Résumé :

Cette thèse est consacrée à l'étude de modèles mathématiques décrivant l'évolution de flammes en boules en présence d'un champ radiatif. Ces flammes ne sont observables qu'en microgravité et à faible nombre de Lewis. Les inconnues sont la température, la fraction massique du carburant et le rayon de la flamme sphérique. Le but de notre travail a été de modéliser le phénomène physique sous la forme d'un problème à frontière libre couplé à l'équation d'Eddington, puis d'étudier la stabilité des solutions au voisinage des états stationnaires, dont l'existence est prouvée en premier lieu. Dans ce but, nous linéarisons le problème à frontière libre, puis construisons une fonction d'Evans qui est analytique et dont les zéros sont les valeurs propres de l'opérateur linéarisé. Nous démontrons également des résultats d'instabilité en faisant appel à la théorie des problèmes paraboliques abstraits totalement non linéaires. Enfin on établit et analyse un modèle intégro-différentiel décrivant la dynamique en temps long du rayon de la flamme.

Mots clés: Flammes en boule, Transfert radiatif, Equation d'Eddington, Problème à frontière libre, Stabilité, Fonction d'Evans, Semi-groupes analytiques, Equation intégro-différentielle

Abstract:

This thesis is devoted to the analysis of mathematical models for flame balls. The latter are tiny, stable, stationary, spherically symmetric flames that occur in combustible gas mixtures. Moreover, they are only visible in a microgravity environment. The main variables are the temperature, the fuel mass fraction and the flame ball radius. We have modelized the physical problem as a Free Boundary Problem (FBP) coupled with the Eddington equation for the radiative transfer. First we prove the existence of stationary solutions. Then we linearize the FBP around a fixed steady solution and construct an Evans function which is analytic, its zeros being the eigenvalues of the linearized operator. We prove rigorously instability results using analytic semi-group techniques. Finally, we derive an integro-differential equation describing the behavior of the flame ball radius for long times.

Key words: Flame balls, Radiative transfer, Eddington equation, Free boundary problem, Stability, Evans function, Analytic semi-groups, Integro-differential equation

N° d'ordre : **3440**

THÈSE
en cotutelle entre

L'UNIVERSITÉ BORDEAUX I

ÉCOLE DOCTORALE DE MATHÉMATIQUES ET INFORMATIQUE

et

LA VRIJE UNIVERSITEIT D'AMSTERDAM

présentée à AMSTERDAM

par **Vincent GUYONNE**

POUR OBTENIR LE GRADE DE

DOCTEUR

SPÉCIALITÉ : **Mathématiques appliquées et calcul scientifique**

****

MODÈLES MATHÉMATIQUES POUR FLAMMES SPHÉRIQUES

****

Soutenue le : 27 Septembre 2007

Après avis de :

Luca LORENZI	Professeur, Université de Parme	**Rapporteurs**
Jean-Michel ROQUEJOFFRE	Professeur, Université Paul Sabatier Toulouse III	

Devant la commission d'examen formée de :

Michel LANGLAIS	Professeur, Université Victor Segalen Bordeaux 2	**Président**
Jean-Michel ROQUEJOFFRE	Professeur, Université Paul Sabatier Toulouse III	**Rapporteur**
Jan Bouwe van den BERG	Professeur, Vrije Universiteit Amsterdam	**Examinateurs**
Claude-Michel BRAUNER	Professeur, Université Bordeaux 1	
Arjen DOELMAN	Professeur, CWI Amsterdam	
Josephus HULSHOF	Professeur, Vrije Universiteit Amsterdam	

- 2007 –

"Entre par la forme, sors de la forme"

Morihei Ueshiba

"Ce qui a été perdu ne se retrouve pas,
vaine quête de jadis, mais se reconstruit..."

Louis René Des Forêts

Contents

Preface v

Acknowledgements vii

Chapter 1. Introduction 1
1.1. Introduction of the physical problem 2
1.2. Governing equations for combustion 4
1.3. Radiative transfer models 9
1.4. Outline of the thesis 13

Chapter 2. Flame balls for a free boundary combustion model with radiative transfer 15
2.1. Introduction 15
2.2. Existence of solutions 23
2.3. Limit cases of the radiative parameters 24
2.4. Numerical calculations 27
2.5. Conclusion 33
2.6. Appendix: Existence proof 34

Chapter 3. Instability in a flame ball problem 41
3.1. Introduction 41
3.2. Function spaces and linearisation 45
3.3. The linear problem 55
3.4. The nonlinear problem 65
3.5. Instability results 69
3.6. Concluding remarks 73
3.7. Appendix A: Technical tools 74
3.8. Appendix B: Proof of Theorem 3.5 77

Chapter 4. On a model of flame ball with radiative transfer 85
4.1. Introduction 85
4.2. Growth model for the radius of flame balls 88
4.3. Mathematical Results 95
4.4. Numerics 98
4.5. Conclusion 100

Chapter 5. Stability properties for a flame ball problem with radiative transfer 103

5.1. Introduction 103
5.2. Linearisation of the free boundary problem 110
5.3. Bifurcation diagram analysis 116
5.4. Stability analysis for the linear Eddington equation 122
5.5. The Evans function for the nonlinear Eddington equation 128

Bibliography 135

Samenvatting 139

Summary 143

Résumé 147

Preface

The subject of this thesis is the mathematical study of a combustion-radiation model for flame balls.

In the introductory Chapter 1 we recapitulate the motivations and physical considerations leading to this study. The governing equations for combustion are revisited and coupled with an appropriate model for radiation phenomena, the free boundary problem to be studied is derived.

Chapter 2 has been published in [**53**] and is joint work with J.B. van den Berg and J. Hulshof. It deals with the existence of stationary solutions.

The content of Chapter 3, are rigorous instability results. It is joint work with Luca Lorenzi and published in [**27**].

The results of Chapter 4 were obtained in collaboration with Pascal Noble and it appeared in [**28**]. An integro-differential equation describing the evolution of the flame ball radius is derived and analysed.

Finally, Chapter 5 concerns stability results for the flame ball problem, and is joint work with J.B. van den Berg and J. Hulshof.

Acknowledgements

This thesis would not exist without the contribution and support of many people and it is time for me to thank them.

I would first like to thank my advisors, Joost Hulshof and Claude-Michel Brauner for giving me the opportunity to write this thesis, to work on a challenging subject, but also to create new contacts and to travel. Thank you for sharing with enthusiasm your knowledge. But I cannot forget to mention my last supervisor Jan Bouwe van den Berg who followed carefully all the details of my thesis. When I had questions, you were always available to answer them, giving good advice. Thank you for this.

This thesis is a joint doctoral thesis between the Vrije Universiteit Amsterdam and the Université Bordeaux 1. I would like to thank the Scientific Department of the French Embassy in Den Haag, and in Bordeaux the International Department and the "Ecole doctorale de mathématiques et informatique" which made this project possible.

I spent two fruitful months in Parma visiting and working with Luca Lorenzi and Alessandra Lunardi. It was a rewarding experience, thank you to both of you.

I would like to thank cordially Arjen Doelman, Michel Langlais, Jean-Michel Roquejoffre and Rob van der Vorst for accepting to be part of my thesis committee.

During my Ph.D., I had the opportunity to work in very good conditions and to be part of a dynamic group. I would like to thank the whole analysis group. We shared some great times. It was a real pleasure to meet and work with you, Pascal, when you joint the group for a post doc. My office mates had to be patient with me and all of them were supportive, so thank you Hala, Guido and Miro.

I also would like to thank Inge for giving me the opportunity to ride horses, it was a real pleasure, and of course I do not forget all the long discussions we had together. I will, definitely, miss the memorable evenings I spend with friends; I am thinking in particular about Guido, the "québécois" Jean-Philippe, Miro (also for some great travelling times!), Tibor and Drahusa. This group would not be complete without the movie team Ewa, Konrad and Wojtek.

I would like to address a special thanks to Wojtek and Alistair who kindly accepted to be my paranimfen. Thank you Wojtek for your true kindness, your imperturbable joy of life and your support. A special thanks to Alistair who was always around, especially during difficult moments, and always offering excellent advise.

Il est enfin temps de remercier mes amis en France, je pense en particulier à Cyril et Carine qui ont toujours été présents. Merci pour toutes ces soirées chaleureuses passées en votre compagnie. Bien évidemment, je ne peux oublier Béatrice toujours aussi heureuse de vivre et avec qui j'espère refouler bientôt les tatamis. Je ne serais complet sans faire une dédicace spéciale à Gaël, l'ami de toujours. Mais aussi je voudrais remercier Hugo, Jean-Philippe (Nicolas), Maxime et Raoul pour être toujours présents après ce long exil.

Enfin et surtout, cet aboutissement n'a pu être réalisé sans ma famille, je tiens à vous remercier tous vivement du fond du cœur. Votre soutien a été des plus précieux depuis toujours, mais surtout durant ces quatre années autant dans les moments heureux que plus difficiles. Merci Arnaud pour ton enthousiasme, ton envie d'aller de l'avant mais aussi pour m'avoir sauvé maintes fois de problèmes informatiques. Merci Hélène pour ton soutien, ton écoute, tes conseils toujours éclairés, mais aussi un grand merci à ta petite famille, Thierry et Martin. Merci pour m'avoir toujours accueilli les bras grand ouverts, avec générosité et enthousiasme.

Je voudrais finir par remercier mes parents, toujours présents, disponibles et concernés. Merci pour vos valeurs inculquées, pour votre soutien sans faille, votre spontanéité et grande générosité.

CHAPTER 1

Introduction

Humans have dealt with combustion since prehistoric times, without understanding its exact mechanism. Scientific efforts to understand combustion processes started with the industrial development occurring in Europe during the XIX-th century. Indeed, the first experimental studies of flame propagation in a gaseous mixture were performed around 1880 by Vieille, Mallard, Le Châtelier and Berthelot amongst other people (see [**20**]). Their motivation was to understand the causes of firedamp explosions in coal mines. Their main interests concerned the velocity of explosion-waves for different gaseous mixtures. It was noticed that the velocity depends on the (maximum) temperature of the flame. In order to relate the temperature and the velocity of explosion-waves, they assumed these waves were propagated as sound waves. In that case, knowing the specific heats, it was possible to relate the velocity and the temperature via an algebraic equation. Moreover, these studies revealed that after an explosion, there exists a deflagration wave corresponding to slower velocities. The first known model to describe the co-existence of such phenomena was derived by Chapman and Jouguet at the beginning of the XX-th century, assuming the flame could be considered as a shock wave. This analogy leads to Rankine-Hugoniot relations from which one can explain the observed phenomena described above.

Half a century later, man's venture into space naturally led to an active scientific interest in physical and other processes in microgravity environments, starting with fundamental physical and biology experiments. In particular, an unexplained spacecraft fire led to experiments with flames. In this thesis we are interested in describing flames in a microgravity environment.

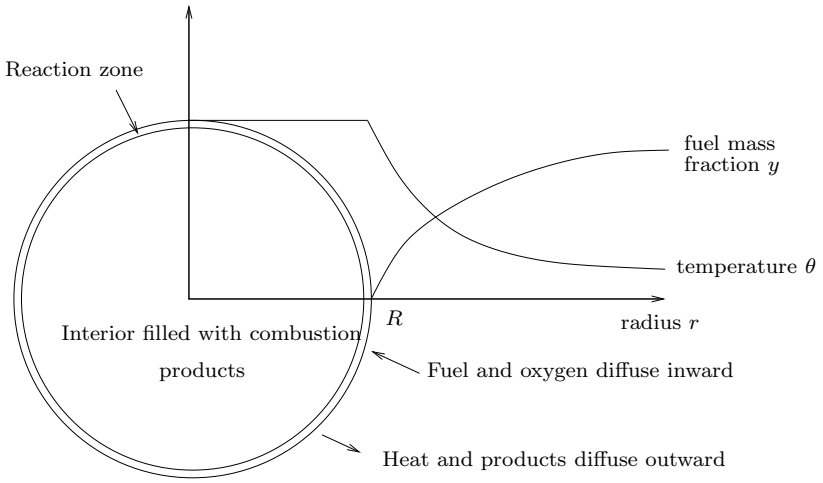

Figure 1.1: Profile of the temperature and the fuel mass fraction variables in the adiabatic case. The radius of the flame ball is denoted by R, corresponding to the flame front.

1.1. Introduction of the physical problem

Flame balls are tiny, stable, stationary, spherically symmetric flames that occur in combustible gas mixtures (such as lean hydrogen-air mixtures), having low Lewis numbers. They are visible only in a microgravity environment. The Lewis number is a measure of the rate of diffusion of fuel into the flame ball relative to the rate of diffusion of heat away from the flame ball. Hydrogen and methane are the only fuels that provide low enough Lewis numbers to produce stable flame balls, even for very weak, barely flammable mixtures. Figure 1.1 provides a sketch of a flame ball and as one can notice, all the combustion takes place in a thin reaction zone. Because the mixture is lean and has a low Lewis number, the flame does not spread across the mixture. It forms a spherical shell filled with combustion products. Fuel and oxygen diffuse inward, while heat and combustion products diffuse outward, and it can only be observed in a microgravity environment, in the absence of buoyant flow that would overwhelm diffusion.

Spherical flame balls are mainly characterised by their radius $R(t)$, which may vary in time. Physicists and mathematicians are interested in describing the behavior of two other quantities, namely the temperature θ and the fuel mass fraction y. As shown in Figure 1.1, these two quantities are supposed to be constant inside the flame ball, in particular the fuel mass fraction is supposed to vanish, meaning that all the fuel has been burnt. Outside the flame ball, in the fresh region, the temperature is decreasing to reach the ambient (or fresh) temperature, while the fuel mass fraction converges to y_f, the initial mass fraction, far away from the flame.

This specific shape of solutions corresponds to the solutions of the first model describing flame balls. This model was derived by Zeldovich [**56**] in 1944. It is quite remarkable that, before scientists knew about the existence of physical flame balls, Zeldovich looked for this special shape of solutions. He showed that the steady heat and mass conservation equations admit a solution corresponding to a stationary spherical flame, just as the same governing equations in a planar geometry admit a steadily propagating flame as a solution for every mixture. The detailed description of the model leading to the explicit expressions of the solutions is discussed in Section 1.3. Zeldovich then studied the stability properties of such solutions. He proved that such flames were unstable. Therefore, he predicted that flame balls would probably not be observable, just as planar flames are frequently subject to instabilities which prevent them from remaining planar.

This was until 1984, when Ronney from NASA (see [**46**]) discovered, during drop tower experiments, the existence of flame balls. From this observation, a physical stabilising effect had to be found. Zeldovich [**56**] had noted the possibility of heat losses stabilising flame balls. The effects of volumetric radiative losses (e.g., due to gas radiation) on flame balls were analysed by Buckmaster and collaborators [**16, 17**]. Noting that the total heat release is proportional to the flame ball surface area and that the total radiative heat loss is proportional to the flame ball volume, one can give a heuristic argument for the stabilisation of flame balls. If the flame radius increases, the surface area to volume ratio decreases, thus the ratio of total heat release to total radiative heat loss increases, thus the flame ball becomes weaker and shrinks. Conversely, if the radius decreases, the flame ball grows stronger and expands. Hence, flame balls with sufficient volumetric losses can be stable to radial disturbances.

It has also been predicted [**34**] that stable flame balls can only exist for mixtures having a Lewis number less than a critical value which is less than unity, which explains why flame balls are not observed for mixtures with Lewis number less than but close to unity (e.g. methane-air) or larger than unity (e.g. propane-air), even for near-extinction mixtures at microgravity.

Flame balls have several unique and interesting properties which indicate a number of practical applications. Since they are quasi one-dimensional, steady and convection-free, they are the simplest possible type of premixed flame structure and therefore provide a useful theoretical and numerical model of the interaction between chemical and transport processes in flames, especially near flammability limits. Flame balls may also be relevant to the turbulent combustion of mixtures with low Lewis number because flame balls are more robust than planar flames. Consequently, sufficiently strong turbulence may extinguish planar flames, whereas flame balls could persist under the

same conditions. Hence, structures reminiscent of flame balls could be the prevalent ones in near-extinction turbulent combustion of lean hydrogen-air mixtures in engines. In other words, it may lead to produce lean-burning car engines, mixing in more air and less fuel, and therefore is more environment friendly. But it can also help to understand fire and explosion hazards in mine shafts, oil refineries and chemical plants. Finally, it can improve spacecraft safety where gases from waste systems or fuel cells could provide a fuel source for long-lived flame balls.

1.2. Governing equations for combustion

To give some background informations, we present a derivation of the mathematical models for flame balls studied in this thesis. More details may be found in [**7, 18, 55**], to name just a few references of a huge list. In the next section we will couple this mathematical model to models with radiative transfer.

The model

As most chemical reactions, flames in gaseous mixtures may involve a large number of reactants and a complicated reaction network. In this study however, we will work with the assumption of simple chemistry. That is, we consider a mixture of only two reactants A_1 and B, and the chemical reaction

$$A_1 + B \to A_2 + \text{ heat } .$$

If we assume furthermore the species B to be abundant compared to A_1, meaning its concentration does not vary much during the chemical reaction, then we get the simplified chemical reaction

$$A_1 \to A_2 + \text{ heat } . \tag{1.1}$$

A mathematical model for (1.1) has to take into account, for each position $\vec{x}$ and at each instant of time t, two densities $\rho_k(\vec{x}, t)$, two velocities $\vec{v}_k(\vec{x}, t)$, two pressures $p_k(\vec{x}, t)$ and temperature θ. We introduce the total mass density ρ, the total velocity $\vec{v}$, and the total pressure p, via the relations

$$\rho(\vec{x}, t) = \sum_k \rho_k(\vec{x}, t),$$

$$\rho\vec{v} = \sum_k \rho_k \vec{v}_k,$$

$$p = \sum_k p_k.$$

Following Truesdell [**52**], ones writes the equations for ρ, $\vec{v}$ and the total energy E per volume as follows:

$$\begin{cases} \dfrac{\partial \rho}{\partial t} + \vec{\nabla} \cdot (\rho \vec{v}) = 0, \\ \dfrac{\partial (\rho v_i)}{\partial t} + \vec{\nabla} \cdot (v_i \rho \vec{v}) = \rho F_i + \displaystyle\sum_{j=1}^{3} \frac{\partial \sigma_{ij}}{\partial x_j}, \quad 1 \leq i \leq 3, \\ \dfrac{\partial E}{\partial t} + \vec{\nabla} \cdot (E \vec{v}) = \displaystyle\sum_{i=1}^{3} \frac{\partial}{\partial x_i} \left(\sum_{j=1}^{3} \sigma_{ij} v_j \right) - \vec{\nabla} \cdot \vec{q} + \vec{F} \cdot \rho \vec{v}, \end{cases} \tag{1.2}$$

provided no momentum and energy are created by the chemical reactions. Moreover, it is assumed that the work of the interaction forces is negligible. Here $(\sigma_{ij})_{1 \leq i,j \leq 3}$ is the tensor of the viscous forces, $\vec{q}$ is the energy flux, $\vec{F}$ is the exterior force per unit of mass. Denoting by $\dot{\rho}_k$ the rate of variation of ρ_k due to the reaction, the system is completed by

$$\frac{\partial \rho_k}{\partial t} + \vec{\nabla} \cdot (\rho_k \vec{v}) = -\vec{\nabla} \cdot (\rho_k \vec{V}_k) + \dot{\rho}_k, \quad k = 1, 2,$$

in which $\vec{V}_k = \vec{v}_k - \vec{v}$ is the diffusion velocity of species A_k.

The total pressure p appears in the viscosity tensor

$$\sigma_{ij} = -\left(p + \frac{2}{3} \mu \vec{\nabla} \cdot \vec{v} \right) \delta_{ij} + \mu \left(\frac{\partial v_i}{\partial x_j} + \frac{\partial v_j}{\partial x_i} \right),$$

the gaseous mixture being Newtonian. Introducing the mass fraction Y_k of A_k by

$$\rho_k = \rho Y_k,$$

the perfect gas law rewrites as

$$p = \sum_k p_k = \rho R \theta \sum_k \frac{Y_k}{m_k},$$

where R is the universal gas constant and m_k the molecular mass of A_k. The internal energy

$$\begin{aligned} e &= \sum_k Y_k e_k = \sum_{Y_k} \left(h_k - \frac{p_k}{\rho_k} \right) \\ &= \sum_k Y_k h_k^0 + \sum_k Y_k \int_{\theta_0}^{\theta} C_p^k d\theta - \frac{p}{\rho}, \end{aligned}$$

involves the individual enthalpies h_k,

$$h_k = h_k^0 + \int_{\theta_0}^{\theta} C_p^k(\theta) d\theta,$$

with C_p^k the specific heat at constant pressure.

We neglect the exterior forces (in particular gravity) and assume $\mu = 0$ in the viscosity tensor. The energy flux $\vec{q}$ reads

$$\vec{q} = -\lambda \vec{\nabla}\theta + \sum_{k=1}^{2} \rho_k h_k \vec{V}_k,$$

in other words, $\vec{q}$ is the sum of a conductive flux given by a Fourier law (λ is the thermal conductivity of the mixture) and diffusive fluxes with the enthalpy of each species. Concerning the mass flux $\rho_k \vec{V}_k$, it is given by Fick's law

$$\rho_k \vec{V}_k = -\rho D \vec{\nabla} Y_k,$$

where $D > 0$ is a diffusion coefficient.

The remaining term to express is the term of reaction $\dot{\rho}_k$. Let us denote by ω the global rate of the reaction (1.1). We suppose that the chemical reaction follows an Arrhenius law of the first order, which reads

$$\omega = B(\theta) \exp\left(-\frac{\mathcal{E}}{R\theta}\right).$$

The quantity $B(\theta)$ is the pre-exponential term and the constant $\mathcal{E}$ is the activation energy of the reaction.

Under the simple chemistry hypothesis and due to the simplifications explained above, writing $Y = Y_1$, System (1.2) can be rewritten as

$$\begin{cases} \dfrac{\partial \rho}{\partial t} + \vec{\nabla} \cdot (\rho \vec{v}) = 0, \\ \dfrac{\partial (\rho v_i)}{\partial t} + \vec{\nabla} \cdot (\rho v_i \vec{v}) = -\dfrac{\partial p}{\partial x_i}, \quad 1 \leq i \leq 3, \\ \dfrac{\partial E}{\partial t} + \vec{\nabla} \cdot (E\vec{v} + p\vec{v}) = \vec{\nabla} \cdot (\lambda \vec{\nabla}\theta) + \vec{\nabla} \cdot (\rho D (h_1 - h_2) \vec{\nabla} Y) \\ \dfrac{\partial \rho Y}{\partial t} + \vec{\nabla} \cdot (\rho Y \vec{v}) = -\rho Y \omega + \vec{\nabla} \cdot (\rho D \vec{\nabla} Y). \end{cases}$$

Moreover, we assume A_1 and A_2 to have the same molecular mass M. In addition, the specific heat at constant pressure C_p and the specific heat at constant volume C_v, are supposed to be independent of θ, and related to each other by Mayer's relation

$$M(C_p - C_v) = R,$$

so that E can be written as

$$E = \frac{1}{2}\rho v^2 + Q\rho Y + \rho(h_2^0 - C_p\theta_0) + \rho C_v \theta.$$

This implies the following coupled system:

$$\begin{cases} \dfrac{\partial \rho}{\partial t} + \vec{\nabla} \cdot (\rho \vec{v}) = 0, \\ \dfrac{\partial (\rho v_i)}{\partial t} + \vec{\nabla} \cdot (\rho v_i \vec{v}) = -\dfrac{\partial p}{\partial x_i}, \quad 1 \leq i \leq 3, \\ \dfrac{\partial \rho C_v \theta}{\partial t} + \vec{\nabla} \cdot (\rho C_p \theta \vec{v}) = Q \rho Y \omega + \vec{\nabla} \cdot (\lambda \vec{\nabla} \theta) \\ \dfrac{\partial \rho Y}{\partial t} + \rho \vec{v} \cdot \vec{\nabla} Y = -\rho Y \omega + \vec{\nabla} \cdot (\rho D \vec{\nabla} Y), \end{cases}$$

where he constant $Q = h_1^0 - h_2^0 > 0$ corresponds to the heat produced by the reaction (1.1) per unit of mass of the reactant. Note that, in the temperature equation, we can replace C_v by C_p via Mayer's relation. In that case, two extra terms appear in the right hand side of the temperature equation, namely $\frac{\partial p}{\partial t}$ and $\vec{v} \cdot \vec{\nabla} p$. Thus, we need to consider an extra hypothesis, namely that the pressure is approximatly constant. This simplification is classical in combustion and is refered to as the combustion approximation or isobaric approximation. The two extra terms will then vanish. Justifications can be found for example in [**18**].

A second hypothesis allows us to decouple the hydrodynamic equations, namely the constant density approximation. This is often used to simplify physical models, even if it is harder to justify on the theoretical level.

As we are looking for flame balls, we will assume our problem to be radially symmetric. Introducing the radial coordinates, the system to consider reads

$$\begin{cases} \rho c(\partial_t \theta + v \partial_r \theta) = \dfrac{\lambda}{r^2} \partial_r (r^2 \partial_r \theta) + Q \rho Y \omega, \\ \rho(\partial_t Y + v \partial_r Y) = \dfrac{1}{r^2} \rho D \partial_r (r^2 \partial_r Y) - \rho Y \omega, \\ \omega = B(\theta) \exp(-\dfrac{\mathcal{E}}{R\theta}), \end{cases}$$

where $c = C_v$. We take the asymptotic conditions

$$\theta \to \theta_f, \rho \to \rho_f, Y \to y_f, \quad \text{for } r \to \infty.$$

Moreover, we will make the assumption that there is almost no convection, meaning that the terms $v \partial_r \theta$ and $v \partial_t Y$ are negligible compared to the Laplacians and the time derivatives $\partial_t Y$ and $\partial_t \theta$. Then we are led to the system

$$\begin{cases} \rho c \partial_t \theta = \lambda \Delta_r \theta + Q \rho Y \omega, \\ \rho \partial_t Y = \rho D \Delta_r Y - \rho Y \omega, \\ \omega = B(\theta) \exp(-\dfrac{\mathcal{E}}{R\theta}), \end{cases}$$

where Δ_r is the radial Laplacian in $\mathbb{R}^3$, i.e. $\Delta_r g = g'' + \frac{2}{r}g'$, where g' is the derivative of g with respect to the radial variable r.

Nondimensionalisation

The next step is to nondimensionalise the equations derived in the previous section. For this purpose, we define

$$\bar{r} = \frac{r}{R_0}, \bar{t} = \frac{\lambda t}{\rho c R_0^2}, \bar{\theta} = \theta \frac{C_v}{Q}, \bar{B} = B \frac{R_0^2 c}{\lambda}, \xi = \frac{\mathcal{E} c}{RQ},$$

where R_0 is a suitable reference flame radius. The variable ξ is the activation energy. We define $\varepsilon = \frac{1}{\xi}$, and in view of the high activation limit assumption, ε will be small. Dropping the bars, the resulting system reads

$$\begin{cases} \partial_t \theta = \Delta \theta + Y\omega, \\ \partial_t Y = \dfrac{1}{\mathrm{Le}} \Delta Y - Y\omega, \\ \omega = B \exp(-\dfrac{1}{\varepsilon \theta}). \end{cases} \tag{1.3}$$

Here the parameter $\mathrm{Le} = \frac{\lambda}{\rho D c}$ is the Lewis number, a classical parameter in combustion theory which plays an important role in the stability analysis. It measures the ratio between the thermal and molecular diffusions.

The flame sheet model

In the previous subsection we derived the common formulation of the (simplified) combustion model as a system of coupled reaction-diffusion equations.

The major consequence of the assumption of high activation energy is that it limits the region in which reaction is significant. In our context, it implies that the reaction occurs in an exponentially (in terms of ε) thin zone located at the flame ball radius $R(t)$. It is therefore reasonable to derive from System (1.3) a free boundary problem.

Physicist and mathematicians have considered both the reaction-diffusion model and the free boundary problem, each approach having its own advantages and disadvantages.

From a modelling point of view, one may start from the assumption that the reaction may be modelled by a balance between (fuel) mass flux going into the flame and heat flux coming out of the flame, where these fluxes will certainly be temperature dependent. Thus we look for a free boundary formulation in which at the free boundary, $Y = 0$, the temperature θ is continuous, and, in case of a flame ball,

$$\frac{1}{\mathrm{Le}}[Y_r] = -[\theta_r] = F(\theta^*),$$

where θ^* is the temperature of the flame front (i.e. the temperature at $r = R(t)$). The function $F(\theta^*)$ is again a reaction rate and a formula for $F(\theta^*)$ has to be derived by means of a formal asymptotic analysis starting from the reaction-diffusion formulation and a high activation energy assumption in which ε is sufficiently small. The analysis is non trivial and, from a mathematical point of view, it is a combination of formal asymptotics and modelling, see [**18, 55**] and also [**22**].

Following [**14**], we will simply impose a reaction rate $F = F(\theta^*)$, which we allow to be of a general form, e.g.

$$F(\theta^*) = B \exp(-\frac{1}{\varepsilon\theta^*}).$$

In [**18, 22, 55**], the authors derive, formally, a free boundary problem obtained from the reaction-diffusion system considering some specific expressions of the reaction rate. In order to obtain such a derivation, several high order effects have been neglected such as, for example, the curvature. A detailed analysis of those effects is performed in [**23**]. To summarise, the free boundary problem derived from the reaction-diffusion system (1.3), reads

$$Y_t = \frac{1}{\mathrm{Le}}\Delta Y \qquad \text{for } r \neq R(t), \tag{1.4a}$$

$$\theta_t = \Delta\theta \qquad \text{for } r \neq R(t). \tag{1.4b}$$

The jump conditions at $r = R(t)$ are

$$[\theta] = Y = 0, \quad -[\theta_r] = \frac{1}{\mathrm{Le}}[Y_r] = F(\theta^*). \tag{1.4c}$$

The asymptotic boundary conditions are

$$Y \to y_f, \qquad \theta \to \theta_f, \qquad \text{as } r \to \infty. \tag{1.4d}$$

1.3. Radiative transfer models

In Section 1.2, we introduced the flame ball model which is known in the literature as the adiabatic model (System (1.4)). It was formulated in 1944 by Zeldovich, who computed the explicit stationary solutions, namely

$$Y(r) = \begin{cases} 0 & \text{for } r \leq R, \\ y_f\left(1 - \dfrac{R}{r}\right) & \text{for } r > R, \end{cases} \tag{1.5}$$

and

$$\theta(r) = \begin{cases} \theta_f + \dfrac{y_f}{\mathrm{Le}} & \text{for } r \leq R, \\ \theta_f + \dfrac{y_f}{\mathrm{Le}}\left(1 - \dfrac{R}{r}\right) & \text{for } r > R, \end{cases} \tag{1.6}$$

where y_f (resp. θ_f) denotes the mass fraction (resp. temperature) in the fresh region far away. Linearising around these stationary solutions

leads to an unexpected stability analysis. Unexpected in the sense that all solutions were proved to be unstable.

The discovery of existing physical flame balls by Ronney in 1984 required reconsideration of this model. It has been argued [**44**] that radiative effects play, on a physical level, an important role for combustion processes in a microgravity environment.

At first, ad hoc heat loss mechanisms were considered and added to System (1.4). We mention the work of Joulin et al. [**16, 17**] and Dold et al. [**22**] for example. In [**16**], the authors considered heat losses to occur in the volume enclosed by the flame sheet only. In this particular situation, bifurcation diagrams were obtained showing the existence of two branches of stationary solutions. These two branches corresponds to two flame balls, one with small radius and one with large radius. The stability analysis performed lead to the following result: provided the Lewis number is less than 1, the solutions related to the small radii are unstable to one- and three-dimensional perturbations. On the other hand, part of the branch corresponding to larger radii consists of solutions stable under three-dimensional perturbations. In [**17**], the authors extend this result by including the effects of heat loss in the far field (fresh gas), and they conclude that far fields losses do not qualitatively change the (stability) properties of the solutions. In [**22**], flame balls are studied in a porous medium that serves to exchange heat with the gas, and two heat loss models are considered. One of these treats the heat loss as being constant in the burnt region and linear in the fresh region. The other does not distinguish between burnt and unburnt gas and is based on a (nonlinear) Stefan's law. For both heat loss models, the authors find, again, two branches of solutions of small and large flame balls, respectively. For Lewis number greater than unity both solutions are unstable, while at Lewis number less than unity, part of the branch of large flame balls becomes stable, solutions with the nonlinear radiative law being stable over a smaller range of parameters. The stable parameter region increases when the heat capacity of the porous medium is increased.

A different approach in the heat loss case was introduce by Rouzaud and al. [**5, 47**]. From a reaction-diffusion heat loss model, the authors derive an integro-differential equation describing the radius long time behavior of flame balls. They are able to show, for an input energy sufficiently large and the Lewis number less than 1, that a flame ball stabilises to a constant radius.

The Eddington model for radiation

Despite these very interesting results, radiation cannot be reduced only to heat loss mechanisms. Radiation involves both the emission and absorption of photons. Emphasising this difference from the heat loss models discussed so far, we speak of radiative transfer models. To

model radiative transfer, let us start with a microscopic description given by the equation

$$\frac{1}{c}\partial_t I + \Omega \cdot \nabla I = \sigma(B(\nu,\theta) - I). \tag{1.7}$$

Here $I = I(x,t,\Omega,\nu)$ is the total radiative intensity, x the position, t the time, Ω the direction of emission, ν the frequency, c the speed of light, σ the opacity of the medium and $B(\nu,\theta)$ the Planck distribution: $B(\nu,\theta) = \frac{2h\nu^3}{c^2}(\exp(\frac{h\nu}{k\theta}) - 1)^{-1}$. Unfortunately, Equation (1.7) is too difficult to analyse even from a numerical point of view. Therefore it is common to consider simplified models such as the (Milne-)Eddington diffusion equations, valid in the limit of isotropic radiation, the Rosseland model, valid for high opacity media, or the optically thin model, valid for nonabsorbent media ([**40, 43**]).

Our goal in this thesis is to study System (1.4) coupled with a simplified radiative transfer equation, namely we deal with the Eddington diffusion model ([**24, 40, 41, 42, 43, 49**]), also known as the P_1 model. It reads

$$-\nabla(\nabla \cdot q) + 3\alpha^2 q = -\alpha\nabla\theta^4, \tag{1.8}$$

where q is the radiative flux and α the opacity of the medium. Coupling the Eddington equation to Problem (1.4), we follow the approach of Buckmaster and Joulin [**14, 31, 32**] in which the divergence of the radiative flux appears with coupling constant β, the Boltzmann constant. Thus β is a measure of the ratio between the radiative and the diffusive flux. By setting $u = -\beta\nabla \cdot q$, it leads to the problem

$$y_t = \frac{1}{\mathrm{Le}}\Delta y \qquad \text{for } r \neq R(t), \tag{1.9a}$$

$$\theta_t = \Delta\theta + u \qquad \text{for } r \neq R(t), \tag{1.9b}$$

$$0 = \Delta u - 3\alpha^2 u + \chi\Delta\theta^k, \tag{1.9c}$$

where $\chi = \alpha\beta$, and we will take k to be either $k = 4$ (black-body radiation) or $k = 1$ (linearised radiation model). Equation (1.9c) is satisfied in the whole space (in the sense of distributions and classically for $r \neq R(t)$). The jump conditions at $r = R(t)$ are

$$[\theta] = y = 0, \quad -[\theta_r] = \frac{1}{\mathrm{Le}}[y_r] = F(\theta(R(t))), \tag{1.9d}$$

with $u + \chi\theta^k$ being smooth (i.e. C^1). The asymptotic boundary conditions are

$$y \to y_f, \quad \theta \to \theta_f, \quad u \to 0 \quad \text{ as } r \to \infty. \tag{1.9e}$$

As mentioned before, the analysis of this problem is the purpose of this thesis. We will first prove the existence of stationary solutions, the multiplicity of such solutions being illustrated via bifurcation diagrams. In order to study stability, we linearise System (1.9) around a fixed

stationary solution and then study its spectral properties. More details about the strategy to tackle this problem can be found in Section 1.4.

Hierarchy of models for the radiative transfer equation

The P_1 model is only the first in a hierarchy of models with increasing physical accuracy. From the microscopic description (Equation (1.7)) it is possible, using the moment closure method for kinetic equations, to derive a hierarchy of macroscopic models which are hyperbolic and locally dissipate the entropy [**35**]. Introducing the radiative intensity, flux and pressure (E_R, F_R and P_R) by

$$E_R = \langle I \rangle = \frac{1}{c} \int_0^\infty \int_{S^2} \phi(\nu, \Omega)\, d\Omega\, d\nu,$$

$$F_R = c\, \langle \Omega\, I \rangle,$$

and

$$P_R = \langle \Omega \otimes \Omega\, I \rangle,$$

the first model of this hierarchy, the M_1 model, is based on the closure assumption

$$P_R = D_R E_R,$$

and can be written as:

$$\begin{cases} \dfrac{\partial E_R}{\partial t} + \nabla \cdot F_R = \sigma c (a T^4 - E_R), \\ \dfrac{1}{c} \dfrac{\partial F_R}{\partial t} + c \nabla (D_R E_R) = -\sigma F_R. \end{cases}$$

The closure assumption contains the Eddington tensor D_R,

$$D_R = \frac{1-\chi}{2} \mathrm{Id} + \frac{3\chi - 1}{2} n \otimes n, \tag{1.10}$$

with $n = \frac{f}{\|f\|}$, $f = \frac{F_R}{cE_R}$, and in which the factor χ is given by

$$\chi = \frac{3 + 4\|f\|^2}{5 + 2\sqrt{4 - 3\|f\|^2}}.$$

Since energy does not travel faster than the speed of light, one always has $\|f\| \leq 1$. This model takes into account the anisotropy of the emission; it is a more realistic model than the Eddington model where the emission is isotropic and time derivatives are neglected, see Dubroca et al. [**24**] for a derivation of this model, numerical simulations and discussions on the effects of the anisotropy.

Note that setting $\chi = \frac{1}{3}$ and $\delta = 0$, we recover the Eddington equation (1.8). An intermediate model between the Eddington and M_1 models is to consider $\chi = \frac{1}{3}$ and $\delta \neq 0$ (i.e. the time derivatives are taken into account), named the P_1 isotropic model. Coupling first this

radiation model to System (1.4) and then the M_1 model would be an interesting extension of the work produced in this thesis.

1.4. Outline of the thesis

The thesis is devoted to the study of System (1.9). First, we are interested in proving the existence of stationary solutions associated to System (1.9). This is the subject of Chapter 2. We do not only prove existence, but also exhibit the multiplicity of existing solutions via bifurcation diagrams. In order to get these diagrams, we will consider mainly two parameters, β and y_f. Limit cases of the radiative parameters are also discussed. We consider four different cases, the limit case $\alpha \to \infty$ with β fixed, the transparent limit $\alpha \to 0$ with β fixed, as well as large Boltzmann numbers $\beta \to \infty$ with α fixed, and finally the transparent limit combined with large Boltzmann numbers, $\alpha \to 0$ and $\alpha\beta = \chi$ fixed.

Since we have multiple solutions, a natural next step is then to perform a stability analysis. For this purpose, one needs first to linearise System (1.9) around a fixed stationary solution and then study the associated eigenvalue problem. In order to get information about the point spectrum, we construct an Evans function $D(\lambda)$. The zeros of this function are the eigenvalues of the problem we consider. For radial perturbations we are able to show that, under a specific range of parameters and provided the Lewis number is less than 1, part of a branch of the bifurcation diagrams obtained in Chapter 2 corresponds to stable solutions. All this is done in Chapter 5.

Chapter 3 is devoted to proving rigorously via analytic semigroups techniques, instability results. After linearising System (1.9) we are able to write such a system in the canonical form

$$\begin{cases} D_t\mathbf{u}(t,\cdot) = \mathcal{A}\mathbf{u}(t,\cdot) + \mathbf{f}(t,\cdot), & t > 0, \\ \mathcal{B}(\mathbf{u}(t,\cdot)) = (0, g_1(t,\cdot), g_2(t,\cdot)), & t > 0. \end{cases}$$

where g_j $(j = 1, 2)$ are given (continuous) functions. One can prove that the realisation A of the operator $\mathcal{A}$ defined in a proper Hölder space generates an analytic semigroup. This allows us to prove instability results for part of a branch of the bifurcations diagrams obtained previously. This chapter was written in collaboration with Luca Lorenzi.

Finally Chapter 4 deals with a different approach of the problem. This chapter was written in collaboration with Pascal Noble. We derive from System (1.9) an integro-differential equation describing the long time evolution of the radius $R(t)$ of the flame ball, namely the equation we considered is of the form

$$\mu R \partial_{1/2} R = R \log R + Eq - \lambda R, t \in \mathbb{R}^+, R(0) = 0,$$

where $\mu > 0$, $\lambda > 0$ and

$$\partial_{1/2} R = \frac{1}{\sqrt{\pi}} \int_0^t \frac{\dot{R}(s)}{\sqrt{t-s}}\, ds = \frac{1}{\sqrt{\pi}} \frac{d}{dt} \int_0^t \frac{R(s)}{\sqrt{t-s}}\, ds.$$

This flame is initiated by a point source energy input $Eq(t)$, to which heat losses of radiative nature are applied, represented by the parameter λ. The intensity of this energy input is measured by the positive constant E , and its time evolution is described by the function q. We prove that when the energy input is sufficiently high, the flame ball stabilises to a constant radius for large time.

CHAPTER 2

Flame balls for a free boundary combustion model with radiative transfer

2.1. Introduction

Combustion processes in gaseous mixtures exhibit a variety of phenomena, such as propagating flame fronts, and, in zero- or microgravity situations, flame balls. The latter are perhaps harder to observe, but the advantage is that they are stationary. From a mathematical point of view they are easier to understand, namely as equilibria rather than traveling wave solutions of the mathematical models used to describe the combustion processes. From a physical point of view, because of the force and speed of the reaction, it is hard to do controlled experiments on flame fronts, whereas the combustion is much less violent in flame balls, which can be observed for prolonged periods of time at the costs of having to transfer the experiment to a microgravity environment. In any case, the high costs and experimental difficulties in combustion research highlight the need for a thorough understanding of the mathematical models.

Since the work of Zeldovich [**56**], flame balls are known to exist for models of combustion with simple chemistry, such as a one step reaction in which a gaseous reactant is converted into a gaseous product. Figure 2.1 is a sketch of a flame ball in the non-radiative case. Note that, in this particular situation, the burnt temperature θ_b is constant inside the ball. In this model, commonly referred to as the adiabatic case, flame balls are linearly unstable, in apparent agreement with the absence of experimentally observed flame balls. That was, until 1984, when Ronney discovered, by surprise, the existence, during drop tower experiments, of physical flame balls, later confirmed by experiments in the Space Shuttle. Since then, several effects have been taken into account in combustion models to explain stabilization of flame balls, in particular (radiative) heat losses from the combustion products inside

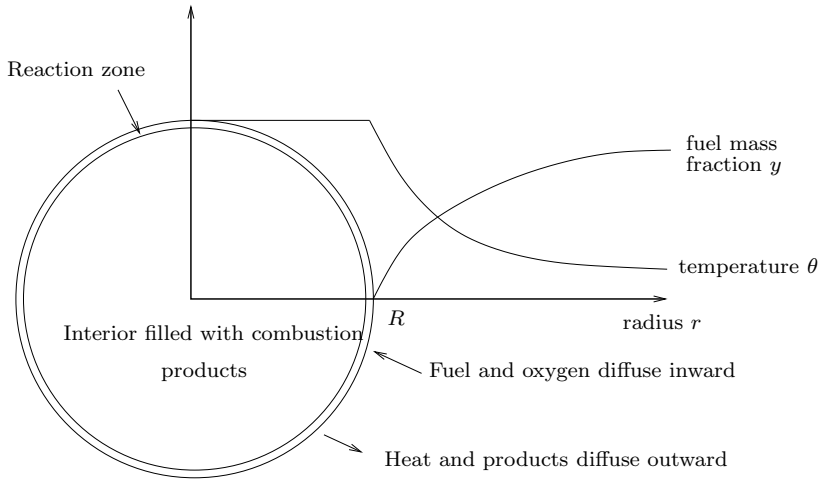

Figure 2.1: Profile of the temperature and the mass fraction variables in the adiabatic case. The radius of the flame ball is denoted by R, corresponding to the flame front.

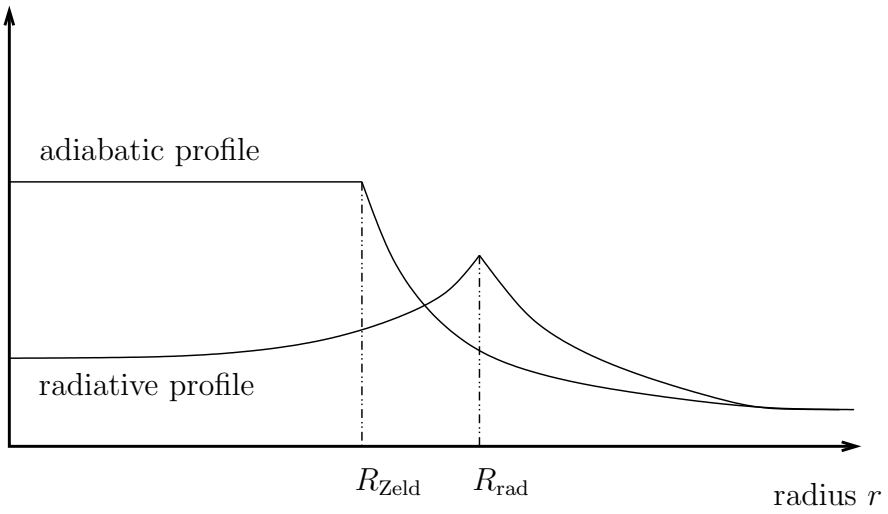

Figure 2.2: Difference of temperature profiles in the adiabatic and in the radiative case.

the flame ball. We refer to [**46**] and references therein, see also the SOFBALL (Structure of Flame Balls at Low Lewis number) link on Paul Ronney's NASA home page [**1**].

In fact, the radiative transfer of heat in combustion processes taking place in inert, not fully transparent media (e.g. dust, porous media, ...), involves both emission and absorption of radiation, and may significantly influence the flame temperature (see Figure 2.2), its propagation speed, and the flammability of the medium itself. This occurs for instance in forest fires and fires in confined spaces, such as tunnels, and the importance of radiative transfer has been noted and stressed in

[**14, 31, 32**]. In this paper, we concentrate on the effects of radiative transfer on flame balls.

There are two common formulations to model combustion processes: the reaction -diffusion and the free boundary formulation. Although both formulations are widely used in the combustion literature, the relation between the two approaches has so far largely been based on numerical simulation and heuristic arguments.

The basic thermo-diffusive model of combustion with simple chemistry is a Reaction Diffusion System (RDS) that is written as:

$$Y_t = \frac{1}{\mathrm{Le}}\Delta Y - YF(\theta), \tag{2.1a}$$

$$\theta_t = \Delta\theta + YF(\theta), \tag{2.1b}$$

where Y denotes the mass fraction of the reactant, θ the temperature, and Le the Lewis number (ratio between conductivity and diffusivity). The function F is an Arrhenius type reaction rate involving a small parameter ε which is the inverse of the activation energy. The Arrhenius law is often modified by the choice of an ignition temperature, below which the reaction rate is taken to be zero. In this framework, (linearly) unstable flame balls are known to exist. For Lewis number close to unity, the growth of the radius has been described using an integro-differential equation which has been derived formally by Joulin [**16**] and rigorously validated by Roquejoffre et al. [**33**].

When one assumes that the flame occurs in a very thin region, it is quite natural to define a Free Boundary Problem (FBP). Its derivation from the RDS formulation has been justified formally in [**22**] under the assumption of high activation energy. Its validity is also confirmed by numerical simulations on the RDS, and its great advantage is that several analytical aspects are simpler to treat. The FBP read as follows:

$$Y_t = \frac{1}{\mathrm{Le}}\Delta Y \qquad \text{for } x \notin R(t), \tag{2.2a}$$

$$\theta_t = \Delta\theta \qquad \text{for } x \notin R(t), \tag{2.2b}$$

with

$$[\theta] = Y = 0, \quad -[\theta_n] = \frac{1}{\mathrm{Le}}[Y_n] = F(\theta), \quad \text{for } x \in R(t), \tag{2.2c}$$

where $R(t)$ represent the location of the free boundary (the flame front), and brackets denote jumps across the free boundary (in the direction of the normal n). The mass flux into the flame is balanced by (reaction) heat flux coming out of the flame, with a (predominantly) temperature dependent reaction rate. Note that at the flame front we impose the condition that $Y = 0$. Usually, one imposes only that the jump $[Y] = 0$, silently assuming that $Y \equiv 0$ on the burnt side of the flame front. Without such an assumption, the FBP formulation with $[Y] = 0$ instead of $Y = 0$ is underdetermined. As a free boundary problem

this model should not be confused with the well-studied NEF model for nearly equidiffusional flames, which was derived by Sivashinsky by means of an asymptotic analysis, in which he coupled the deviation of the Lewis number from unity to ε, the inverse of the activation energy, see [**12, 50**], and derived what is now known as the Kuramoto-Sivashinsky equation.

The remaining step is to incorporate a model for the radiative effects. The first models developed by Joulin et al. [**16, 17**] and Dold et al. [**22**] for example, are based on rather ad hoc heat loss assumptions (whereas in the present paper we will consider a more thorough radiative transfer model). We would like to recall at this point some results obtained in this context. In [**16**], heat losses are assumed to occur in the volume enclosed by the flame sheet only. In this framework two stationary solution branches exist, corresponding to small and large radius. Concerning the ensuing stability issues, the authors showed that, provided the Lewis number is less than unity, all small flames are unstable to one-dimensional (radial) perturbations. Large flames are unstable to three-dimensional perturbations, but only if they have a radius greater than some critical value. Thus there is a band of large flames, lying between the quenching point and unstable flames, that are stable. In [**17**], the authors extend this result by including the effects of heat loss in the far field (unburned gas), and they conclude that far fields losses do not qualitatively change the (stability) properties of the solutions. Finally, in [**22**], flame balls are studied in a porous medium that serves to exchange heat with the gas, and two heat loss models are considered. One of these treats the heat loss as being constant in the burnt region and linear in the unburned region. The other does not distinguish between burnt and unburnt gas and is based on a (nonlinear) Stefan's law. For both heat loss models, the authors find, again, two branches of solutions of small and large flame balls, respectively. For Lewis number greater than unity the solutions are unstable, while at Lewis number less than unity part of the branch of large flame balls becomes stable, solutions with the nonlinear radiative law being stable over a smaller range of parameters. The stable parameter region increases when the heat capacity of the porous medium is increased. It is clear from the considerations in [**16, 17, 22**] that the stability properties depend strongly on the Lewis number. More details and a comparison with our model can be found in Section 2.4.

In this paper, we would like to go one step further in the description of the radiative effects and introduce a physically more realistic radiative transfer model. Let us start with a microscopic description of the radiative transfer, which is given by the equation

$$\frac{1}{c}\partial_t I + \Omega \cdot \nabla I = \sigma(B(\nu,\theta) - I),$$

where $I = I(x, t, \Omega, \nu)$ is a total radiative intensity, x the position, t the time, Ω the direction of emission vector, ν the frequency, σ the opacity of the medium and $B(\nu, \theta)$ the Planck distribution: $B(\nu, \theta) = \frac{2h\nu^3}{c^2}(\exp(\frac{h\nu}{k\theta}) - 1)^{-1}$. Since numerical simulations of this model are very cumbersome, radiation is most commonly described by simplified models, such as the (Milne-)Eddington diffusion equations, valid in the limit of isotropic radiation, the Rosseland model, valid for high opacity media, or the optically thin model, valid for nonabsorbent media ([**40, 43**]).

In this paper we adopt the Eddington diffusion model ([**24, 40, 41, 42, 43, 49**]), namely,

$$-\nabla(\nabla \cdot q) + 3\alpha^2 q = -\alpha \nabla \theta^4, \tag{2.3}$$

where q is the radiative flux. Thus, the radiative effects are a direct consequence of temperature variations. Following Joulin and Buckmaster [**14, 31, 32**], these radiative effects couple back to the temperature equation, in which the divergence of the radiative flux appears with coupling constant β, the Boltzmann constant. Thus β is a measure of the ratio between the radiative and the diffusive flux. For flame fronts, this extended model was proposed and studied in [**14, 31, 32**], and in [**6, 10**].

In this paper we study equilibria of the resulting FBP in the radially symmetric case, i.e. steady spherically symmetric flame balls. If we set $r = |x|$, we may thus write the Laplacian operator as $\Delta = \partial_{rr} + \frac{2}{r}\partial_r$, so that the problem can be viewed as a system of ordinary differential equations. Hence, throughout the paper all functions depend on the radial coordinate r only, and they all have zero derivative at $r = 0$. To make the mathematical analysis easier, we do not use the vector equation (2.3) but work with the scalar equation

$$-\Delta u + 3\alpha^2 u - \alpha \Delta \theta^4 = 0,$$

where $-u = \nabla \cdot q$, the divergence of the radiation flux as it appears in the modified temperature equation. This equation is nonlinear and therefore does not allow us to compute explicit solutions for the full problem defined below. On the other hand, if one would consider θ instead of θ^4, i.e. the "linear" problem, one can write down explicitly the solution, and in Section 2.4 we compare the solutions of the linear and nonlinear equations. The free boundary problem reads

$$\frac{1}{\mathrm{Le}}\Delta Y = 0 \qquad \text{for } r \neq R, \tag{2.4a}$$

$$-\Delta\theta - \beta u = 0 \qquad \text{for } r \neq R, \tag{2.4b}$$

$$-\Delta u + 3\alpha^2 u - \alpha \Delta \theta^4 = 0. \tag{2.4c}$$

Equation (2.4c) is satisfied in the whole space in the sense of the distributions (and classically for $r \neq R$). The jump conditions at $r = R$

are

$$[\theta] = Y = 0, \quad -[\theta_r] = \frac{1}{\mathrm{Le}}[Y_r] = F(\theta(R)), \tag{2.4d}$$

with u being continuous, while the size of the jump in u_r follows automatically from (2.4c) and (2.4d). The asymptotic boundary conditions are

$$Y \to Y_f, \quad \theta \to \theta_f, \quad u \to 0 \quad \text{as } r \to \infty. \tag{2.4e}$$

The parameters θ_f and Y_f denote the temperature and the mass fraction far away in the fresh region. We recall that R is the free boundary variable corresponding to the flame front and that $F(\theta(R))$ is the reaction rate evaluated at $r = R$. Note that we will not specify the reaction rate and work only with general reaction rates F. The reason is that, to prove existence properties, we only need to know that F is a positive function of the temperature at the flame front. The main result of this paper is the following:

Theorem 2.1 (Existence). *Let $\alpha \geq 0$, $\beta \geq 0$, let F be continuous and positive and let $\theta_f > 0$, $Y_f > 0$. Then there exists a radial solution $(\theta(r), Y(r), u(r), R)$ to (2.4). Moreover, for generic choices of the parameters the number of solutions is odd.*

Let us briefly outline the method of the proof. We first observe that the FBP formulation, with the Arrhenius law only acting on the flame front, allows to decouple equation (2.4a) for Y from the two others, (2.4b) and (2.4c). The only bounded function Y which solves (2.4a) and satisfies $Y = 0$ at $r = R$ and $Y \to Y_f$ as $r \to \infty$, is given by

$$Y(r) = \begin{cases} 0 & \text{for } r \leq R, \\ Y_f\left(1 - \frac{R}{r}\right) & \text{for } r > R. \end{cases} \tag{2.5}$$

Here R is still unknown. We now drop one of the free boundary condition, namely the last equality in (2.4d), and solve the problem with R as a parameter. In other words, we drop the reaction rate and fix R. The next theorem provides us with a unique solution of the resulting reduced problem, parameterized by the now prescribed flame ball radius R.

Theorem 2.2 (Uniqueness and existence for $\boldsymbol{R}$ fixed). *Fix $R > 0$ and let $\alpha \geq 0$, $\beta \geq 0$, $\theta_f > 0$, $Y_f > 0$. Then there exists a unique solution $(\theta_R(r), Y_R(r), u_R(r))$ to (2.4), with $\theta > 0$.*

To prove this theorem, we will first decompose the temperature as $\theta = \theta_h + w$ where θ_h is an adiabatic profile with an arbitrary fixed radius R. Because we seek radial solutions, we can explicitly compute θ_h, namely

$$\theta_h = \theta_f + \frac{Y_f}{\mathrm{Le}} \min\left(1, \frac{R}{r}\right). \tag{2.6}$$

Then, we show that w satisfies a nonlinear elliptic equation defined on all $\mathbb{R}$. Thus θ_h is the temperature component of the solution of the

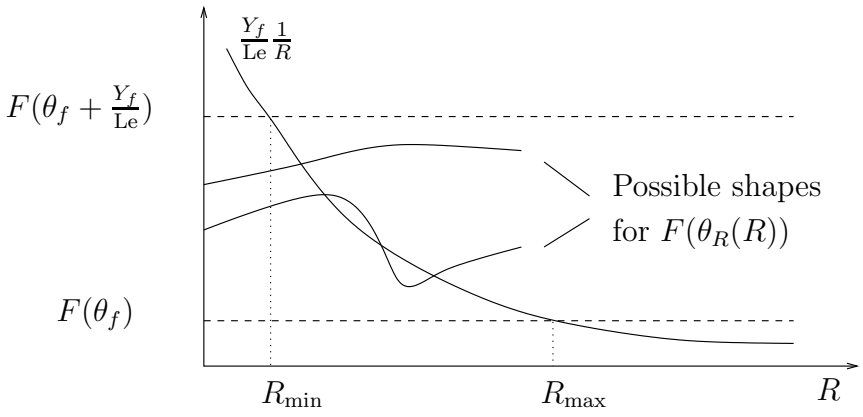

Figure 2.3: Sketch of the graphs occurring in Equation (2.7). The dashed lines are the bounds on $F(\theta_R(R))$; they are depicted here for the case of increasing F.

reduced problem with given R, in the case that $\beta = 0$. The subscript h stands for "homogeneous", because θ_h is the solution of the homogeneous part of (2.4b) which satisfies the jump condition. The other part w in the splitting will then be the solution of the full inhomogeneous equation (2.4b) which is smooth (i.e. $[w] = [w_r] = 0$) across $r = R$. Hence w satisfies the equation $-\Delta w = u$ globally, just as u solves (2.4c) globally, in the sense of the distributions. To solve this equation, we consider the problem on a bounded domain, more precisely on a ball $B_\rho = B(0, \rho) \subset \mathbb{R}^3$, with $\rho > R$ large. Using sub- and supersolution arguments, one obtains a solution on the bounded domain. Then we let $\rho \to \infty$, and, by a diagonal process, this leads to a solution on $\mathbb{R}^3$. Uniqueness is proved using classical arguments (see Section 2.2 for details).

Remark 2.1.3. We only consider positive θ, the solution $\theta_R(r)$ depends continuously on R, and θ_R is bounded between θ_f and $\theta_f + \frac{Y_f}{\mathrm{Le}}$.

Going back to the proof of Theorem 2.1, we need to find a value of R for which $\theta_R(r)$ satisfies the final free boundary condition in (2.4d). As we know Y explicitly, we are left with one "algebraic" equation

$$\frac{Y_f}{\mathrm{Le}}\frac{1}{R} = F(\theta_R(R)). \tag{2.7}$$

Thus only at this final stage the reaction rate F plays a role in the analysis. From Figure 2.3 we can easily see that Equation (2.7) has at least one solution (see Section 2.2 for more details). This ends the proof of Theorem 2.1.

Remark 2.1.4. When solving Equation (2.7), one can easily see from Remark 2.1.3 and Figure 2.3 that the radiative radius R_{rad} is bounded between two values. If the reaction rate F is an increasing function of the temperature, as it is usually the case, the lower bound on the

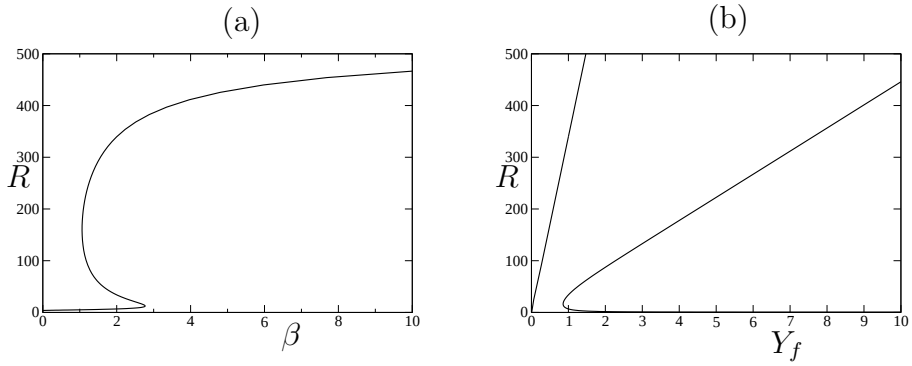

Figure 2.4: Bifurcation curves exhibiting turning points: (a) with β used as bifurcation parameter; (b) with Y_f as the parameter.

flame radius is given by the adiabatic or Zeldovich radius $R_{\text{Zeld}} = \frac{Y_f}{\text{Le}} \frac{1}{F(\theta_f + Y_f/\text{Le})}$ (i.e. the radius in absence of radiative effects, see Section 2.2 for more details), whereas the upper bound is $\frac{Y_f}{\text{Le}} \frac{1}{F(\theta_f)}$.

In Section 2.3 we examine limit cases of Problem (2.4). The cases $\alpha \to \infty$ with β fixed, and $\alpha \to 0$ (or transparent limit) lead to the adiabatic case and are the easiest to justify. A more subtle analysis is needed to treat the cases $\beta \to \infty$ (large Boltzmann limit) and $\alpha \to 0$ supposing $\alpha\beta = \chi$ fixed (transparent limit combined with large Boltzmann numbers). In the large Boltzmann limit, we prove that the temperature profile converge to a constant profile, namely to the fresh temperature θ_f. On the other hand, in the transparent limit combined with large Boltzmann numbers, the temperature profile does not converge to a constant profile, but to a radiative one (cf. Figure 2.2).

Finally, in Section 2.4 we compare the analytic expressions in the asymptotic limits to numerical computations for the full problem. We also make a comparison with analytic calculations for a "linearized" system, see Section 2.4 for details. As an example, in Figure 2.4a we depict a typical bifurcation diagram, where β is used as the bifurcation parameter. For a range of parameter values there are three distinct flame ball solutions (for the adiabatic (non-radiative) problem there is always only one solution). Examining the corresponding solution profiles, the upper branch turns out to be physically irrelevant, since the temperature profile is almost identically equal to θ_f. In Figure 2.4b the fuel mass fraction Y_f in the fresh region is used as a bifurcation parameter. Again, multiple solutions are obtained, on two disconnected branches.

2.2. Existence of solutions

In this section we sketch the arguments that lead to Theorem 2.2 and subsequently to Theorem 2.1. All remaining details of the proofs are provided in Appendix 2.6. We recall that in order to fix R, we consider Problem (2.4) and we drop the equation involving the reaction rate F in (2.4d). The expression for Y is of course given by (2.5). Theorem 2.1 follows immediately from Theorem 2.2 when we combine it with the fact that the algebraic equation (2.7) has a solution.

To begin with, we reduce equations (2.4b) and (2.4c) to one elliptic equation. To do so, we first need to introduce a splitting of the solution θ we are looking for, writing

$$\theta = \theta_h^R + w. \tag{2.8}$$

Here θ_h^R is the solution of

$$-\Delta\theta_h^R = 0 \qquad \text{for } r \neq R, \tag{2.9a}$$

with jumps conditions

$$[\theta_h^R] = 0, \quad -[\frac{\partial\theta_h^R}{\partial r}] = \frac{1}{\mathrm{Le}}[\frac{\partial Y}{\partial r}], \quad \text{at } r = R, \tag{2.9b}$$

and the asymptotic boundary condition

$$\theta_h^R \to \theta_f \quad \text{as } r \to \infty. \tag{2.9c}$$

We note that (2.9) can be solved explicitly, where θ_h^R is given by (2.6). The advantage of the splitting (2.8) is that w must have zero jumps:

$$[w] = [w_r] = 0,$$

and $w \to 0$ as $r \to \infty$. Hence it must be a solution of

$$-\Delta w = \beta u \tag{2.10}$$

on the *whole space* in the sense of the distributions.

Next we observe that (2.4c) implies that

$$u = \alpha(3\alpha^2 - \Delta)^{-1}\Delta\theta^4,$$

which expresses u in terms of θ^4 by means of the bounded operator

$$\alpha(3\alpha^2 - \Delta)^{-1}\Delta = \alpha\Delta(3\alpha^2 - \Delta)^{-1},$$

which operates from $L^\infty \to L^\infty$. Note that the Laplacian and its resolvent commute because $3\alpha^2 > 0$. Combining with (2.10), it follows that

$$\Delta\left(w + \alpha\beta(3\alpha^2 - \Delta)^{-1}\theta^4\right) = 0,$$

whence, since both w and θ^4 are bounded, $w + \alpha\beta(3\alpha^2 - \Delta)^{-1}\theta^4$ must be a constant:

$$w + \alpha\beta(3\alpha^2 - \Delta)^{-1}\theta^4 = C.$$

Subtracting θ_f^4 from θ^4 only changes the constant. Moreover, $\theta^4 - \theta_f^4$ has zero limit at infinity ($r \to \infty$), a property which is preserved by the

resolvent $(3\alpha^2 - \Delta)^{-1}$, and also $w \to 0$ as $r \to \infty$. Thus $w + \alpha\beta(3\alpha^2 - \Delta)^{-1}(\theta^4 - \theta_f^4) = 0$. Applying $(3\alpha^2 - \Delta)^{-1}$ to both sides, we arrive at

$$(3\alpha^2 - \Delta)w + \alpha\beta\left((w + \theta_h^R)^4 - \theta_f^4\right) = 0, \tag{2.11a}$$

which again should hold globally, with asymptotic boundary condition

$$w \to 0 \quad \text{as } r \to \infty. \tag{2.11b}$$

We note that $w(r)$ is a solution of a second order ordinary differential equation (globally). Thus it has zero jumps $[w]$ and $[w_r]$ at $r = R$. We have split the problem for θ, which was inhomogeneous because of the jump in $r = R$ and the nonzero limit as $r \to \infty$ on the one hand, and the presence of βu in (2.4b) on the other, into two parts. The first part, θ_h^R, takes care of the jumps and limits, while the second, w, corresponds to the inhomogeneous term βu in (2.4b).

The crucial idea in the existence proof is the above redution of the system of two equations (2.4b) and (2.4c) to one elliptic equation (2.11a). Therefore, existence of a solution pair (θ, u) for (2.4b) and (2.4c) is equivalent to the existence of a solution w for Problem (2.11). In order to solve this problem, we first consider (2.11a) on a ball $B_\rho \subset \mathbb{R}^3$, with the boundary condition (2.11b) being replaced by $w = 0$ on ∂B_ρ. Then, using classical momotone iteration methods, we can prove existence on this finite domain. Finally, we take the limit $\rho \to \infty$ and arrive at

Lemma 2.5. *For R fixed, there exists a unique solution w_R of Problem* (2.11) *satisfying the bound*

$$-\frac{Y_f}{\mathrm{Le}} \min\left(1, \frac{R}{|x|}\right) \le w \le 0. \tag{2.12}$$

The solution w_R is $C^2(\mathbb{R})$, radially symmetric, monotonically increasing in $|x|$, and depends continuously on R.

Thus, this proves Theorem 2.2 and shows that, omitting the reaction rate from the problem formulation, there exists for every $R > 0$ a unique solution triple (θ, Y, u) with $\theta > 0$. It remains, in order to prove Theorem 2.1, to solve (2.7) with $\theta_R(R)$ given by Theorem 2.2. Lemma 2.5 shows that $\theta_R(R)$ depends continuously on R. Moreover, in view of estimate (2.12), $\theta_f \le \theta_R(R) \le \theta_f + \frac{Y_f}{\mathrm{Le}}$. Hence, Theorem 2.1 is an easy consequence of the intermediate value theorem applied to Equation (2.7). All details of the proof, as well as additional estimates, can be found in the appendix.

2.3. Limit cases of the radiative parameters

In this section we examine some singular limit cases. We recall that we introduced the splitting $\theta = \theta_h^R + w$. Throughout this section, we

consider a couple $(\theta_{\text{par}}, R_{\text{par}})$ depending on some parameters, and we seek a limit. Let us start by the following:

Remark 2.3.6. As R_{par} lies in a compact set, see Remark 2.6.19, one can extract a subsequence converging to a limit, called R. Along the subsequence, $\theta_h^{R_{\text{par}}}$ converges to θ_h^R (uniformly).

The limit case $\alpha \to \infty$ with β fixed

The limit $\alpha \to \infty$, β fixed is usually called the optically thick limit for an opaque medium. In this limit the effect of the radiation is lost. Indeed, we have

Lemma 2.7. *The solution w of Problem* (2.11) *converges to zero uniformly as $\alpha/\beta \to \infty$.*

As a consequence of this lemma, and in view of (2.19), the flame ball solution has a temperature profile that converges to the Zeldovich solution, and also the flame ball radius converges to the Zeldovich radius as $\alpha/\beta \to \infty$.

Proof. We simply modify the subsolution in the proof of Lemma 2.14 in such a way that it pushes the solution obtained in Lemma 2.5 and thereby w itself, to zero. A negative constant w is a subsolution provided

$$3\alpha^2 w + \beta\alpha\left((\theta_h^R + w)^4 - \theta_f^4\right) \leq 0.$$

this is certainly the case if

$$\left(\theta_f + \frac{Y_f}{\text{Le}} + w\right)^4 - \theta_f^4 = -\frac{3\alpha}{\beta} w,$$

which has a unique solution $w \in (-\frac{Y_f}{\text{Le}}, 0)$, which is easily seen to converge to zero as $\alpha/\beta \to \infty$. This completes the proof. □

Remark 2.3.8. Note that the limit is the same as the one for α fixed and $\beta \to 0$, i.e. radiative flux negligible with respect to convective flux.

The transparent limit $\alpha \to 0$ with β fixed

Surprisingly, as opposed to the traveling wave case, see [**10**], this limit also reproduces the adiabatic (Zeldovich) flames. As in the previous section we have

Lemma 2.9. *The solution w of Problem* (2.11) *converges to zero uniformly if $\alpha \to 0$ with β fixed.*

Proof. We have, in view of (2.12),

$$-\Delta w = -3\alpha^2 w - \alpha\beta\left((\theta_h^R + w)^4 - \theta_f^4\right) \to 0$$

uniformly, as $\alpha \to 0$ and $\alpha\beta \to 0$. Also, again because of (2.12), w is uniformly small for large r. By the maximum principle for the Laplacian this implies that $w \to 0$ uniformly as $\alpha \to 0$ and $\alpha\beta \to 0$. $\square$

Large Boltzmann numbers $\beta \to \infty$ with α fixed

With large Boltzmann numbers the solution loses its physical meaning because the temperature profile becomes flat. We have

Lemma 2.10. *For α fixed and $\beta \to \infty$ the temperature profile θ converges to θ_f uniformly.*

Proof. Let us set $w_n = w_{\beta_n}$, with $\beta_n \to \infty$ as $n \to \infty$. We are looking for a limit of the problem

$$-\Delta w_n = -3\alpha^2 w_n - \alpha\beta((\theta_h^{R_n} + w_n)^4 - \theta_f^4). \tag{2.13}$$

with asymptotic boundary condition $w_n \to 0$ as $|x| \to \infty$.

Writing the weak formulation of (2.13) and dividing by β_n we find that, for any test function $\varphi \in C_c^\infty([0,\infty))$, in view of (2.12),

$$\int \left((\theta_h^{R_n} + w_n)^4 - \theta_f^4\right)\varphi = -\frac{1}{\beta_n}\int 3\alpha^2 w_n\varphi + \frac{1}{\alpha\beta_n}\int w_n\Delta\varphi \to 0,$$

as $n \to \infty$. By the bound (2.12), the functions

$$(\theta_h^{R_n} + w_n)^4 - \theta_f^4 \tag{2.14}$$

are nonnegative. Thus we may conclude that they converge to the zero function in L^1_{loc} strongly. Next, we rewrite (2.14) as

$$G(Z_{R_n} + w_n),$$

where $G(\xi) = (\theta_f + \xi)^4 - \theta_f^4$ and $Z_R(r) = \frac{Y_f}{\text{Le}}\min\left(1, \frac{R}{r}\right)$.

Again in view of (2.12), the variable $\xi = Z_R + w$ ranges between 0 and Z_R. In this range G' is positive and bounded away from zero and infinity. Consequently, the functions $Z_{R_n} + w_n$ also converge strongly to zero in L^1_{loc}. But Z_{R_n} converges if we restrict to a further subsequence, along which R_n converges, not only in L^1_{loc} but also in L^∞.

We claim that for any sequence R_n bounded away from zero and infinity, and for any sequence $\beta_n \to \infty$, the corresponding solutions w_n of (2.11) have the property that $\theta_n = \theta_h^{R_n} + w_n \to \theta_f$, uniformly on $[0,\infty)$. To prove this, we apply the following simple lemma.

Lemma 2.11. *Let f_n and g_n be functions on $\mathbb{R}_+$ such that*

- *$f_n + g_n \geq 0$,*
- *$f_n + g_n \to 0$ in $L^1(0,\rho)$ for all $\rho > 0$,*
- *$f_n' \geq -C$ in a weak sense,*
- *$g_n' \geq 0$,*

then $f_n + g_n \to 0$ in $L^\infty(0,\rho)$ for all $\rho > 0$.

Proof. Immediate from the estimate

$$f_n(r) + g_n(r) \geq f_n(r_0) + g_n(r_0) - C(r - r_0),$$

if $r > r_0 > 0$. □

This lemma applies to $f_n = Z_{R_n}$ and $g_n = w_n$, which is monotone by Lemma 2.5. As before, we conclude that $\theta_n - \theta_f \to 0$ in $L^\infty(\mathbb{R})$. □

The transparent limit combined with large Boltzmann numbers: $\alpha \to 0$ with $\alpha\beta = \chi$ fixed

Finally, we consider the limit $\alpha \to 0$, $\alpha\beta = \chi > 0$ fixed, which was also treated in the traveling wave context, see [**10, 6**]. We show that in this limit solutions of the radiative transfer problem converge to solutions of a radiative heat loss problem, where θ solves

$$\Delta\theta - \chi(\theta^4 - \theta_f^4) = 0 \qquad r \neq R,$$

and R is the flame radius of the limit solution. This will follow along the same lines in the previous sections from

Lemma 2.12. *In the limit $\alpha \to 0$ with $\alpha\beta = \chi > 0$ fixed, the solution w of* (2.11) *converges along subsequences to a solution of*

$$-\Delta w + \chi((\theta_h^R + w)^4 - \theta_f^4) = 0, \tag{2.15}$$

with $w \to 0$ as $r \to \infty$.

Proof. In view of the *a priori* bounds on w and on R, and in view of Remark 2.6.16 we know that w, w' and w'' are (uniformly) equicontinuous on bounded balls. This suffices again to conclude that, as $\alpha \to 0$, a subsequence converges in $C^2(\overline{B_\rho})$, for any $\rho > 0$, to a solution of (2.15). As before, a diagonal process finishes the proof. □

Remark 2.3.13. In this limit w remains non-trivial in the sense that it does not coincide with one of the bounds in (2.12). Thus, in the limit we will have a bifurcation diagram given by

$$\frac{Y_f}{\mathrm{Le}R} = F\left(\theta_f + \frac{Y_f}{\mathrm{Le}} + w(R)\right),$$

and the right hand side truly depends on R.

2.4. Numerical calculations

In this section we examine the flame balls numerically. We will compare the outcome of the computations with analytic formulas for the "linearized" problem, which we present below.

Analytic solutions for the linear case

In this first part, we derive a bifurcation diagram equation for the linear case. Namely, we still consider Problem (2.4), except that (2.4c) is replaced by the linear equation

$$-\Delta u + 3\alpha^2 u - \alpha\Delta\theta = 0. \tag{2.16}$$

We can compute explicit formulas for the temperature θ and the variable u. To simplify the notation we introduce

$$\mu = \mu_{\alpha\beta} = \sqrt{3\alpha^2 + \alpha\beta}.$$

Then

$$\theta(r) = \begin{cases} \dfrac{B_1}{r}\sinh(\mu r) + B_3 + \theta_f & \text{for } r \le R, \\ \dfrac{B_2}{r}\exp(-\mu r) + \dfrac{B_3 R}{r} + \theta_f & \text{for } r > R, \end{cases}$$

where the constants are given by

$$B_1 = \frac{\alpha\beta Y_f}{\mathrm{Le}\mu^3}\,\exp(-\mu R), \qquad B_2 = \frac{\alpha\beta Y_f}{\mathrm{Le}\mu^3}\sinh(\mu R), \qquad B_3 = \frac{3\alpha^2 Y_f}{\mathrm{Le}\mu^2}.$$

The expression for u is

$$u(r) = \begin{cases} -\dfrac{B_1\mu^2}{\beta r}\sinh(\mu r) & \text{for } r \le R, \\ -\dfrac{B_2\mu^2}{\beta r}\exp(-\mu r) & \text{for } r > R. \end{cases}$$

Finally, the equation that fixes the flame radius R, and that determines the bifurcation diagrams, reads

$$F\left(\frac{\alpha\beta Y_f}{2\mu^3\mathrm{Le}R}\left[1 - 2\mu R - e^{-2\mu R}\right] + \frac{Y_f}{\mathrm{Le}} + \theta_f\right) = \frac{Y_f}{\mathrm{Le}R}. \tag{2.17}$$

Bifurcation diagrams

Let us turn to the numerical investigation of the problem. Since we know from Theorem 2.1 that a solution is uniquely determined by its flame radius R, we exhibit diagrams in which the flame ball is represented by R along the vertical axis, and the horizontal axis is reserved for a control parameter, such as Y_f or one of the radiative parameters α or β.

We can only do numerical simulations on bounded domains, so we choose a large ball B_ρ on which we impose Dirichlet boundary conditions, as used in the existence proof. From the proof of Lemma 2.5 we know that the solution on the bounded ball B_ρ approaches the solution on $\mathbb{R}^3$ as $\rho \to \infty$, and in the numerical calculations we always make sure that $\rho \gg R$. Since the flame balls are radially symmetric, the problem is thus reduced to a boundary value problem for an ODE,

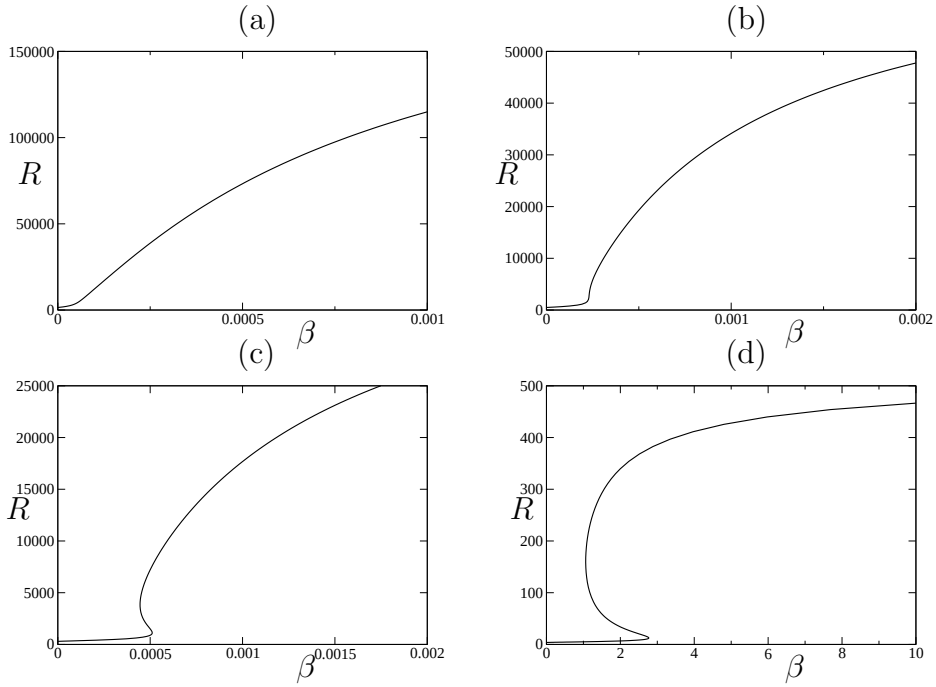

Figure 2.5: Bifurcation diagrams with β as the bifurcation parameter for (a) $A = 0.1$; (b) $A = 0.3$; (c) $A = 0.5$; (d) $A = 40$.

and we use the continuation software [**21**] to compute the bifurcation diagrams.

We need an explicit expression for the reaction rate. Following the literature, e.g. [**55, 18**], we choose a simple Arrhenius law

$$F(\theta(R)) = A \exp\left(-\frac{1}{\varepsilon\theta(R)}\right), \tag{2.18}$$

where ε is a normalized inverse activation energy and $A > 0$ is the pre-exponential factor. Next we must choose values for the parameters. Unless mentioned otherwise, in all computations we take

$$\theta_f = 1, \quad Y_f = 1, \quad \mathrm{Le} = 1, \quad \varepsilon = 0.1, \quad A = 40, \quad \alpha = 10^{-4}, \quad \beta = 2.$$

In fact, the parameters Y_f and Le appear in the stationary problem only in the combination Y_f/Le, so we will use this ratio as a parameter in what follows.

In Figure 2.5 bifurcation diagrams are shown with β as the bifurcation parameter, for various values of the pre-exponential constant A. We see that a turning point appears in the bifurcation diagram as we increase A. Hence, for A sufficiently large there is a range of values of the Boltzmann number β for which there exist multiple stationary flame balls. Increasing A corresponds to making the function in the Arrhenius law (2.18) steeper. In the context of traveling wave solutions (moving flame fronts) it was already observed (and extensively

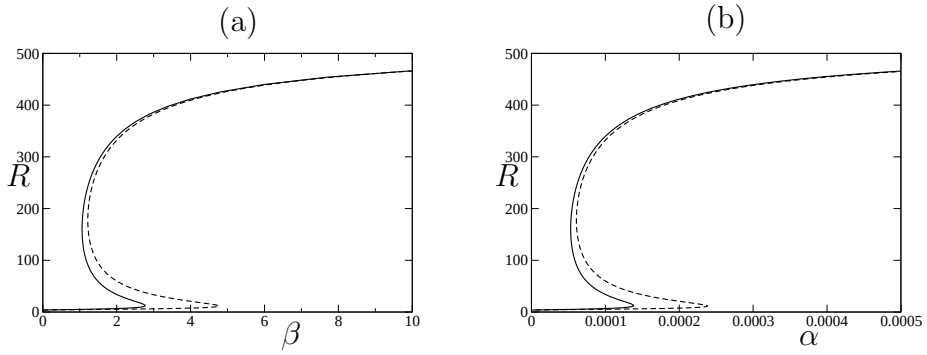

Figure 2.6: Comparison between the nonlinear problem (solid line) and the linearized one (dashed line) with (a) β and (b) α as the bifurcation parameter.

analyzed) that a steeper Arrhenius law may lead to turning points in bifurcation diagrams, see [**6**]. We note that the presence of turning points is due to the radiative effects being incorporated in the model, since uniqueness of the adiabatic flame ball implies the absence of turning points in the adiabatic problem.

Figure 2.5 also corroborates the study of the limit cases in Section 2.3. In the limit $\beta \to 0$ the flame radius R converges to the Zeldovich radius (the minimal possible radius), see Remarks 2.1.4 and 2.3.8. On the other hand, as proved in Lemma 2.10, in the limit $\beta \to \infty$ the temperature profile converges to θ_f, which corresponds to the maximal radius (see again Remark 2.1.4).

To make a useful comparison between the full, nonlinear problem and the "linearized" equation (2.16) from Section 2.4, we need to linearize the term θ^4 around some *characteristic temperature* θ_c: $\theta^4 \approx \theta_c^4 + 4\theta_c^3(\theta - \theta_c)$. Introducing the rescaled variable $\tilde{u} = \beta u$, we then arrive at the system

$$\begin{cases} \Delta\theta + \tilde{u} = 0, \\ \Delta\tilde{u} - 3\alpha^2\tilde{u} + 4\alpha\beta\theta_c^3\Delta\theta = 0. \end{cases}$$

Therefore, solutions of the full problem should be compared to solutions of the linearized problem for $\tilde{\beta} = 4\beta\theta_c^3$. Hence, in all figures, for the (dashed) curves representing the analytic expression (2.17) for the linearized problem, the scaling factor $4\theta_c^3$ is taken into account. As characteristic temperature we simply adopt $\theta_c = \theta_f$ throughout.

In Figure 2.6 we compare the outcome of the numerical computations on the nonlinear problem with the analytic expression for the linearized one, using both α and β as bifurcation parameters. In Figure 2.6a we see that the nonlinear and linear problems are qualitatively very similar. In the limit $\beta \to \infty$ we know from Lemma 2.10 that $\theta \to \theta_f$ uniformly, so our choice of $\theta_c = \theta_f$ leads to quantitative

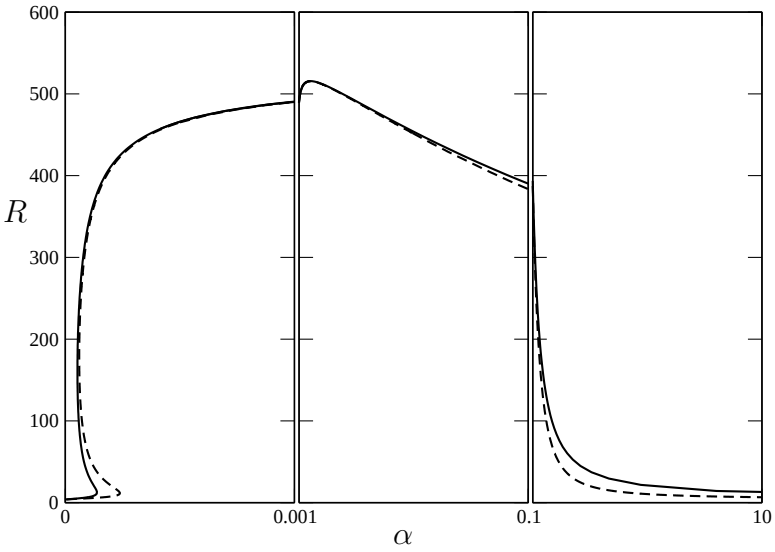

Figure 2.7: The complete (α, R) bifurcation diagram, on three different scales.

agreement for large β. In the adiabatic limit, i.e. $\beta \to 0$, the solution becomes independent of the radiative effect, irrespective of the equations being linear or not.

Figure 2.6b is, up to a scaling in the horizontal direction, the same as Figure 2.6a. The reason is that α is so small that α^2 is negligible compared to $\alpha\beta$, so that to good approximation the solution in this parameter regime only depends on the combination $\alpha\beta$.

From Lemma 2.7 we know that for large α the solution converges to the adiabatic one, and the radius decreases towards the Zeldovich radius. Indeed, when we continue the bifurcation curve of Figure 2.6b for larger values of α we obtain Figure 2.7, where we need three different scales to be able to see the full picture. In accordance with Lemmas 2.7 and 2.9 the flame radius R tends to the $\frac{Y_f}{\mathrm{Le}}\frac{1}{F(\theta_f+Y_f/\mathrm{Le})}$ in both limits $\alpha \to 0$ and $\alpha \to \infty$, while it makes an excursion near $\frac{Y_f}{\mathrm{Le}}\frac{1}{F(\theta_f)}$ in between.

In Figure 2.8 we employ Y_f/Le as the bifurcation parameter. For Y_f/Le sufficiently large there are again three solutions, and we need to examine two different scales to see them. The linearized problem does not mimic the nonlinear one too closely, since for large values of Y_f/Le the temperature varies too much to be adequately represented by the characteristic temperature θ_c.

The linear behavior of the curves in Figure 2.8 can be understood from the fact that α is chosen very small. In this asymptotic regime it

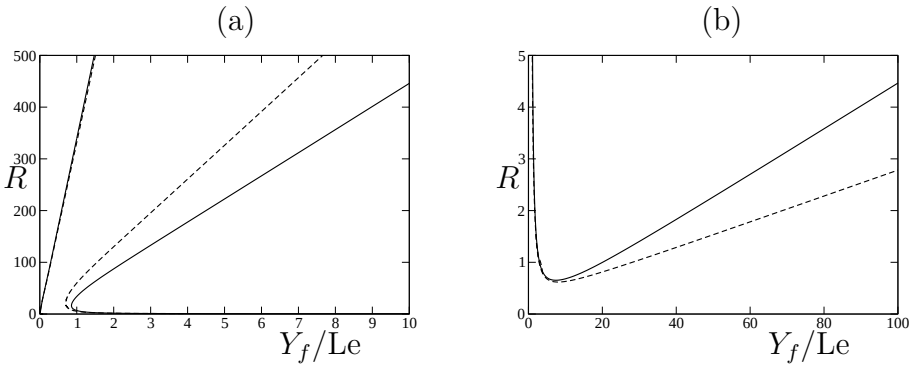

Figure 2.8: Comparison between the nonlinear problem (solid line) and the linearized one (dashed line) with Y_f/Le as bifurcation parameter, depicted at two different scales.

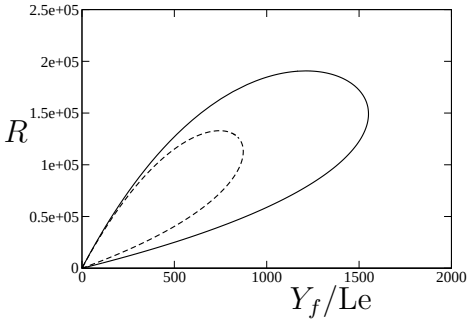

Figure 2.9: The global picture of the $(Y_f/\mathrm{Le}, R)$ bifurcation diagram. Note that there is a branch of solutions (almost) coinciding with the horizontal axis.

is not hard to calculate the slopes for the linearized problem. In fact $R \sim C_i \frac{Y_f}{\mathrm{Le}}$, where the two slopes $C_{1,2}$ in Figure 2.8a are approximately given by the two largest solutions of $F(\frac{1}{2\sqrt{\alpha\beta}}C^{-1} + \theta_f) = C^{-1}$, while the slope C_3 in Figure 2.8b is approximately equal to A^{-1}. Of course, the reason we can determine these slopes is that we have the explicit expression (2.17) for the bifurcation curve in the linearized problem. For the nonlinear problem, determining the slopes is an exercise in asymptotic analysis that falls outside the scope of this paper. Note that near the origin the slope is given by $F(\theta_f)^{-1}$ for both the linearized and the nonlinear problem.

Finally, while Figure 2.8a suggests that there are two disconnected solution branches, the global bifurcation diagram depicted in Figure 2.9 shows that these branches are in fact connected to each other for large values of R and Y_f/Le.

The multiplicity of flame ball solutions, also found in heat loss models [**16, 22, 17**], leads to questions about stability, which we intend to

study in future work. As in the heat loss case, it is in these stability issues that the Lewis number, which plays a somewhat subdued role in the analysis of the stationary problem, will be crucial.

Multiplicity of solutions and stability in the heat loss case are discussed in the introduction. At this point we would like to make some comparisons with our results using the Eddington equation for radiative transfer. One may notice that for some range of parameter values there are three branches of stationary solutions compared to two in the heat loss models, see for example Figure 2.5. Here one needs to keep in mind that for large R (i.e. the extreme part of the upper branch) the temperature profile is almost flat and therefore does not correspond to a physical flame ball. On the other hand, near the turning point, there are truly three stationary flame balls, of which we expect the *middle* one (see also Figure 2.6) to be stable, at least in some range of the parameters. In the bifurcation diagram in Figure 2.8 we may also expect stability of the middle branch. Detailed analysis of stability is the subject of current research. Some preliminary *in*stablity results have been obtained in [**27**].

2.5. Conclusion

Radiation can significantly influence combustion processes. In this paper we investigate a free boundary model for combustion in a gaseous mixture, where we couple the usual diffusion equations to the radiation field. The radiation itself is described by the Eddington equation, which models radiative transfer in a dusty medium under (near) isotropic conditions. This model thus incorporates both emission and absorption of radiation, in contrast to the usual simplified heat loss models, cf. [**31, 22**]. Mathematically, this leads to the addition of an elliptic equation describing the radiation field, which is coupled to the (parabolic) diffusion equations.

In this context we prove the existence of radially symmetric stationary solutions, or *flame balls*, which are physically observed in microgravity environments [**46**]. We find that a solution exists for any combination of the parameters in the model. Since we consider a free boundary model, determining the radius of the flame is part of the problem. Our strategy is to split the analysis in two parts. First we fix the free boundary and solve an elliptic problem on a fixed domain. Subsequently, we solve the remaining algebraic equation to select the correct flame radius.

Having proved the existence of stationary flame balls, we then turn our attention to asymptotic regimes of the radiative parameters, namely the opacity α of the medium and the Boltzmann number β. In both the limits $\alpha \to 0$ and $\alpha \to \infty$ we recover the adiabatic (non-radiative, or "Zeldovich") flames. The same limit is obtained in the

limit $\beta \to 0$, whereas when $\beta \to \infty$ the temperature profile becomes flat. The limit $\alpha \to 0$, $\beta \to \infty$ with fixed $\alpha\beta$, leads to a nontrivial limit problem with a truly radiative asymptotic profile.

Finally, by using numerical computations and by examining analytically a "linearized" problem, we investigate the multiplicity of solutions (for fixed parameter values). We find large parameter regimes where multiple stationary flame balls exist. This of course raises interesting stability questions, which we plan to address in a forthcoming paper (extending the work of Joulin et al. [**16**] on the heat loss case). We expect the Lewis number Le, which is of minor importance for the stationary problem, to play a crucial role in the stability issues for radiative flame balls.

2.6. Appendix: Existence proof

In this appendix we collect the details of the proofs of the statements in Section 2.2, in particular Lemma 2.5. We also provide additional uniform estimates on the function w.

Existence on a bounded domain

Let us consider (2.11) on a ball $B_\rho = B(0,\rho) \subset \mathbb{R}^3$, the boundary condition (2.11b) being replaced by $w = 0$ on ∂B_ρ. We assume $\rho > R$.

Lemma 2.14. *For fixed $0 < R < \rho$, there is a unique solution w of* (2.11a) *with $\theta = \theta_h^R + w \geq 0$ on B_ρ and $w = 0$ on ∂B_ρ. The solution is radial and as such it belongs to $C^2([0,\rho])$ as well as to $C^2(\overline{B_\rho})$. It satisfies the bounds*

$$-\frac{Y_f}{\mathrm{Le}} \min\left(1, \frac{R}{|x|}\right) \leq w \leq 0.$$

Remark 2.6.15. The estimate (2.12) is independent of the parameters α and β. It provides us with a uniform estimate on the decay rate of w towards zero as $r \to \infty$.

Proof. We first establish the existence of w. The function $\overline{w} \equiv 0$ is a supersolution of (2.11a) with zero Dirichlet boundary data, because substituting $w = \overline{w} \equiv 0$ in (2.11a), we end up with $\alpha\beta((\theta_h^R)^4 - \theta_f^4) > 0$. On the other hand, the function $\underline{w} = -\frac{Y_f}{\mathrm{Le}} \min(1, \frac{R}{r})$ is a subsolution: it is negative in $r = \rho$, and substituting $w = \underline{w}$ we obtain $3\alpha^2\underline{w} - \Delta\underline{w}$. The first term is negative, the latter too, but in the sense of the distributions. More precisely, $-\Delta\underline{w}$ is a negative "Dirac" measure supported on $r = R$. It is straightforward to mollify $\underline{w}$ into a family of smooth subsolutions $\underline{w}^\varepsilon$ with $\underline{w}^\varepsilon \to \underline{w}$ uniformly as $\varepsilon \to 0$, and $\underline{w}^\varepsilon \equiv \underline{w}$ outside the interval $(R-\varepsilon, R+\varepsilon)$. By standard arguments, e.g. [**25**], it follows that there is a solution of (2.11a) with $w = 0$ in $r = \rho$ which lies between $\underline{w}$ and $\overline{w}$. This solution is obtained using an

iteration argument starting from either the sub- or the supersolution, both of which are radial. As a consequence, the constructed solution is also radial. The regularity of w, i.e. $w \in C^2(B_\rho)$, follows directly from ODE arguments. In fact the bounded solutions w of (2.11a) with $w = 0$ on ∂B_ρ are in $C^2(\overline{B_\rho})$, see again [**25**].

If w_1 and w_2 are two such solutions, then we set

$$f(x, w) = \alpha\beta \left((w + \theta_h^R(x))^4 - \theta_f^4 \right),$$

and

$$c(x) = \int_0^1 \frac{\partial f}{\partial w}(x, tw_1(x) + (1-t)w_2(x))dt.$$

The function $v = w_1 - w_2$ is a solution of

$$\begin{cases} -\Delta v + (3\alpha^2 + c(x))v = 0 & \text{in } B_\rho, \\ v = 0 & \text{on } \partial B_\rho, \end{cases}$$

where $c \in C(\overline{B}_\rho)$. By the maximum principle, see [**25**], $v \equiv 0$ if c is nonnegative. Thus we have uniqueness in the class of functions w which satisfy $w(x) + \theta_h^R(x) \geq 0$, i.e., the functions w for which the corresponding temperature profile θ is positive, and it is natural to restrict to this class. This completes the proof. □

Remark 2.6.16. Writing (2.11a) as an ODE, i.e.,

$$w'' = -\frac{2}{r}w' + 3\alpha^2 w + \alpha\beta \left(\left(w + \theta_h^R(r) \right)^4 - \theta_f^4 \right),$$

with initial conditions $w(0) = w_0$ and $w'(0) = 0$, this initial value problem is well-posed and behaves nicely in terms of continuous dependence on parameters. In particular, w, w', w'' and w''' are uniformly bounded on bounded intervals (for bounded ranges of α^2 and $\alpha\beta$). Alternatively, to examine regularity, one could proceed from the PDE (2.11a) directly using bootstrap arguments and Hölder estimates for elliptic equations, see e.g. [**25**].

Remark 2.6.17. We emphasize that w is defined for $0 \leq r \leq \rho$ and that ρ as well as R are parameters with $0 < R < \rho$. Thus we write $w = w_\rho^R$.

Solutions on the whole space

In this section we take the limit $\rho \to \infty$ to prove existence of a solution w of Problem (2.11).

Lemma 2.18. *For R fixed, there exists a solution w of Problem* (2.11) *which satisfies the bound* (2.12). *The solution belongs to $C^2(\mathbb{R})$ and is unique in the class of radial and nonradial functions.*

Proof. Take a sequence $\rho_n \to \infty$ as $n \to \infty$, and set $w_n = w^R_{\rho_n}$, so w_n is a solution of

$$\begin{cases} -\Delta w_n + 3\alpha^2 w_n = -\alpha\beta\left((w_n + \theta_h^R)^4 - \theta_f^4\right) & \text{in } B_{\rho_n}, \\ w_n = 0 & \text{on } \partial B_{\rho_n}, \end{cases}$$

as constructed in Section 2.6. We extend w_n to the whole of $\mathbb{R}^3$ by setting $w_n \equiv 0$ for $r \geq \rho_n$. Clearly estimate (2.12) continues to hold for w_n.

Now fix some $\rho = \bar{\rho}$ and consider the solutions w_n with $\rho_n > \bar{\rho}$, and in particular their restrictions to $B_{\bar{\rho}}$. It follows directly from Remark 2.6.16 that w_n and its first and second order derivatives are bounded and equicontinuous. Note that the nonlinear term in (2.11) is Lipschitz continuous if w is. Thus, we may extract a subsequence along which w_n converges in $C^2(\overline{B_{\bar{\rho}}})$. Choosing $\bar{\rho} = 1, 2, 3, \ldots$ a standard diagonal argument now produces a subsequence along which w_n converges in $C^2(\overline{B_{\bar{\rho}}})$ for every $\bar{\rho} > 0$. It follows that the limit w exists on the whole space, and that it satisfies (2.11a) as well as the bound (2.12). Clearly w corresponds to a temperature profile $\theta = \theta_h^R + w > 0$ on $\mathbb{R}^3$.

Now suppose we have two such profiles. Reasoning as in the uniqueness proof in Lemma 2.14 we find that $v = w_1 - w_2$ is bounded and satisfies

$$-\Delta v + (3\alpha^2 + c(x))v = 0 \quad \text{in } \mathbb{R}^3.$$

When $v \to 0$ as $|x| \to \infty$ (uniformly) the maximum principle implies that $v \equiv 0$, provided the coefficient $3\alpha^2 + c(x)$ of v is nonnegative. Thus we have uniqueness in the class of solutions w which have $w(x) \to 0$ as $|x| \to \infty$ uniformly. □

Proof of Theorem 2.1

In the previous section we proved Theorem 2.2 and showed that, omitting the reaction rate from the problem formulation, there exists for every $R > 0$ a unique solution triple (θ, Y, u) with $\theta > 0$. It remains to solve (2.7) with $\theta_R(R)$ given by Theorem 2.2.

Remark 2.6.19. In view of the estimate (2.12) the flame temperature $\theta(R)$ is bounded between θ_f and $\theta_f + \frac{Y_f}{\mathrm{Le}}$. As F is a continuous positive function, let us define the positive numbers

$$m = \min_{\theta \in [\theta_f,\, \theta_f + Y_f/\mathrm{Le}]} F(\theta) \quad \text{and} \quad M = \max_{\theta \in [\theta_f,\, \theta_f + Y_f/\mathrm{Le}]} F(\theta).$$

Then any solution of the full flame ball problem must satisfy

$$\frac{Y_f}{\mathrm{Le}}\,\frac{1}{M} \leq R \leq \frac{Y_f}{\mathrm{Le}}\,\frac{1}{m}. \tag{2.19}$$

Equation (2.7) has a left hand side which goes from $+\infty$ to 0 as R goes from 0 to ∞. Its right hand side is bounded between m and M. Thus the existence of the solution in Theorem 2.1 is immediate once

we know that Remark 2.1.3 (about continuity of $\theta_R(R)$) is true. More precisely:

Lemma 2.20. *If $R_n \to R > 0$, then the corresponding functions θ_{R_n} converge uniformly to θ_R on $[0, \infty)$.*

Proof. Clearly this will follow from the same statement for w_R, where w_R is the solution of (2.11) obtained in Lemma 2.5. In view of the bound (2.12), uniform convergence on bounded subsets implies uniform convergence on $[0, \infty)$. By exactly the same arguments as in the proof of Lemma 2.5 in Section 2.6, it follows that along a subsequence of $n \to \infty$, w_{R_n} (as well as its first and second order derivatives) converges uniformly on any bounded interval to a solution of (2.11) satisfying (2.12). Since this solution is unique, it follows that $w_{R_n} \to w_R$, along this subsequence. In fact, every sequence of $n \to \infty$ has a subsequence for which this is the case. But then there cannot be a sequence of n for which $||w_{R_n} - w_R||_\infty$ is bounded away from zero. This completes the proof of Lemma 2.20 and thereby of Theorem 2.1. □

Remark 2.6.21. Instead of using this sequence argument, one could also invoke an implicit function argument to conclude that $R \to \theta_R(R)$ (or $R \to w_R(R)$) is smooth. Furthermore, assuming the derivatives of left and right hand sides of (2.7) to be different at solutions, it follows immediately that the number of solutions is odd. This is the statement that in general situations the number of solutions is odd.

Uniform estimates

As we have seen, solutions of the flame ball problem are given by $\theta = \theta_h^R + w_R$, where R is such that (2.7) holds, and where w_R is a C^2-function (of course θ_h^R is not). Moreover, w_R satisfies (2.11). In this section we show that w is monotone in r

Lemma 2.22. *The solution $w = w_R$ of (2.11) has $w' \geq 0$.*

Proof. w solves

$$-w'' - \frac{2}{r}w' = g(r, w) = -3\alpha^2 w - \alpha\beta\left((w + \theta_h^R(r))^4 - \theta_f^4\right), \qquad (2.20)$$

where g satisfies

$$\frac{\partial g}{\partial w} < 0 \quad \text{and} \quad \frac{\partial g}{\partial r} \geq 0,$$

the latter being discontinuous in $r = R$ of course, but with limits existing from both sides. Moreover, $w'(0) = 0$ by symmetry.

If w' is negative somewhere, then there must be points r_1 and r_2 such that $w'(r_1) = w'(r_2) = 0$, while $w' < 0$ on (r_1, r_2). This follows from $w'(0) = 0$ and $0 > w(r) \to 0$ as $r \to \infty$.

Clearly then $g(r_1, w_1(r_1)) = -w''(r_1) \geq 0$ and $g(r_2, w_1(r_2)) = -w''(r_2) \leq 0$, contradicting

$$\frac{d}{dr} g(r, w(r)) = \frac{\partial g}{\partial r} + \frac{\partial g}{\partial w}\frac{\partial w}{\partial r} > 0 \quad \text{on } (r_1, r_2).$$

□

Lemma 2.23. *There exists a constant C depending on α^2 and $\alpha\beta$ such that*

$$\int_0^\infty w'(r)^2 dr < C.$$

Proof. Multiplying (2.20) by w and integrating from r_1 to r_2 ($0 < r_1 < r_2 < \infty$) we obtain

$$-\int_{r_1}^{r_2} w'' w dr = \int_{r_1}^{r_2} \frac{2}{r} w' w dr + \int_{r_1}^{r_2} g(r, w) w dr,$$

so that

$$\int_{r_1}^{r_2} |w'|^2 dr + w'(r_1)w(r_1) = w'(r_2)w(r_2) + \int_{r_1}^{r_2} \frac{2}{r} w' w dr + \int_{r_1}^{r_2} g(r, w)\, w dr.$$

Letting $r_1 \to 0$ and using $w' \geq 0$, $w < 0$, it follows that, also using (2.12),

$$\int_0^{r_2} |w'|^2 dr \leq \int_0^{r_2} g(r, w(r))\, w(r) dr \leq C,$$

where C is a constant depending linearly on α^2 and $\alpha\beta$, but not on r_2. This proves the claim. □

Going one step further, we get the following.

Lemma 2.24. *w belongs to $H^2(0, \infty)$.*

Proof. Multiplying (2.20) by $-w''$ and integrating from r_1 to r_2 we find

$$\int_{r_1}^{r_2} |w''|^2 dr + \int_{r_1}^{r_2} \frac{2}{r} w' w'' dr + \int_{r_1}^{r_2} g(r, w)\, w'' dr = 0.$$

Hence, with e.g. $r_1 = 2$,

$$\int_2^{r_2} |w''|^2 dr \leq \left(\int_2^{r_2} |w'|^2 dr\right)^{\frac{1}{2}} \left(\int_2^{r_2} |w''|^2 dr\right)^{\frac{1}{2}} + \left(\int_2^{r_2} |g(r, w(r))|^2 dr\right)^{\frac{1}{2}} \left(\int_2^{r_2} |w''|^2 dr\right)^{\frac{1}{2}}.$$

In view of (2.12), (2.20) and Lemma 2.23 we conclude that

$$\int_2^\infty |w''|^2 dr \leq C,$$

where C depends on α^2 and $\alpha\beta$. The fact that w is C^2 implies that also $\int_0^\infty |w''|^2$ is bounded. Lemma 2.23 and inequality (2.12) finish the proof. □

Remark 2.6.25. If we consider the problem in $\mathbb{R}^3$, one can easily check that w belongs to $W^{2,p}(\mathbb{R}^3)$ if $p > 3$.

CHAPTER 3

Instability in a flame ball problem

3.1. Introduction

In this paper, we deal with a mathematical model, proposed in [**53**], to describe the evolution of flame balls. Before going into mathematical considerations, let us first briefly introduce the physical problem.

It is well known that combustion processes in gravity or in microgravity environments exhibit different features: the most known one is the appearance of flame balls in microgravity, which differently from flame fronts, are stationary states.

The first models in which flame balls are taken into account, have been proposed by Zeldovich (see [**56**]) to describe combustion processes with simple chemistry (such as a one step reaction in which the gaseous reactant is converted into a gaseous product). In such (non radiative) models, the combustion processes are described in terms of two main quantities: the temperature θ and the mass fraction y of the reactant. These two quantities are assumed to be constant inside the flame ball. In particular, y identically vanishes inside the flame ball. The following figure provides us with a sketch of the situation. In such models, flame balls are shown to be unstable, which is in seeming agreement with the absence of experimentally observed flame balls.

In 1984, P.D. Ronney discovered, surprisingly, the existence of physical flame balls, and this fact was later confirmed by experiments in Space Shuttle. Since then, several effects have been taken into account in combustion models to explain stabilization of flame balls, in particular (radiative) heat losses from the combustion products inside the flame ball. Indeed, the radiative transfer of heat in combustion processes, taking place in inert, not fully transparent media (e.g. dust, porous media, etc.), involves both emission and absorption of radiation. Such phenomena may significantly influence the temperature of the flame, its propagation speed (see e.g. [**10**]) and the flammability of the medium itself. And, of course, these facts may be responsible for the stability of flame balls. For more physical details, we refer the reader to [**46**] and the references therein. See also the SOFBALL

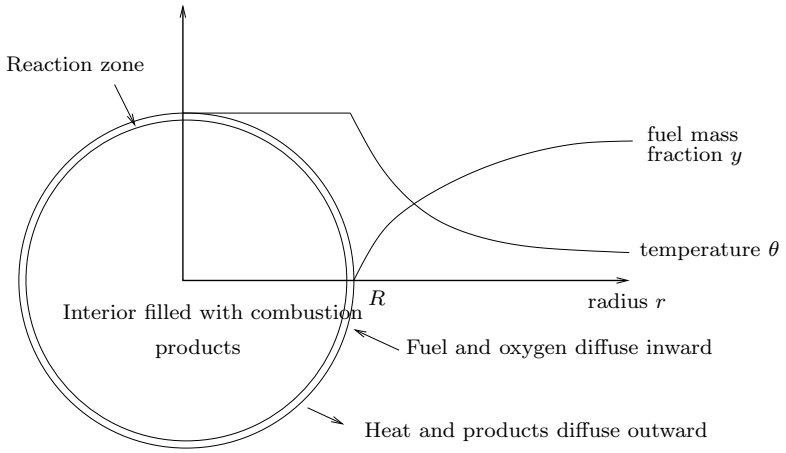

Figure 3.1: Profile of the temperature and the mass fraction variables in the adiabatic case. The radius of the flame ball is denoted by R, corresponding to the flame front.

(Structure of Flame Balls at Low Lewis number) link on Paul Ronney's NASA home page [**1**].

Here, we focus our attention on the model proposed in [**53**], which takes into account the effects of the radiative transfer on the flame balls. To derive their model, the authors consider a derivation of a radiative transfer equation, known as the Eddington equation (see e.g. [**24, 40**]), coupled with the usual Reaction Diffusion System for the temperature and mass fraction of the reactant, under the assumption that the reaction occurs in a very thin region which bounds the burnt region $\Omega(t)$. This leads them to the following free boundary problem:

$$\begin{cases} y_t(t,x) = \dfrac{1}{\mathrm{Le}}\Delta y(t,x), & t>0, \quad x \in \mathbb{R}^3 \setminus \overline{\Omega(t)}, \\ y(t,x) = 0, & t>0, \quad x \in \Omega(t), \\ \theta_t(t,x) = \Delta\theta(t,x) + \beta u(t,x), & t>0, \quad x \notin \partial\Omega(t), \\ \Delta u(t,x) - 3\alpha^2 u(t,x) + \alpha\Delta\theta^4(t,x) = 0, & t>0, \quad x \notin \partial\Omega(t), \end{cases} \tag{3.1}$$

associated with the jump conditions on $\partial\Omega(t)$:

$$[\theta(t,\cdot)] = [y(t,\cdot)] = 0, \qquad -\left[\frac{\partial\theta}{\partial\nu}(t,\cdot)\right] = \frac{1}{\mathrm{Le}}\left[\frac{\partial y}{\partial\nu}(t,\cdot)\right], \tag{3.2}$$

$$\frac{1}{\mathrm{Le}}\left[\frac{\partial y}{\partial\nu}(t,\cdot)\right] = F(\theta(t,\cdot)) \qquad u(t,\cdot) + \alpha\theta(t,\cdot) \quad \text{smooth}, \tag{3.3}$$

for $t>0$.

We note that the later condition amounts to posing the last equation in (3.1) on $\mathbb{R}^3$ in the sense of the distributions. The asymptotic conditions

at infinity, inherited from the initial conditions for Y and θ, are

$$y(t,x) \to Y_f, \quad \theta(t,x) \to \Theta_f, \quad u(t,x) \to 0, \tag{3.4}$$

as $|x| \to \infty$ and $t > 0$.

As above, the variables θ and y correspond, respectively, to the temperature and the fuel mass fraction, whereas u is a measure of the radiation flux. Θ_f and Y_f denote the temperature and the mass fraction away in the fresh region. The parameters Le (Lewis number), α and β denote respectively the ratio between conductivity and diffusivity, the opacity of the medium and the ratio between the radiative and the diffusive flux. The space variable x belongs to $\mathbb{R}^3$, $\partial\Omega(t)$ is the free boundary variable corresponding to the flame front and $F(\theta(t,\cdot))$ is the reaction rate evaluated at $\partial\Omega(t)$, a simplified Arrhenius law, F being a smooth positive and increasing function. Finally, ν denotes the unit outward normal to $\partial\Omega(t)$.

Here, we deal only with the case $\alpha > 0$. If $\alpha = 0$ the equation for u in System (3.1) reduces to $\Delta u = 0$, so that u is zero. Hence, we are then left with the nonradiative problem. However, if we scale u with β and take $\alpha\beta$ fixed, the limit $\alpha \to 0$ does make sense and leads to a heat loss combustion model. See also [**6, 15, 22, 32**].

From a mathematical and also from a physical viewpoint, it is interesting to understand if the steady state radial solutions to Problem (3.1)-(3.4), determined in [**53**] (see the forthcoming Theorem 3.3), are stable or unstable with respect to small perturbations. In this paper we give a partial answer to this question. More precisely, we determine a set of values of the parameters $(\alpha, \beta, \mathrm{Le})$, which imply that such radial steady state solutions are unstable with respect to smooth radial perturbations. Of course, looking for radial solutions simplifies the analysis of the problem. We follow the approach considered in [**6**], where the authors consider travelling wave solutions in a free boundary combustion-radiation problem. Numerical investigations show that the main features of the problem are preserved in the case when the term θ^4 in the last equation of Problem (3.1)-(3.4) is replaced with θ. Therefore, in this paper we do such a reduction. This simplification will imply some nice consequences, the most significant one is that it allows us to write an explicit Evans function, whose knowledge is a fundamental tool to prove stability/instability results.

Since we look for radial solutions, with this simplification, System (3.1)-(3.4) can be reduced to the following 1D problem for the radial

unknowns (y, θ, u) and for the free boundary R:

$$\begin{cases} y_t(t,r) = \dfrac{1}{\mathrm{Le}}\left(y_{rr}(t,r) + \dfrac{2}{r}y_r(t,r)\right), & t>0, \quad r > R(t), \\ y(t,r) = 0, & t>0, \quad r < R(t), \\ \theta_t(t,r) = \theta_{rr}(t,r) + \dfrac{2}{r}\theta_r(t,r) + \beta u(t,r), & t>0, \quad r \neq R(t), \\ u_{rr}(t,r) + \dfrac{2}{r}u_r(t,r) - 3\alpha^2 u(t,r) \\ \qquad +\alpha\left(\theta_{rr}(t,r) + \dfrac{2}{r}\theta_r(t,r)\right) = 0, & t>0, \quad r \neq R(t), \end{cases} \tag{3.5}$$

associated with the jump conditions at $r = R(t)$:

$$\begin{cases} [\theta(t,\cdot)] = [y(t,\cdot)] = 0, \\ [\theta_r(t,\cdot)] = -\dfrac{1}{\mathrm{Le}}[y_r(t,\cdot)] = -F(\theta(R(t))), \\ u(t,\cdot) + \alpha\theta(t,\cdot) \quad \text{smooth}, \end{cases} \tag{3.6}$$

for any $t > 0$, and the asymptotic conditions inherited from the initial data:

$$y(t,r) \to y_f, \quad \theta(t,r) \to \theta_f, \quad u(t,r) \to 0 \quad \text{as } r \to +\infty, \qquad t > 0. \tag{3.7}$$

The paper is structured as follows. In Section 3.2 we introduce the Banach spaces we deal with in this paper, which are spaces of (Hölder) continuous functions. Moreover, we transform our problem into an equivalent one in a fixed domain. We are so led to the study of the problem

$$\begin{cases} D_t\mathbf{u}(t,\cdot) = \mathcal{A}\mathbf{u}(t,\cdot) + \mathcal{F}(\mathbf{u}(t,\cdot), \mathbf{p}(t,\cdot)), & t>0, \\ \mathcal{L}(\mathbf{u}(t,\cdot), \mathbf{p}(t,\cdot)) = \mathbf{0}, & t>0, \\ \mathcal{B}(\mathbf{u}(t,\cdot), \mathbf{p}(t,\cdot)) = \mathcal{G}(\mathbf{u}(t,\cdot), \mathbf{p}(t,\cdot)), & t>0, \\ \mathbf{u}(0,\cdot) = \mathbf{u}_0, \end{cases} \tag{3.8}$$

$\mathcal{A}$ and $\mathcal{L}$ being second-order elliptic operators, $\mathcal{B}$ being a first-order boundary differential operator, $\mathcal{F}$ being a *fully nonlinear* and non-local operator depending not only on $\mathbf{u}$ but also on its space derivatives up to the second-order, and $\mathcal{G}$ being a nonlinear boundary differential operator depending on $\mathbf{u}$, $\mathbf{p}$ and their first-order derivatives. In Section 3.3 we prove that the realization A of $\mathcal{A}$ in a suitable space of bounded and continuous functions generates an analytic semigroup. We show that, for any values of the parameters α and β, the halfline $(-\infty, 0]$ lies in $\sigma(A)$. In particular, when α and β satisfy (3.49), $\sigma(A)$ contains at least one positive eigenvalue. We also provide Schauder type estimates that will be basic tools to prove, in Section 3.4, the existence and some regularity properties of the solution to Problem (3.8). In Section 3.5,

we prove the instability results. Finally, in Appendices A and B, we prove some technical results and the existence of positive eigenvalues of A, under condition (3.49).

Notation: For any $k > 0$ and any interval $I \subset \mathbb{R}$, we denote by $C_b^k(I)$ the set of bounded functions $f : I \to \mathbb{K}$ ($\mathbb{K}$ being either $\mathbb{R}$ or $\mathbb{C}$) which are differentiable up to the $[k]$-th order inside I, with bounded derivatives, and such that $f^{[k]}$ is α-Hölder continuous in I. When I is bounded we simply write $C^k(I)$ instead of $C_b^k(I)$. The previous spaces are normed with the classical Euclidean norms. By $C_c^\infty(I)$, we denote the space of functions f which are infinitely many times differentiable in I and are compactly supported in I.

For any $\gamma, \theta > 0$ and any pair of intervals $I, J \subset \mathbb{R}$, we denote by $C_b^{\gamma,\theta}(I \times J)$ the set of functions $f : I \times J \to \mathbb{R}$ such that $f(t, \cdot) \in C_b^\theta(J)$ for any $t \in I$, $f(\cdot, x) \in C_b^\gamma(I)$ for any $x \in J$ and $\|f\|_{C_b^{\gamma,\theta}(I\times J)} < +\infty$, where

$$\|f\|_{C_b^{\gamma,\theta}(I\times J)} := \sup_{t\in I} \|u(t,\cdot)\|_{C_b^\theta(J)} + \sup_{x\in J} [u(\cdot,x)]_{C_b^\gamma(I)}.$$

Further, given a Banach space X and $r > 0$, we denote by $B(0,r) \subset X$ the open ball with centre at $x = 0$ and radius r, and by $\overline{B}(0,r)$ its closure. If X and Y are two Banach spaces, we denote by $L(X,Y)$ the set of all linear bounded operators from X in Y. We simply write $L(X)$ when $X = Y$. If M is a linear operator (not necessarily bounded), we denote by $\sigma(M)$ its spectrum and, when M is bounded, we denote by r its spectral radius, i.e. $r = \sup\{|\lambda| : \lambda \in \sigma(M)\}$. Given three Banach spaces $Y \subset Z \subset X$ (where the embeddings are continuous), we say that Z belongs to the class J_θ ($\theta \in [0,1]$) between X and Y (shortly, $Z \in J_\theta(X,Y)$) if there exists a positive constant C, such that $\|x\|_Z \le C\|x\|_X^{1-\theta}\|x\|_Y^\theta$ for any $x \in Y$.

Finally, we set $I_1^- = [0,1]$ and $I_1^+ = [1,+\infty)$ and denote by $\sqrt{\lambda}$ the principal root of $\lambda \in \mathbb{C} \setminus (-\infty, 0]$.

3.2. Function spaces and linearisation

We split this section into several subsections.

Function spaces

Definition 3.1. *For any $k \in [0,3)$ and any fixed $R > 0$, we denote by $\mathcal{X}_k$ the space defined by*

$$\mathcal{X}_k = \Big\{\mathbf{f} = (f_1, f_2, f_3) : f_1, f_3 \in C_b^k([R,+\infty)),\ f_2 \in C^k([0,R]),$$
$$\lim_{x\to+\infty} (|f_1(x)| + |f_3(x)|) = 0\Big\},$$

endowed with the Euclidean norm, i.e.

$$\|\mathbf{f}\|_{\mathcal{X}_k} = \|f_1\|_{C_b^k([R,+\infty))} + \|f_2\|_{C^k([0,R])} + \|f_3\|_{C_b^k([R,+\infty))}.$$

When $k = 0$, we simply write $\mathcal{X}$ instead of $\mathcal{X}_0$. Similarly, for any $k \geq 1$, we denote by $\mathcal{X}_k^0$ the subset of $\mathcal{X}_k$ of functions $\mathbf{f}$ such that $D_x f_2(0) = 0$. We endow $\mathcal{X}_k^0$ with the norm of $\mathcal{X}_k$.
Moreover, for any $\theta \in (0,1)$ and any $T > 0$, we denote by $\mathcal{X}_{\theta/2,\theta}(0,T)$ the set of functions $\mathbf{u} = (v, w_1, w_2)$ such that $\mathbf{u}(t,\cdot) \in \mathcal{X}_\theta$ for any $t \in [0,T]$,

$$\sup_{0\leq t\leq T} \|\mathbf{u}(t,\cdot)\|_{\mathcal{X}_\theta} < +\infty,$$

$v(\cdot,x), w_1(\cdot,y), w_2(\cdot,x) \in C^{\theta/2}([0,T])$ for any $x \in I_R^+$ and any $y \in I_R^-$, and

$$\begin{aligned}[[\mathbf{u}]]_\theta := & \sup_{x\in I_R^+} \|v(\cdot,x)\|_{C^{\theta/2}([0,T])} + \sup_{x\in I_R^-} \|w_1(\cdot,x)\|_{C^{\theta/2}([0,T])} \\ & + \sup_{x\in I_R^+} \|w_2(\cdot,x)\|_{C^{\theta/2}([0,T])} < +\infty.\end{aligned}$$

Similarly, we set

$$\mathcal{X}_{1+\theta/2,2+\theta}(0,T) = \left\{\mathbf{u} : D_t^{\alpha_1} D_x^{\alpha_2}\mathbf{u} \in \mathcal{X}_{\theta/2,\theta}(0,T), \text{ for } 2\alpha_1 + \alpha_2 \leq 2\right\}.$$

The spaces $\mathcal{X}_{\theta/2,\theta}(0,T)$ and $\mathcal{X}_{1+\theta/2,2+\theta}(0,T)$ are Banach spaces when endowed with the norms

$$\|\mathbf{u}\|_{\mathcal{X}_{\theta/2,\theta}(0,T)} = \sup_{0\leq t\leq T} \|\mathbf{u}(t,\cdot)\|_{\mathcal{X}_\theta} + [[\mathbf{u}]]_\theta,$$

for $\mathbf{u} \in \mathcal{X}_{\theta/2,\theta}(0,T)$, and

$$\|\mathbf{u}\|_{\mathcal{X}_{1+\theta/2,2+\theta}(0,T)} = \sum_{2\alpha_1+\alpha_2\leq 2} \|D_t^{\alpha_1} D_x^{\alpha_2}\mathbf{u}\|_{\mathcal{X}_{\theta/2,\theta}(0,T)},$$

for $\mathbf{u} \in \mathcal{X}_{1+\theta/2,2+\theta}(0,T)$.

Definition 3.2. *For any $k \in [0,3)$ and any fixed $R > 0$, we denote by $\mathcal{Y}_k$ the set of functions $\mathbf{f} = (f_1, f_2)$ such that $f_1 \in C^k([0,R])$, $f_2 \in C_b^k([R,+\infty))$ and $\lim_{x\to+\infty} f_2(x) = 0$. We endow this space with the Euclidean norm, i.e. $\|\mathbf{f}\|_{\mathcal{Y}_k} = \|f_1\|_{C^k([0,R])} + \|f_2\|_{C_b^k([R,+\infty))}$ for any $\mathbf{f} \in \mathcal{Y}_k$.*

For any $\gamma, \theta \in [0,1)$ and any $T > 0$, we set

$$\begin{aligned}\mathcal{Y}_{\gamma,\theta}(0,T) = \Big\{\mathbf{f} \in \mathcal{Y}_0 : f_1 \in C^{\gamma,\theta}([0,T]\times[0,R]), \\ f_2 \in C_b^{\gamma,\theta}([0,T]\times[R,+\infty))\Big\},\end{aligned}$$

and we norm it by setting

$$\begin{aligned}\|\mathbf{f}\|_{\mathcal{Y}_{\gamma,\theta}(0,T)} := & \|f_1\|_{C^{\gamma,\theta}([0,T]\times[0,R])} + \sup_{t\in[0,T]} [f_2(t,\cdot)]_{C_b^\theta([R,+\infty))} \\ & + \sup_{x\in[R,+\infty)} [f_2(\cdot,x)]_{C^\gamma([0,T])},\end{aligned}$$

for any $\mathbf{f} \in \mathcal{Y}_{\gamma,\theta}(0,T)$. *Similarly, for any* $\theta \in (0,1)$, *we denote by* $\mathcal{Y}_{\theta/2,2+\theta}(0,T)$, *the space of functions* $\mathbf{f}$ *such that* $D_x^j \mathbf{f} := (D_x^j f_1, D_x^j f_2) \in \mathcal{Y}_{\theta/2,\theta}(0,T)$ *for any* $j = 0,1,2$. *We endow* $\mathcal{Y}_{\theta/2,2+\theta}(0,T)$ *with the norm*

$$\|\mathbf{f}\|_{\mathcal{Y}_{\theta/2,2+\theta}(0,T)} = \sum_{j=0}^{2} \|D_x^j \mathbf{f}\|_{\mathcal{Y}_{\theta/2,\theta}(0,T)}, \qquad \mathbf{f} \in \mathcal{Y}_{\theta/2,2+\theta}(0,T).$$

Existence of stationary solutions

Here, we recall the main result obtained in [**53**].

Theorem 3.3 (Existence of steady state solutions). *Let* $\alpha, \beta \geq 0$, *let* F *be continuous, positive and increasing, and let* $\Theta_f > 0$, $Y_f > 0$. *Then there exists a radial solution* $(Y(r), \Theta(r), U(r), R)$ *to* (3.5), (3.6) *and* (3.7). *Such a solution for the* Y *equation is given by*

$$Y(r) = Y_f \left(1 - \frac{R}{r}\right), \qquad r > R.$$

To simplify the notation we introduce

$$\mu = \mu_{\alpha\beta} = \sqrt{3\alpha^2 + \alpha\beta}.$$

Then

$$\Theta(r) = \begin{cases} \dfrac{B_1}{r}\sinh(\mu r) + B_3 + \Theta_f & \text{for } r \leq R, \\ \dfrac{B_2}{r}\exp(-\mu r) + \dfrac{B_3 R}{r} + \Theta_f & \text{for } r > R, \end{cases}$$

where the constants are given by

$$B_1 = \frac{\alpha\beta Y_f}{\mathrm{Le}\mu^3}\exp(-\mu R), \qquad B_2 = \frac{\alpha\beta Y_f}{\mathrm{Le}\mu^3}\sinh(\mu R), \qquad B_3 = \frac{3\alpha^2 Y_f}{\mathrm{Le}\mu^2}.$$

The expression for u *is*

$$u(r) = \begin{cases} -\dfrac{B_1\mu^2}{\beta r}\sinh(\mu r) & \text{for } r \leq R, \\ -\dfrac{B_2\mu^2}{\beta r}\exp(-\mu r) & \text{for } r > R. \end{cases}$$

where R *is determined through the equation*

$$F\left(\frac{\alpha\beta Y_f}{2\mu^3 \mathrm{Le} R}\left[1 - 2\mu R - e^{-2\mu R}\right] + \frac{Y_f}{\mathrm{Le}} + \Theta_f\right) = \frac{Y_f}{\mathrm{Le} R}. \tag{3.9}$$

Moreover, for generic choices of the parameters, the number of steady state solutions to Problem (3.5), (3.6) *and* (3.7) *is odd.*

Linearisation of the parabolic equations

Let us now fix a stationary solution (Θ, Y, U, R) of system (3.5)-(3.7). To linearize the system around this equilibrium, we follow the method developed in [**13, 11, 12**]. For this purpose, first of all we introduce the function $\tilde{Y}$, $\tilde{\Theta}$, $\tilde{U}$ defined by $\tilde{Y}(x) = Y(Rx)$, $\tilde{\Theta}(x) = \Theta(Rx)$, $\tilde{U}(x) = RU(Rx)$. Note that the triplet $(\tilde{Y}, \tilde{\Theta}, \tilde{U})$ is a stationary solution of Problem (3.5)-(3.7) corresponding to $R(\cdot) \equiv 1$ and with α, β, F being replaced with $\tilde{\alpha} = R\alpha$, $\tilde{\beta} = R\beta$ and RF.

Now, we assume that (y, θ, u) is a smooth radial solution to Problem (3.5)-(3.7). As a first step, we make the front steady by setting

$$\tau = \frac{t}{R^2}, \qquad x = \frac{r}{R(t)}, \qquad R(t) = R(1 + s(\tau)), \tag{3.10}$$

when r varies in $[0, R(t)]$ and

$$\tau = \frac{t}{R^2}, \qquad x = \frac{r - R(t) + R}{R}, \qquad R(t) = R(1 + s(\tau)), \tag{3.11}$$

when r varies in $[R(t), +\infty)$. The change of coordinates and unknowns in (3.10) is convenient for radial problems in bounded domains: x is a new radial variable which varies from $x = 0$ to $x = 1$. On the contrary, this change of unknowns is not useful when r varies in $[R(t), +\infty)$. This is the reason why we use (3.11) to fix the boundary at $x = 1$ when r varies in $[R(t), +\infty)$. Next we set, for $r \in [R(t), +\infty)$

$$\begin{cases} (i) & y(t,r) = \tilde{Y}(x) + s(\tau)\tilde{Y}_x(x) + v(\tau, x), \\ (ii) & \theta^+(t,r) = \tilde{\Theta}^+(x) + s(\tau)\tilde{\Theta}^+_x(x) + w^+(\tau, x), \\ (iii) & Ru^+(t,r) = \tilde{U}^+(x) + s(\tau)\tilde{U}^+_x(x) + p^+(\tau, x), \end{cases} \tag{3.12a}$$

and for $r \in [0, R(t)]$

$$\begin{cases} (iv) & \theta^-(t,r) = \tilde{\Theta}^-(x) + s(\tau)x\tilde{\Theta}^-_x(x) + w^-(\tau, x), \\ (v) & Ru^-(t,r) = \tilde{U}^-(x) + s(\tau)x\tilde{U}^-_x(x) + p^-(\tau, x), \end{cases} \tag{3.12b}$$

where θ^- and θ^+ are obtained extending by continuity $\theta_{|[0,R(t))}$ and $\theta_{|(R(t),+\infty)}$ up to $r = R(t)$. In the same way, we define the functions u^+, u^-, $\tilde{\Theta}^+$, $\tilde{\Theta}^-$, $\tilde{U}^+$ and $\tilde{U}^-$. The splitting in (3.12)(ii) and (3.12)(iv) is adapted from a similar trick in [**13**] and is suitable for problems in bounded domains. A similar argument, already considered in [**12, 29, 37, 36, 38**], is used to obtain the splitting in (3.12)(i), (3.12)(iii) and (3.12)(v).

The final equation for v. For notation convenience, we write everywhere t instead of τ. Note that evaluating (3.12)(i) at $x = 1$ and observing that $\tilde{Y}(1) = 0$ and $\tilde{Y}_x(1) = Y_f$, allows us to write s in terms of v. In fact,

$$s(t)\tilde{Y}_x(1) + v(t,1) = s(t)Y_f + v(t,1) = 0, \qquad t > 0. \tag{3.13}$$

Replacing the expressions of y, given by (3.12), in the first differential equation in (3.5), recalling that $\tilde{Y}$ is a stationary solution of the first differential equation in Problem (3.5) (with $R = 1$), and taking (3.13) into account, we can show that the function v turns out to solve the differential equation

$$v_t(t,x) = \frac{1}{\mathrm{Le}}\left(v_{xx}(t,x) + \frac{2}{x}v_x(t,x)\right) + (\tilde{\mathcal{F}}_1(v(t,\cdot)))(x), \tag{3.14}$$

for any $t > 0$ and any $x \in I_1^+$, where

$$(\tilde{\mathcal{F}}_1(v(t,\cdot)))(x) = \left\{ -\frac{v_t(t,1)}{Y_f} + \frac{2v(t,1)}{\mathrm{Le}(Y_f x - v(t,1))x}\right\}$$
$$\times\left(v_x(t,x) - \frac{v(t,1)}{Y_f}\tilde{Y}_{xx}(x)\right) + \frac{2(v(t,1))^2}{\mathrm{Le}Y_f x^2(Y_f x - v(t,1))}\tilde{Y}_x(x), \tag{3.15}$$

for $t > 0,\ x \in I_1^+$. Evaluating the differential equation (3.14) at $x = 1$, we can get rid of the term $v_t(t,1)$ in the right-hand side of (3.15). In fact, we get

$$v_t(t,1) = \frac{1}{\mathrm{Le}}\left(1 + \frac{v_x(t,1)}{Y_f} + \frac{2v(t,1)}{Y_f}\right)^{-1}$$
$$\times\left\{v_{xx}(t,1) + 2v_x(t,1) + \frac{2v(t,1)}{Y_f - v(t,1)}\left(v_x(t,1) + 3v(t,1)\right)\right\}, \tag{3.16}$$

for any $t > 0$, so that we can replace the function $\tilde{\mathcal{F}}_1(v(t,\cdot))$ in (3.15) with the function $\mathcal{F}_1(v(t,\cdot))$ defined by

$$(\mathcal{F}_1(v(t,\cdot)))(x) = \left\{ -\frac{1}{\mathrm{Le}}\left[v_{xx}(t,1) + 2v_x(t,1)\right.\right.$$
$$\left.+\frac{2v(t,1)}{Y_f - v(t,1)}\left(v_x(t,1) + 3v(t,1)\right)\right] \times \left(Y_f + v_x(t,1) + 2v(t,1)\right)^{-1}$$
$$\left.+\frac{2}{\mathrm{Le}}\frac{v(t,1)}{x(Y_f x - v(t,1))}\right\}\left(v_x(t,x) - \frac{1}{Y_f}v(t,1)\tilde{Y}_{xx}(x)\right)$$
$$+\frac{2}{\mathrm{Le}}\frac{(v(t,1))^2}{Y_f x^2(Y_f x - v(t,1))}\tilde{Y}_x(x), \tag{3.17}$$

for any $x \in I_1^+$.

The final equations for w^- and w^+. Arguing similarly and taking (3.16) into account whenever it is necessary, one can check that the functions $w^\pm$ and $p^\pm$ solve the differential equations

$$w_t^\pm(t,x) = w_{xx}^\pm(t,x) + 2x^{-1}w_x^\pm(t,x) + \tilde{\beta}p^\pm(t,x)$$
$$+(\hat{\mathcal{F}}_2^\pm(v(t,\cdot),w^\pm(t,\cdot)))(x), \tag{3.18}$$

and

$$3\tilde{\alpha}^2 p^\pm(t,x) = p_{xx}^\pm(t,x) + 2x^{-1}p_x^\pm(t,x) + \tilde{\alpha}\left(w_{xx}^\pm(t,x) + 2x^{-1}w_x^\pm(t,x)\right)$$
$$+(\mathcal{F}_3(v(t,\cdot),w^\pm(t,\cdot),p^\pm(t,\cdot)))(x), \tag{3.19}$$

for any $t>0$ and any $x\in I_1^{\pm}$, and

$$(\hat{\mathcal{F}}_2^-(v(t,\cdot),w^-(t,\cdot)))(x)=-\frac{1}{\mathrm{Le}}\bigg(1+\frac{1}{Y_f}v_x(t,1)+\frac{2}{Y_f}v(t,1)\bigg)^{-1}$$
$$\times\frac{x}{Y_f-v(t,1)}\bigg(w_x^-(t,x)-\frac{v(t,1)}{Y_f}x\Theta_{xx}^-(x)\bigg)$$
$$\times\bigg\{v_{xx}(t,1)+2v_x(t,1)+2\frac{v(t,1)}{Y_f-v(t,1)}\big(v_x(t,1)+3v(t,1)\big)\bigg\}$$
$$-\frac{(v(t,1))^2}{(Y_f-v(t,1))^2}\bigg(\tilde{\Theta}_{xx}^-(x)+\frac{2}{x}\tilde{\Theta}_x^-(x)\bigg)$$
$$-\tilde{\beta}\frac{(v(t,1))^3-2Y_f(v(t,1))^2}{Y_f(Y_f-v(t,1))^2}x\tilde{U}_x^-(x)$$
$$-\frac{(v(t,1))^2-2Y_fv(t,1)}{(Y_f-v(t,1))^2}\bigg(w_{xx}^-(t,x)+\frac{2}{x}w_x^-(t,x)\bigg),\tag{3.20a}$$

for $t>0$ and $x\in I_1^-$. We also get

$$(\hat{\mathcal{F}}_2^+(v(t,\cdot),w^+(t,\cdot)))(x)=$$
$$\bigg\{-\frac{1}{\mathrm{Le}}\bigg[v_{xx}(t,1)+2v_x(t,1)+\frac{2v(t,1)}{Y_f-v(t,1)}\big(v_x(t,1)+3v(t,1)\big)\bigg]$$
$$\times\big(Y_f+v_x(t,1)+2v(t,1)\big)^{-1}+\frac{2v(t,1)}{x(Y_fx-v(t,1))}\bigg\}$$
$$\times\bigg(w_x^+(t,x)-\frac{1}{Y_f}v(t,1)\tilde{\Theta}_{xx}^+(x)\bigg)$$
$$+\frac{2(v(t,1))^2}{Y_fx^2(Y_fx-v(t,1))}\tilde{\Theta}_x^+(x),\tag{3.20b}$$

for any $t>0$ and any $x\in I_1^+$, whereas

$$(\mathcal{F}_3^-(v(t,\cdot),w^-(t,\cdot),p^-(t,\cdot)))(x)=-\frac{(v(t,1))^2-2Y_fv(t,1)}{(Y_f-v(t,1))^2}$$
$$\times\bigg\{p_{xx}^-(t,x)+\frac{2}{x}p_x^-(t,x)+\tilde{\alpha}\bigg(w_{xx}^-(t,x)+\frac{2}{x}w_x^-(t,x)\bigg)\bigg\}$$
$$-\frac{(v(t,1))^2}{(Y_f-v(t,1))^2}\bigg\{\tilde{U}_{xx}^-(x)+\frac{2}{x}\tilde{U}_x^-(x)+\tilde{\alpha}\bigg(\tilde{\Theta}_{xx}^-(x)+\frac{2}{x}\tilde{\Theta}_x^-(x)\bigg)\bigg\}$$
$$+3\tilde{\alpha}^2\frac{(v(t,1))^3-2Y_f(v(t,1))^2}{Y_f(Y_f-v(t,1))^2}x\tilde{U}_x^-(x),\qquad t>0,\ \ x\in I_1^-,\tag{3.21a}$$

and

$$(\mathcal{F}_3^+(v(t,\cdot),w^+(t,\cdot),p^+(t,\cdot)))(x)=$$

$$\frac{2(v(t,1))^2}{Y_f x^2(Y_f x - v(t,1))}\big(\tilde{U}_x^+(x) + \tilde{\alpha}\tilde{\Theta}_x^+(x)\big)$$
$$-\frac{2(v(t,1))^2}{Y_f x(Y_f x - v(t,1))}\big(\tilde{U}_{xx}^+(x) + \tilde{\alpha}\tilde{\Theta}_{xx}^+(x)\big)$$
$$+\frac{2v(t,1)}{x(Y_f x - v(t,1))}\big(p_x^+(t,x) + \tilde{\alpha}w_x^+(t,x)\big), \tag{3.21b}$$

for any $t > 0$ and any $x \in I_1^+$.

Linearisation of the jump conditions

Now, we rewrite the jump conditions in (3.6) in terms of the new unknowns $v, w^\pm, p^\pm$. Recalling that

$$\tilde{Y}_x(1) = -\mathrm{Le}\big(\tilde{\Theta}_x^+(1) - \tilde{\Theta}_x^-(1)\big) \tag{3.22}$$

and, taking (3.13) into account, we can transform the condition $[\theta] = 0$ into the following equivalent condition for v and w:

$$w^+(t,1) - w^-(t,1) = -(\mathrm{Le})^{-1}v(t,1), \qquad t > 0. \tag{3.23}$$

As far as the condition $[\theta_r(t,\cdot)] = -(\mathrm{Le})^{-1}y_r(t,R(t))$, is concerned, we preliminarily observe that, using (3.12)(ii) and (3.12)(iii), we can rewrite it as follows:

$$w_x^+(t,1) - w_x^-(t,1) + \frac{1}{\mathrm{Le}}v_x(t,1) = -s(t)\Big(\tilde{\Theta}_{xx}^+(1) - \tilde{\Theta}_{xx}^-(1) + \frac{1}{\mathrm{Le}}\tilde{Y}_{xx}(1)\Big)$$
$$-\frac{s(t)}{1+s(t)}\big(\tilde{\Theta}_{xx}^-(1)s(t) + w_x^-(t,1)\big). \tag{3.24}$$

Now, we observe that, since $\tilde{\Theta}^- \in C^2([0,1])$, $\tilde{\Theta}^+ \in C_b^2([1,+\infty))$ and $\tilde{\Theta}_{xx}^\pm(x) = -2x^{-1}\tilde{\Theta}_x^\pm(x) - \tilde{\beta}\tilde{U}^\pm(x)$, for any $x \in I_1^\pm$, we get $\tilde{\Theta}_{xx}^+(1) - \tilde{\Theta}_{xx}^-(1) = -2(\tilde{\Theta}_x^+(1) - \tilde{\Theta}_x^-(1)) - \tilde{\beta}(\tilde{U}^+(1) - \tilde{U}^-(1))$. The continuity of the functions $\tilde{\Theta}$ and $\tilde{\Theta} + \tilde{\alpha}\tilde{U}$ at $x = 1$ implies that $\tilde{U}$ is continuous at $x = 1$ as well. Therefore,

$$\tilde{\Theta}_{xx}^+(1) - \tilde{\Theta}_{xx}^-(1) = -2\big(\tilde{\Theta}_x^+(1) - \tilde{\Theta}_x^-(1)\big). \tag{3.25}$$

Similarly, $\tilde{Y}_{xx}(1) = -2\tilde{Y}_x(1)$. Therefore, taking (3.13) into account, the condition (3.24) reduces to

$$w_x^+(t,1) - w_x^-(t,1) + (\mathrm{Le})^{-1}v_x(t,1) = \mathcal{F}_4(v(t,\cdot), w^-(t,\cdot)), \tag{3.26}$$

for $t > 0$, where

$$(\mathcal{F}_4(v(t,\cdot), w^-(t,\cdot)) = \frac{v(t,1)}{Y_f(Y_f - v(t,1))}\big(Y_f w_x^-(t,1) - \tilde{\Theta}_{xx}^-(1)v(t,1)\big), \tag{3.27}$$

and $t > 0$. To write the condition $y(t,R(t)) = -\mathrm{Le}F(\theta(R(t)))$ in terms of v, w, we begin by observing that

$$F(\theta(t,R(t))) = F(\tilde{\Theta}^+(1) + s(t)\tilde{\Theta}_x^+(1) + w^+(t,1))$$

$$= F(\tilde{\Theta}^+(1)) + F'(\tilde{\Theta}^+(1))(s(t)\tilde{\Theta}^+_x(1) + w^+(t,1)) + Q(s(t), w^+(t,\cdot)), \tag{3.28}$$

for any $t > 0$, where $(\xi, \zeta) \mapsto Q(\xi, \zeta)$ is a smooth function, quadratic with respect to the pair (ξ, ζ). Taking (3.13), (3.22) and (3.23) into account, we easily deduce that

$$s(t)\big(\tilde{\Theta}^+_x(1) - \tilde{\Theta}^-_x(1)\big) = -w^+(t,1) + w^-(t,1). \tag{3.29}$$

Replacing this expression of $s(t)$ in the last side of (3.28) and recalling that $\tilde{\Theta}^+_x(1) - \tilde{\Theta}^-_x(1) = -RF(\tilde{\Theta}(1))$, we get

$$F(\theta(t, R(t))) = F(\tilde{\Theta}^+(1))$$
$$+\frac{F'(\tilde{\Theta}^+(1))}{RF(\tilde{\Theta}^+(1))}\Big(\tilde{\Theta}^-_x(1)w^+(t,1) - \tilde{\Theta}^+_x(1)w^-(t,1)\Big) + Q(s(t), w^+(t,\cdot)), \tag{3.30}$$

for any $t > 0$. Therefore, the jump condition

$$y_r(t, R(t)) = \mathrm{Le} F(\theta(R(t))),$$

reads (in terms of v and w) as follows:

$$v_x(t,1) + 2v(t,1) = \mathrm{Le}\,\frac{F'(\tilde{\Theta}(1))}{F(\tilde{\Theta}(1))}\Big(\tilde{\Theta}^-_x(1)w^+(t,1) - \tilde{\Theta}^+_x(1)w^-(t,1)\Big)$$
$$+\mathcal{F}_5(v(t,\cdot), w^\pm(t,\cdot)), \tag{3.31}$$

for any $t > 0$, where

$$\mathcal{F}_5(v(t,\cdot), w^\pm(t,\cdot)) = \mathrm{Le}\, RF\left(\tilde{\Theta}^+(1) - \frac{v(t,1)}{Y_f}\tilde{\Theta}^+_x(1) + w^+(t,1)\right)$$
$$-\mathrm{Le}\, RF(\tilde{\Theta}(1)) - \mathrm{Le}\frac{F'(\tilde{\Theta}^+(1))}{F(\tilde{\Theta}^+(1))}\big(\tilde{\Theta}^-_x(1)w^+(t,1) - \tilde{\Theta}^+_x(1)w^-(t,1)\big). \tag{3.32}$$

Let us now compute the jump conditions for u. For this purpose, we observe that the continuity of the function $\tilde{U}$ at $x = 1$, the equalities $[\tilde{U}_x] = -\tilde{\alpha}[\tilde{\Theta}_x]$ and (3.29) allow us to rewrite the jump condition $[u(t,\cdot)] = 0$, for any $t > 0$ as follows:

$$p^+(t,1) - p^-(t,1) = -\tilde{\alpha}\big(w^+(t,1) - w^-(t,1)\big), \qquad t > 0. \tag{3.33}$$

Finally, arguing as in the proof of (3.26), and observing that $\tilde{U}^+_{xx}(1) + \tilde{\alpha}\tilde{\Theta}^+_{xx}(1) - \tilde{U}^-_{xx}(1) - \tilde{\alpha}\tilde{\Theta}^-_{xx}(1) = 0$, we can rewrite the jump condition $[u_r(t,\cdot)] = -\tilde{\alpha}[\theta_r(t,\cdot)]$ as follows:

$$p^+_x(t,1) - p^-_x(t,1) = -\tilde{\alpha}\big(w^+_x(t,1) - w^-_x(t,1)\big)$$
$$+\mathcal{F}_6(v(t,\cdot), w^-(t,\cdot), p^-(t,\cdot)), \tag{3.34}$$

for any $t > 0$, where

$$\mathcal{F}_6(v(t,\cdot), w^-(t,\cdot), p^-(t,\cdot)) = -\frac{(v(t,1))^2}{Y_f(Y_f - v(t,1))}\big(\tilde{U}^-_{xx}(1) + \tilde{\alpha}\tilde{\Theta}^-_{xx}(1)\big)$$

$$+\frac{v(t,1)}{Y_f - v(t,1)}\big(p_x^-(t,1) + \tilde{\alpha} w_x^-(t,1)\big).$$

The problem for $(v, w^\pm, p^\pm)$: summary

Summing up, the problem for the unknowns $(v, w^\pm, p^\pm)$ reads as follows for $t > 0$

$$\begin{cases} v_t(t,x) = (\mathrm{Le})^{-1}\big(v_{xx}(t,x) + 2x^{-1}v_x(t,x)\big) + (\mathcal{F}_1(v(t,\cdot)))(x), \\ \qquad\qquad\qquad\qquad\qquad\qquad\qquad\qquad\qquad\qquad x \in I_1^+, \\ w_t^\pm(t,x) = w_{xx}^\pm(t,x) + 2x^{-1}w_x^\pm(t,x) + \tilde{\beta} p^\pm(t,x) \\ \qquad\qquad + (\hat{\mathcal{F}}_2^\pm(v(t,\cdot), w^\pm(t,\cdot)))(x), \qquad\qquad x \in I_1^\pm, \\ 3\tilde{\alpha}^2 p^\pm(t,x) = p_{xx}^\pm(t,x) + 2x^{-1}p_x^\pm(t,x) \\ \qquad\qquad + \tilde{\alpha}\big(w_{xx}^\pm(t,x) + 2x^{-1}w_x^\pm(t,x)\big) \\ \qquad\qquad + (\mathcal{F}_3^\pm(v(t,\cdot), w^\pm(t,\cdot), p^\pm(t,\cdot)))(x), \qquad x \in I_1^\pm, \end{cases} \tag{3.35}$$

with the boundary conditions:

$$\begin{cases} \mathcal{B}(v(t,\cdot), w^-(t,\cdot), w^+(t,\cdot)) = \\ \qquad\qquad (0, \mathcal{F}_4(v(t,\cdot), w^-(t,\cdot)), \mathcal{F}_5(v(t,\cdot), w^\pm(t,\cdot))), \\ B_4(w^-(t,\cdot), w^+(t,\cdot), p^-(t,\cdot), p^+(t,\cdot)) = 0, \\ B_5(w^-(t,\cdot), w^+(t,\cdot), p^-(t,\cdot), p^+(t,\cdot)) = \\ \qquad\qquad \mathcal{F}_6(v(t,\cdot), w^-(t,\cdot), p^-(t,\cdot)), \end{cases} \tag{3.36}$$

for any $t > 0$, where the nonlinear terms $\mathcal{F}_1$, $\hat{\mathcal{F}}_2$ and $\mathcal{F}_j$ $(j = 3, \dots, 6)$ are given by (3.17), (3.20), (3.21), (3.27), (3.32) and (3.35),

$$\mathcal{B}(v, w^-, w^+) = (B_1(v, w^-, w^+), B_2(v, w^-, w^+), B_3(v, w^-, w^+)), \tag{3.37}$$

with

$$B_{j+1}(v, w^-, w^+) = D_x^j w^+(1) - D_x^j w^-(1) + (\mathrm{Le})^{-1} D_x^j v(1), \quad j = 0, 1, \tag{3.38}$$

$$B_3(v, w^-, w^+) = v_x(1) + 2v(1) - \mathrm{Le}\big(a\, w^+(1) + b\, w^-(1)\big), \tag{3.39}$$

$$B_{4+j}(w^-, w^+, p^-, p^+) = D_x^j p^+(1) + \tilde{\alpha}\, D_x^j w^+(1) - D_x^j p^-(1) - \tilde{\alpha}\, D_x^j w^-(1), \tag{3.40}$$

for $j = 0, 1$ and

$$a := \frac{F'(\tilde{\Theta}(1))}{F(\tilde{\Theta}(1))}\tilde{\Theta}_x^-(1), \qquad b := -\frac{F'(\tilde{\Theta}(1))}{F(\tilde{\Theta}(1))}\tilde{\Theta}_x^+(1). \tag{3.41}$$

Since F is an Arrhenius function, we know that it is a positive increasing function. Moreover, as the profile of the temperature in the radiative case indicates (see [**53**]), $\tilde{\Theta}_x^-(1)$ is positive, whereas $\tilde{\Theta}_x^+(1)$ is negative. As a consequence, the two quantities a and b are nonnegative.

Let us simplify a bit more Problem (3.35)-(3.36). For this purpose, we observe that, from the third differential equation in (3.35) coupled with the last two boundary conditions in (3.36), we immediately see that the function z defined by

$$z(t,x) = (p^-(t,x) + \tilde{\alpha} w^-(t,x))\chi_{[0,1]}(x)$$

$$+(p^+(t,x) + \tilde{\alpha} w^+(t,x) - \psi(x)\mathcal{F}_6(v(t,\cdot), w^-(t,\cdot), p^-(t,\cdot)))\chi_{(1,+\infty)}(x),$$

for any $t > 0$ and any $x \in [0, +\infty)$, where $\psi \in C_c^\infty((0,+\infty))$ is any smooth function such that $\psi(1) = 0$ and $\psi'(1) = 1$, satisfies (for any fixed t) the assumptions of Lemma 3.14 and solves the differential equation (3.91) with $\gamma = 3\tilde{\alpha}^2$ and

$$g(t,x) = (3\tilde{\alpha}^3 w^-(t,x) + (\mathcal{F}_3^-(v(t,x), w^-(t,x), p^-(t,\cdot)))(x))\chi_{[0,1]}(x)$$

$$+(3\tilde{\alpha}^3 w^+(t,x) + (\mathcal{F}_3^+(v(t,\cdot), w^+(t,\cdot), p^+(t,\cdot)))(x))\chi_{(1,+\infty)}(x)$$

$$+\mathcal{F}_6(v(t,\cdot), w^-(t,\cdot), p^-(t,\cdot))\left(\psi''(x) + 2x^{-1}\psi'(x) - 3\tilde{\alpha}^2\psi(x)\right)\chi_{[1,+\infty)}(x)$$

$$:= 3\tilde{\alpha}^3 w(t,x) + (\mathcal{F}_7(v(t,\cdot), w^\pm(t,\cdot), p^\pm(t,\cdot)))(x), \tag{3.42}$$

for any $t > 0$ and any $x \in [0, +\infty)$. Therefore,

$$p^\pm(t,x) = \frac{\sqrt{3}\tilde{\alpha}^2}{2x}\int_x^{+\infty} y e^{\sqrt{3}\tilde{\alpha}(x-y)} w(t,y)dy$$

$$-\frac{\sqrt{3}\tilde{\alpha}^2}{2x}\int_0^{+\infty} y e^{-\sqrt{3}\tilde{\alpha}(x+y)} w(t,y)dy + \frac{\sqrt{3}\tilde{\alpha}^2}{2x}\int_0^{x} y e^{\sqrt{3}\tilde{\alpha}(y-x)} w(t,y)dy$$

$$-\tilde{\alpha} w^\pm(x) + \psi^\pm(x)\mathcal{F}_6(v(t,\cdot), w^-(t,\cdot), p^-(t,\cdot))$$

$$+\frac{1}{2\sqrt{3}\tilde{\alpha}x}\int_x^{+\infty} y e^{\sqrt{3}\tilde{\alpha}(x-y)}(\mathcal{F}_7(v(t,\cdot), w^\pm(t,\cdot), p^\pm(t,\cdot)))(y)dy$$

$$-\frac{1}{2\sqrt{3}\tilde{\alpha}x}\int_0^{+\infty} y e^{-\sqrt{3}\tilde{\alpha}(x+y)}(\mathcal{F}_7(v(t,\cdot), w^\pm(t,\cdot), p^\pm(t,\cdot)))(y)dy$$

$$+\frac{1}{2\sqrt{3}\tilde{\alpha}x}\int_0^{x} y e^{\sqrt{3}\tilde{\alpha}(y-x)}(\mathcal{F}_7(v(t,\cdot), w^\pm(t,\cdot), p^\pm(t,\cdot)))(y)dy$$

$$:= (\Gamma^\pm(w^-(t,\cdot), w^+(t,\cdot)))(x)$$

$$+(\mathcal{F}_8^\pm(v(t,\cdot), w^-(t,\cdot), w^+(t,\cdot), p^-(t,\cdot), p^+(t,\cdot)))(x), \tag{3.43}$$

for any $t > 0$ and any $x \in I_1^\pm$, where $\Gamma^\pm$ is the linearization at zero of the operator in the right-hand side of (3.43), $\psi^- = 0$, $\psi^+ = \psi$ and $w = w^-\chi_{[0,R)} + w^+\chi_{[R,+\infty)}$. Replacing (3.43) in the first two differential equations in (3.35), and writing $\mathbf{u} := (v, w^-, w^+)$, we obtain the

following system for $t > 0$

$$\begin{cases} D_t\mathbf{u}(t,\cdot) = \mathcal{A}\mathbf{u}(t,\cdot) + \mathcal{F}(\mathbf{u}(t,\cdot), p^-(t,\cdot), p^+(t,\cdot)), \\ \mathcal{B}(\mathbf{u}(t,\cdot)) = \mathcal{G}(\mathbf{u}(t,\cdot)), \\ 3\tilde{\alpha}^2 p^\pm(t,x) = p^\pm_{xx}(t,x) + 2x^{-1}p^\pm_x(t,x) \\ \qquad\qquad +\tilde{\alpha}\big(w^\pm_{xx}(t,x) + 2x^{-1}w^\pm_x(t,x)\big) \\ \qquad\qquad +(\mathcal{F}^\pm_3(v(t,\cdot), w^\pm(t,\cdot), p^\pm(t,\cdot)))(x), \quad x \in I^\pm_1, \\ B_{4+j}(w^-, w^+, p^-, p^+) = j\,\mathcal{F}_6(v(t,\cdot), w^-(t,\cdot), p^-(t,\cdot)), \quad j = 0,1, \end{cases} \tag{3.44}$$

where

$$\begin{aligned} (\mathcal{A}\mathbf{u})(x) = \Bigg(& \frac{v_{xx}(x) + 2x^{-1}v_x(x)}{\mathrm{Le}}, \\ & w^-_{xx}(x) + 2x^{-1}w^-_x(x) + \tilde{\beta}(\Gamma^-(w^-, w^+))(x), \\ & w^+_{xx}(x) + 2x^{-1}w^+_x(x) + \tilde{\beta}(\Gamma^+(w^-, w^+))(x)\Bigg), \end{aligned} \tag{3.45}$$

$$\mathcal{F}(\mathbf{u}, p^-, p^+) = (\mathcal{F}_1(\mathbf{u}), \mathcal{F}^-_2(\mathbf{u}, p^-, p^+), \mathcal{F}^+_2(\mathbf{u}, p^-, p^+)),$$
$$\mathcal{G}(\mathbf{u}) = (0, \mathcal{G}_1(\mathbf{u}), \mathcal{G}_2(\mathbf{u}))$$

and

$$\mathcal{F}_1(\mathbf{u}) = \mathcal{F}_1(v), \quad \mathcal{F}^\pm_2(\mathbf{u}) = \hat{\mathcal{F}}^\pm_2(v, w^\pm) + \tilde{\beta}\mathcal{F}^\pm_8(v, w^-, w^+, p^-, p^+), \tag{3.46}$$

$$\mathcal{G}_1(\mathbf{u}) = \mathcal{F}_4(v), \quad \mathcal{G}_2(\mathbf{u}) = \mathcal{F}_5(v, w^-, w^+) \tag{3.47}$$

and the operator $\mathcal{B}$ is given by (3.37)-(3.39).

Remark 3.2.4. In view of the formulas (3.12), it is immediate to check that the stability/instability of the steady state solution (Y, Θ, U) of Problem (3.5)-(3.7) is equivalent to the stability/instability of the null solution of Problem (3.35)-(3.36).

3.3. The linear problem

In this section we study the main properties of the linearized problem (at $(\mathbf{u}, p^-, p^+) = (\mathbf{0}, 0, 0)$) associated with Problem (3.44), i.e. with the problem

$$\begin{cases} D_t\mathbf{u}(t,\cdot) = \mathcal{A}\mathbf{u}(t,\cdot) + \mathbf{f}(t,\cdot), & t > 0, \\ \mathcal{B}(\mathbf{u}(t,\cdot)) = (0, g_1(t,\cdot), g_2(t,\cdot)), & t > 0, \\ 3\tilde{\alpha}^2 p^\pm(t,x) = p^\pm_{xx}(t,x) + 2x^{-1}p^\pm_x(t,x) & \\ \qquad +\tilde{\alpha}\big(w^\pm_{xx}(t,x) + 2x^{-1}w^\pm_x(t,x)\big) + f^\pm_3(t,x), & t > 0, \ x \in I^\pm_1, \\ B_{4+j}(w^-, w^+, p^-, p^+) = j\,g_3(t,\cdot), & t > 0, \ j = 0,1, \end{cases} \tag{3.48}$$

where $\mathbf{f} = (f_1, f^-_2, f^+_2)$, f^-_3, f^+_3 and g_j $(j = 1,2,3)$ are given (continuous) functions.

Since Problem (3.48) is easily decoupled, taking Lemma 3.14 into account, it is immediate to check that we can limit ourselves to study the linear problem

$$\begin{cases} D_t\mathbf{u}(t,\cdot) = \mathcal{A}\mathbf{u}(t,\cdot) + \mathbf{f}(t,\cdot), & t > 0, \\ \mathcal{B}(\mathbf{u}(t,\cdot)) = (0, g_1(t,\cdot), g_2(t,\cdot)), & t > 0. \end{cases}$$

Analyzing the realization of the operator $\mathcal{A}$ in $\mathcal{X}$: I, a generation result

In this subsection, we prove that the realization A of the operator $\mathcal{A}$ in (3.45) in $\mathcal{X}$, with domain $D(A) = \big\{\mathbf{u} \in \mathcal{X}_2^0 : \ \mathcal{A}\mathbf{u} \in \mathcal{X},\ \mathcal{B}(\mathbf{u}) = 0\big\}$, generates an analytic semigroup.

Theorem 3.5. *For any $\alpha > 0$ and any $\beta, a, b \geq 0$, the operator $(A, D(A))$ generates an analytic semigroup in $\mathcal{X}$. Moreover, $\sigma(A) \supset (-\infty, 0]$ and, if (α, β, R) satisfies the condition*

$$1 + \frac{(2R\mu + 1)\exp(-2R\mu) - 1}{2\mu^3}\alpha\beta F'(\Theta(R)) > 0, \tag{3.49}$$

where $\mu = \sqrt{3\alpha^2 + \alpha\beta}$, then $\sigma(A)$ contains positive real eigenvalues and $\sigma(A) \cap \{\lambda \in \mathbb{C} : \mathrm{Re}\lambda > 0\}$ consists of eigenvalues of A. Any of such eigenvalues admits a corresponding eigenfunction $\mathbf{u} = (v, w^-, w^+) \in D(A)$ with v never vanishing in I_1^+.

Proof. Here, we limit ourselves to proving that the following operator $(A, D(A))$ generates an analytic semigroup in $\mathcal{X}$. We postpone to Appendix 3.8 the proofs of the properties of the spectrum of A, since they are rather technical. Of course, to prove that A generates an analytic semigroup in $\mathcal{X}$, it suffices to consider the case when $\beta = 0$. Indeed, the general case then will follow by a straightforward perturbation argument.

For notational convenience, throughout the proof, we denote by C positive constants, independent of λ, $\mathbf{f}$ and $\mathbf{u}$, which may vary from line to line. We stress that the functions we deal with throughout this proof are complex-valued functions.

Let us fix $\lambda \in \mathbb{C}$. We are going to show that, if $\mathrm{Re}\,\lambda$ is sufficiently large, then, for any $\mathbf{f} = (f_1, f_2^-, f_2^+) \in \mathcal{X}$, the equation $\lambda\mathbf{u} - \mathcal{A}\mathbf{u} = \mathbf{f}$ admits a unique solution in $D(A)$ and

$$\|\mathbf{u}\|_\infty \leq C|\lambda|^{-1}\|\mathbf{f}\|_\infty. \tag{3.50}$$

According to [**39**, Proposition 2.1.11], this will imply that $(A, D(A))$ generates an analytic semigroup in $\mathcal{X}$.

Let us begin by solving the differential equations for v, w^- and w^+ in (3.48). Arguing as in the proof of Lemma 3.14, it is immediate to

check that, if $\lambda \notin (-\infty, 0]$, the more general solution $\mathbf{u} = (v, w^-, w^+)$ in $\mathcal{X}_2$ of the differential equations in (3.48) is given by

$$\begin{aligned} v(x) \,=\, & \left(\frac{1}{2\sqrt{\lambda \mathrm{Le}}} \int_x^{+\infty} t e^{-\sqrt{\lambda \mathrm{Le}}\, t} f_1(t) dt\right) \frac{e^{\sqrt{\lambda \mathrm{Le}}\, x}}{x} \\ & + \left(c + \frac{1}{2\sqrt{\lambda \mathrm{Le}}} \int_1^x t e^{\sqrt{\lambda \mathrm{Le}}\, t} f_1(t) dt\right) \frac{e^{-\sqrt{\lambda \mathrm{Le}}\, x}}{x}, \qquad x \in I_1^+, \end{aligned}$$

$$\begin{aligned} w^-(x) \,=\, & \frac{1}{2\sqrt{\lambda}\, x} \int_0^1 t e^{\sqrt{\lambda}\,(x+t)} f_2^-(t) dt - \frac{1}{2\sqrt{\lambda}\, x} \int_0^x t e^{\sqrt{\lambda}\,(x-t)} f_2^-(t) dt \\ & - \frac{1}{2\sqrt{\lambda}\, x} \int_x^1 t e^{\sqrt{\lambda}\,(t-x)} f_2^-(t) dt - 2 \frac{\sinh(\sqrt{\lambda} x)}{x} d^-, \qquad x \in I_1^-, \end{aligned}$$

$$\begin{aligned} w^+(x) \,=\, & \frac{1}{2\sqrt{\lambda}} \left(\int_x^{+\infty} t e^{-\sqrt{\lambda}\, t} f_2^+(t) dt \right) \frac{e^{\sqrt{\lambda}\, x}}{x} \\ & + \left(d^+ + \frac{1}{2\sqrt{\lambda}} \int_1^x t e^{\sqrt{\lambda}\, t} f_2^+(t) dt \right) \frac{e^{-\sqrt{\lambda}\, x}}{x}, \qquad x \in I_1^+, \end{aligned}$$

c, d^-, d^+ being arbitrary complex constants.

Let us now impose the boundary conditions in (3.48). Since we are interested in proving (3.50) for $\lambda \in \mathbb{C}$ with sufficiently large real parts, we can assume that $\sqrt{\lambda \mathrm{Le}} \neq 1$.
In such a case, the condition $B_3(v, w^-, w^+) = 0$ allows us to uniquely write the constant c in terms of d^- and d^+. So, finally, we get

$$\begin{aligned} v(x) \,=\, & \frac{e^{\sqrt{\lambda \mathrm{Le}}\, x}}{2x\sqrt{\lambda \mathrm{Le}}} \int_x^{+\infty} t e^{-\sqrt{\lambda \mathrm{Le}}\, t} f_1(t) dt + \frac{e^{-\sqrt{\lambda \mathrm{Le}}\, x}}{2x\sqrt{\lambda \mathrm{Le}}} \int_1^x t e^{\sqrt{\lambda \mathrm{Le}}\, t} f_1(t) dt \\ & + \frac{(\sqrt{\lambda \mathrm{Le}} + 1) e^{(2-x)\sqrt{\lambda \mathrm{Le}}}}{2x(\sqrt{\lambda \mathrm{Le}} - 1)\sqrt{\lambda \mathrm{Le}}} \int_1^{+\infty} t e^{-\sqrt{\lambda \mathrm{Le}}\, t} f_1(t) dt \\ & + \frac{\mathrm{Le}\, e^{\sqrt{\lambda \mathrm{Le}}}}{1 - \sqrt{\lambda \mathrm{Le}}} (a\, w^+(1) + b\, w^-(1)) \frac{e^{-\sqrt{\lambda \mathrm{Le}}\, x}}{x}, \qquad x \in I_1^+. \quad (3.51) \end{aligned}$$

We recall that a and b are defined by (3.41).

To determine the constants d^- and d^+, we compute the boundary conditions $B_j(v, w^-, w^+) = 0$ $(j = 1, 2)$. A long but straightforward computation shows that such constants can be uniquely determined if and only if λ is not a zero of the Evans function $\mathcal{E}$ defined by

$$\begin{aligned} \mathcal{E}(\lambda, a, b, \mathrm{Le}) \,=\, & -2\sqrt{\lambda} - \frac{a(\sqrt{\lambda \mathrm{Le}} + \sqrt{\lambda})}{1 - \sqrt{\lambda \mathrm{Le}}} + \frac{a(\sqrt{\lambda \mathrm{Le}} - \sqrt{\lambda})}{1 - \sqrt{\lambda \mathrm{Le}}} e^{-2\sqrt{\lambda}} \\ & + \frac{b(\sqrt{\lambda} - \sqrt{\lambda \mathrm{Le}})}{1 - \sqrt{\lambda \mathrm{Le}}} (1 - e^{-2\sqrt{\lambda}}). \qquad (3.52) \end{aligned}$$

In such a case,

$$d^- = \frac{1}{\mathcal{E}(\lambda,a,b,\mathrm{Le})}\times$$
$$\Big\{ -\left(2+\frac{a(\sqrt{\mathrm{Le}}+1)}{(1-\sqrt{\lambda\mathrm{Le}})}-\frac{b(1-\sqrt{\mathrm{Le}})}{(1-\sqrt{\lambda\mathrm{Le}})}\right)\int_0^1 t\sinh(\sqrt{\lambda}\,t)f_2^-(t)dt$$
$$+\frac{\sqrt{\lambda}-1-a}{(\sqrt{\lambda\mathrm{Le}}-1)\mathrm{Le}}\left(\int_1^{+\infty} te^{-\sqrt{\lambda\mathrm{Le}}\,t}f_1(t)dt\right)e^{(\sqrt{\lambda\mathrm{Le}}-\sqrt{\lambda})}$$
$$+\frac{1-\sqrt{\lambda\mathrm{Le}}+a}{1-\sqrt{\lambda\mathrm{Le}}}\int_1^{+\infty} te^{-\sqrt{\lambda}t}f_2^+(t)dt\Big\}$$

and

$$d^+ = \frac{1}{\mathcal{E}(\lambda,a,b,\mathrm{Le})}\times$$
$$\Big\{ -2\frac{1-\sqrt{\lambda\mathrm{Le}}-b}{1-\sqrt{\lambda\mathrm{Le}}}\int_0^1 t\sinh(\sqrt{\lambda}\,t)f_2^-(t)dt$$
$$+\left[\frac{\sqrt{\lambda}+1}{\mathrm{Le}\,(\sqrt{\lambda\mathrm{Le}}-1)}e^{(\sqrt{\lambda\mathrm{Le}}+\sqrt{\lambda})}+\frac{\sqrt{\lambda}-1}{\mathrm{Le}\,(\sqrt{\lambda\mathrm{Le}}-1)}e^{(\sqrt{\lambda\mathrm{Le}}-\sqrt{\lambda})}\right.$$
$$\left.+\frac{2b}{\mathrm{Le}\,(1-\sqrt{\lambda\mathrm{Le}})}e^{\sqrt{\lambda\mathrm{Le}}}\sinh(\sqrt{\lambda})\right]\int_1^{+\infty} te^{-\sqrt{\lambda\mathrm{Le}}\,t}f_1(t)dt$$
$$+\left(1+\frac{(\sqrt{\mathrm{Le}}+1)e^{2\sqrt{\lambda}}+1-\sqrt{\mathrm{Le}}}{2(1-\sqrt{\lambda\mathrm{Le}})}\,a+\frac{(\sqrt{\mathrm{Le}}+1)(e^{2\sqrt{\lambda}}-1)}{2(1-\sqrt{\lambda\mathrm{Le}})}\,b\right)$$
$$\times\int_1^{+\infty} te^{-\sqrt{\lambda}t}f_2^+(t)dt\Big\}.$$

Let us now estimate the sup-norm of the functions v, w^- and w^+. To begin with, we observe that, for any fixed a, b and Le, $|\mathcal{E}(\lambda,a,b,\mathrm{Le})|$ behaves as $2|\lambda|^{1/2}$ as $|\lambda|$ tends to $+\infty$ and $\mathrm{Re}\lambda$ is positive. Therefore, there exists $M = M(a,b,\mathrm{Le}) > 0$ such that the function $\mathcal{E}(\cdot,a,b,\mathrm{Le})$ does not admit roots with real part greater than M and, consequently, the functions v, w^- and w^+ are well defined for such λ's.

To estimate the function v in (3.51), we observe that a straightforward computation shows that

$$\|v\|_\infty \le \left\{\frac{1}{(\mathrm{Re}\sqrt{\lambda\mathrm{Le}})^2}\left(1+\frac{1}{2\mathrm{Re}\sqrt{\lambda\mathrm{Le}}}\right)\right.$$
$$\left.+\frac{1}{2}\frac{|\sqrt{\lambda\mathrm{Le}}+1|}{|\sqrt{\lambda\mathrm{Le}}-1|}\frac{(\mathrm{Re}\sqrt{\lambda\mathrm{Le}})+1}{(\mathrm{Re}\sqrt{\lambda\mathrm{Le}})^3}\right\}\|f_1\|_\infty$$
$$+\frac{\mathrm{Le}}{|1-\sqrt{\lambda\mathrm{Le}}|}(a\,|w^+(1)|+b\,|w^-(1)|). \tag{3.53}$$

Moreover,

$$\left|d^- - \frac{1}{\sqrt{\lambda}}\int_0^1 t\sinh(\sqrt{\lambda}\,t)f_2^-(t)dt\right| \le \frac{C}{|\lambda|}e^{-\mathrm{Re}\sqrt{\lambda}}\|\mathbf{f}\|_{\mathcal{X}},$$

and

$$|d^+| \leq \frac{C}{|\lambda|} e^{\mathrm{Re}\sqrt{\lambda}} \|\mathbf{f}\|_{\mathcal{X}},$$

for any $\lambda \in \mathbb{C}$ with sufficiently large real part. Therefore,

$$|w^-(1)| + \|w^+\|_\infty \leq C|\lambda|^{-1}\|\mathbf{f}\|_{\mathcal{X}}, \tag{3.54}$$

for such λ's. Hence, from (3.53) and (3.54) we deduce that

$$\|v\|_\infty \leq C|\lambda|^{-1}\|\mathbf{f}\|_{\mathcal{X}}, \tag{3.55}$$

for any $\lambda \in \mathbb{C}$ with sufficiently large real part.

To estimate the sup-norm of w^-, we use a slight different technique based on well-known estimates for the Laplacian in the whole of $\mathbb{R}^3$. For this purpose, we introduce the function u defined as follows for $x \in [0, +\infty)$,

$$u(x) = w^-(x)\chi_{[0,1]}(x) + \left(w^+(x) + (\mathrm{Le})^{-1}v(x)\right)\chi_{(1,+\infty)}(x). \tag{3.56}$$

All the above results show that

$$u \in C^1_b([0,+\infty)) \cap C^2([0,1]) \cap C^2_b([1,+\infty)).$$

Moreover, if we denote by $\tilde{u} : \mathbb{R}^3 \to \mathbb{C}$ the function defined by $\tilde{u}(x) = u(|x|)$ for any $x \in \mathbb{R}^3$, it is immediate to check that $\tilde{u} \in C^1(\mathbb{R}^3)$ (since $u'(0) = 0$) and $\tilde{u} \in W^{2,p}_{\mathrm{loc}}(\mathbb{R}^3)$ for any $p \in [1, +\infty)$. Moreover, $\tilde{u}$ solves the elliptic equation $\lambda\tilde{u} - \Delta\tilde{u} = \tilde{f}_\lambda$, in $\mathbb{R}^3$, where the function $\tilde{f}_\lambda \in L^\infty(\mathbb{R}^3)$ is defined by

$$\tilde{f}_\lambda(x) = f_2^-(|x|)\chi_{B(0,1)}(x)$$
$$+ \left\{ f_2^+(|x|) + \lambda\left(\frac{1}{\mathrm{Le}} - 1\right) v(|x|) + f_1(|x|) \right\} \chi_{\mathbb{R}^3\setminus B(0,1)}(x),$$

for any $x \in \mathbb{R}^3$. The estimate (3.55) implies that $\sup_{x\in\mathbb{R}^3} |\tilde{f}_\lambda(x)| \leq C\|\mathbf{f}\|_{\mathcal{X}}$, for any $\lambda \in \mathbb{C}$ with a sufficiently large real part. Now, [**39**, Proposition 2.1.11] shows that

$$\sup_{x\in\mathbb{R}^3} |\tilde{u}(x)| \leq C|\lambda|^{-1} \sup_{x\in\mathbb{R}^3} |\tilde{f}_\lambda(x)| \leq C\|\mathbf{f}\|_{\mathcal{X}},$$

for any λ as above. Hence, taking (3.54) into account, we get

$$\|w^-\|_\infty \leq C|\lambda|^{-1}\|\mathbf{f}\|_{\mathcal{X}}, \tag{3.57}$$

for $\lambda \in \mathbb{C}$ with sufficiently large real part. Now, from (3.54), (3.55) and (3.57), we get (3.50). □

The following proposition shows that the set of the parameter α and β satisfying (3.49) is not empty.

Proposition 3.6. *For any choice of a smooth, positive and increasing function F, and any $Y_f > 0$, $\Theta_f > 0$, there exist positive values of the parameters α and β satisfying* (3.49).

Proof. We split the proof into three steps. For notation convenience, throughout the proof, we denote by C positive constants, independent of α, that may vary from line to line

Step 1. Here, we prove that, if $R = R(\alpha, \beta)$ is an arbitrary solution of (3.9), then the function $\Theta(R)$ stays bounded when (α, β) tends to $(0, 0)$. Indeed, from (3.3) it follows that if $R = R(\alpha, \beta)$ is a solution of (3.9), then $\Theta(R)$ satisfies the estimate

$$\Theta(R) \leq \frac{Y_f}{\mathrm{Le}} \left(\frac{\sinh(z)}{ze^z} + 1 \right) + \Theta_f, \tag{3.58}$$

where $z = (3\alpha^2 + \alpha\beta)^{1/2} R(\alpha, \beta)$. A straightforward computation now shows that the function defined by the right-hand side of (3.58) is bounded in $\mathbb{R}$ and this, of course, implies that $\Theta(R)$ is bounded itself by a positive constant which is independent of α, β and of the solution of (3.9) corresponding to such a choice of (α, β).

Step 2. Now, we show that if we take $\beta = \alpha^\kappa$ for some $\kappa > 5/2$, then any function $(\alpha, \beta) \mapsto R(\alpha, \alpha^\kappa)$, implicitly defined through (3.9), is such that

$$\lim_{\alpha \to 0} (3\alpha^2 + \alpha^{\kappa+1})^{1/2} R(\alpha, \alpha^\kappa) = 0.$$

Indeed, if this was not the case, up to a subsequence we can assume that the previous limit (say L) belongs to $(0, +\infty]$. This, in particular, would imply that $R(\alpha, \alpha^\kappa)$ blows up as α tends to 0. It follows that the modulus of the term

$$\frac{\alpha^\kappa Y_f (1 - 2(3\alpha^2 + \alpha^{\kappa+1})^{1/2} R - e^{-2(3\alpha^2 + \alpha^{\kappa+1})^{1/2} R})}{2\alpha^2 (3\alpha + \alpha^\kappa)^{3/2} \mathrm{Le}\, R} \tag{3.59}$$

could be estimated by

$$C \frac{\alpha^{\kappa - 1/2} (3\alpha^2 + \alpha^{\kappa+1}) R^2}{(3\alpha^2 + \alpha^{\kappa+1})^{3/2} R} = C \frac{\alpha^{\kappa - 1/2}}{3\alpha^2 + \alpha^{\kappa+1}} (3\alpha^2 + \alpha^{\kappa+1})^{1/2} R$$

$$\leq 2CL\alpha^{\kappa - 5/2},$$

if $L \in (0, +\infty)$ and α is sufficiently small. Therefore, taking the limit as α tends to 0 in both the sides of (3.9), gives

$$F\left(\frac{Y_f}{\mathrm{Le}} + \Theta_f \right) = 0, \tag{3.60}$$

which, combined with the positivity of F, leads us to a contradiction.

Similarly, we can argue when $L = +\infty$. Indeed, in such a case, we can estimate (3.59) by

$$C \frac{\alpha^{\kappa - 1/2}}{(3\alpha^2 + \alpha^{\kappa+1})} \leq C\alpha^{\kappa - 5/2},$$

as α tends to 0. As above, this leads us to (3.60).

Step 3. Now, we are almost done. Indeed, since F is a smooth function, from the above results it follows that the term $F'(\Theta(R))$ is bounded uniformly with respect to (α, β) and the particular solution of (3.9) that we consider. Therefore,

$$1 + \frac{(2R\sqrt{3\alpha^2+\alpha^{\kappa+1}}+1)\exp(-2R\sqrt{3\alpha^2+\alpha\beta})-1}{2(3\alpha^2+\alpha\beta)^{3/2}}\alpha\beta F'(\Theta(R)) > 0$$

$$\geq 1 - C\frac{R^2(3\alpha^2+\alpha^{\kappa+1})\alpha^{\kappa+1}}{(3\alpha^2+\alpha^{\kappa+1})^{3/2}}$$

$$\geq 1 - C\alpha^{\kappa-2}. \tag{3.61}$$

It follows that, the left-hand side of (3.49) is positive if we take $\beta = \alpha^\kappa$ (for some $\kappa > 5/2$) and, then, α sufficiently small. □

Analyzing the realization of the operator $\mathcal{A}$ in $\mathcal{X}$: II, characterization of some interpolation spaces

In this subsection we characterize the interpolation spaces $D_A(\theta/2, \infty)$, $D_A(1/2, \infty)$ and $D_A(1+\theta/2, \infty)$, $\theta \in (0,1)$. This characterization will provide us with a fundamental tool to prove the forthcoming Theorem 3.8.

Proposition 3.7. *For any $\theta \in (0,1)$ the following characterizations hold:*

$$D_A(\theta/2, \infty) = \{\mathbf{u} \in \mathcal{X}_\theta : B_1\mathbf{u} = 0\}, \tag{3.62a}$$

$$D_A(1+\theta/2, \infty) = \{\mathbf{u} \in \mathcal{X}^0_{2+\theta} : \mathcal{B}\mathbf{u} = 0,\ B_1 A\mathbf{u} = 0\}, \tag{3.62b}$$

with equivalence of the respective norms. Moreover,

$$\big\{\mathbf{u} \in \mathcal{X}_1 : B_1\mathbf{u} = 0\big\} \subset D_A(1/2, \infty), \tag{3.63}$$

with continuous embedding.

Proof. The proof we provide is similar to that in [**12**, Theorem 5.5] and is based on the method developed in [**2**] in the case of a single equation. Throughout the proof, we denote by C positive constants, independent of $\mathbf{u}$, $\mathbf{w}$, λ, k_1, k_2 and t, which may vary from line to line.

We begin by proving the inclusion "$\supset$" in (3.62a), and (3.63). For this purpose, we fix $\mathbf{u} = (v, w^-, w^+)$ in the space defined by the right-hand side of (3.62a) (resp. in the left-hand side of (3.63)). Next, we extend the functions v, w^- and w^+ to the whole of $\mathbb{R}$ with the functions $\hat{v}$, $\hat{w}^-$ and $\hat{w}^+$ defined as follows: $\hat{v}$ is obtained extending w^+ by symmetry with respect to the point $x = 1$, whereas $\hat{w}^-$ is obtained, first extending w^- to $(-\infty, 0]$ by setting $\hat{w}^-(x) = w^-(-x)$, if $x \in [-1, 0]$, and $\hat{w}^-(x) = \hat{w}^-(-1)\max\{x+2, 0\}$, if $x \in (-\infty, -1]$, and then extending the so obtained function by symmetry (with respect to $x = 1$) to the whole of $\mathbb{R}$. Finally, $\hat{w}^+$ is extended to $\mathbb{R}$ by setting

$\hat w^+(x)=2\hat w^-(2-x)-\hat w^+(2-x)-2(\mathrm{Le})^{-1}v(2-x)$ for any $x\in(-\infty,1]$. By construction, $\hat v,\hat w^-,\hat w^+$ belong to $C_b^\theta(\mathbb{R})$ and

$$\|\hat v\|_{C_b^\theta(\mathbb{R})}+\|\hat w^-\|_{C_b^\theta(\mathbb{R})}+\|\hat w^+\|_{C_b^\theta(\mathbb{R})}\le C\|\mathbf{u}\|_{\mathcal{X}_\theta}.$$

Now, we regularize the previous three functions by convolution setting

$$v_\xi(x)=\int_{\mathbb{R}}\hat v(x+\xi y)\varphi(y)dy,\quad w_\xi^\pm(x)=\int_{\mathbb{R}}\hat w^\pm(x+\xi y)\varphi(y)dy,\quad x\in\mathbb{R},$$

for any $\xi\in(0,1)$. Here, $\varphi\in C_c^\infty(\mathbb{R})$ is any smooth, positive and even function, compactly supported in $(-1,1)$ and such that $\|\varphi\|_{L^1(\mathbb{R})}=1$. As it is immediately seen, the function $\mathbf{u}_\xi:=(v_\xi,w_\xi^-,w_\xi^+)$ is smooth and satisfies $B_1\mathbf{u}_\xi=0$ for any $\xi\in(0,1)$. Moreover, the following estimates are satisfied:

$$\|\mathbf{u}_\xi-\mathbf{u}\|_{\mathcal{X}}\le C\xi^\theta\|\mathbf{u}\|_{\mathcal{X}_\theta},\quad \|\mathbf{u}_\xi\|_{\mathcal{X}_1}\le\frac{C}{\xi^{1-\theta}}\|\mathbf{u}\|_{\mathcal{X}_\theta},\quad \|\mathbf{u}_\xi\|_{\mathcal{X}_2}\le\frac{C}{\xi^{2-\theta}}\|\mathbf{u}\|_{\mathcal{X}_\theta},\tag{3.64}$$

for any $\xi\in(0,1)$ and some positive constant C, independent of ξ. Finally, v_ξ and w_ξ^+ vanish as x tends to $+\infty$ and, since $\hat w^-$ is even in $[-1,1]$, then $D_xw_\xi^-(0)=0$ for any $\xi\in(0,1)$. This implies that the function $((v_\xi)_{|_{[1,+\infty)}},(w_\xi^-)_{|_{[0,1]}},(w_\xi^+)_{|_{[1,+\infty)}})$ belongs to $D(A)$.

Let now $\lambda_0>\max\{1,R^2\}$ and M be two positive constants such that

$$\|AR(\lambda,A)\|_{\mathcal{X}}\le M,\qquad \lambda>\lambda_0.\tag{3.65}$$

Taking (3.64) and (3.65) into account, it is immediate to check that

$$\begin{aligned}&\|\lambda^{\theta/2}AR(\lambda,A)\mathbf{u}\|_{\mathcal{X}}\\ &\le\|\lambda^{\theta/2}AR(\lambda,A)(\mathbf{u}-\mathbf{u}_{\lambda^{-1/2}})\|_{\mathcal{X}}+\|\lambda^{\theta/2}AR(\lambda,A)\mathbf{u}_{\lambda^{-1/2}}\|_{\mathcal{X}}\\ &\le M\lambda^{\theta/2}\|\mathbf{u}-\mathbf{u}_{\lambda^{-1/2}}\|_{\mathcal{X}}+\|\lambda^{\theta/2}AR(\lambda,A)\mathbf{u}_{\lambda^{-1/2}}\|_{\mathcal{X}}\\ &\le MC\|\mathbf{u}\|_{\mathcal{X}_\theta}+\|\lambda^{\theta/2}AR(\lambda,A)\mathbf{u}_{\lambda^{-1/2}}\|_{\mathcal{X}}.\end{aligned}\tag{3.66}$$

To estimate the $\mathcal{X}$-norm of the function

$$\mathbf{v}:=AR(\lambda,A)\mathbf{u}_{\lambda^{-1/2}}=-\mathbf{u}_{\lambda^{-1/2}}+\lambda R(\lambda,A)\mathbf{u}_{\lambda^{-1/2}},$$

we observe that such a function solves the problem

$$\begin{cases}\lambda\mathbf{v}-A\mathbf{v}=A\mathbf{u}_{\lambda^{-1/2}},\\ \mathcal{B}\mathbf{v}=(0,-B_2\mathbf{u}_{\lambda^{-1/2}},-B_3\mathbf{u}_{\lambda^{-1/2}}).\end{cases}\tag{3.67}$$

Hence, it suffices to show that any solution $\mathbf{w}\in\mathcal{X}_2^0$ of the problem

$$\begin{cases}\lambda\mathbf{w}-A\mathbf{w}=\mathbf{f},\\ \mathcal{B}\mathbf{w}=(0,k_1,k_2),\end{cases}\tag{3.68}$$

where $\mathbf{f}\in\mathcal{X}$ and $k_1,k_2\in\mathbb{R}$, satisfies, for λ large, the estimate

$$\lambda\|\mathbf{w}\|_{\mathcal{X}}\le C\big\{\|\mathbf{f}\|_{\mathcal{X}}+\lambda^{1/2}(|k_1|+|k_2|)\big\}.\tag{3.69}$$

Indeed, applying (3.69) to Problem (3.67) and taking (3.64) into account, we get

$$\begin{aligned}\lambda\|\mathbf{v}\|_{\mathcal{X}} &\le C\big\{\|A\mathbf{u}_{\lambda^{-1/2}}\|_{\mathcal{X}} + \lambda^{1/2}(|B_2\mathbf{u}_{\lambda^{-1/2}}| + |B_3\mathbf{u}_{\lambda^{-1/2}}|)\big\}\\ &\le C\big\{\|\mathbf{u}_{\lambda^{-1/2}}\|_{\mathcal{X}_2} + \lambda^{1/2}\|\mathbf{u}_{\lambda^{-1/2}}\|_{\mathcal{X}_1}\big\}\\ &\le C\lambda^{1-\theta/2}\|\mathbf{u}\|_{\mathcal{X}_\theta}.\end{aligned}$$

Therefore, we can complete the estimate (3.66), obtaining that

$$\lambda^{\theta/2}\|AR(\lambda,A)\mathbf{u}\|_{\mathcal{X}} \le C\|\mathbf{u}\|_{\mathcal{X}_\theta}, \tag{3.70}$$

for λ large. Now, (3.70) implies that $\mathbf{u} \in D_A(\theta/2,\infty)$ and (see [**2**]),

$$\|\mathbf{u}\|_{D_A(\theta/2,\infty)} \le C\|\mathbf{u}\|_{\mathcal{X}_\theta}.$$

The inclusion "$\supset$" in (3.62a), and (3.63) follow. So, to conclude this part of the proof, let us check the estimate (3.69). We begin by proving it in the case when $\tilde\beta = 0$. For notational convenience we denote by A_0 the operators A corresponding to $\tilde\beta = 0$. Arguing as in the proof of the quoted theorem, it is not an hard task to show that the (unique) solution to Problem (3.68) (with A being replaced with A_0) which belongs to $\mathcal{X}_2^0$ is given by $\mathbf{w} = R(\lambda,A_0)\mathbf{f} + \mathbf{z}$, for λ real and sufficiently large, where $\mathbf{z} = (z_1, z_2^-, z_2^+)$ is defined by

$$z_1(x) = \frac{(a+b)\mathrm{Le}\,(1-e^{-2\sqrt{\lambda}})k_1 - 2\sqrt{\lambda}k_2}{(1-\sqrt{\lambda\mathrm{Le}})\mathcal{E}(\lambda)} \cdot \frac{e^{-\sqrt{\lambda\mathrm{Le}}(x-1)}}{x}, \tag{3.71}$$

for any $x \in I_1^+$,

$$\begin{aligned}z_2^-(x) = &-\frac{2}{\mathcal{E}(\lambda)}\frac{\sinh(\sqrt{\lambda}\,x)}{x}e^{-\sqrt{\lambda}}\\ &\times\left(\frac{1-\sqrt{\lambda\mathrm{Le}}+a}{(\sqrt{\lambda\mathrm{Le}}-1)}k_1 + \frac{\sqrt{\lambda\mathrm{Le}}-\sqrt{\lambda}}{(\sqrt{\lambda\mathrm{Le}}-1)\mathrm{Le}}k_2\right),\end{aligned} \tag{3.72}$$

for any $x \in I_1^-$,

$$z_2^+(x) = \frac{2}{\mathcal{E}(\lambda)}\frac{e^{-\sqrt{\lambda}x}}{x} \tag{3.73}$$

$$\times\left(\frac{(b-1+\sqrt{\lambda\mathrm{Le}})\sinh(\sqrt{\lambda})}{(\sqrt{\lambda\mathrm{Le}}-1)}k_1 - \frac{\sqrt{\lambda\mathrm{Le}}\sinh(\sqrt{\lambda})+\sqrt{\lambda}\cosh(\sqrt{\lambda})}{(\sqrt{\lambda\mathrm{Le}}-1)\mathrm{Le}}k_2\right)$$

for any $x \in I_1^+$, where $\mathcal{E}(\lambda) = \mathcal{E}(\lambda,a,b,\mathrm{Le})$ is given by (3.52). Now, from (3.50), (3.71)-(3.73) and recalling that $|\mathcal{E}(\lambda)|$ behaves like $\lambda^{-1/2}$ as λ tends to $+\infty$, we immediately obtain (3.69) in this case.

To prove the estimate (3.69) in the general case when the operator A_0 is replaced with the operator A, it suffices to observe that the solution to Problem (3.68) is a fixed point of the operator $\Lambda : \mathcal{X} \to \mathcal{X}_2^0$ defined by

$$\Lambda(\mathbf{u}) = R(\lambda,A_0)\mathbf{f} - \tilde\beta R(\lambda,A_0)(0,\Gamma^-(w^-,w^+),\Gamma^+(w^-,w^+)) + \mathbf{z},$$

where $\mathbf{u} = (v, w^-, w^+)$, the function $\mathbf{z}$ is as above and the operators Γ^-, Γ^+ are given by (3.43). A straightforward computation shows that Λ is a contraction in $\mathcal{X}$, provided that λ is sufficiently large. Therefore, for such λ's, Problem (3.68) admits a unique solution $\mathbf{w} \in D(A)$ and satisfies

$$\begin{aligned}\|\mathbf{w}\|_{\mathcal{X}} &\leq \|R(\lambda, A_0)\mathbf{f}\|_{\mathcal{X}} \\ &+\tilde{\beta}\|R(\lambda, A_0)(0, \Gamma^-(w^-, w^+), \Gamma^+(w^-, w^+))\|_{\mathcal{X}} + \|\mathbf{z}\|_{\mathcal{X}} \\ &\leq \frac{C}{\lambda}\|\mathbf{f}\|_{\mathcal{X}} + \frac{1}{2}\|\mathbf{u}\|_{\mathcal{X}} + \frac{C}{\sqrt{\lambda}}(|k_1| + |k_2|),\end{aligned}$$

from which the estimate (3.69) follows immediately.
Now, we check the inclusion "$\subset$" in (3.62a). Since

$$\mathcal{X} \subset \mathcal{C}^0 := C_b([1, +\infty)) \times C([0, 1]) \times C_b([1, +\infty))$$

and

$$D(A) \subset \mathcal{C}^2 := C_b^2([1, +\infty)) \times C^2([0, 1]) \times C_b([1, +\infty))$$

with continuous embedding, from a general result in interpolation theory (see, e.g. [**51**]), it follows that

$$D_A(\theta/2, \infty) \subset (\mathcal{C}^0, \mathcal{C}^2)_{\theta/2,\infty}.$$

Now, observing that $(X_1 \times X_2, Y_1 \times Y_2) = (X_1, Y_1)_{\theta,\infty} \times (X_2, Y_2)_{\theta,\infty}$, with equivalence of the corresponding norms, for any quadruplet of Banach spaces $Y_i \subset X_i$ $(i = 1, 2)$ (see again [**51**]), we can easily show that

$$\begin{aligned}D_A(\theta/2, \infty) &\subset (C_b([1, +\infty)), C_b^1([1, +\infty)))_{\theta,\infty} \\ &\times (C_b([0, 1]), C_b^1([0, 1]))_{\theta,\infty} \times (C_b([1, +\infty)), C_b^1([1, +\infty)))_{\theta,\infty} \\ &= C_b^\theta([1, +\infty)) \times C_b^\theta([0, 1]) \times C_b^\theta([1, +\infty)),\end{aligned}$$

with equivalence of the corresponding norms, where the last equality follows from [**39**, Theorem 1.2.17]. Moreover, since $D_A(\theta/2, \infty)$ is contained in the closure (with respect to the $\mathcal{X}$-norm) of the space $\mathcal{X}_2$, it follows that, if $\mathbf{u} = (v, w^-, w^+)$ belongs to $D_A(\theta/2, \infty)$, then $B_1\mathbf{u} = 0$ and $\lim_{x\to+\infty} v(x) = \lim_{x\to+\infty} w^+(x) = 0$. The inclusion "$\subset$" in (3.62a) now follows.

To conclude the proof of the proposition, let us check the set equality (3.62b). Showing the embedding "$\supset$" is immediate in view of (3.62a), observing that, if $z \in C^{2+\theta}([0, 1])$, then the function $x \mapsto z_x(x)/x$ belongs to $C^\theta([0, 1])$ and its C^θ-norm is bounded from above by $C\|z\|_{C^{2+\theta}([0,1])}$. To prove the other inclusion, we fix $\mathbf{u} \in D_A(1+\theta/2, \infty)$ and write $\mathbf{u} = R(\lambda, A)(\lambda\mathbf{u} - A\mathbf{u})$ for some λ sufficiently large. Taking (3.62a) into account, it is immediate to check that the function $\lambda\mathbf{u} - A\mathbf{u}$ belongs to $\mathcal{X}_\theta$ and

$$\|\lambda\mathbf{u} - A\mathbf{u}\|_{\mathcal{X}_\theta} \leq C\|\mathbf{u}\|_{D_A(1+\theta/2,\infty)}.$$

Now, arguing as in the proof of the estimate (3.94), it is easy to check that the function $\mathbf{u}$ belongs to $\mathcal{X}_{2+\theta}$ and

$$\|\mathbf{u}\|_{\mathcal{X}^0_{2+\theta}} \le C\|\mathbf{u}\|_{D_A(1+\theta/2,\infty)}.$$

Therefore, the inclusion "$\subset$" in (3.62b) follows. This completes the proof. □

Solving the nonhomogeneous linear Problem (3.48)

Now, arguing as in the proof of [**39**, Theorem 5.1.18(iii)] and taking Proposition 3.7 and Lemma 3.15 into account, the following theorem, which is the main result of this subsection, can be proved.

THEOREM 3.8. *Fix $T > 0$, $\tilde{\alpha}, \tilde{\beta}, a, b \ge 0$ and $\theta \in (0,1)$, and suppose that $\mathbf{f} \in \mathcal{X}_{\theta/2,\theta}(0,T)$, $\mathbf{u}_0 \in \mathcal{X}^0_{2+\theta}$ and $g_1, g_2 \in C^{(1+\theta)/2}([0,T])$. Further, assume that the following compatibility conditions hold:*

$$\mathcal{B}\mathbf{u}_0 = (0, g_1(0), g_2(0)), \qquad B_1(\mathcal{A}\mathbf{u}_0 + \mathbf{f}(0,\cdot)) = 0. \tag{3.74}$$

Then, Problem (3.48) admits a unique solution $\mathbf{u} \in \mathcal{X}_{1+\theta/2,2+\theta}(0,T)$. The function $\mathbf{u}$ can be represented by

$$\begin{aligned}\mathbf{u}(t,\cdot) \,=\, & e^{tA}\mathbf{u}_0 + \int_0^t e^{(t-s)A}\big(\mathbf{f}(s,\cdot) + \mathcal{A}\mathcal{N}(g_1(s), g_2(s))\big)ds \\ & -A\int_0^t e^{(t-s)A}\mathcal{N}(g_1(s), g_2(s))ds,\end{aligned} \tag{3.75}$$

for any $t \in (0,T]$, where $\mathcal{N}(c,d) = \mathcal{M}(0,c,d,0)$ for any $c, d \in \mathbb{R}$, and $\mathcal{M}$ is the lifting operator defined in Lemma 3.15. Moreover, there exists a positive constant C_0, independent of $\mathbf{u}_0$, $\mathbf{f}$, g_1 and g_2, such that

$$\begin{aligned}\|\mathbf{u}\|_{\mathcal{X}_{1+\theta/2,2+\theta}(0,T)} \le C_0\big\{ & \|\mathbf{u}_0\|_{\mathcal{X}_{2+\theta}} + \|\mathbf{f}\|_{\mathcal{X}_{\theta/2,\theta}(0,T)} \\ & + \|g_1\|_{C^{(1+\theta)/2}([0,T])} + \|g_2\|_{C^{(1+\theta)/2}([0,T])}\big\}.\end{aligned} \tag{3.76}$$

3.4. The nonlinear problem

We are now in a position to solve Problem (3.44). For notational convenience, throughout this section we denote by $\mathbf{p}$ the vector function $\mathbf{p} = (p^-, p^+)$. In view of the formula (3.43) and Theorem 3.8, under suitable assumptions on $\mathbf{u}_0$, any solution $(\mathbf{u}, \mathbf{p})$ to Problem (3.44), belonging to the space $\mathcal{Z}_\theta(0,T) := \mathcal{X}_{1+\theta/2,2+\theta}(0,T) \times \mathcal{Y}_{\theta/2,2+\theta}(0,T)$ (endowed with the norm

$$\|(\mathbf{u},\mathbf{p})\|_{\mathcal{Z}_\theta(0,T)} := \|\mathbf{u}\|_{\mathcal{X}_{1+\theta/2,2+\theta}(0,T)} + \|\mathbf{p}\|_{\mathcal{Y}_{\theta/2,2+\theta}(0,T)},$$

for any $(\mathbf{u},\mathbf{p}) \in \mathcal{Z}_\theta(0,T)$) and satisfying the following conditions

$$\mathbf{u}(0,\cdot) = \mathbf{u}_0, \qquad D_x w^-(t,0) = 0, \qquad t \ge 0,$$

is a fixed point of the operator $\mathcal{R} = (\mathcal{R}_1, \mathcal{R}_2)$ defined by

$$(\mathcal{R}_1(\mathbf{u},\mathbf{p}))(t,\cdot) = e^{tA}\mathbf{u}_0$$

$$+\int_0^t e^{(t-s)A}\big\{\mathcal{F}(\mathbf{u}(s,\cdot),\mathbf{p}(s,\cdot))+\mathcal{A}\mathcal{N}\mathcal{G}(\mathbf{u}(s,\cdot))\big\}ds$$

$$-A\int_0^t e^{(t-s)A}\mathcal{N}\mathcal{G}(\mathbf{u}(s,\cdot))ds,$$

$$(\mathcal{R}_2(\mathbf{u},\mathbf{p}))(t,\cdot)=((\mathcal{R}_{21}(\mathbf{u},\mathbf{p}))(t,\cdot),(\mathcal{R}_{22}(\mathbf{u},\mathbf{p}))(t,\cdot))$$

where

$$(\mathcal{R}_{21}(\mathbf{u},\mathbf{p}))(t,\cdot)=\Gamma^-((\mathcal{R}_1(\mathbf{u},\mathbf{p}))(t,\cdot))+\mathcal{F}_8^-(\mathbf{u}(t,\cdot),\mathbf{p}(t,\cdot)),$$
$$(\mathcal{R}_{22}(\mathbf{u},\mathbf{p}))(t,\cdot)=\Gamma^+((\mathcal{R}_1(\mathbf{u},\mathbf{p}))(t,\cdot))+\mathcal{F}_8^+(\mathbf{u}(t,\cdot),\mathbf{p}(t,\cdot)),$$

for any $t\in[0,T]$, any $\mathbf{u}\in\mathcal{X}_{1+\theta/2,2+\theta}(0,T)$, with a sufficiently small norm, and any $\mathbf{p}\in\mathcal{Y}_{\theta,2+\theta}(0,T)$. Here, the operators Γ^-, Γ^+, $\mathcal{F}_8^\pm$, $\mathcal{F}$ and $\mathcal{G}$ are given, respectively, by (3.43), (3.46) and (3.47).

If not otherwise specified, throughout this section we assume that $\tilde\alpha>0$, $\tilde\beta,a,b\in[0,+\infty)$. To begin with, let us prove the following lemma.

Lemma 3.9. *There exists $\hat\rho_0>0$ such that, if $\mathbf{u}_0\in\overline{B}(0,\hat\rho_0)\subset\mathcal{X}^0_{2+\theta}$, the equation $\mathbf{r}=\mathcal{R}_2(\mathbf{r},\mathbf{u_0})$ admits a unique solution $\mathbf{r}\in\mathcal{Y}_{2+\theta}$ and there exists a positive constant C, independent of $\mathbf{u}_0$, such that*

$$\|\mathbf{r}\|_{\mathcal{Y}_{2+\theta}}\le C\|\mathbf{u}_0\|_{\mathcal{X}_{2+\theta}}.$$

Proof. Taking (3.94), Lemma 3.16 and the definitions of the operators $\mathcal{F}_3^\pm$, $\mathcal{F}_6$ and $\mathcal{F}_7$ into account (see (3.21), (3.35) and (3.42)), it is immediate to check that $\mathcal{R}_2(\cdot,\mathbf{u}_0)$ maps $\mathcal{Y}_{2+\theta}$ into itself and

$$\|\mathcal{R}_2(\mathbf{r}_2,\mathbf{u}_0)-\mathcal{R}_2(\mathbf{r}_1,\mathbf{u}_0)\|_{\mathcal{Y}_{2+\theta}(0,T)}$$

$$\le C_1\big(\|\mathcal{F}_7(\mathbf{u}_0,\mathbf{r}_2)-\mathcal{F}_7(\mathbf{u}_0,\mathbf{r}_1)\|_{\mathcal{Y}_\theta}$$

$$+\|\psi\|_{C_b^{4+\theta}([1,+\infty))}|\mathcal{F}_6(\mathbf{u}_0,\mathbf{r_2})-\mathcal{F}_6(\mathbf{u}_0,\mathbf{r_1})|\big)$$

$$\le C_2\big(\|\mathcal{F}_3(\mathbf{u}_0,\mathbf{r}_2)-\mathcal{F}_3(\mathbf{u}_0,\mathbf{r}_1)\|_{\mathcal{Y}_\theta}$$

$$+\|\psi\|_{C_b^{4+\theta}([1,+\infty))}|\mathcal{F}_6(\mathbf{u}_0,\mathbf{r_2})-\mathcal{F}_6(\mathbf{u}_0,\mathbf{r_1})|\big)$$

$$\le C_3\|\mathbf{u}_0\|_{\mathcal{X}_{2+\theta}}\|\mathbf{r}_2-\mathbf{r}_1\|_{\mathcal{Y}_{2+\theta}},$$

for any $\mathbf{r}_1,\mathbf{r}_2\in\mathcal{Y}_{2+\theta}$ and some positive constants C_1, C_2 and C_3, independent of $\mathbf{u}_0$, $\mathbf{r}_1$ and $\mathbf{r}_2$. It follows that $\mathcal{R}_2(\cdot,\mathbf{u}_0)$ is a contraction in $\mathcal{Y}_{2+\theta}$ provided that $\hat\rho_0<\max\{L_2^{-1},Y_f\}$. This completes the proof. □

We can now prove the main result of this section. For this purpose we denote by $\mathbf{p}_0(\mathbf{u_0})$ the fixed point of the operator $\mathbf{r}\mapsto\mathcal{R}_2(\mathbf{r},\mathbf{u}_0)$ provided by the previous lemma.

Theorem 3.10. *For any $T > 0$ and any $\theta \in (0,1)$, there exists $\rho_0 = \rho_0(T)$ such that, for any $\mathbf{u}_0 \in B(0,\rho_0) \subset \mathcal{X}^0_{2+\theta}$ satisfying the following compatibility conditions:*

$$\mathcal{B}\mathbf{u}_0 = \mathcal{G}(\mathbf{u}_0), \quad B_1(\mathcal{A}\mathbf{u}_0 + \mathcal{F}(\mathbf{u}_0, \mathbf{p}_0(\mathbf{u}_0))) = 0, \tag{3.77}$$

Problem (3.44) *admits a unique solution $(\mathbf{u},\mathbf{p}) \in \mathcal{Z}_\theta(0,T)$ such that $\mathbf{u}(0,\cdot) = \mathbf{u}_0$. Moreover, there exists a positive constant $C > 0$, independent of $\mathbf{u}_0$, such that*

$$\|(\mathbf{u},\mathbf{p})\|_{\mathcal{Z}_\theta(0,T)} \le C\|\mathbf{u}_0\|_{\mathcal{X}_{2+\theta}}. \tag{3.78}$$

Proof. We limit ourselves to proving that there exist ρ_0, $\rho > 0$, with $\rho_0 \le \hat{\rho}_0$ (where $\hat{\rho}_0$ is as in the statement of Lemma 3.9) such that, for any $\mathbf{u}_0 \in \overline{B}(0,\rho) \subset \mathcal{X}^0_{2+\theta}$ satisfying (3.77), Problem (3.44) admits a unique solution $(\mathbf{u},\mathbf{p}) \in B(0,\rho) \subset \mathcal{Z}_\theta(0,T)$. Then, a standard argument will show that the previous one is, actually, the unique solution to Problem (3.44) belonging to $\mathcal{Z}_\theta(0,T)$. For more details we refer the reader, e.g., to [**37**, Theorem 4.2].

Throughout the proof, we denote by K_j ($j \in \mathbb{N}$) positive functions of ρ, which may depend also on T, but are independent of $\mathbf{u}_0$ and $\mathbf{u}$, such that $\lim_{\rho\to 0} K_j(\rho) = 0$. Similarly, we denote by C_j ($j \in \mathbb{N}$) positive constants, independent of $\mathbf{u}_0$ and $\mathbf{u}$.

We are going to show that the operator $\mathcal{R}$ is a contraction in the closed set

$$B(0,\mathbf{u}_0,\rho) = \big\{(\mathbf{u},\mathbf{p}) \in \mathcal{Z}_\theta(0,T) : \\ \|(\mathbf{u},\mathbf{p})\|_{\mathcal{Z}_\theta(0,T)} \le \rho,\ \mathbf{u}(0,\cdot) = \mathbf{u}_0,\ \mathbf{p}(0,\cdot) = \mathbf{p}_0(\mathbf{u}_0)\big\}.$$

For this purpose, we observe that a long but straightforward computation and Lemmas 3.14 and 3.16 show that, if $\rho < 3^{-1}Y_f$, then $\mathcal{F}(\mathbf{u},\mathbf{p}) \in \mathcal{X}_{\theta/2,\theta}$ for any $(\mathbf{u},\mathbf{p}) \in B(0,\mathbf{u}_0,\rho)$ and

$$\|\mathcal{F}(\mathbf{u},\mathbf{p})\|_{\mathcal{X}_{\theta/2,\theta}(0,T)} \le K_1(\rho)\|(\mathbf{u},\mathbf{p})\|_{\mathcal{Z}_\theta(0,T)}. \tag{3.79}$$

Similarly,

$$\|\mathcal{F}(\mathbf{u}_2,\mathbf{p}_2) - \mathcal{F}(\mathbf{u}_1,\mathbf{p}_1)\|_{\mathcal{X}_{\theta/2,\theta}(0,T)} \le K_2(\rho)\|(\mathbf{u}_2,\mathbf{p}_2) - (\mathbf{u}_1,\mathbf{p}_1)\|_{\mathcal{Z}_\theta(0,T)}, \tag{3.80}$$

for any $(\mathbf{u}_1,\mathbf{p}_1)$ and any $(\mathbf{u}_2,\mathbf{p}_2) \in B(0,\mathbf{u}_0,\rho)$.

To estimate the function $\mathcal{G}$, we first show that $\mathcal{X}_{1+\theta/2,2+\theta}(0,T)$ is embedded in $C^{(1+\theta)/2}([0,T];\mathcal{X}_1)$ and

$$\|\mathbf{u}\|_{C^{(1+\theta)/2}([0,T];\mathcal{X}_1)} \le C_1\|\mathbf{u}\|_{\mathcal{X}_{1+\theta/2,1+\theta}(0,T)}, \quad \mathbf{u} \in \mathcal{X}_{1+\theta/2,2+\theta}(0,T). \tag{3.81}$$

Once (3.81) is proved, it is immediate to show that

$$\mathcal{G}(\mathbf{u}) \in C^{(1+\theta)/2}([0,T]) \times C^{(1+\theta)/2}([0,T]),$$

for any $\mathbf{u} \in \overline{B}(0,\rho) \subset \mathcal{X}_{1+\theta/2,2+\theta}(0,T)$ and

$$\|\mathcal{G}(\mathbf{u}_2) - \mathcal{G}(\mathbf{u}_1)\|_{C^{(1+\theta)/2}([0,T])^2} \le K_3(\rho)\|\mathbf{u}_2 - \mathbf{u}_1\|_{\mathcal{X}_{1+\theta/2,2+\theta}(0,T)}, \tag{3.82}$$

for any $\mathbf{u}_1, \mathbf{u}_2 \in \overline{B}(0,\rho) \subset \mathcal{X}_{1+\theta/2,2+\theta}(0,T)$, $(j = 1,2)$.

To prove (3.81) we can take advantage of [**39**, Lemma 5.1.1]. To apply the quoted lemma to our situation, we just need to show that $\mathcal{X}_1 \in J_{(1-\theta)/2}(\mathcal{X}_\theta, \mathcal{X}_{2+\theta})$. This can be done easily observing that $C_b^1(I) \in J_{(1-\theta)/2}(C_b^\theta(I), C_b^{2+\theta}(I))$ for any closed interval $I \subset \mathbb{R}$ (see e.g. [**39**, Proposition 1.1.3]). Hence, $\mathcal{C}^1 \in J_{(1-\theta)/2}(\mathcal{C}^\theta, \mathcal{C}^{2+\theta})$. Here, for any $\gamma \geq 0$, $\mathcal{C}^\gamma = C_b^\gamma([1,+\infty)) \times C^\gamma([0,1]) \times C_b^\gamma([1,+\infty))$ (endowed with the product norm). The claim now follows, observing that the norms of $\mathcal{X}_\gamma$ and $\mathcal{C}^\gamma$ ($\gamma = \theta, 1, 2+\theta$) coincide.

Since, by (3.77), the triplet $(\mathbf{u}_0, \mathcal{F}(\mathbf{u}, \mathbf{p}_0(\mathbf{u_0})), \mathcal{G}(\mathbf{u}_0))$ satisfies the compatibility conditions (3.74), Theorem 3.8 and the estimates (3.79) and (3.82) show that the function $\mathcal{R}_1(\mathbf{u}, \mathbf{p})$ belongs to $\mathcal{X}_{1+\theta/2,2+\theta}(0,T)$ and

$$\begin{aligned} &\|\mathcal{R}_1(\mathbf{u},\mathbf{p})\|_{\mathcal{X}_{1+\theta/2,2+\theta}(0,T)} \\ &\leq C_0\big(\|\mathbf{u}_0\|_{\mathcal{X}_{2+\theta}} + \|\mathcal{F}(\mathbf{u},\mathbf{p})\|_{\mathcal{X}_{\theta/2,\theta}(0,T)} + \|\mathcal{G}(\mathbf{u},\mathbf{p})\|_{C^{(1+\theta)/2}([0,T])^2}\big) \\ &\leq C_0\big(\|\mathbf{u}_0\|_{\mathcal{X}_{2+\theta}} + K_4(\rho)\|(\mathbf{u},\mathbf{p})\|_{\mathcal{Z}_\theta(0,T)}\big), \end{aligned} \tag{3.83}$$

for any $(\mathbf{u}, \mathbf{p}) \in B(0, \mathbf{u}_0, \rho)$, where C_0 is the constant in (3.76). The same argument, applied to the triplet $(\mathbf{0}, \mathcal{F}(\mathbf{u}_2, \mathbf{p}_2) - \mathcal{F}(\mathbf{u}_1, \mathbf{p}_1), \mathcal{G}(\mathbf{u}_2) - \mathcal{G}(\mathbf{u}_1))$, and the estimates (3.80) and (3.82) show that

$$\begin{aligned} &\|\mathcal{R}_1(\mathbf{u}_2,\mathbf{p}_2) - \mathcal{R}_1(\mathbf{u}_1,\mathbf{p}_1)\|_{\mathcal{X}_{1+\theta/2,2+\theta}(0,T)} \\ &\leq K_5(\rho)\|(\mathbf{u}_2,\mathbf{p}_2) - (\mathbf{u}_1,\mathbf{p}_1)\|_{\mathcal{Z}_\theta(0,T)}, \end{aligned} \tag{3.84}$$

for any $(\mathbf{u}_j, \mathbf{p}_j) \in B(0, \mathbf{u}_0, \rho)$, $(j = 1, 2)$.

As far as the function $\mathcal{R}_2$ is concerned, we observe that Lemma 3.14 and the estimate (3.83) imply that $\mathcal{R}_2(\mathbf{u}, \mathbf{p})$ belongs to $\mathcal{Y}_{0,2+\theta}(0,T)$. Moreover,

$$\begin{aligned} \|\mathcal{R}_2(\mathbf{u},\mathbf{p})\|_{\mathcal{Y}_{0,2+\theta}(0,T)} &\leq L_2\big(\|\mathcal{R}_1(\mathbf{u},\mathbf{p})\|_{\mathcal{X}_{0,\theta}(0,T)} + \|\mathcal{F}_8(\mathbf{u},\mathbf{p})\|_{\mathcal{Y}_{0,\theta}(0,T)}\big) \\ &\leq C_2\left(\|\mathbf{u}_0\|_{\mathcal{X}_{2+\theta}} + K_6(\rho)\|(\mathbf{u},\mathbf{p})\|_{\mathcal{Z}_\theta(0,T)}\right) \end{aligned}$$

and

$$\begin{aligned} &\|(\mathcal{R}_2(\mathbf{u},\mathbf{p}))(t,\cdot) - (\mathcal{R}_2(\mathbf{u},\mathbf{p}))(s,\cdot)\|_{\mathcal{Y}_2} \\ &\leq L_1\big(\|(\mathcal{R}_1(\mathbf{u},\mathbf{p}))(t,\cdot) - (\mathcal{R}_1(\mathbf{u},\mathbf{p}))(s,\cdot)\|_{\mathcal{X}} \\ &\qquad + \|\mathcal{F}_8(\mathbf{u}(t,\cdot),\mathbf{p}(t,\cdot)) - \mathcal{F}_8(\mathbf{u}(s,\cdot),\mathbf{p}(s,\cdot))\|_{\mathcal{X}}\big) \\ &\leq K_7(\rho)\|(\mathbf{u},\mathbf{p})\|_{\mathcal{Z}_\theta(0,T)}|t-s|^{\theta/2}, \end{aligned}$$

for any $t, s \in [0,T]$, where the constants L_1 and L_2 are given by (3.93) and (3.94). Therefore,

$$\|\mathcal{R}_2(\mathbf{u},\mathbf{p})\|_{\mathcal{Y}_{\theta,2+\theta}(0,T)} \leq C_3\left(\|\mathbf{u}_0\|_{\mathcal{X}_{2+\theta}} + K_8(\rho)\|(\mathbf{u},\mathbf{p})\|_{\mathcal{Z}_\theta(0,T)}\right).$$

Similarly, taking (3.84) into account, we get

$$\begin{aligned} &\|\mathcal{R}_2(\mathbf{u}_2,\mathbf{p}_2) - \mathcal{R}_2(\mathbf{u}_1,\mathbf{p}_1)\|_{\mathcal{Y}_{\theta/2,2+\theta}(0,T)} \\ &\leq K_9(\rho)\|(\mathbf{u}_2,\mathbf{p}_2) - (\mathbf{u}_1,\mathbf{p}_1)\|_{\mathcal{Z}_\theta(0,T)}, \end{aligned} \tag{3.85}$$

for any $(\mathbf{u}_j, \mathbf{p}_j) \in B(0, \mathbf{u}_0, \rho)$, $(j = 1, 2)$. Now, from the estimates (3.83)-(3.85) it follows immediately that the operator $\mathcal{R}$ is a contraction in $B(0, \mathbf{u}_0, \rho)$ provided that

$$\begin{cases} \rho_0 < \min\{\rho, \hat{\rho}_0\}, \quad \rho < Y_f, \\ \big(C_0 + C_3\big)\rho_0 + \big(C_0 K_4(\rho) + C_3 K_8(\rho)\big)\rho \leq \rho, \quad K_5(\rho) + K_9(\rho) \leq \frac{1}{2}. \end{cases} \tag{3.86}$$

This completes the proof. □

Remark 3.4.11. We stress that there exist initial data

$$\mathbf{u}_0 = (v, w^-, w^+) \in \mathcal{X}_{2+\theta}$$

which satisfy the compatibility conditions (3.77). For instance, in the case when $v(1) = v_x(1) = v_{xx}(1) = 0$ the nonlinear terms $\mathcal{F}_j(\mathbf{u}_0, \mathbf{p})$ $(j = 1, 2, 3)$ identically vanish for any choice of $\mathbf{p} \in \mathcal{Y}_{2+\theta}$. Therefore, (3.77) reduces to $\mathcal{B}\mathbf{u} = \mathcal{G}(\mathbf{u}_0)$ and $B_1 \mathcal{A}\mathbf{u}_0 = 0$, which is satisfied, for instance, when $w^-(1) = w^+(1) = 0$ and $w_x^-(1) = w_x^+(1) = w_{xx}^-(1) = w_{xx}^+(1)$.

3.5. Instability results

In this section, the main body of the paper, we prove the instability results. We recall that, according to Remark 3.2.4, solutions of Problem (3.35)-(3.36) close to 0 correspond to solutions of Problem (3.5)-(3.7) close to the steady-state solution (Θ, Y, U, R) provided by Theorem 3.3. Therefore, to prove the instability of the steady state solution (Y, Θ, U, R), with respect to smooth (radial) perturbations, we just need to prove the instability of the trivial solution of Problem (3.35)-(3.36).

As Theorem 3.5 shows, in the case when the parameters $a, b, \tilde{\alpha}, \tilde{\beta}$ satisfy (3.49), the spectrum of the operator A contains points with positive real parts. The difficulty of having a complete analysis of the Evans function (i.e. of the set of the eigenvalues of the operator A), prevents us from applying the Linearized Stability Principle (see e.g. [**39**, Section 9.1.1]) to prove our results [1]. To overcome this problem we will show that the argument in [**12**, Section 5] can be adapted to our situation. Such an argument is a bit more technical than the Linearized Stability Principle, but it provides stronger results, see the forthcoming Main Theorem. This is another reason explaining why we choose to follow this way to prove our instability results.

The main tool we use to prove the instability results is provided by the following proposition from [**12**, Theorem 4.6]. To state it, we need

[1] Indeed, since the subset of $\sigma(A)$ with positive real part is, a priori, not a spectral set (and it does not contain any spectral set), there is no hope of constructing an unstable manifold. This difficulty arises typically in problems in unbounded domains.

to introduce some quantities. Let X, η, K and $\{T_n\}$ be, respectively a real Banach space, two positive numbers and a family of operators defined in $B(0,\eta)$ with the following property: there exist $M \in L(X)$ and two constants $L > 0$, $p > 1$ such that

$$\|T_n(x) - Mx\| \le L\|x\|^p, \qquad x \in B(0,\eta).$$

Moreover, assume that the spectral radius r of the operator M is greater than 1 and is an eigenvalue of M. Finally, let K and σ be positive constants such that

$$\|M^n\|_{L(X)} \le K\left(\frac{r^p + r}{2}\right)^n, \qquad n \in \mathbb{N}, \tag{3.87a}$$

$$\sigma = \frac{1}{2}\min\left\{\frac{\eta}{2}, \left(\frac{r^p - r}{2^{p+2}LK}\right)^{1/(p-1)}\right\}. \tag{3.87b}$$

Proposition 3.12. *Let $\{T_n\}$, M and σ be as above. Then, for any $\delta \in (0,\eta)$, there exists $u \in X$ with the following properties: there exist $N \in \mathbb{N}$ (depending on δ) and $x_0 \in B(0,\delta) \subset X$, such that the sequence $x_{n+1} = T_n(x_n)$, is well defined for any $n \le N-1$ and $x'(x_N) \ge \sigma|x'(u)|^{p/(p-1)}/2$ for any operator $x' \in L(X,\mathbb{R})$ such that $|x'(u)| \ne 0$ and $\|x'\| \le 1$.*

In order to apply Proposition 3.12 to our situation, let us now define the operator $\mathbb{P} \in L(\mathcal{X}^0_{2+\theta})$ by setting

$$\mathbb{P}\mathbf{u} = \mathbf{u} - \mathcal{M}(\mathcal{B}\mathbf{u}, B_1\mathcal{A}\mathbf{u}), \qquad \mathbf{u} \in \mathcal{X}^0_{2+\theta}, \tag{3.88}$$

where $\mathcal{M}$ is the lifting operator defined in Lemma 3.15. By construction, $\mathbb{P}\mathbf{u} \in \mathcal{X}^0_{2+\theta}$, $\mathcal{B}\mathbb{P}\mathbf{u} = 0$ and $B_1\mathcal{A}\mathbb{P}\mathbf{u} = 0$, so that $\mathbb{P}\mathbf{u} \in D_A(1+\theta/2,\infty)$ (see (3.63)). Moreover, since $\mathbb{P}$ is a projection, then $\mathcal{X}^0_{2+\theta} = D_A(1+\theta/2,\infty) \oplus (I-\mathbb{P})(\mathcal{X}^0_{2+\theta})$. It follows that the restriction of the operator $\mathbf{u} \mapsto (\mathcal{B}\mathbf{u}, B_1\mathcal{A}\mathbf{u})$ to $(I-\mathbb{P})(\mathcal{X}^0_{2+\theta})$ is an isomorphism between $(I-\mathbb{P})(\mathcal{X}^0_{2+\theta})$ and $\mathbb{R}^4$.

Let us now denote by $\mathcal{I}_\rho$ the set

$$\mathcal{I}_\rho = \big\{\mathbf{u} \in \mathcal{X}^0_{2+\theta} :$$

$$\|\mathbf{u}\|_{\mathcal{X}_{2+\theta}} \le \rho,\ \mathcal{B}(\mathbf{u}) = \mathcal{G}(\mathbf{u}),\ B_1(\mathcal{A}\mathbf{u} + \mathcal{F}(\mathbf{u}, \mathbf{p}_0(\mathbf{u}))) = 0\big\},$$

where the operator $\mathbf{p}_0$ is defined before Theorem 3.10, and $\rho < Y_f$. Of course, $\mathcal{I}_\rho = F^{-1}(\mathbf{0})$, where the (smooth) function $F : B(0,\rho) \subset \mathcal{X}^0_{2+\theta} \to \mathbb{R}^4$ is given by

$$F(\mathbf{u}) = (\mathcal{B}(\mathbf{u}) - \mathcal{G}(\mathbf{u}), B_1(\mathcal{A}\mathbf{u} + \mathcal{F}(\mathbf{u}, \mathbf{p}_0(\mathbf{u})))).$$

Since $F'(\mathbf{0}) = (\mathcal{B}, B_1\mathcal{A})$, applying the Implicit Function Theorem, it follows that there exist $\rho_1, \eta > 0$ and a smooth function $\Phi : B(0,\eta) \subset D_A(1+\theta/2,\infty) \to (I-\mathbb{P})(\mathcal{X}^0_{2+\theta})$ with $\Phi'(\mathbf{0}) = \mathbf{0}$ and such that $\mathcal{I}_{\rho_1}$ is the graph of Φ.

Main Theorem.

Theorem 3.13. *Suppose that the quintuplet* (a, b, Le) *satisfies Equation* (3.49)*. Then, the null solution of Problem* (3.35)-(3.36) *is unstable with respect to* $\mathcal{X}_{2+\theta}$*-smooth perturbations* ($\theta \in (0,1)$) *in the following sense: there exists* $C > 0$ *such that for any* $\rho_0 > 0$*, there exist an initial datum* $u_0 \in B(0,\rho_0) \subset \mathcal{X}_{2+\theta}$ *and* $N \in \mathbb{N}$ *such that the solution* $(\mathbf{u}, \mathbf{p})$ *of Problem* (3.35)-(3.36) *exists (at least) in the time domain* $[0, N]$ *and* $\|\mathbb{P}\mathbf{u}(N,\cdot)\|_{\mathcal{X}} \geq C$*. In the particular case when* $a, b \neq 0$*, it follows that* $|v(N,1)| \geq C$*, where, as usually, we have set* $\mathbf{u} = (v, w^-, w^+)$*. This, in view of the formulas* (3.10) *and* (3.13)*, implies the instability of the front* $t \mapsto R(t)$ *in Problem* (3.5)-(3.7)*.*

Proof. To begin with, we observe that, in view of formula (3.13), we can limit ourselves to proving the instability of the function $v(\cdot,1)$. We fix $\rho \leq \min\{\rho_0(1), \rho_1\}$, where $\rho_0(1)$ is given by Theorem 3.10 and ρ_1 is as above. With this choice of ρ it follows that for any $\mathbf{u}_0 \in \mathcal{X}^0_{2+\theta}$, satisfying the compatibility conditions (3.77), the initial value problem $\mathbf{u}(0,\cdot) = \mathbf{u}_0$ associated with Problem (3.35)-(3.36) admits a unique solution $(\mathbf{u}(\cdot,\mathbf{u}_0,0), \mathbf{p}(\cdot,\mathbf{u}_0,0)) \in \mathcal{X}_{1+\theta/2,2+\theta}(0,1)\times\mathcal{Y}_{\theta/2,2+\theta}(0,1)$. Since Problem (3.35)-(3.36), is autonomous, for any $n \in \mathbb{N}$ and any $\mathbf{u}_0 \in B(0,\eta) \subset D_A(1+\theta/2,\infty)$ such a problem with initial condition $\mathbf{u}(n-1,\cdot) = \mathbf{u}_0 + \Phi(\mathbf{u}_0)$ admits a unique solution $(\mathbf{u}(\cdot,\mathbf{u}_0+\Phi(\mathbf{u}_0), n-1), \mathbf{p}(\cdot,\mathbf{u}_0+\Phi(\mathbf{u}_0), n-1)) \in \mathcal{X}_{1+\theta/2,2+\theta}(n-1,n) \times \mathcal{Y}_{\theta/2,2+\theta}(n-1,n)$, provided that $(1+\|\Phi\|_{L(\mathcal{X}_{2+\theta})})\eta \leq \rho_0(1)$. Moreover, for $t \in [n-1,n]$,

$$(\mathbf{u}(t,\cdot,\mathbf{u}_0+\Phi(\mathbf{u}_0),n-1), \mathbf{p}(t,\cdot,\mathbf{u}_0+\Phi(\mathbf{u}_0),n-1)) =$$
$$(\mathbf{u}(t-n+1,\cdot,\mathbf{u}_0+\Phi(\mathbf{u}_0),0), \mathbf{p}(t-n+1,\cdot,\mathbf{u}_0+\Phi(\mathbf{u}_0),0)).$$

Therefore, the operator

$$\begin{aligned}\mathbf{u}_0 \mapsto T_n(\mathbf{u}_0) &= \mathbb{P}(\mathbf{u}(n,\cdot,\mathbf{u}_0+\Phi(\mathbf{u}_0),n-1))\\ &= \mathbb{P}(\mathbf{u}(1,\cdot,\mathbf{u}_0+\Phi(\mathbf{u}_0),0)),\end{aligned}$$

is well defined in $B(0,\eta) \subset D_A(1+\theta/2,\infty)$ with values in $D_A(1+\theta/2,\infty)$, for any $n \in \mathbb{N}$. Here, $\mathbb{P}$ is the projection defined in (3.88). Now, we observe that the Fréchet derivative of T_n at $\mathbf{u}_0 = \mathbf{0}$ is the restriction to $D_A(1+\theta/2,+\infty)$ of the operator e^A. For this purpose, we observe that, according to the previous remarks and Formula (3.75), it follows that

$$\begin{aligned}&\mathbf{u}(n,\cdot,\mathbf{u}_0+\Phi(\mathbf{u}_0),n-1)\\ &= e^A(\mathbf{u}_0+\Phi(\mathbf{u}_0)) - A\int_0^1 e^{(1-s)A}\mathcal{M}\mathcal{G}(\mathbf{u}(s,\mathbf{u}_0+\Phi(\mathbf{u}_0),0))ds\\ &+\int_0^1 e^{(1-s)A}\big\{\mathcal{F}(\mathbf{u}(s,\cdot,\mathbf{u}_0+\Phi(\mathbf{u}_0),0), \mathbf{p}(s,\mathbf{u}_0+\Phi(\mathbf{u}_0),0))\\ &+\mathcal{A}\mathcal{M}\mathcal{G}(\mathbf{u}(s,\mathbf{u}_0+\Phi(\mathbf{u}_0),0))\big\}ds,\end{aligned}$$

and

$$\mathbf{p}(n,\cdot,\mathbf{u}_0+\Phi(\mathbf{u}_0),n-1) =$$
$$\mathcal{R}_2(\mathbf{u}(1,\cdot,\mathbf{u}_0+\Phi(\mathbf{u}_0),0), \mathbf{p}(1,\cdot,\mathbf{u}_0+\Phi(\mathbf{u}_0),0)).$$

Taking the estimate (3.78) into account and recalling that $\mathcal{F}$, $\mathcal{G}$ and Φ are quadratic near $\mathbf{0}$ and $\mathbb{P}e^A = e^A$ on $D_A(1+\theta/2,\infty)$, it is immediate to check that

$$\begin{aligned}\|T_n(\mathbf{u}_0) - e^A\mathbf{u}_0\|_{\mathcal{X}_{2+\theta}} \leq \\ \|\mathbb{P}\|_{L(D_A(1+\theta/2,\infty))}\|\mathbf{u}(1,\cdot,\mathbf{u}_0+\Phi(\mathbf{u}_0),0) - e^A\mathbf{u}_0\|_{\mathcal{X}_{2+\theta}} \\ \leq L\|\mathbf{u}_0\|^2_{\mathcal{X}_{2+\theta}},\end{aligned} \tag{3.89}$$

for any $n \in \mathbb{N}$ and some positive constant L, independent of $\mathbf{u}_0$. Since, according to Theorem 3.5, the operator A admits eigenvalues with positive real part when the condition (3.49) is satisfied, it follows that for such values of the parameters $a, b, \tilde{\alpha}, \tilde{\beta}, \mathrm{Le}$, the spectral radius r of the operator e^A is larger than 1. Moreover, from the spectral mapping theorem (see e.g. [**39**, Corollary 2.3.7]) and Theorem 3.5, we easily deduce that there exists an eigenvalue λ_0 of A such that $r = e^{\mathrm{Re}\lambda_0}$.

We first assume that $\lambda_0 > 0$. According to Theorem 3.5, there exists an eigenfunction $\mathbf{u} = (v, w^-, w^+)$ corresponding to λ_0 with v never vanishing on $[1,+\infty)$. As a byproduct, $\mathbf{u}$ is an eigenfunction of e^A corresponding to e^λ. Therefore, we can apply Proposition 3.12 with x' being given by $x'(\mathbf{z}) = z_1(1)$ ($\mathbf{z} = (z_1, z_2^-, z_2^+)$). It follows that for any $\delta > 0$ there exists a function $\mathbf{u}_0 \in B(0,\delta) \subset D_A(1+\theta/2,\infty)$, ($\mathbf{u}_0 = (v_0, w_0^-, w_0^+)$) such that the sequence $\mathbf{x}_n = T_{n-1}(\mathbf{x}_{n-1})$ is well defined for any $n = 0,\dots,N$ (for some $N \in \mathbb{N}$) and $|x'(\mathbf{x}_N)| \geq \sigma|v_0(1)|/2$, where σ is given by (3.87b) with L being given by (3.89) and K being defined according to (3.87a). Note that $\mathbf{u}(1,\cdot,\mathbf{u}_0+\Phi(\mathbf{u}_0),0) \in \mathcal{I}_{\rho_1}$ and $(I-\mathbb{P})\mathbf{u}(1,\cdot,\mathbf{u}_0+\Phi(\mathbf{u}_0),0) = \Phi(T_0(\mathbf{u}_0))$. By the arguments in the first part of the proof, it follows that, if $N > 1$, $\mathbf{x}_2$ is the projection on $\mathbb{P}(\mathcal{X}_{2+\theta})$ of the value at $t = 2$ of the solution of Problem (3.35)-(3.36), with datum $\mathbf{u}_0+\Phi(\mathbf{u}_0)$. Iterating this argument shows that the solution of Problem (3.35)-(3.36) with datum $\mathbf{u}_0+\Phi(\mathbf{u}_0)$ at $t = 0$ exists at least in the time domain $[0,N]$ and $\mathbf{x}_N = \mathbb{P}\mathbf{u}(N,\cdot,\mathbf{u}_0+\Phi(\mathbf{u}_0),0)$. By Proposition 3.12, with $p = 2$, it follows that

$$\begin{aligned}\|\mathbb{P}\mathbf{u}(N,\cdot,\mathbf{u}_0+\Phi(\mathbf{u}_0),0)\|_{\mathcal{X}} &\geq |v_{\mathbb{P}}(N,R,\mathbf{u}_0+\Phi(\mathbf{u}_0),0)| \\ &= |x'(\mathbb{P}\mathbf{u}(N,\cdot,\mathbf{u}_0+\Phi(\mathbf{u}_0),0))| \geq \frac{\sigma}{2}|v_0(1)|,\end{aligned}$$

where $v_{\mathbb{P}}(\cdot,\mathbf{u}_0+\Phi(\mathbf{u}_0))$ is the first component of the function $\mathbb{P}\mathbf{u}(\cdot,\mathbf{u}_0+\Phi(\mathbf{u}_0))$. Now, the first part of the assertion follows in this case. In particular, when a and b differ from 0, $v_{\mathbb{P}}(\cdot,\mathbf{u}_0+\Phi(\mathbf{u}_0))$ is the first component of $\mathbf{u}(\cdot,\mathbf{u}_0+\Phi(\mathbf{u}_0))$. Hence, the instability of the front follows.

Now, suppose that $\lambda_0 \in \mathbb{C}\setminus\mathbb{R}$. Arguing as above, it is immediate to check that there exists an eigenfunction $\tilde{\mathbf{u}}_0 = (\tilde{v}_0, \tilde{w}_0^-, \tilde{w}_0^+)$ of the operator e^A (viewed as an operator defined on complex-valued functions) corresponding to e^{λ_0}, such that $\tilde{v}_0$ never vanishes in I_1^+. Since $\tilde{\mathbf{u}}_0$ is a complex-valued function and we are interested in real-valued solutions to Problem (3.35)-(3.36), we cannot apply directly Proposition 3.12. To

overcome this difficulty, we begin by observing that we can fix $N \in \mathbb{N}$ such that $N\mathrm{Im}\lambda \notin \pi/2 + \pi\mathbb{Z}$. Indeed, if $m\mathrm{Im}(\lambda) \in \pi/2 + \pi\mathbb{Z}$, for some $m \in \mathbb{N}$, then $(m+1)\mathrm{Im}(\lambda) \notin \pi/2 + \pi\mathbb{Z}$, since $(m+1)\mathrm{Im}(\lambda) \in \pi/2 + \pi\mathbb{Z}$ would imply that $\mathrm{Im}(\lambda) \in \pi\mathbb{Z}$ and, consequently, $m\mathrm{Im}(\lambda)$ would belong to $\pi\mathbb{Z}$, which is a contradiction. Choosing properly the constant $c \in \mathbb{C} \setminus \{0\}$, we can assume that the function $\hat{\mathbf{u}}_0 := c\tilde{\mathbf{u}}_0 = (\hat{v}_0, \hat{w}_0^-, \hat{w}_0^+)$ satisfies $e^{\lambda_0 N}\hat{v}_0(1) = \xi \in \mathbb{R} \setminus \{0\}$ and $\|\mathrm{Re}(\hat{\mathbf{u}}_0)\|_{\mathcal{X}} + \|\mathrm{Im}(\hat{\mathbf{u}}_0)\|_{\mathcal{X}} \leq 1$. Writing $\hat{v}_0(1) = e^{-\lambda_0 N}\xi$ and recalling the choice of N, it is immediate to check that $\mathrm{Re}(\hat{v}_0(1)) \neq 0$.

Now, we set $\mathbf{u}_0 = \mathrm{Re}(\hat{\mathbf{u}}_0) := (v_0, w_0^-, w_0^+)$ and take x' as above. Of course, $\mathbf{u}_0 \neq \mathbf{0}$ (since $v_0(1) \neq 0$) and $\mathbf{u}_0 \in D_A(1+\theta/2, \infty)$. Moreover, since $\mathrm{Re}(e^{tA}\hat{\mathbf{u}}_0) = e^{tA}\mathbf{u}_0$ for any $t > 0$, it follows that $M^n\mathbf{u}_0 = \mathrm{Re}(e^{\lambda_0 n}\hat{\mathbf{u}}_0)$ for any $n \in \mathbb{N}$, so that

$$\begin{aligned} |x'(M^N\mathbf{u}_0)| &= |e^{\lambda_0 N}\hat{v}_0(1)| = e^{N\mathrm{Re}\,\lambda_0}|\hat{v}_0(1)| \\ &\geq e^{N\mathrm{Re}\,\lambda_0}|v_0(1)| = e^{N\mathrm{Re}\,\lambda_0}|x'(\mathbf{u}_0)| = r^N|x'(\mathbf{u}_0)|. \end{aligned} \tag{3.90}$$

Now, we can apply the proof of Proposition 3.12 (as given in [**12**]) with T_n as above and $\mathbf{x}_0 = \sigma_0 e^{-\mathrm{Re}\lambda\, N}\mathbf{u}_0$, and taking (3.90) into account, we can easily show that the sequence $\mathbf{x}_n = T_{n-1}(\mathbf{x}_{n-1})$ is well defined for any $n = 1, \ldots, N$. Moreover, since

$$|x'(M^N\mathbf{u}_0)| = \mathrm{Re}(e^{\lambda n}\hat{v}(1)) = |e^{\lambda n}\hat{v}(1)| = e^{\mathrm{Re}\lambda N}|v(1)|,$$

it follows that $|x'(\mathbf{x}_N)| \geq 2^{-1}\sigma_0|v(1)|$. Hence, the conclusion follows as in previous case. □

3.6. Concluding remarks

Let us make a few remarks on the instability results and relate them to the bifurcation diagrams obtained in [**53**] (Figure 3.2 below reproduces some bifurcation diagrams for different continuation parameters). Note that the curve in Figure (3.2b) closes for big values of R, so that the two branches are not disconnected. Let us suppose that the bifurcation diagram equation (3.9) defines a curve, then one can check (via the implicit function theorem) that the vertical turning points occur when the Evans function $D(\lambda)$ in 0 is 0. Note that $D(0)$ is exactly the expression on the right-hand side of Condition (3.49). Starting from $R = Y_f = 0$ in Figure (3.2b) for example, it is positive and remains positive until the first vertical turning point, which is not visible in Figure (3.2b). All along this part of the bifurcation curve, there is one unstable mode. This suggests that flames with a slightly perturbed larger R will have $R(t) \to \infty$, while a smaller R gives a flame with either $R(t) \to 0$ or converging to a solution on the middle branch, provided such a solution is stable. In both figures, stability can only occur between the two vertical turning points. As $\beta \to 0$ in Figure (3.2a), we recover the instability of the adiabatic solution.

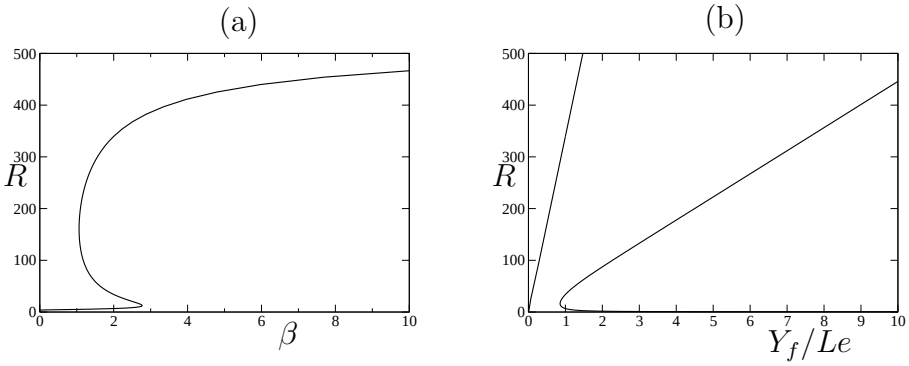

Figure 3.2: Bifurcation diagrams with (a) β and (b) Y_f/Le as the bifurcation parameters.

3.7. Appendix A: Technical tools

In this appendix, we collect some results which have been used in the paper.

Lemma 3.14. *Suppose that*

$$z \in C_b^1([0,+\infty)) \cap C^2([0,1]) \cap C_b^2([1,+\infty))$$

satisfies the differential equation

$$\gamma z(x) - z_{xx}(x) - 2x^{-1} z_x(x) = g(x), \tag{3.91}$$

for any $x \in [0,+\infty)$, some $\gamma > 0$ and $g \in L^\infty((0,+\infty))$ such that $g \in C([0,1]) \cap C_b([1,+\infty))$. Then,

$$\begin{aligned} z(x) \;=\; & \frac{1}{2\sqrt{\gamma}\,x} \int_x^{+\infty} t e^{\sqrt{\gamma}(x-t)} g(t)dt - \frac{1}{2\sqrt{\gamma}\,x} \int_0^{+\infty} t e^{-\sqrt{\gamma}(t+x)} g(t)dt \\ & + \frac{1}{2\sqrt{\gamma}\,x} \int_0^{x} t e^{\sqrt{\gamma}(t-x)} g(t)dt, \end{aligned} \tag{3.92}$$

for any $x \in [0,+\infty)$. Moreover, z goes to 0 at infinity, if g does, and there exists a positive constant L_1, independent of g, such that

$$\|z\|_{C^2([0,1])} + \|z\|_{C_b^2([1,+\infty))} \le L_1 \|g\|_{L^\infty((0,+\infty))}. \tag{3.93}$$

Further, if f belongs to $C^\theta([0,1]) \cap C_b^\theta([1,+\infty))$ for some $\theta \in (0,1)$, then $z \in C^{2+\theta}([0,1]) \cap C_b^{2+\theta}([1,+\infty))$ and there exists a positive constant L_2, independent of g, such that

$$\|z\|_{C^{2+\theta}([0,1])} + \|z\|_{C_b^{2+\theta}([1,+\infty))} \le L_2 \big\{ \|g\|_{C^\theta([0,1])} + \|g\|_{C_b^\theta([1,+\infty))} \big\}. \tag{3.94}$$

Proof. Setting $\widetilde{z}(x) = xz(x)$ for any $x > 0$, the differential equation for z in (3.48) transforms into the equation

$$\gamma \widetilde{z}(x) - \widetilde{z}_{xx}(x) = xg(x), \qquad x \in [0,1) \cup (1,+\infty),$$

which can be easily solved. Coming back to z, we deduce that the more general solution $z \in C^2((0,1]) \cap C_b^2([1,+\infty))$ of the differential equation (3.91), which vanishes at infinity, is given by

$$z(x) = \left(d_1^- - \frac{1}{2\sqrt{\gamma}} \int_1^x t e^{-\sqrt{\gamma}\, t} g(t) dt \right) \frac{e^{\sqrt{\gamma}\, x}}{x}$$

$$+ \left(d_2^- + \frac{1}{2\sqrt{\gamma}} \int_1^x t e^{\sqrt{\gamma}\, t} g(t) dt \right) \frac{e^{-\sqrt{\gamma}\, x}}{x},$$

for any $x \in (0,1)$ and

$$z(x) = \left(\frac{1}{2\sqrt{\gamma}} \int_x^{+\infty} t e^{-\sqrt{\gamma}\, t} g(t) dt \right) \frac{e^{\sqrt{\gamma}\, x}}{x}$$

$$+ \left(d_1^+ + \frac{1}{2\sqrt{\gamma}} \int_1^x t e^{\sqrt{\gamma}\, t} g(t) dt \right) \frac{e^{-\sqrt{\gamma}\, x}}{x},$$

for any $x \in (1,+\infty)$, where d_1^-, d_2^+ and d_1^+ are arbitrary constants. Note that z vanishes at infinity if g does. Imposing that z is twice continuously differentiable at $x = 0$ and $z'(0) = 0$, yields

$$z(x) = \frac{1}{2\sqrt{\gamma}\, x} \bigg(\int_0^1 t e^{\sqrt{\gamma}\,(t+x)} g(t) dt - \int_0^x t e^{\sqrt{\gamma}\,(x-t)} g(t) dt$$

$$+ \int_1^x t e^{\sqrt{\gamma}\,(t-x)} g(t) dt \bigg) - 2 d_2^- \frac{\sinh(\sqrt{\lambda} x)}{x}, \tag{3.95}$$

for any $x \in I_1^-$. Moreover, imposing the continuity of z and z' at $x = 1$, leads us immediately to the formula (3.92).

Next, a straightforward computation shows the estimate (3.93).

Finally, let us assume that $g \in C^\theta([0,1]) \cap C_b^\theta([1,+\infty))$. Since z satisfies the differential equation in (3.91), then it is immediate to see that $z_{xx} \in C_b^\theta([1,+\infty))$. So, we just need to show that $z_{xx} \in C^\theta([0,1])$. For this purpose, it suffices to prove that the second order derivative of the function in (3.95), where we take $d_2^- = 0$, belongs to $C^\theta([0,1])$. We still denote by z such a function. A straightforward computation and an asymptotic analysis near $x = 0$, show that

$$z_{xx}(x) = \frac{2}{\sqrt{\gamma}} \frac{1}{x^3} \int_0^x t \sinh(\sqrt{\gamma} t) g(t) dt - g(x)$$

$$+ \frac{1}{2\sqrt{\gamma}} \bigg(\int_1^x t\, e^{\sqrt{\gamma} t} g(t) dt \bigg) h_1(x)$$

$$+ \bigg(\frac{1}{2\sqrt{\gamma}} \int_0^1 t e^{\sqrt{\gamma} t} g(t) dt - \frac{1}{2\sqrt{\gamma}} \int_0^x t\, e^{-\sqrt{\gamma} t} g(t) dt \bigg) h_2(x), \tag{3.96}$$

for any $x \in I_1^-$, where h_1 and h_2 belong to $C^1([0,1])$. Therefore, we can limit ourselves to showing that the first term in the right-hand side

of (3.96) defines a function $q \in C^\theta([0,1])$. For this purpose, for any $x \in (0,1]$, we split $q(x)$ as follows:

$$q(x) = \frac{2g(0)}{\gamma^{3/2}}\left(\sqrt{\gamma}\frac{\cosh(\sqrt{\gamma}x)}{x^2} - \frac{\sinh(\sqrt{\gamma}x)}{x^3}\right)$$

$$+\frac{2}{\sqrt{\gamma}}\frac{1}{x^3}\int_0^x t\sinh(\sqrt{\gamma}t)(g(t)-g(0))dt. \tag{3.97}$$

The first term in the right-hand side of (3.97) is smooth in $[0,1]$, whereas the latter one is differentiable in $[0,1]$ and its first-order derivative can be estimated by $C[g]_{C^\theta([0,1])}x^{\theta-1}$ for any $x \in (0,1]$. It follows that q belongs to $C^\theta([0,1])$ and

$$\|q\|_{C^\theta([0,1])} \leq C\|g\|_{C^\theta([0,1])}, \tag{3.98}$$

for some positive constant C. ¿From (3.96) and the estimate (3.98) we deduce that $z_{xx} \in C^\theta([0,1])$ and satisfies (3.98) (with, possibly, a different constant). □

Lemma 3.15. *There exists a lifting operator $\mathcal{M} : \mathbb{R}^4 \to \mathcal{X}_\infty$ such that*

$$\mathcal{B}\mathcal{M}(q_1,q_2,q_3,q_4) = (q_1,q_2,q_3), \qquad B_1\mathcal{A}\mathcal{M}(q_1,q_2,q_3,q_4) = q_4,$$

for any $(q_1,q_2,q_3,q_4) \in \mathbb{R}^4$.

Proof. To determine the operator $\mathcal{M}$, we fix a quadruplet (q_i), $i = 1,..,4$ belonging to $\mathbb{R}^4$ and set $\mathcal{M}(q_1,q_2,q_3,q_4) = (v,w^-,w^+)$. Observing that

$$\Gamma^+(w^-,w^+)(1) - \Gamma^-(w^-,w^+)(1) = \tilde{\alpha}(w^+(1) - w^-(1)),$$

where Γ^- and Γ^+ are the operators defined by (3.43), we easily see that the triplet (v,w^-,w^+) needs to solve the linear system

$$\begin{cases} D_x^j w^+(1) - D_x^j w^-(1) + (\mathrm{Le})^{-1}D_x^j v(1) = q_{j+1}, \quad j = 0,1, \\ v_x(1) + 2v(1) - \mathrm{Le}\big(aw^+(1) + bw^-(1)\big) = q_3, \\ w^+_{xx}(1) + 2w^+_x(1) + \tilde{\alpha}\tilde{\beta}w^+(1) - w^-_{xx}(1) - 2w^-_x(1) \\ \quad -\tilde{\alpha}\tilde{\beta}w^-(1) + (\mathrm{Le})^{-2}\big(v_{xx}(1) + 2v_x(1)\big) = q_4. \end{cases} \tag{3.99}$$

In the case when a and b differ from 0, we can look for a triplet (v,w^-,w^+) of the type

$$\begin{aligned} &v(x) = 0, \qquad w^-(x) = w_0^-, \qquad x \in I_1^-, \\ &w^+(x) = (w_0^+ + w_1^+(x-1) + w_2^+(x-1)^2)\phi(x), \qquad x \in I_1^+, \end{aligned}$$

where $\phi \in C_c^\infty((0,+\infty))$ $(j = 1,2)$ is any smooth function such that $\phi \equiv 1$ in a neighborhood of $x = 1$. A straightforward computation

shows that we can take

$$w_0^- = -\frac{a\mathrm{Le}\, q_1 + q_3}{\mathrm{Le}(a+b)}, \qquad w_0^+ = \frac{b\mathrm{Le}\, q_1 - q_3}{\mathrm{Le}(a+b)},$$
$$w_1^+ = q_2, \qquad w_2^+ = \frac{1}{2}\Big(q_4 - \tilde{\alpha}\tilde{\beta} q_1 - \frac{2}{R} q_2\Big).$$

Finally, in the case when $a = b = 0$, we can look for a solution of the system (3.99) of the type

$$v(x) = v_0\phi(x), \quad x \in I_1^+,$$
$$w^+(x) = (w_0^+ + w_1^+(x-1) + w_2^+(x-1)^2)\phi(x), \quad x \in I_1^+,$$
$$w^-(x) = 0, \quad x \in I_1^-.$$

We find

$$v_0 = \frac{1}{2} q_3, \qquad w_0^+ = q_1 - \frac{1}{2\mathrm{Le}} q_3,$$
$$w_1^+ = q_2, \qquad w_2^+ = \frac{1}{2}\left\{ q_4 - 2q_2 - \tilde{\alpha}\tilde{\beta}\left(q_1 - \frac{1}{2\mathrm{Le}} q_3 \right) \right\}.$$

□

Lemma 3.16. *Suppose that u belongs to $C_b^{2+\theta}([1,+\infty))$, for some $\theta \in (0,1)$, and satisfies $\lim_{x\to+\infty} u(x) = 0$. Then,*

$$\lim_{x\to+\infty} u'(x) = \lim_{x\to+\infty} u''(x) = 0.$$

Proof. The proof follows by an interpolation argument. It suffices to observe that there exists a positive constant C, independent of v, such that

$$\|v\|_{C_b^2([0,+\infty))} \le C \|v\|^{\theta/(2+\theta)}_{C_b([0,+\infty))} \|v\|^{2/(2+\theta)}_{C_b^{2+\theta}([0,+\infty))}, \quad v \in C_b^{2+\theta}([0,+\infty)),$$

(see [**39**, Proposition 1.1.3]) and to apply such an estimate to the function $x \mapsto v(x) := u(x+M)$, letting, then, M go to $+\infty$. □

3.8. Appendix B: Proof of Theorem 3.5

In this appendix, we conclude the proof of Theorem 3.5. More precisely we prove that

- **(a)** for any choice of the parameters $a, b, \alpha, \beta, \mathrm{Le}$ and R, it holds that $\sigma(A) \supset (-\infty, 0]$;
- **(b)** if condition (3.49) is satisfied, then A admits a positive eigenvalue. Moreover, any $\lambda \in \sigma(A)$ with positive real part is an eigenvalue of A. Finally, if λ is an eigenvalue of A with positive real part, then there exists a corresponding eigenfunction $\mathbf{u} = (v, w^-, w^+)$ such that $v(x) \neq 0$ for any $x \in I_1^+$.

Proof of (a)

Of course, we can limit ourselves to proving that $(-\infty, 0) \subset \sigma(A)$. For this purpose, we look for nontrivial solutions $\mathbf{u} \in D(A)$ of the equation $\lambda\mathbf{u} - A\mathbf{u} = \mathbf{0}$. In view of Lemma 3.14, this is equivalent to looking for nontrivial solutions $(v, w^-, w^+, p^-, p^+) \in \mathcal{X}_2 \times \mathcal{Y}_2$ of the system

$$\begin{cases} \lambda v(x) - (\mathrm{Le})^{-1}\left(v_{xx}(x) + 2x^{-1}v_x(x)\right) = 0, & x \in I_1^+, \\ \lambda w^\pm(x) - w^\pm_{xx}(x) - 2x^{-1}w^\pm_x(x) - \tilde\beta p^\pm(x) = 0, & x \in I_1^\pm, \\ 3\tilde\alpha^2 p^\pm(x) - p^\pm_{xx}(x) - 2x^{-1}p^\pm_x(x) \\ \qquad -\tilde\alpha\left(w^\pm_{xx}(x) + 2x^{-1}w^\pm_x(x)\right) = 0, & x \in I_1^\pm, \\ \mathcal{B}(v, w^\pm) = 0, \qquad B_j(w^\pm, p^\pm) = 0, \quad j = 4, 5, \end{cases} \tag{3.100}$$

which satisfy the additional conditions $w^-_x(0){=}p^-_x(0) = 0$. Arguing as in the proof of Lemma 3.14, it is immediate to check that the more general solution of the first differential equation in (3.100) is given by

$$v(x) = c_1\frac{e^{\sqrt{\lambda\mathrm{Le}}\,x}}{x} + c_2\frac{e^{-\sqrt{\lambda\mathrm{Le}}\,x}}{x}, \qquad x \in I_1^+,$$

where c_1 and c_2 are arbitrary complex constants. As far as the other two equations in (3.100) are concerned, setting, as usually, $w^\pm(x) = \tilde w^\pm(x)/x$ and $p(x) = \tilde p(x)/x$, we get the following system of equations for $w^\pm$ and $p^\pm$:

$$\begin{cases} \lambda\tilde w^\pm - \tilde w^\pm_{xx} - \tilde\beta\tilde p^\pm = 0, & \text{in } I_1^\pm, \\ 3\tilde\alpha^2\tilde p^\pm - \tilde p^\pm_{xx} - \tilde\alpha\tilde w^\pm_{xx} = 0, & \text{in } I_1^\pm. \end{cases} \tag{3.101}$$

By the first equation, we can write $p^\pm$ in terms of $w^\pm$ and, replacing into the second equation, we finally get the following fourth order equations for w^- and w^+:

$$\tilde w^\pm_{xxxx}(x) - (\tilde\alpha\tilde\beta + \lambda + 3\tilde\alpha^2)\tilde w^\pm_{xx}(x) + 3\tilde\alpha^2\lambda\tilde w^\pm(x) = 0, \qquad x \in I_1^\pm, \tag{3.102}$$

whose characteristic polynomial is $P(\mu) = \mu^4 - (\tilde\alpha\tilde\beta + \lambda + 3\tilde\alpha^2)\mu^2 + 3\tilde\alpha^2\lambda$. Let us denote by μ_j $(j = 1, \dots, 4)$ the four roots of the polynomial P. Since, $\lambda < 0$, we have $\mu_j = (-1)^j\sqrt{\xi_1}$ $(j = 1, 2)$ and $\mu_j = (-1)^j\sqrt{\xi_2}$ $(j = 3, 4)$ for some $\xi_1, \xi_2 \in \mathbb{R}$ with $\xi_1 \neq \xi_2$. Now, a straightforward computation shows that the functions w^- and w^+ solving the equation (3.102) (with $w^-_x(0) = 0$) are uniquely determined up to four complex constants (if $\mathrm{Re}\,\mu_j > 0$ for $j = 1, 3$) and up to five complex constants (if $0 = \mathrm{Re}\,\mu_3 < \mathrm{Re}\,\mu_1$). Using the first differential equation in (3.101), allows us to determine explicitly the function p^- and p^+ in terms of w^- and w^+. In particular, we see that $p^-_x(0) = 0$. Next, computing the boundary conditions in (3.100), we are led to a system of five equations

in (at least) six unknowns which, of course, cannot be uniquely solvable. Hence $(-\infty, 0) \in \sigma(A)$.

Proof of (b)

Let us now show that if $\lambda \in \sigma(A)$ has positive real part, then λ is an eigenvalue of A. So, we fix $\mathbf{f} \in \mathcal{X}$ ($\mathbf{f} = (f_1, f_2^-, f_2^+)$) and we look for nontrivial solutions of the system (3.100) (where we replace the right-hand sides of the differential equations, respectively, with f_1 and $f_2^\pm$), corresponding to $\lambda \in \mathbb{C}$ with positive real part. Let us first assume that $\mathbf{f} \in \mathcal{X}_2$. Since the more general solution of the equation for v, which goes to 0 at infinity, is given by

$$v(x) = c\frac{e^{-\sqrt{\lambda \mathrm{Le}}x}}{x}, \qquad x \in I_1^+,$$

where c is a complex constant, we just need to pay attention to the equations for $w^\pm$ and $p^\pm$. Arguing as usually, we are led to solving the system

$$\begin{cases} \lambda\tilde{w}^\pm(x) - \tilde{w}^\pm_{xx}(x) - \tilde{\beta}\tilde{p}^\pm(x) = xf_2^\pm(x), & x \in I_1^\pm, \\ 3\tilde{\alpha}^2\tilde{p}^\pm(x) - \tilde{p}^\pm_{xx}(x) - \tilde{\alpha}\tilde{w}^\pm_{xx}(x) = 0, & x \in I_1^\pm. \end{cases} \tag{3.103}$$

Since, by assumption, $f_2^\pm$ is twice continuously differentiable in $I_1^\pm$, we can differentiate twice the first differential equation in (3.103), and, plugging the so obtained expression for $\tilde{p}$ and $\tilde{p}_{xx}$ into the second differential equation, we get the equations $\tilde{w}^\pm_{xxxx} - (\tilde{\alpha}\tilde{\beta} + \lambda + 3\tilde{\alpha}^2)\tilde{w}^\pm_{xx} + 3\tilde{\alpha}^2\lambda\tilde{w}^\pm = 3\tilde{\alpha}^2 x f^\pm - 2f^\pm_x - xf^\pm_{xx}$ in $I_1^\pm$. Denote by $\pm\mu_1$ and $\pm\mu_3$ the roots of the polynomial P. Let us first assume that $\mu_1 = \mu_3$, where μ_1 and μ_3 are as in the proof of point (a). This is the case when $\lambda = \lambda_0 := \tilde{\alpha}(\sqrt{3\tilde{\alpha}} \pm i\sqrt{\tilde{\beta}})^2$ and $\mu_1^2 = \mu_{1,0}^2 := \tilde{\alpha}\sqrt{3\tilde{\alpha}}(\sqrt{3\tilde{\alpha}} \pm i\sqrt{\tilde{\beta}})$. Hence, $\mathrm{Re}\,\mu_{1,0} > 0$. Then, the more general solutions $w^- \in C^2((0,1])$ and $w^+ \in C^2([1,+\infty))$ to the previous differential equations are given by

$$\begin{aligned} w^\pm(x) = &\left(d_1^\pm - \frac{1}{4\mu_{1,0}^3}\int_1^x (\mu_{1,0}t + 1)e^{-\mu_{1,0}t}g^\pm(t)dt\right)\frac{e^{\mu_{1,0}x}}{x} \\ &+\left(d_2^\pm + \frac{1}{4\mu_{1,0}^2}\int_1^x e^{-\mu_{1,0}t}g^\pm(t)dt\right)e^{\mu_{1,0}x} \\ &+\left(d_3^\pm + \frac{1}{4\mu_{1,0}^3}\int_1^x e^{\mu_{1,0}t}(1 - \mu_{1,0}t)g^\pm(t)dt\right)\frac{e^{-\mu_{1,0}x}}{x} \\ &+\left(d_4^\pm + \frac{1}{4\mu_{1,0}^2}\int_1^x e^{\mu_{1,0}t}g^\pm(t)dt\right)e^{-\mu_{1,0}x}, \end{aligned}$$

where $d_j^\pm$ $j = 1, \ldots, 4$ are arbitrary complex constants and $g^\pm(x) = 3\tilde{\alpha}^2 x f_2^\pm(x) - 2D_x f_2^\pm(x) - xD_{xx}f_2^\pm(x)$, for any $x \in I_1^\pm$. Integrating by parts the terms containing the derivatives of the functions $f_2^\pm$ and

imposing that w^- is twice continuously differentiable in $x=0$ and w^+ is bounded at infinity, we finally get the following formula for $w^\pm$:

$$\begin{aligned} w^-(x) = -\Bigg(& d_1^- + \frac{3\tilde{\alpha}^2-\mu_{1,0}^2}{2\mu_{1,0}^2}\int_0^1 t^2\cosh(\mu_{1,0}t)f_2^-(t)dt \\ & -\frac{3\tilde{\alpha}^2-\mu_{1,0}^2}{2\mu_{1,0}^2}\int_0^1 t\sinh(\mu_{1,0}t)f_2^-(t)dt \\ & -\frac{3\tilde{\alpha}^2}{4\mu_{1,0}^3}\int_x^1 t(\mu_{1,0}t+1)e^{-\mu_{1,0}t}f_2^-(t)dt \\ & -\frac{1}{4\mu_{1,0}}\int_x^1 t(1-\mu_{1,0}t)e^{-\mu_{1,0}t}f_2^-(t)dt\Bigg)\frac{e^{\mu_{1,0}x}}{x} \\ & +\Bigg(d_1^- - \frac{3\tilde{\alpha}^2}{4\mu_{1,0}^3}\int_x^1 t(1-\mu_{1,0}t)e^{\mu_{1,0}t}f_2^-(t)dt \\ & -\frac{1}{4\mu_{1,0}}\int_x^1 t(1+\mu_{1,0}t)e^{\mu_{1,0}t}f_2^-(t)dt\Bigg)\frac{e^{-\mu_{1,0}x}}{x} \\ & +\Bigg(d_2^- - \frac{3\tilde{\alpha}^2-\mu_{1,0}^2}{2\mu_{1,0}^2}\int_0^1 t\sinh(\mu_{1,0}t)f_2^-(t)dt \\ & -\frac{3\tilde{\alpha}^2-\mu_{1,0}^2}{4\mu_{1,0}^2}\int_x^1 te^{-\mu_{1,0}t}f_2^-(t)dt\Bigg)e^{\mu_{1,0}x} \\ & +\Bigg(d_2^- - \frac{3\tilde{\alpha}^2-\mu_{1,0}^2}{4\mu_{1,0}^2}\int_x^1 te^{\mu_{1,0}t}f_2^-(t)dt\Bigg)e^{-\mu_{1,0}x}, \end{aligned} \tag{3.104}$$

and

$$\begin{aligned} w^+(x) = & \Bigg(\frac{3\tilde{\alpha}^2}{4\mu_{1,0}^3}\int_x^{+\infty} t(\mu_{1,0}t+1)e^{-\mu_{1,0}t}f_2^+(t)dt \\ & +\frac{1}{4\mu_{1,0}}\int_x^{+\infty} t(1-\mu_{1,0}t)e^{-\mu_{1,0}t}f_2^+(t)dt\Bigg)\frac{e^{\mu_{1,0}x}}{x} \\ & -\Bigg(\frac{3\tilde{\alpha}^2-\mu_{1,0}^2}{4\mu_{1,0}^2}\int_x^{+\infty} te^{-\mu_{1,0}t}f_2^+(t)dt\Bigg)e^{\mu_{1,0}x} \\ & +\Bigg(d_2^+ + \frac{3\tilde{\alpha}^2-\mu_{1,0}^2}{4\mu_{1,0}^2}\int_1^x te^{\mu_{1,0}t}f_2^+(t)dt\Bigg)e^{-\mu_{1,0}x} \\ & +\Bigg(d_1^+ + \frac{3\tilde{\alpha}^2}{4\mu_{1,0}^3}\int_1^x t(1-\mu_{1,0}t)e^{\mu_{1,0}t}f_2^+(t)dt \\ & +\frac{1}{4\mu_{1,0}}\int_1^x t(1+\mu_{1,0}t)e^{\mu_{1,0}t}f_2^+(t)dt\Bigg)\frac{e^{-\mu_{1,0}x}}{x}, \end{aligned} \tag{3.105}$$

where $d_1^\pm$ and $d_2^\pm$ are arbitrary complex constants. Then, replacing the expressions of $w^\pm$ so far obtained in the first differential equation in (3.103), we get

$$p^-(x) = \frac{\mu_{1,0}^2-\lambda}{\tilde{\beta}}w^-(x) + 2\mu_{1,0}\Bigg(d_2^- - \frac{3\tilde{\alpha}^2-\mu_{1,0}^2}{2\mu_{1,0}^2}\int_0^1 t\sinh(\mu_{1,0}t)f_2^-(t)dt$$

$$+\frac{3\tilde{\alpha}^2-\mu_{1,0}^2}{4\mu_{1,0}^2}\int_1^x te^{-\mu_{1,0}t}f_2^-(t)dt\Big)\frac{e^{\mu_{1,0}x}}{x}$$

$$-2\mu_{1,0}\Big(d_2^-+\frac{3\tilde{\alpha}^2-\mu_{1,0}^2}{4\mu_{1,0}^2}\int_1^x te^{\mu_{1,0}t}f_2^-(t)dt\Big)\frac{e^{-\mu_{1,0}x}}{x},\quad x\in I_1^-,\ (3.106)$$

and

$$p^+(x)=\frac{\mu_{1,0}^2-\lambda}{\tilde{\beta}}w^+(x)-\Big(\frac{3\tilde{\alpha}^2-\mu_{1,0}^2}{2\mu_{1,0}\tilde{\beta}}\int_x^{+\infty}te^{-\mu_{1,0}t}f_2^+(t)dt\Big)\frac{e^{\mu_{1,0}x}}{x}$$

$$-2\frac{\mu_{1,0}}{\tilde{\beta}}\Big(d_2^++\frac{3\tilde{\alpha}^2-\mu_{1,0}^2}{4\mu_{1,0}^2}\int_1^x te^{\mu_{1,0}t}f_2^+(t)dt\Big)\frac{e^{-\mu_1 x}}{x},\quad x\in I_1^+.\ (3.107)$$

Now, a density argument shows that the formulas (3.104)-(3.107) define the solution of the system (3.100) (with the right-hand side of the differential equations for v and w, being replaced with the functions f_1 and $f_2^{\pm}$, respectively) also in the case when $\mathbf{f}\in\mathcal{X}$. Imposing the boundary conditions, we are led to a linear system of five equations in five unknowns that is uniquely solvable if and only if the matrix $M^{(1)}$ defined by

$$M^{(1)}=\begin{pmatrix} m_{11}^{(1)}e^{-\sqrt{\lambda_0\mathrm{Le}}} & m_{12}^{(1)}e^{-\mu_{1,0}} & m_{13}^{(1)}e^{-\mu_{1,0}} & m_{14}^{(1)} & m_{15}^{(1)}\\ m_{21}^{(1)}e^{-\sqrt{\lambda_0\mathrm{Le}}} & m_{22}^{(1)}e^{-\mu_{1,0}} & m_{23}^{(1)}e^{-\mu_{1,0}} & m_{24}^{(1)} & m_{25}^{(1)}\\ m_{31}^{(1)}e^{-\sqrt{\lambda_0\mathrm{Le}}} & m_{32}^{(1)}e^{-\mu_{1,0}} & m_{33}^{(1)}e^{-\mu_{1,0}} & m_{34}^{(1)} & m_{35}^{(1)}\\ 0 & m_{42}^{(1)}e^{-\mu_{1,0}} & m_{43}^{(1)}e^{-\mu_{1,0}} & m_{44}^{(1)} & m_{45}^{(1)}\\ 0 & m_{52}^{(1)}e^{-\mu_{1,0}} & m_{53}^{(1)}e^{-\mu_{1,0}} & m_{54}^{(1)} & m_{55}^{(1)}\end{pmatrix},$$

where

$$\mathrm{Le}\,m_{11}^{(1)}=m_{12}^{(1)}=m_{13}^{(1)}=1,\quad m_{14}^{(1)}=-\sinh(\mu_{1,0}),$$
$$m_{15}^{(1)}=-\cosh(\mu_{1,0}),\quad \mathrm{Le}\,m_{21}^{(1)}=\sqrt{\lambda_0\mathrm{Le}}+1,$$
$$m_{22}^{(1)}=\mu_{1,0}+1,\quad m_{23}^{(1)}=\mu_{1,0},$$
$$m_{24}^{(1)}=\mu_{1,0}\cosh(\mu_{1,0})-\sinh(\mu_{1,0}),\quad m_{25}^{(1)}=\mu_{1,0}\sinh(\mu_{1,0}),$$
$$m_{31}^{(1)}=\sqrt{\lambda_0\mathrm{Le}}-1,\quad m_{32}^{(1)}=m_{33}^{(1)}=\mathrm{Le}\,a,$$
$$m_{34}^{(1)}=\mathrm{Le}\,b\sinh(\mu_{1,0}),\quad m_{35}^{(1)}=\mathrm{Le}\,b\cosh(\mu_{1,0}),$$
$$m_{42}^{(1)}=\pm i\tilde{\alpha}\sqrt{3\tilde{\alpha}\tilde{\beta}},\quad m_{43}^{(1)}=\pm i\tilde{\alpha}\sqrt{3\tilde{\alpha}\tilde{\beta}}+2\mu_{1,0},$$
$$m_{44}^{(1)}=\mp i\tilde{\alpha}\sqrt{3\tilde{\alpha}\tilde{\beta}}\sinh(\mu_{1,0}),$$
$$m_{45}^{(1)}=\mp i\tilde{\alpha}\sqrt{3\tilde{\alpha}\tilde{\beta}}\cosh(\mu_{1,0})+2\mu_{1,0}\sinh(\mu_{1,0}),$$
$$m_{52}^{(1)}=\pm i\alpha\sqrt{3\tilde{\alpha}\tilde{\beta}}(\mu_{1,0}+1),\quad m_{53}^{(1)}=\{\pm i\tilde{\alpha}\sqrt{3\tilde{\alpha}\tilde{\beta}}+2(\mu_{1,0}+1)\}\mu_{1,0},$$
$$m_{54}^{(1)}=\pm i\tilde{\alpha}\sqrt{3\tilde{\alpha}\tilde{\beta}}\{\mu_{1,0}\cosh(\mu_{1,0})-\sinh(\mu_{1,0})\},$$
$$m_{55}^{(1)}=\mu_{1,0}\{\pm i\tilde{\alpha}\sqrt{3\tilde{\alpha}\tilde{\beta}}\sinh(\mu_{1,0})-2\mu_{1,0}\cosh(\mu_{1,0})+2\sinh(\mu_{1,0})\},$$

is not singular. Therefore, if λ_0 is in $\sigma(A)$, then λ_0 is an eigenvalue of A.

Let us now suppose that $\mu_1^2 \neq \mu_3^2$. Then, $\operatorname{Re}\mu_1 \geq \operatorname{Re}\mu_3 > 0$. Arguing as above, we can easily show that the solutions $w^{\pm}$ and $p^{\pm}$ of System (3.103) are given by:

$$\begin{aligned} w^-(x) = &-\Bigg(d_1^- + \frac{3\tilde{\alpha}^2-\mu_1^2}{\mu_1(\mu_1^2-\mu_3^2)}\int_0^1 t\sinh(\mu_1 t) f_2^-(t)dt \\ &+\frac{3\tilde{\alpha}^2-\mu_1^2}{2\mu_1(\mu_1^2-\mu_3^2)}\int_x^1 te^{-\mu_1 t} f_2^-(t)dt\Bigg)\frac{e^{\mu_1 x}}{x} \\ &+\Bigg(d_1^- + \frac{3\tilde{\alpha}^2-\mu_1^2}{2\mu_1(\mu_1^2-\mu_3^2)}\int_x^1 te^{\mu_1 t} f_2^-(t)dt\Bigg)\frac{e^{-\mu_1 x}}{x} \\ &+\Bigg(d_2^- - \frac{3\tilde{\alpha}^2-\mu_3^2}{2\mu_3(\mu_1^2-\mu_3^2)}\int_x^1 te^{\mu_3 t} f_2^-(t)dt\Bigg)\frac{e^{-\mu_3 x}}{x} \\ &-\Bigg(d_2^- - \frac{3\tilde{\alpha}^2-\mu_3^2}{\mu_3(\mu_1^2-\mu_3^2)}\int_0^1 t\sinh(\mu_3 t) f_2^-(t)dt \\ &-\frac{3\tilde{\alpha}^2-\mu_3^2}{2\mu_3(\mu_1^2-\mu_3^2)}\int_x^1 te^{-\mu_3 t} f_2^-(t)dt\Bigg)\frac{e^{\mu_3 x}}{x} \\ &:= w_1^-(x)+w_2^-(x)+w_3^-(x)+w_4^-(x), \end{aligned}$$

for any $x \in I_1^-$,

$$\begin{aligned} w^+(x) = &\Bigg(d_1^+ - \frac{3\tilde{\alpha}^2-\mu_1^2}{2\mu_1(\mu_1^2-\mu_3^2)}\int_1^x te^{\mu_1 t} f_2^+(t)dt\Bigg)\frac{e^{-\mu_1 x}}{x} \\ &-\frac{3\tilde{\alpha}^2-\mu_1^2}{2\mu_1(\mu_1^2-\mu_3^2)}\Bigg(\int_x^{+\infty} te^{-\mu_1 t} f_2^+(t)dt\Bigg)\frac{e^{\mu_1 x}}{x} \\ &+\Bigg(d_2^+ + \frac{3\tilde{\alpha}^2-\mu_3^2}{2\mu_3(\mu_1^2-\mu_3^2)}\int_1^x te^{\mu_3 t} f_2^+(t)dt\Bigg)\frac{e^{-\mu_3 x}}{x} \\ &+\frac{3\tilde{\alpha}^2-\mu_3^2}{2\mu_3(\mu_1^2-\mu_3^2)}\Bigg(\int_x^{+\infty} te^{-\mu_3 t} f_2^+(t)dt\Bigg)\frac{e^{\mu_3 x}}{x} \\ &:= w_1^+(x)+w_2^+(x)+w_3^+(x)+w_4^+(x), \end{aligned}$$

for any $x \in I_1^+$,

$$p^{\pm} = \frac{\mu_1^2-\lambda}{\tilde{\beta}}(w_1^{\pm}+w_2^{\pm}) + \frac{\mu_3^2-\lambda}{\tilde{\beta}}(w_3^{\pm}+w_4^{\pm}),$$

where $d_1^{\pm}$ and $d_2^{\pm}$ are arbitrary complex constants. Imposing the boundary conditions we are led to a system of five equations in the unknowns

$(c, d_1^+, d_2^+, d_1^-, d_2^-)$, whose associated matrix $M_\lambda^{(2)}$ is given by

$$M_\lambda^{(2)} = \begin{pmatrix} m_{11}^{(2)} e^{-\sqrt{\lambda \mathrm{Le}}} & m_{12}^{(2)} e^{-\mu_1} & m_{13}^{(2)} e^{-\mu_3} & m_{14}^{(2)} & m_{15}^{(2)} \\ m_{21}^{(2)} e^{-\sqrt{\lambda \mathrm{Le}}} & m_{22}^{(2)} e^{-\mu_1} & m_{23}^{(2)} e^{-\mu_3} & m_{24}^{(2)} & m_{25}^{(2)} \\ m_{31}^{(2)} e^{-\sqrt{\lambda \mathrm{Le}}} & m_{32}^{(2)} e^{-\mu_1} & m_{33}^{(2)} e^{-\mu_3} & m_{34}^{(2)} & m_{35}^{(2)} \\ 0 & m_{42}^{(2)} e^{-\mu_1} & m_{43}^{(2)} e^{-\mu_3} & m_{44}^{(2)} & m_{45}^{(2)} \\ 0 & m_{52}^{(2)} e^{-\mu_1} & m_{53}^{(2)} e^{-\mu_3} & m_{54}^{(2)} & m_{55}^{(2)} \end{pmatrix},$$

where

$$\mathrm{Le}\, m_{11}^{(2)} = m_{12}^{(2)} = m_{13}^{(2)} = 1, \qquad m_{1\,4+j}^{(2)} = -\sinh(\mu_{2j+1}), \quad (j = 0, 1),$$

$$\mathrm{Le}\, m_{21}^{(2)} = \sqrt{\lambda \mathrm{Le}} + 1, \qquad m_{2\,2+j}^{(2)} = \mu_{2j+1} + 1,$$

$$m_{2\,4+j}^{(2)} = \mu_{2j+1} \cosh(\mu_{2j+1}) - \sinh(\mu_{2j+1}), \quad (j = 0, 1),$$

$$m_{31}^{(2)} = \sqrt{\lambda \mathrm{Le}} - 1, \quad m_{32}^{(2)} = m_{33}^{(2)} = \mathrm{Le}\, a,$$

$$m_{3\,4+j}^{(2)} = \mathrm{Le}\, b \sinh(\mu_{2j+1}), \quad m_{4\,2+j}^{(2)} = \lambda - \mu_{2j+1}^2 + \tilde{\alpha}\tilde{\beta}, \quad (j = 0, 1),$$

$$m_{4\,4+j}^{(2)} = (\mu_{2j+1}^2 - \lambda - \tilde{\alpha}\tilde{\beta}) \sinh(\mu_{2j+1}), \quad (j = 0, 1),$$

$$m_{5\,2+j}^{(2)} = -(\mu_{2j+1}^2 - \lambda - \tilde{\alpha}\tilde{\beta})(\mu_{2j+1} + 1), \quad (j = 0, 1),$$

$$m_{5\,4+j}^{(2)} = -(\mu_{2j+1}^2 - \lambda - \tilde{\alpha}\tilde{\beta})\{\mu_{2j+1} \cosh(\mu_{2j+1}) - \sinh(\mu_{2j+1})\}, \quad (j = 0, 1).$$

It follows that $\lambda \in \sigma(A)$ if and only if λ is a root of the Evans function $\mathcal{E} : \{\lambda \in \mathbb{C} : \ \mathrm{Re}\, \lambda > 0\} \setminus \{\lambda_0\} \to \mathbb{C}$, defined by $\mathcal{E}(\lambda) = \det M_\lambda$, where $M_\lambda = M_\lambda^{(2)}$, if $\mu_1^2 \neq \mu_2^3$, and $M_\lambda = M^{(1)}$ otherwise.

Summing up, we have proved that if $\lambda \in \sigma(A)$ has positive real part, then it is an eigenvalue of A.

To conclude this point of the proof, let us observe that $\mathcal{E}(\lambda) = \mu_1\mu_3(\mu_1^2 - \mu_3^2)^2 e^{-\sqrt{\lambda \mathrm{Le}}} \tilde{\mathcal{E}}(\lambda)$ for any $\lambda \in \mathbb{C}$ with positive real part and some function $\tilde{\mathcal{E}}$. Since $\mu_1 \neq \mu_3$ and they both differ from 0, we can limit ourselves to showing that, under the condition (3.49), the function $\tilde{\mathcal{E}}$ has a positive zero. For this purpose, it suffices to observe that $\tilde{\mathcal{E}}(\lambda)$ tends to $+\infty$ as λ tends to $+\infty$ and

$$\tilde{\mathcal{E}}(\lambda) = -1 - \frac{(2R\mu + 1)\exp(-2R\mu) - 1}{2\mu^3} \alpha\beta F'(\Theta(R)) + o(1),$$

where $\mu = \sqrt{3\alpha^2 + \alpha\beta}$, as λ tends to 0^+. Therefore, if the condition (3.49) is satisfied, the function $\tilde{\mathcal{E}}$ should admit a positive root λ_1. Equivalently, the matrix M_{λ_1} is singular, so that λ_1 is in the spectrum of A.

Finally, showing that, if $\lambda \in \sigma(A)$ has positive real part, then there exists a eigenfunction $\mathbf{u} = (v, w^-, w^+)$ corresponding to such λ, with $v(x) \neq 0$ for any $x \in I_1^+$, is an immediate consequence of the previous computations. Indeed, the matrices $\tilde{M}^{(1)}$ and $\tilde{M}_\lambda^{(2)}$ (for any λ with positive real part), obtained, respectively, from $M^{(1)}$ and $M_\lambda^{(2)}$ by erasing

the first column and the third row are invertible since their determinant are given, respectively, by

$$\det M^{(1)} = 4\mu_1^4 e^{2\mu_1}, \qquad \det M_\lambda^{(2)} = -\mu_1\mu_3(\mu_1^2 - \mu_3^2)^2 e^{\mu_1+\mu_3}.$$

This means that we can uniquely determine the constants $d_1^\pm$ and $d_2^\pm$ in terms of c or, equivalently, that there exists an eigenfunction $\mathbf{u}$ with $v \neq 0$. This completes the proof of Theorem 3.5. □

CHAPTER 4

On a model of flame ball with radiative transfer

4.1. Introduction

Spherical flame balls have been found to exist as stable objects for small enough Lewis number during some experiments carried out at microgravity [**45, 46**]. Since Zeldovich, "adiabatic" flame balls are unstable to one-dimensional radial perturbations, a stabilizing effect has to be identified. It has been argued [**44**] that radiation is physically important in near limit combustion at low gravity. Then, it is natural to consider a heat loss mechanism through radiation as a stabilizing effect. Moreover it is worth noting that halon (CF_3Br) is added to experimental mixtures (to increase the luminosity of flame balls) which augment the radiation through soot formation.
Buckmaster et al. [**16, 17**] proposed different models to take into account the heat loss through radiation. They considered first constant heat losses in the burnt gases [**16**]: when the heat losses are not too large, they proved the existence of two possible steady flame balls: a small one and a large one. It is proved that they have different linear stability properties: the small flame ball, similar to the Zeldovich flame is unstable under radial perturbations whereas the large flame ball is stable under radial perturbations but unstable under three dimensional perturbation if its radius is too large. Similar results have been obtained for a refined version of the previous model where linear far field heat loss are considered [**17**]. Using matched asymptotic expansions for large activation energy, Buckmaster et al. [**16, 17**] derived an integro-differential model for the nonlinear radial motion of the flame when $Le < 1$:

$$\partial_{1/2} R(\tau) = \log R(\tau) - \lambda R(\tau)^2 + \frac{Eq(\tau)}{R(\tau)},\ R(0) = 0,$$

with $\partial_{1/2}R = \frac{d}{dt}\int_0^t \frac{R(s)}{\sqrt{\pi(t-s)}}ds$ and $Eq(\tau)$ represents the amount of energy injected in the system. Numerical simulations of this model suggested that the small flame ball is unstable and the large one is stable. Recently, Rouzaud [**47**] carried out a rigorous study of the long time behaviour of flame balls for this equation which confirms this qualitative behaviour. Moreover, Rouzaud et al. developed adaptated numerical schemes for this kind of equations that possess similar mathematical properties and exhibit the same type of asymptotic behaviour [**5**].

More refined models have been considered with reaction taking place within an unbounded medium that contains a small volume fraction of porous solid which only exchange heat with the gas [**22**]. Heat losses through radiation are modeled in two different ways: either they are constant in the burnt gas and linear in the unburnt gas (similarly to Buckmaster et al. studies) either they are a continuous dimensionless form of Stefan's law having a linear part that dominates close to ambient temperatures and a fourth power that dominates at higher temperatures. Similarly, two branches of solutions are found, the branch of large flame balls being linearly stable and the smaller one being unstable.

Recently, Guyonne et al. [**53**] proposed an other mechanism to take into account the radiation and considered a model of flame with *radiative transfer*. Indeed the presence of particles in the mixture generates a radiation field approximated by the well known Eddington equation

$$-\nabla\nabla\cdot q + 3\alpha^2 q + \alpha\nabla\theta^4 = 0,$$

where q represents the radiative flux, θ the temperature and α the opacity of the medium. This system is coupled with a classical free boundary combustion model with simple chemistry $F \to B$, where F is the fresh gas and B the burnt gas. This model is derived in the high activation limit, the reaction occurring in a reaction sheet located at $r = R(t)$ and can be written:

$$\begin{aligned} &\partial_t Y - \frac{1}{\mathrm{Le}}\Delta Y = 0,\ r > R(t),\ Y = 0,\ r < R(t),\\ &\partial_t\theta - \Delta\theta = -\beta\nabla\cdot q, \qquad\qquad r \neq R(t), \end{aligned}$$

with the jump conditions at $r = R(t)$

$$[\theta] = [y] = 0,\ \frac{1}{Le}[Y_r] = -[\theta_r] = F_\epsilon(\theta(R(t))),$$

where $F_\epsilon(\theta)$ is the reaction rate modeled by an Arrhenius law. It is proved that there exists steady flame balls for this model. Moreover, numerical simulations with numerical continuation software show that for the same set of parameters there exist several steady flames. Then

the question of their stability arises. Even in the simpler case where a linearized Eddington law is considered:

$$-\nabla\nabla\cdot q + 3\alpha^2 q + \alpha\nabla\theta = 0,$$

the question of the linear and nonlinear stability of steady flame ball is far from being understood: we shall mention here the works of Guyonne, Hulshof and Van den Berg [**54**] on the numerical analysis of the Evans function for the linear and nonlinear Eddington law and the paper of Guyonne and Lorenzi [**27**] which proves that spectral instability implies nonlinear instability with semi-group techniques. Getting nonlinear stability within this framework is quite a hard problem and is an open problem.

The purpose of this paper is to analyze the stabilizing effect of *radiative transfer* with the view point developed by Buckmaster et al. [**16, 17**]. Indeed to study the nonlinear growth of radial solutions, they derived an integro-differential equation using matched asymptotic expansions. This approach has been justified rigorously by Roquejoffre et al. [**33**] for the adiabatic model with a direct derivation from the reaction diffusion system. Moreover the asymptotic behaviour of this kind of integro-differential equations is now well understood and efficient numerical schemes are available. The aim of this paper is two fold: through the formal derivation of the same type of integro-differential equations for the flame balls growth, the mathematical and numerical analysis of this model, we want, on the one hand, to study the stabilizing effect of the *radiative transfer* in the formation of flame balls. On the other hand, for this particular model of radiative transfer (the linearized Eddington equation), we want to discuss directly the dynamic of flame balls and the stability of steady flame balls *under radial perturbations* obtained in [**53**]. We are not concerned here with the stability of flame balls under three dimensional perturbations. It is worth noting that the approach proposed is very complementary to the indirect approach which consists in studying the linear stability and then getting informations for the full nonlinear free boundary problem problem. Moreover, if it is possible to justify rigorously this formal derivation similarly to the paper of Roquejoffre et al. [**33**], this should give a complete answer on the nonlinear stability of flame balls *under radial perturbations* in the presence of radiative transfer, but this justification is a hard issue.

The paper is organized as follow: in Section 4.2, we derive an integro differential equation for the nonlinear radial motion of a flame ball using matched asymptotic expansions:

$$\partial_{1/2}R(\tau) = \log R(\tau) - \lambda R(\tau) + \frac{Eq(\tau)}{R(\tau)}\cdot \tag{4.1}$$

The dynamic is articulated around the two steady flame balls with radius $R_1 < R_2$ solutions of $\log R = \lambda R$, provided that $\lambda < \frac{1}{e}$. In Section 4.3 we study mathematically the asymptotic behaviour of the solutions of (4.1) and discuss the stability of the "large" flame ball with radius R_2 and instability of the "small" flame ball with radius R_1. In Section 4.4, we carry out numerical computations on Equation (4.1) using the numerical schemes designed by Rouzaud et al.

4.2. Growth model for the radius of flame balls

We consider the following model of combustion with simple chemistry coupled with the *linearized* Eddington equation:

$$\begin{array}{l} \partial_t y - \dfrac{1}{Le}\Delta y = 0, r > R(t),\ y = 0, r < R(t), \\ \partial_t \theta - \Delta\theta = \beta u,\ -\Delta u + 3\alpha^2 u = \alpha\Delta\theta,\ r \neq R(t), \end{array} \tag{4.2}$$

where u denotes $u = -\nabla \cdot q$, supplemented with the jump conditions at $r = R(t)$

$$\begin{array}{l} [u] = [\theta] = [y] = 0, \\ [u_r] = -\alpha[\theta_r],\ \dfrac{1}{Le}[y_r] = -[\theta_r] = F_\epsilon(\theta(R(t))). \end{array} \tag{4.3}$$

Moreover the functions (y, θ, u) must satisfy the conditions at infinity

$$\lim_{r\to\infty}(y(r), \theta(r), u(r)) = (1, 0, 0). \tag{4.4}$$

The reaction rate F_ϵ is given by an Arrhenius law $F_\epsilon(\theta) = A \exp -\frac{1}{\epsilon\theta}$: the constant A is a pre-exponential factor and ϵ^{-1} is the activation energy which is assumed to be large ($0 < \epsilon << 1$). In order to derive an equation for the growth of a flame ball, we follow the methodology introduced by G. Joulin and divide the space into two concentric regions: a quasi-stationary zone where time derivatives are neglected where the combustion occurs and a far field zone where the only phenomenons that are taken into account are diffusion of the reactant and the temperature. The radiative effects are considered both in the reaction zone and the far field zone. We then obtain an equation for the radius by matching the derivatives of the inner quasi-stationary solution and the outer solution.

Steady solutions

Before computing quasi-steady solutions, let us first compute the steady solutions of (4.2, 4.3, 4.4). Let us fix the radius $R > 0$ and define η as $\eta = \eta_{\alpha\beta} = \sqrt{3\alpha^2 + \alpha\beta}$. Then there exists a unique steady

solution with the following analytic expression:

$$u(r) = \begin{cases} -\dfrac{B_1\eta^2}{\beta r}\sinh(\eta r) & \text{for } r \le R, \\ -\dfrac{B_2\eta^2}{\beta r}\exp(-\eta r) & \text{for } r > R. \end{cases} \tag{4.5}$$

where the constants are given by

$$B_1 = \frac{\alpha\beta}{\mathrm{Le}\eta^3}\exp(-\eta R), \qquad B_2 = \frac{\alpha\beta}{\mathrm{Le}\eta^3}\sinh(\eta R), \qquad B_3 = \frac{3\alpha^2}{\mathrm{Le}\eta^2}.$$

The expression for θ is

$$\theta(r) = \begin{cases} \dfrac{B_1}{r}\sinh(\eta r) + B_3 & \text{for } r \le R, \\ \dfrac{B_2}{r}\exp(-\eta r) + \dfrac{B_3 R}{r} & \text{for } r > R, \end{cases} \tag{4.6}$$

Finally the solution for the mass fraction variable is expressed by

$$y(r) = \max(0, 1 - \frac{R}{r}). \tag{4.7}$$

Then the temperature at the front is given by

$$Le\theta(R) = 1 + \frac{\alpha\beta}{\eta^2}\Big(\frac{1-\exp(-2\eta R)}{2\eta R} - 1\Big).$$

Note that the dependence of the temperature at the front with respect to the flame radius in the case where radiative transfer is taken into account is different from the case where heat loss radiative terms are considered. In the latter case, the dependence is *parabolic* [**16**].

It is easily seen with equation (4.7) that $[y_r]_{|r=R} = \frac{1}{R}$. Then the steady flame balls are the steady solutions (y, θ, u) defined by (4.5, 4.6, 4.7) such that R is solution of

$$F_\epsilon(\theta(R)) = \frac{1}{RLe} \tag{4.8}$$

The case where $\alpha, \beta \to 0$ as $\epsilon \to 0$ is of particular interest: as a matter of fact, Buckmaster et al. [**16, 17**] also considered vanishing heat loss terms as $\epsilon \to 0$. As a consequence, in some asymptotic parameter regimes, it is possible to simplify Equation (4.8). Under the scaling, $\beta = \overline{\beta}\epsilon$ and $\alpha >> \beta$ (we can choose $\alpha = O(\epsilon^\mu)$ with $0 < \mu < 1$) and $0 < \epsilon << 1$, we find that

$$\theta(R) = \frac{1}{Le} - \frac{\overline{\beta}\epsilon}{Le\sqrt{3}}R + O(\epsilon^2).$$

Inserting this relation into (4.8) and letting $\epsilon \to 0$, one finds

$$\log\frac{R}{R_{ad}} = \frac{\overline{\beta}Le}{\sqrt{3}}R, \tag{4.9}$$

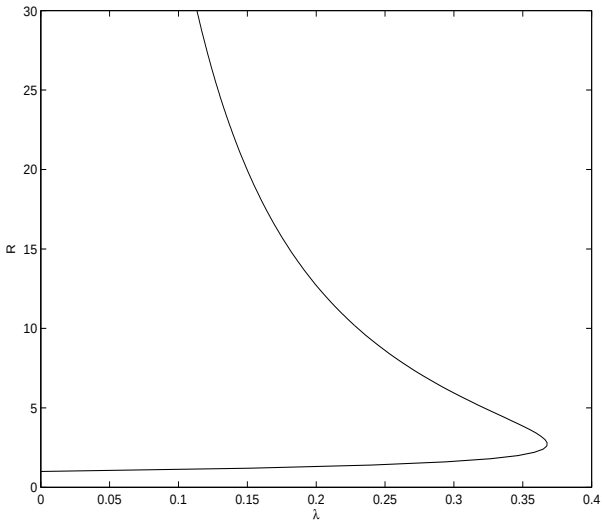

Figure 4.1: Diagram of bifurcation of equation (4.9) in the $(\lambda = \frac{\overline{\beta} Le}{\sqrt{3}}, R)$ plane.

where R_{ad} denotes the adiabatic radius. The set of solutions of equation (4.9) is plotted in Figure 4.1 in the (R, λ)-plane where $\lambda = \frac{\overline{\beta} Le}{\sqrt{3}}$.

We can see that for $\lambda > \lambda_{cr} = \frac{1}{R_{ad} e}$, no solution exists and for $\lambda < \lambda_{cr}$, there exists two solutions $R_1 < R_2$ which corresponds to steady flame balls. The smaller flame ball converges to the flame ball constructed by Zeldovich in the limit $\lambda \to 0$.

It is important to note the difference between the equation for steady flame balls (4.9) when *radiative transfer* is taken into account and the equation for steady flame balls when *radiative heat losses* are considered (which are constant in the burnt phase of order $O(\epsilon)$, linear in the fresh phase and of order $O(\epsilon^2)$). In that case, the equation for steady flame balls reads

$$\log(\frac{R}{R_{ad}}) = \Lambda \, R^2,$$

where Λ is a constant depending on heat loss terms. The difference between the two equations is that, considering *constant heat loss term* in the burnt gas, the temperature at the front $\theta(R)$ is a *parabolic* function of the flame radius whereas in the case of radiative transfer, the temperature at the front is a *linear* function of the flame radius (in the parameter regime considered previously).

Inner solutions

Now we consider the non stationary case and we suppose that the flame has a spherical symmetry with a flame radius at $r = R(t)$. The purpose is to compute an equation satisfied by $R(t)$. Let us denote (Y, Θ, U) the steady solution computed at the previous section and fix $\nu \in (0,1)$. We are first going to compute an approximation of the solution (y, θ, u) on $B(0, \epsilon^{-\nu})$, considering that it is a quasi steady solution with a flame radius $r = R(t) << \epsilon^{-\nu}$. We write the solution (y, θ, u) as

$$(y, \theta, u) = (1 + \epsilon v(t))\big(Y, \Theta, U\big) + (0, \epsilon w(t), 0).$$

This solution satisfies the steady equations and the jump conditions provided that

$$\frac{1 + \epsilon v(t)}{RLe} = F_\epsilon\big(\Theta(R) + \epsilon(\Theta(R)v + w)\big).$$

This equation reads, up to order $O(\epsilon)$

$$v + \frac{w}{\Theta(R)} = -\log(RLe) - \log\Big(F_\epsilon\big(\Theta(R)\big)\Big).$$

The boundary conditions at $r = \epsilon^{-\nu}$ are given by:

$$\begin{aligned}
\theta(t, \epsilon^{-\nu}) &= \frac{3\alpha^2}{Le(3\alpha^2 + \alpha\beta)} R\epsilon^\nu + \epsilon w(t) + O(\epsilon^{\nu+1}), \\
y(t, \epsilon^{-\nu}) &= 1 - \epsilon^\nu R(t) + \epsilon v(t) + O(\epsilon^{\nu+1}), \\
u(t, \epsilon^{-\nu}) &= -\frac{\alpha(1 + \epsilon v(t))\epsilon^\nu}{Le\sqrt{3\alpha^2 + \alpha\beta}} \sinh(R\sqrt{3\alpha^2 + \alpha\beta}) \exp(-\frac{\sqrt{3\alpha^2 + \alpha\beta}}{\epsilon^\nu}) \\
&= O(\epsilon^{\nu+3}).
\end{aligned} \tag{4.10}$$

The last estimate on u is valid provided that $\sqrt{3\alpha^2 + \alpha\beta} = O(\epsilon^\mu)$ with $\mu < \nu$.

Outer solution

We compute an approximate solution (y, θ, u) outside $B(0, \epsilon^{-\nu})$ of

$$\partial_t y - \frac{1}{Le}\Delta y = 0, \;\; \partial_t \theta - \Delta\theta = \beta u, \;\; -\Delta u + 3\alpha^2 u = \alpha\Delta\theta,$$

supplemented with the boundary conditions (4.10); the conditions at infinity are given by $\lim_{r\to\infty}(y, \theta, u) = (1, 0, 0)$ and the initial conditions will be specified later. Following the derivation of Joulin, we rescale time and space: $\tau = \epsilon^2 t$, $\rho = \epsilon r$ and define

$$(\overline{y}, \overline{\theta}, \overline{u})(\tau, \rho) = \big(\frac{y(t,r) - 1}{\epsilon}, \frac{\theta(t,r)}{\epsilon}, \frac{u(t,r)}{\epsilon^3}\big), \overline{R}(\tau) = R(t).$$

Then $(\overline{y},\overline{\theta},\overline{u})$ satisfies the rescaled system

$$\partial_\tau \overline{y} - \frac{1}{Le}\Delta\overline{y} = 0,\ \ \partial_\tau\overline{\theta} - \Delta\overline{\theta} = \beta\overline{u},\ \ -\epsilon^2\Delta\overline{u} + 3\alpha^2\overline{u} = \alpha\Delta\overline{\theta},$$

with the boundary conditions

$$\begin{aligned}
&\overline{y}(\tau,\epsilon^{1-\nu}) = -\epsilon^{\nu-1}\overline{R}(\tau) + \overline{v}(\tau) + O(\epsilon^\nu),\\
&\overline{\theta}(\tau,\epsilon^{1-\nu}) = \epsilon^{\nu-1}\frac{3\alpha^2}{Le(3\alpha^2+\alpha\beta)}\overline{R}(\tau) + \overline{w}(\tau) + O(\epsilon^\nu),\\
&\overline{u}(\tau,\epsilon^{1-\nu}) = O(\epsilon^\nu).
\end{aligned}$$

We are only interested in the jumps of the radial derivatives, namely $(\rho\overline{y})_\rho$, $(\rho\overline{\theta})_\rho$ evaluated at the point $\rho = \epsilon^{1-\nu}$. Let us start with

$$\frac{\partial}{\partial\rho}(\rho\overline{y})_{|\rho=\epsilon_+^{1-\nu}}$$

and define $Y = \rho\overline{y}$ for all $\rho > \epsilon^{1-\nu}$. Then extend Y on $\mathbb{R}$ by an odd function $\overline{Y}$ so that

$$\overline{Y}(\tau,\rho) = \begin{cases} Y(\tau,\frac{1}{\sqrt{Le}}\rho + \epsilon^{1-\nu}) - Y(\tau,\epsilon^{1-\nu}), & \text{for } \rho > 0,\\ -Y(\tau,-\frac{1}{\sqrt{Le}}\rho + \epsilon^{1-\nu}) + Y(\tau,\epsilon^{1-\nu}), & \text{for } \rho < 0. \end{cases}$$

Denote $\psi(\tau) = Y(\tau,\epsilon^{1-\nu}) = -\overline{R}(\tau) + O(\epsilon^{1-\nu})$: $\overline{Y}$ satisfies the equation

$$\overline{Y}_\tau - \overline{Y}_{\rho\rho} = \dot\psi(\tau)\big(1_{]-\infty,0[}(\rho) - 1_{]0,\infty[}(\rho)\big),$$

with initial condition

$$\overline{Y}(0,\rho) = \begin{cases} Y(0,\frac{1}{\sqrt{Le}}\rho + \epsilon^{1-\nu}) - \psi(0), & \text{for } \rho > 0,\\ -Y(0,-\frac{1}{\sqrt{Le}}\rho + \epsilon^{1-\nu}) + \psi(0), & \text{for } \rho < 0. \end{cases}$$

Then we find that

$$\begin{aligned}
\overline{Y}(\tau,\rho) = &\frac{1}{\sqrt{4\pi\tau}}\int_0^\infty \big(Y(0,\frac{x}{\sqrt{Le}} + \epsilon^{1-\nu}) - \psi(0)\big)\big(e^{-\frac{|x-\rho|^2}{4\tau}} - e^{-\frac{|x+\rho|^2}{4\tau}}\big)dx\\
&- \int_0^\tau\int_0^\infty \dot\psi(s)\frac{e^{-\frac{|x-\rho|^2}{4(\tau-s)}} - e^{-\frac{|x+\rho|^2}{4(\tau-s)}}}{\sqrt{4\pi(\tau-s)}}dxds.
\end{aligned}$$

Derive $\overline{Y}$ with respect to ρ and take the value at point $\rho = 0$:

$$\frac{\partial}{\partial\rho}(\rho\overline{y})_{|\rho=\epsilon^{1-\nu}} = \sqrt{Le}\frac{\partial\overline{Y}}{\partial\rho}_{|\rho=0} = -\sqrt{Le}\partial_{1/2}\psi(\tau) + \phi_y(\tau),$$

where ϕ_y is only function of the initial data $y(0,x)$, given by

$$\phi_y(\tau) = \frac{Le^{\frac{3}{2}}}{\sqrt{4\pi\tau}}\int_{\epsilon^{1-\nu}}^\infty \big(x\overline{y}(0,x) - \epsilon^{1-\nu}\overline{y}(0,\epsilon^{1-\nu})\big)\frac{x-\epsilon^{1-\nu}}{\tau}e^{-Le\frac{(x-\epsilon^{1-\nu})^2}{4\tau}},$$

and the fractional derivative $\partial_{1/2}\psi(\tau)$ is the function

$$\partial_{1/2}\psi(\tau) = \frac{d}{dt}\int_0^t \frac{\psi(s)}{\sqrt{\pi(t-s)}}ds.$$

As a conclusion, we find that

$$\frac{\partial}{\partial\rho}(\rho\overline{y})^+_{|\rho=\epsilon^{1-\nu}} = \sqrt{Le}\partial_{1/2}\overline{R} + \phi_y(\tau) + O(\epsilon^{1-\nu}).$$

We compute the derivative of $\rho\overline{\theta}$ at point $\rho = \epsilon^{1-\nu}$: following the analysis made previously, one introduces the functions $T = \rho\overline{\theta}$, $V = \rho\overline{u}$ and defines

$$\overline{T}(\tau,\rho) = \begin{cases} T(\tau,\rho+\epsilon^{1-\nu}) - T(\tau,\epsilon^{1-\nu}), & \text{for } \rho > 0, \\ -T(\tau,-\rho+\epsilon^{1-\nu}) + T(\tau,\epsilon^{1-\nu}), & \text{for } \rho < 0, \end{cases}$$

and

$$\overline{V}(\tau,\rho) = \begin{cases} V(\tau,\rho+\epsilon^{1-\nu}) - V(\tau,\epsilon^{1-\nu}), & \text{for } \rho > 0, \\ -V(\tau,-\rho+\epsilon^{1-\nu}) + V(\tau,\epsilon^{1-\nu}), & \text{for } \rho < 0. \end{cases}$$

The functions $\overline{T}, \overline{V}$ satisfy the system

$$\begin{array}{l} \partial_\tau\overline{T} - \overline{T}_{\rho\rho} = \beta\overline{V} + \dot{\overline{T}}_\epsilon H(\rho) - \beta\overline{V}_\epsilon(\tau)H(\rho), \\ -\epsilon^2\overline{V}_{\rho\rho} + 3\alpha^2\overline{V} = \alpha\overline{T}_{\rho\rho} + 3\alpha^2\overline{V}_\epsilon(\tau)H(\rho), \end{array} \tag{4.11}$$

with $H(\rho) = 1_{]-\infty,0[}(\rho) - 1_{]0,\infty[}$ and $(\overline{T}_\epsilon, \overline{V}_\epsilon) = \epsilon^{1-\nu}(\overline{\theta},\overline{u})(\tau,\epsilon^{1-\nu})$. Take the Fourier Transform of the system (4.11): this yields

$$\begin{array}{l} \partial_\tau\hat{\overline{T}} + \xi^2\hat{\overline{T}} = \beta\hat{\overline{V}} + \dot{\overline{T}}_\epsilon(\tau)\hat{H}(\xi) - \beta\overline{V}_\epsilon(\tau)\hat{H}(\xi), \\ (3\alpha^2+\epsilon^2\xi^2)\hat{\overline{V}} = -\alpha\xi^2\hat{\overline{T}} + 3\alpha^2\overline{V}_\epsilon(\tau)\hat{H}(\xi). \end{array} \tag{4.12}$$

Eliminating $\hat{\overline{V}}$ from (4.12) yields the equation on $\hat{\overline{T}}$:

$$\partial_\tau\hat{\overline{T}} + \xi^2(1+\frac{\alpha\beta}{3\alpha^2+\epsilon^2\xi^2})\hat{\overline{T}} = \dot{\overline{T}}_\epsilon\hat{H}(\xi) + \beta\overline{V}_\epsilon(\tau)(\frac{3\alpha^2}{3\alpha^2+\epsilon^2\xi^2} - 1)\hat{H}(\xi).$$

The function $\hat{\overline{T}}$ is given by

$$\begin{aligned} \hat{\overline{T}}(\tau,\xi) = & e^{-(1+\frac{\alpha\beta}{3\alpha^2+\epsilon^2\xi^2}\xi^2\tau)}\hat{\overline{T}}(0,\xi) + \int_0^\tau e^{-(1+\frac{\alpha\beta}{3\alpha^2+\epsilon^2\xi^2})\xi^2(\tau-s)}\hat{H}(\xi)\dot{\overline{T}}_\epsilon(s)ds \\ & - \int_0^\tau \overline{V}_\epsilon(s)\frac{\beta\epsilon^2\xi^2}{3\alpha^2+\epsilon^2\xi^2}\hat{H}(\xi)e^{-(1+\frac{\alpha\beta}{3\alpha^2+\epsilon^2\xi^2})\xi^2(\tau-s)}ds. \end{aligned}$$

The analysis is now completely similar to the case treated previously for the derivative of $\rho\overline{y}$ at the boundary: take the inverse Fourier transform of $\hat{\overline{T}}$ and derive $\overline{T}$ with respect to ρ. There exists ϕ_θ which is only a function of $\theta(0,.)$ such that

$$\frac{\partial}{\partial\rho}(\rho\overline{\theta})_{|\rho=\epsilon^{1-\nu}} = -\frac{1}{Le(1+\frac{\alpha\beta}{3\alpha^2})^{\frac{3}{2}}}\partial_{1/2}\overline{R} + \phi_\theta(\tau) + O(\epsilon^{1-\nu}).$$

Matching of the derivatives

Recall that the analysis of the outer solution yields

$$\begin{aligned}\frac{\partial}{\partial\rho}(\rho\overline{\theta})^{+}_{|\rho=\epsilon^{1-\nu}} &= -\frac{1}{Le(1+\frac{\alpha\beta}{3\alpha^2})^{\frac{3}{2}}}\partial_{1/2}\overline{R}+\phi_\theta(\tau)+O(\epsilon^{1-\nu}),\\ \frac{\partial}{\partial\rho}(\rho\overline{y})^{+}_{|\rho=\epsilon^{1-\nu}} &= \sqrt{Le}\partial_{1/2}\overline{R}+\phi_y(\tau)+O(\epsilon^{1-\nu}).\end{aligned}\tag{4.13}$$

Moreover it is easily proved using the expression of the inner solution that

$$\frac{\partial}{\partial\rho}(\rho\overline{\theta})^{-}_{|\rho=\epsilon^{1-\nu}}=w(\tau),\ \ \frac{\partial}{\partial\rho}(\rho\overline{y})^{-}_{|\rho=\epsilon^{1-\nu}}=v(\tau).\tag{4.14}$$

The jump conditions at the free boundary are given by

$$v(\tau)+\frac{w}{\Theta(R)}=-\log(RLe)-\log\Big(F_\epsilon\big(\Theta(R)\big)\Big).\tag{4.15}$$

Eliminating v, w from (4.13, 4.14, 4.15) and up to order $O(\epsilon^{1-\nu})$, we find the equation for the radius $\overline{R}$ of the flame ball:

$$\left(\frac{(Le\Theta(\overline{R}))^{-1}}{(1+\frac{\alpha\beta}{3\alpha^2})^{\frac{3}{2}}}-\sqrt{Le}\right)\partial_{1/2}\overline{R}=\log(RLe)$$

$$+\log(F_\epsilon(\Theta(\overline{R})))+\frac{\phi_\theta(\tau)}{\Theta(\overline{R})}+\phi_y(\tau).$$

This expansion is valid provided we have chosen $\sqrt{3\alpha^2+\alpha\beta}=O(\epsilon^\mu)$ with $\mu<\nu$. This condition is satisfied when β,α are $O(\epsilon^\mu)$.

Let us choose the scaling $\alpha=\overline{\alpha}\epsilon^\mu$ and $\beta=\overline{\beta}\epsilon$ which clearly satisfies the hypothesis $\beta,\alpha=O(\epsilon^\mu)$. In this case, we can simplify the equation of growth. The front temperature is given by

$$\Theta(R)=\frac{1}{Le}-\frac{\overline{\beta}\epsilon}{Le\sqrt{3}}R+(\text{h.o.t}).$$

Then the equation for the radius growth can be written

$$(1-\sqrt{Le})\partial_{1/2}\overline{R}=\log(\frac{\overline{R}}{R_{ad}})-\frac{Le\overline{\beta}}{\sqrt{3}}R+\Phi(\tau).$$

where R_{ad} is the adiabatic radius. The function Φ is only a function of the initial data $y(0,.)$ and $\theta(0,.)$.
It is remarkable to see the influence of the radiative transfer through the term $-\lambda R$ instead of the heat loss term of radiation $-\lambda R^2$ derived in other analysis [**16, 17**].

Now if we consider a reaction initiated by the input of energy of order $O(\epsilon)$ at the origin, we choose initial conditions so that $\Phi(\tau)=0$

and the only difference comes from the near field equations: we have to solve the quasi stationary equations

$$\begin{array}{l} -\Delta\,\theta = \beta\,u + \epsilon\,\mathcal{Q}(t)\delta(r=0), \\ -\Delta\,u + 3\alpha^2\,u = \alpha\Delta\,\theta, \end{array} \tag{4.16}$$

where $\mathcal{Q}$ represents the amount of energy input in the system at the origin (see [**30**] for more details). This system is completed with jump conditions detailed in Section 4.2. The stationary solution of (4.16) with jump conditions is the sum of the stationary solution computed in Section 4.2 and a particular solution (u_p, θ_p) which is smooth at point $r = R(t)$. It is a Fourier transform exercise to prove that a particular solution (u_p, θ_p) of this system is given by

$$u_p = \alpha\epsilon\mathcal{Q}(t)\frac{\mathrm{sh}(\sqrt{3\alpha^2+\alpha\beta})r}{4\pi\,r},$$

and

$$\theta_p = \frac{\epsilon\mathcal{Q}(t)}{4\pi\,r} - \frac{\alpha\beta\epsilon\mathcal{Q}(t)}{4\pi(3\alpha^2+\alpha\beta)}\frac{\mathrm{sh}\sqrt{3\alpha^2+\alpha\beta}r}{r}.$$

Thus in the asymptotic $\alpha = O(\epsilon^\mu)$ with $0 < \mu < 1$ and $\beta = \overline{\beta}\epsilon$, the temperature at the front is given by

$$\Theta(R) = \frac{1}{Le} - \frac{\overline{\beta}\epsilon}{Le\sqrt{3}}R + \frac{\epsilon\mathcal{Q}(t)}{4\pi\,R} + (\text{h.o.t}). \tag{4.17}$$

As a consequence, we find the growth equation

$$(1-\sqrt{Le})\partial_{1/2}\overline{R} = \log\frac{\overline{R}}{R_{ad}} - \frac{Le\overline{\beta}}{\sqrt{3}}\overline{R} + \frac{Le^2}{4\pi}\frac{\mathcal{Q}(\tau)}{\overline{R}}.$$

In the sequel, we put the last term concerning the energy input at origin in the form $\frac{Eq(\tau)}{\overline{R}}$. Here E represents the intensity of the energy input and $q(\tau)$ corresponds to the time fluctuations of this energy input. In the next sections, we are going to analyze mathematically and numerically

$$(1-\sqrt{Le})\partial_{1/2}\overline{R} = \log\frac{\overline{R}}{R_{ad}} - \frac{Le\overline{\beta}}{\sqrt{3}}\overline{R} + \frac{Eq(\tau)}{\overline{R}}.$$

4.3. Mathematical Results

In this section, we consider the more generalized equation,

$$\mu R\partial_{1/2}R = R\log R + Eq - \lambda R, t \in \mathbb{R}^+, R(0) = 0, \tag{4.18}$$

where $\mu > 0$, $\lambda > 0$ and

$$\partial_{1/2}R = \frac{1}{\sqrt{\pi}}\int_0^t \frac{\dot{R}(s)}{\sqrt{t-s}}\,ds = \frac{1}{\sqrt{\pi}}\frac{d}{dt}\int_0^t \frac{R(s)}{\sqrt{t-s}}\,ds. \tag{4.19}$$

It describes the evolution of a spherical flame, initiated by a point source energy input $Eq(t)$, at which are applied heat losses of radiative

nature, represented by the parameter λ. The intensity of this energy input is measured by the positive constant E , and its time evolution is described by the function q. This one is a smooth, nonnegative function, with connected support and unit total mass, its initial values satisfy the following assumption,

$$q(t) \sim q_0 t^\beta \text{ as } t \to 0 \text{ with } 0 \leq \beta < 1/2, \tag{4.20}$$

and as $t \to +\infty$, q tends to 0. Finally the parameter μ can be viewed as a time rescaling (see Section 4.4), and is assumed, in this section, to be a positive real number, fixed to 1.
Mathematical results of Equation (4.18) are, according to minor modifications in the proofs, similar to the ones written in [**4, 47**]. Therefore proofs are omitted, only comments are mentioned when necessary.

Let us begin to state existence results for the Cauchy problem.

Proposition 4.1. *Let us assume q positive on $[0, t_0]$, $q(0) = q_0$. Then, there exists $t_1 \in]0, t_0]$, such that* (4.18) *admits a solution in $C^{3/2}([0, t_1])$ satisfying,*

$$R(t) \sim R_0 t^{1/4}, \qquad \text{with } R_0^2 = \frac{E q_0}{\sqrt{\pi}} \int_0^1 t^{-\frac{1}{4}} (1-t)^{-\frac{1}{2}} dt.$$

In order to prove the existence of a unique maximal solution, the flame radius is expressed as the trace at $x = 0$ of a function $u(t, x)$, solution of the following parabolic equation,

$$\begin{cases} u_t - u_{xx} = 2\delta_{x=0}\big(\log u + \dfrac{Eq}{u} - \lambda u\big) & \text{for } x \in \mathbb{R}, \\ u(0, \cdot) = 0. \end{cases} \tag{4.21}$$

This formulation is essential to characterize the long-time behavior of the flame. Then we consider more general Cauchy problems, such as

$$\begin{cases} u_t - u_{xx} = 2\delta_{x=0}\big(\log u + \dfrac{Eq}{u} - \lambda u\big) & \text{for } x \in \mathbb{R}, \\ u(0, \cdot) = u_0(x), \end{cases} \tag{4.22}$$

where u_0 is even, Lipschitz, square-integrable, non-negative function. This is equivalent to solving,

$$\begin{cases} u_t - u_{xx} = 0, \quad x > 0 \\ u_x(t, 0) = -\big(\log u + \dfrac{Eq}{u} - \lambda u\big) & \text{for } x \in \mathbb{R}, \\ u(0, \cdot) = u_0(x). \end{cases}$$

Such a writing allow us to prove the

Theorem 4.2. *Let q satisfy Condition* (4.20). *We suppose there exists $t_0 > 0$ such that $q(t) > 0$ on $]0, t_0[$, and $q(t) = 0$ if $t \geq t_0$, then*

i) *if $t_0 = +\infty$,* (4.22) *has a unique global positive solution, except at $t = 0$. Moreover u is C^∞ on $\mathbb{R}_+^* \times \mathbb{R}^*$ and $t \mapsto u(t, 0)$ is C^∞ on $\mathbb{R}_+^*$.*

ii) *if $t_0 < +\infty$, (4.22) has a unique maximal solution u defined on an interval $[0, t_{max}[$, positive, except at $t = 0$. Moreover u is C^∞ on $]0, t_{max}[$. If $t_{max} < +\infty$, there exists $t_n \to t_{max}$ such that $\lim_{n\to+\infty} u(t_n, 0) = 0$.*

In particular, a consequence of this theorem is the existence of a solution of Equation (4.18). The uniqueness of u is based on a comparison principle (see [**47**] for more details).

These results now recalled, we may discuss different cases where either quenching or stabilization of the flame occurs. For this purpose, we denote u_E the solution of (4.21) and $R_E(t) := u_E(t, 0)$ the corresponding radius of the flame. Let us turn to the asymptotic behavior of the radius. In order to prove the following results, monotonicity methods (cf. [**48**]) are of major importance. Indeed, sub or supersolutions are computed and create, therefore, an admissible range for the solutions. At this stage, a comparison principle coupled to a relevant choice of the bounds, tells us either quenching or stabilization of the flame.

Before going further, we make a remark on the role played by the parameter λ. The stationary solutions of

$$u_t - u_{xx} = 2\delta_{x=0}(\log u - \lambda u),$$

are the constants R satisfying,

$$\log R = \lambda R,$$

hence the values of λ_{cr} and the distinction we have to make between the cases $\lambda < \lambda_{cr}$ and $\lambda > \lambda_{cr}$. Please note that we do not consider the case $\lambda = \lambda_{cr}$, the study being identical to [**47**]. Moreover λ is assumed nonnegative in the sequel so that u_E solution of (4.22) is a bounded function.

We first consider the supercritical case, $\lambda > \lambda_{cr}$, corresponding to high radiative heat losses. Then, the loss of energy is too important and the flame quenches. We state the following proposition.

Proposition 4.3. *Assume $\lambda > \lambda_{cr}$.*

i) *If $q > 0$ on $\mathbb{R}_+^*$, then the solution of (4.21) is global and $\lim_{t\to+\infty} R_E(t) = 0$.*

ii) *If q is compactly supported, R_E quenches on finite time.*

We now consider the sub-critical case, $\lambda < \lambda_{cr}$. This situation leads to different properties, more complex because depending on the quantities E and q, i.e. the amount of energy we input in the system and the time length of this injection. We have

Theorem 4.4. *Assume $\lambda < \lambda_{cr}$ and $q > 0$ on $\mathbb{R}_+^*$. Then equation (4.18) has a unique global solution $R_E(t)$ and there exists $E_{cr}(q) > 0$ such that*

i) *if* $E < E_{cr}(q)$, $\lim_{t\to+\infty} R_E(t) = 0$,
ii) *if* $E > E_{cr}(q)$, $\lim_{t\to+\infty} R_E(t) = R_2$,
iii) *if* $E = E_{cr}(q)$, $\lim_{t\to+\infty} R_E(t) = R_1$,

If q *is compactly supported, with support* $]0, t_0[$, *then equation* (4.18) *has a unique solution* $R_E(t)$ *and there exists* $E_{cr}(q) > 0$ *such that*

i) *if* $E < E_{cr}(q)$, R_E *quenches in finite time,*
ii) *if* $E \geq E_{cr}(q)$, *the previous result holds again.*

This theorem can be proved with minor changes in the sub and supersolutions in the proofs developed in [**47**]. For more details on the theoretical study on this type of equations, we refer the reader to [**4, 47**].

As a conclusion, we have verified that the equation derived in Section 4.2,

$$(1 - \sqrt{Le})\partial_{1/2}\overline{R} = \log \frac{\overline{R}}{R_{ad}} - \frac{Le\overline{\beta}}{\sqrt{3}}\overline{R} + \frac{Eq(\tau)}{\overline{R}}, \tag{4.23}$$

is well posed provided that $Le < 1$ and the flame ball quenches if $Le\overline{\beta}$ exceed a threshold. When $Le\overline{\beta}$ is small enough, there exists two steady flame balls. The small one is unstable and the large one is stable under radial perturbations. Since we have computed nonlinear evolutions of radial perturbations, these results shall be understood as nonlinear stability properties of the steady flame balls.

There are different explanations to justify the assumption Le $<$ 1. From a mathematical point of view, Equation (4.23) is ill posed for Lewis numbers greater than one. Indeed, in this case, we face a retrograd parabolic equation in which instabilities can occur (see for example [**9, 8**]). The special case Le $= 1$ with high activation energy has been studied in [**26**]. From a physical point of view, as the Lewis number is the ratio between thermal and molecular diffusion, the condition $Le < 1$ is equivalent saying gas molecules diffuse faster than heat. In this configuration, flame balls are willing to exist, whereas for Lewis numbers greater than one, flames vanish. Considering the experiments performed by Ronney et al. (see for example [**46**]), flame balls are observed only for lean reactants mixtures which Lewis number is between 0.06 and 0.5. So that the restriction Le < 1 is reasonable and in fact is a necessary condition for stationary flame balls to exist.

4.4. Numerics

In this section, we follow the methods developed in [**5**]. We first present the numerical scheme and then turn to numerical investigations.

Presentation of the scheme

We recall that the radius R can be seen as the trace on the axis $x = 0$ of the solution $u(x,t)$ of the diffusive problem (4.22). A suitable scheme to study long time behaviour of such equations is an implicit Euler scheme in time. The scheme reads,

$$\begin{cases} \dfrac{u^{n+1}-u^n}{\tau} - u_{xx}^{n+1} = 0 \quad \text{for } x > 0, \\ u_x^{n+1}(0) = -\log u^{n+1}(0) - \dfrac{Eq^{n+1}}{u^{n+1}(0)} + \lambda u^{n+1}(0) \\ u^0 = 0, \end{cases}$$

where τ denotes the time step and $q^n = q(n\tau)$. The discretized heat equations can be solved explicitly using Fourier transform so that system (4.4) determines explicitly the quantity in which we are really interested, i.e. the sequence $R^n := u^n(0)$. Moreover by induction and because of the maximum principle, we have $u^n \geq 0$.
Before going further, we define two quantities needed later on by

$$\begin{cases} \alpha^n = \displaystyle\int_{\mathbb{R}} \frac{\hat{u}^{n-1}(\xi)d\xi}{1+4\pi^2\xi^2\tau} = \sqrt{\tau}\sum_{k=1}^{n-1}\theta_{n-k+1}g^k, \quad \hat{u}^0 = 0, \\ g^n = f^n(\alpha^n + \sqrt{\tau}g^n), \quad n \geq 1, \end{cases}$$

where

$$\theta_{p+1} = \int_{\mathbb{R}} \frac{2\sqrt{\tau}}{(1+4\pi^2\xi^2\tau)^{p+1}}d\xi = \frac{2p-1}{2p}\theta_p = \frac{C_{2p-1}^p}{2^{2p-1}}\theta_1, \qquad \text{with } \theta_1 = 1.$$

The radius R is then expressed in term of these quantities, namely $R^n = \alpha^n + \sqrt{\tau}g^n > 0$. The unknown g^n being determined by successive resolutions of the following implicit equation

$$\Phi(g^n) := g^n - \log(\alpha^n + \sqrt{\tau}g^n) - \frac{Eq(n\tau)}{\alpha^n + \sqrt{\tau}g^n} + \lambda(\alpha^n + \sqrt{\tau}g^n) = 0. \quad (4.24)$$

In order to be consistent with Equation (4.18), we need to introduce the parameter μ different from 1. It enters Equation (4.24) as

$$\Phi(g^n) := \mu g^n - \log(\alpha^n + \sqrt{\tau}g^n) - \frac{Eq(n\tau)}{\alpha^n + \sqrt{\tau}g^n} + \lambda(\alpha^n + \sqrt{\tau}g^n) = 0. \quad (4.25)$$

This implicit equation is solved by a Newton method with initial data g^{n-1}.
The properties of this scheme remain unchanged so that by [**5**], the convergence and comparison properties still hold. The numerical scheme also sustained similar qualitative properties to the continuous model of flame ball growth (see [**5**] for more details).

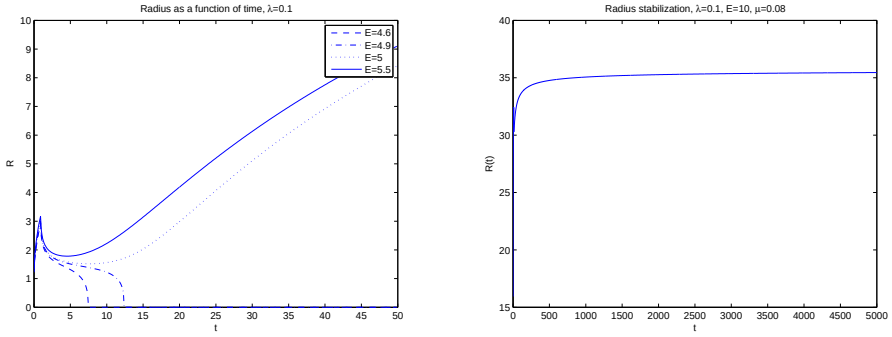

Figure 4.2: Evolution of the radius when $\lambda < \lambda_{cr}$ and E variable; from extinction to stabilization.

Numerical results

We now turn on the numerical investigation of the problem. For this purpose, we consider an input energy $q = \chi_{[0,1]}$. In Figure 4.2, we fix a value for the parameter λ, namely $\lambda = 0.1 < \lambda_{cr} = 1/e$ and plot the different radius evolution possibilities for different energy inputs. We note that (picture on the left) we recover the expected behavior of the radius: when E is small, the flame quenches whereas when it is larger, the behavior cannot be guessed with this time scale and numerical simulations have to be performed for longer times. For this purpose, we perform a time rescaling. Writing $t = \tau/\epsilon$ in Formula (4.18) and dividing by R, implies a new expression $\tilde{\mu}\partial_{1/2}R$, where $\tilde{\mu} = \sqrt{\epsilon}\mu$. So that, dropping the tilde, we are able to simulate large time scale t via a smaller time scale τ only by taking values of μ less than one. Figure 4.2 (right), shows the stabilization towards the radius R_2 in the time coordinate τ.

Finally, in Figure 4.3, the energy E is fixed and we consider different values for λ. For important radiative heat losses, the flame quenches, whereas it stabilize to the corresponding critical radius, depending on the value of λ.

4.5. Conclusion

In this paper, we have studied the stabilizing effect of *radiative transfer* on the formation of flame balls. In the formation of flame balls, radiation is an important physical effect. Instead of considering radiative heat loss, just as Buckmaster et al. did in [**16, 17**] through simplified versions of Stefan's law, we have considered radiative transfer using the well known (linearized) Eddington law. In some asymptotic parameter regime, we obtain the existence of two steady flame balls. In our study, the asymptotic equation for the radius of the steady

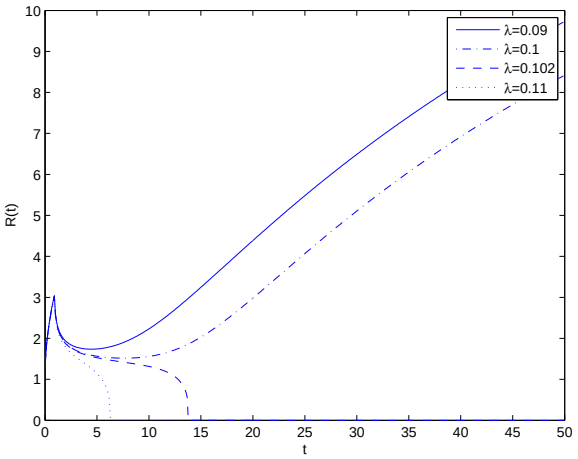

Figure 4.3: Evolution of the radius when E fixed and λ variable.

flame ball is $\log R = \lambda R$ and it is different from the one obtained by Buckmaster et al, $\log R = \Lambda R^2$. The difference in the power of R comes from the fact that the dependence of the front temperature with respect to R is different whether we consider heat loss terms (in that case, the dependence is parabolic) or radiative transfer (in that case it is linear). This has an influence on the size of the steady flame balls. For the linearized Eddington equation of radiative transfer, we have derived, using an approach initiated by Buckmaster et al., an integro-differential equation for the growth of a flame ball. This equation differs again from the one obtained by Buckmaster et al. with a loss term proportional to R instead of R^2. The equation obtained in this paper describes the *nonlinear evolution* of *radial perturbation* of steady flame balls and falls into a class of integro-differential equations that are mathematically and numerically well understood [**4, 5, 47**]: we have used this framework to study mathematically and numerically the asymptotic behaviour of this equation. When two steady flame balls exist, the smaller one is unstable (except for particular values of the parameters) and the larger one is stable similarly to the results obtained in [**16, 17**]. This gives a partial answer to the stability properties of flame balls obtained in [**53**] since the perturbations considered in the paper have the *radial* symmetry. Finally, we shall mention that the derivation carried out in this paper is only formal and it would be interesting to make this derivation rigorously: for that purpose, instead of starting from the free boundary problem, we shall consider the reaction diffusion system with a singular reaction term and follow the method developed by Roquejoffre et al. in the adiabatic case [**33**].

CHAPTER 5

Stability properties for a flame ball problem with radiative transfer

5.1. Introduction

The purpose of this thesis is to study stability properties for a flame ball Free Boundary Problem (FBP) with radiative transfer. This chapter deals with the stability issues of this FBP and is therefore the confluence of all the previous work. To reach this goal, different steps were needed. Let us then start this introduction by a recapitulation of these different steps and then state the mathematical results obtained in this chapter.

The first mathematical model to describe such flames goes back to Zeldovich [**56**] in 1944. This model leads to the existence of solutions which are unstable under radially symmetric perturbations. This model, known as the non-radiative or adiabatic model, describes combustion processes with simple chemistry (such as a one step reaction in which the gaseous reactant is converted into a gaseous product). In such models, we are interested in two quantities: the temperature θ and the fuel mass fraction y, which are assumed, in the adiabatic context, to be constant inside the flame, in particular $y \equiv 0$, see Figure 5.1.

It was then believed that physical flame balls do not exist, until 1984, when, surprisingly, Ronney (see e.g. [**16, 17**]) discovered during drop tower experiments the existence of physical flame balls. Therefore, a stabilizing effect has to be identified. It has been argued [**44**] that radiation is physically important in near limit combustion at low gravity. Indeed, flame balls are, so far, the weakest flames known. They are difficult to see and exist close to the extinction limit. Several models were then established incorporating heat losses as radiative effects (see e.g [**16, 17, 22**]). These heat-loss models only take into consideration the loss of heat due to radiation. A more realistic physical model will describe radiation effects by considering a radiative transfer equation. Indeed, the radiative transfer of heat in combustion processes, taking place in inert, not fully transparent media (e.g. dust, porous media,

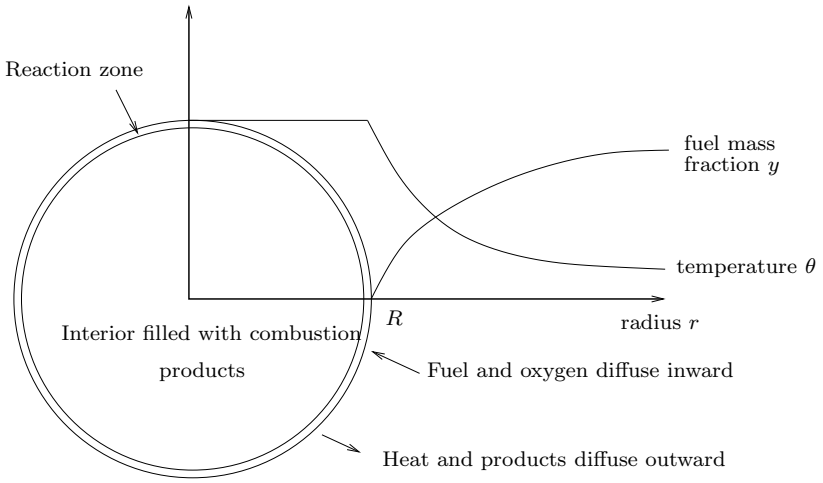

Figure 5.1: Profile of the temperature and the mass fraction variables in the adiabatic case. The radius of the flame ball is denoted by R, corresponding to the flame front.

etc.), involves both emission and absorption of radiation. Such phenomena may significantly influence the temperature of the flame, its propagation speed (see e.g. [**10**]) and the flammability of the medium itself. For more physical details, we refer the reader to [**46**] and the references therein. See also the SOFBALL (Structure of Flame Balls at Low Lewis number) link on Paul Ronney's NASA home page [**1**].

Throughout our study, we indeed go one step further in the description of the radiative effects and introduce a physically more realistic radiative transfer model. Namely, we adopt the Eddington diffusion model ([**24, 40, 41, 42, 43, 49**])

$$-\nabla(\nabla \cdot q) + 3\alpha^2 q = -\alpha \nabla \theta^4, \tag{5.1}$$

where q is the radiative flux and α is the opacity of the medium. Thus, the radiative effects are a direct consequence of temperature variations. Following Joulin and Buckmaster [**14, 31, 32**], these radiative effects couple back to the temperature equation, in which the divergence of the radiative flux appears with coupling constant β, the so-called Boltzmann constant. Thus β is a measure of the ratio between the radiative and the diffusive flux. For flame fronts, this extended model was proposed and studied in [**14, 31, 32**], and in [**6, 10**]. To streamline the mathematical analysis, we do not use the vector equation (5.1) but work with the scalar equation for the divergence of the flux

$$-\Delta u + 3\alpha^2 u - \alpha \Delta \theta^4 = 0,$$

where $u = -\beta \nabla \cdot q$ is a suitable multiple of the divergence of the radiation flux as it appears in the modified temperature equation. Assuming our problem to be spherically symmetric, the free boundary problem

then reads

$$y_t = \frac{1}{\mathrm{Le}}\Delta y \qquad \text{for } r \neq R(t), \tag{5.2a}$$

$$\theta_t = \Delta\theta + u \qquad \text{for } r \neq R(t), \tag{5.2b}$$

$$0 = \Delta u - 3\alpha^2 u + \chi\Delta\theta^k, \tag{5.2c}$$

where $\chi = \alpha\beta$. The artificial parameter k will be taken either $k = 4$ (black-body radiation) or $k = 1$ (linearised radiation model). Equation (5.2c) is satisfied in the whole space in the sense of the distributions (and classically for $r \neq R(t)$). The jump conditions at $r = R(t)$ are

$$[\theta] = y = 0, \quad -[\theta_r] = \frac{1}{\mathrm{Le}}[y_r] = F(\theta(R(t))), \tag{5.2d}$$

with $u + \chi\theta^k$ being continuously differentiable, as follows from (5.2c) if θ is merely bounded. The asymptotic boundary conditions are

$$y \to y_f, \quad \theta \to \theta_f, \quad u \to 0 \quad \text{as } r \to \infty. \tag{5.2e}$$

The parameters θ_f and y_f denote the temperature and the mass fraction far away in the fresh region. We recall that $R(t)$ is the free boundary variable corresponding to the flame front and that $F(\theta(R))$ is the reaction rate evaluated at $r = R$. Note that, for the analytical results, we will not specify the reaction rate and work only with general reaction rates F. We only need to know that F is a positive function of the temperature at the flame front. On the other hand, when performing numerics, we will need to specify one reaction rate which will be taken as an Arrhenius type law.

Once the mathematical model is written down, the next step is to prove existence of stationary solutions for Problem (5.2):

$$\frac{1}{\mathrm{Le}}\Delta Y = 0 \qquad \text{for } r \neq R, \tag{5.3a}$$

$$\Delta\Theta + U = 0 \qquad \text{for } r \neq R, \tag{5.3b}$$

$$\Delta U - 3\alpha^2 U + \chi\Delta\Theta^k = 0. \tag{5.3c}$$

Here R is a stationary flame radius, Equation (5.3c) is again satisfied in the whole space in the sense of the distributions (and classically for $r \neq R$). The jump conditions at $r = R$ are

$$[\Theta] = Y = 0, \quad -[\Theta_r] = \frac{1}{\mathrm{Le}}[Y_r] = F(\Theta(R)), \tag{5.3d}$$

with, as above, $U + \chi\Theta^k$ smooth (i.e. C^1). The asymptotic boundary conditions are

$$Y \to y_f, \quad \Theta \to \theta_f, \quad U \to 0 \quad \text{as } r \to \infty. \tag{5.3e}$$

Note that we are looking for radial solutions in $\mathbb{R}^3$, therefore the Laplacian can be written, for an arbitrary function f, as $\Delta f = f'' + \frac{2}{r}f'$, where primes denote derivatives in the radial coordinate r. We recall the main result obtained in [**53**]

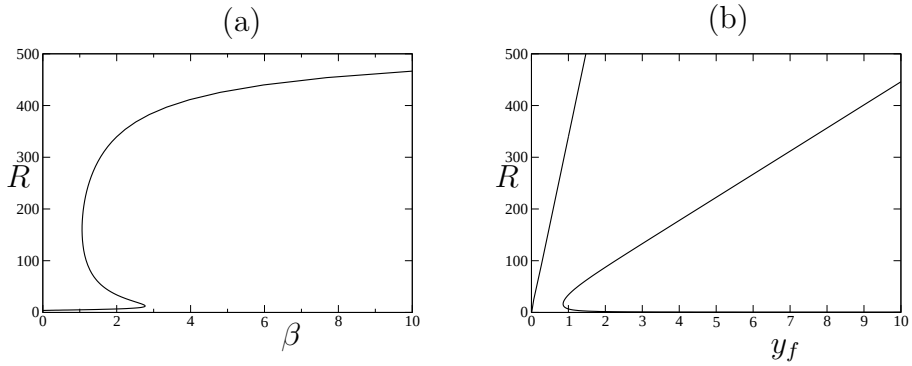

Figure 5.2: Bifurcation curves exhibiting turning points: (a) with β used as bifurcation parameter; (b) with Y_f as the parameter.

Theorem 5.1 (Existence). *Let $\alpha \geq 0$, $\beta \geq 0$, let F be continuous and positive and let $\theta_f > 0$, $y_f > 0$. Then there exists a radial solution $(\Theta(r), Y(r), U(r), R)$ to the stationary System (5.3). Moreover, for generic choices of the parameters the number of solutions is odd.*

Concerning the stationary problem, the mass fraction equation is independent from the two others, and one can compute the explicit formula

$$Y(r) = \begin{cases} 0 & \text{for } r \leq R, \\ y_f \left(1 - \frac{R}{r}\right) & \text{for } r > R. \end{cases} \tag{5.4}$$

Different bifurcation diagrams are shown in [**53**], depending either on the parameters β or y_f, which give an example of multiplicity of stationary solutions, reproduced in Figure 5.2. The pictures suggest that the bifurcation diagrams consist of curves, and for the linearised Eddington equation ($k = 1$) we prove, in Section 5.3, that this is indeed the case. Moreover one may ask whether Figures 5.2a and 5.2b depict *all* solution curves. Again, for $k = 1$ we prove that the answer is affirmative, see Section 5.3.

From now on, let us fix a stationary solution (Y, Θ, U, R) of Problem (5.3). As we are interested in stability properties of System (5.2), we start by perturbing a fixed stationary solution. We consider radially symmetric perturbations. Thus the first task is to linearise the FBP (5.2). Our analysis is based on [**8**] in which the authors derive a general method to linearise such problems. As we are dealing with a radially symmetric problem, we will also consider [**11**], in which a suitable change of variable for radial problems is obtained. We will derive the linearised problem for our model in Section 5.2.

After proving the existence of stationary solutions and linearising around a fixed one, we concentrate on the main body of this chapter, namely the study of the stability issues. In order to understand the point spectrum of our problem, we define an Evans function. Let us

explain briefly how one can derive such a function. Let λ be a candidate eigenvalue. As suggested in Figure 5.1, one can split the space into two regions, namely the burnt region (inside the ball) corresponding to the interval $[0, R(t)]$ and the fresh region (outside the ball) corresponding to the interval $[R(t), +\infty)$. Our goal is then to define and compute eigenfunctions on each interval described above. In order to define an eigenfunction on the whole space, one sees that the remaining step will be to match the two eigenfunctions at the free boundary $r = R$. At this point precisely, the two functions should satisfy the linearised jump conditions. Therefore, we are left with a linear system to solve which involves a matrix needing to have a nontrivial kernel. Note that this matrix depends on the candidate eigenvalue λ. By definition, the determinant of the matrix is called the Evans function, denoted $D(\lambda)$ in the literature. It is an analytic function in λ and its zeros give the point spectrum of our problem.

On the one hand we consider a linearised Eddington equation ($k = 1$) for which we can derive explicit formulas for the Evans function. On the other hand, when considering the black-body model ($k = 4$), there is no hope to derive explicit formulas and numerical techniques are needed to compute the Evans function.

In this thesis we only consider radially symmetric perturbations. The "linear" case is treated in Section 5.4 while Section 5.5 concerns the nonlinear one. In the "linear" case, the expression of the Evans function is quite complicated and only a numerical study of the eigenvalues is possible. The main result is summarised in Figure 5.3 and will briefly be discussed now.

As we are interested in relating the stability results to the bifurcation diagrams, we draw in Figure 5.3 a magnification around the first vertical turning point of a bifurcation diagram, where β is the natural bifurcation parameter. Let us explain Figure 5.3b, which is a catalogue for the spectral radial radius R. We recall that, for every R there exists a unique flame ball with radius R, if we leave the reaction rate $F(\theta^*)$ unspecified in (5.3d). Scaling r and u by R, this stationary solution only depends on $\tilde{\alpha} = R\alpha$, $\tilde{\beta} = R\beta$, θ_f, y_f and Le. In particular the flame temperature θ^* only depends on $\tilde{\alpha}$, $\tilde{\beta}$, θ_f and $\frac{y_f}{\mathrm{Le}}$. Any reaction rate F with $F(\theta^*) = F(\theta(R)) = \frac{y_f}{R\mathrm{Le}}$ then makes this flame ball a stationary solution of the FBP (5.2). Then we can, for given values of y_f, θ_f and Le, for given flame ball radius R, and hence for given $F(\theta^*)$, $F(\theta^*)$ being just a number, examine the spectral stability varying basically $F'(\theta^*)$ (vertically in the stability diagram) versus the scaled radiative parameters $\tilde{\alpha}$ and $\tilde{\beta}$. The combustion parameters θ_f, y_f, Le, or combinations thereof, may also be varied.

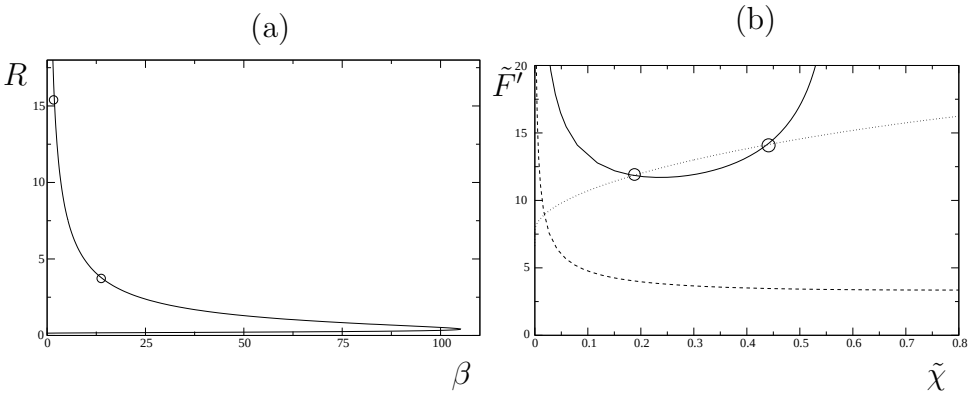

Figure 5.3: Relation between the stability on the bifurcation diagram (a) and the stable area (b) for Le $= 0.7$, $A = 2.29.10^6$, $\varepsilon = 3.35.10^{-2}$ and $k = 1$

We will do all the spectral stability analysis for $R = 1$, because of the scaling

$$\tilde{y}(r) = y(Rr), \quad \tilde{\theta}(r) = \theta(Rr), \quad \tilde{u}(r) = Ru(Rr), \tag{5.5a}$$

$$\tilde{\alpha} = R\alpha, \quad \tilde{\beta} = R\beta, \quad \tilde{\chi} = R^2\alpha\beta. \tag{5.5b}$$

Note that the reaction rate $F(\theta)$ also has to be scaled: $\tilde{F}(\theta) = RF(\theta)$.

As we trace the solution curve in the bifurcation diagram 5.3a, in which only β is varied, the radius R, and hence both $\tilde{\alpha}$ and $\tilde{\beta}$ vary, and the spectral stability depends on $F'(\theta^*)$, or more precisely on $\tilde{F}'(\theta^*)$, as we shall see from the Evans function. The solution curve itself defines a curve in the $(\tilde{\alpha}, \tilde{\beta})$-plane, which we put horizontally. Vertically above each point of this curve, we put $\tilde{F}'(\theta^*) = RF'(\theta^*)$, where R is the (unscaled) radius of the flame ball and $F'(\theta^*)$ the derivative in θ^* of $F(\theta) = A\exp(-\frac{1}{\varepsilon\theta})$, the reaction rate function used to make the bifurcation diagram.

As $\tilde{\chi} = R^2\alpha\beta$ turns out to be monotone along the solution curve, we sketch the resulting curve in Figure 5.3b in a diagram with $\tilde{\chi}$ horizontally and $RF'(\theta^*)$ vertically. In this diagram we draw in fact three curves

- dotted: bifurcation curve,
- dashed: $D(0) = 0$,
- solid: Hopf bifurcation curve (2 conjugate purely imaginary eigenvalues).

Turning points correspond to intersections of the dotted and dashed curves. The interpretation is as follows. We start on the bifurcation diagram 5.3a at $\beta = 0$ and R small. We are moving along this curve until we reach the vertical turning point. This branch of the diagram corresponds to the dotted line, in 5.3b, for small values of $\tilde{\chi}$ until it hits the vertical turning point line. We go back to Picture 5.3a considering the middle branch of the diagram. This middle branch

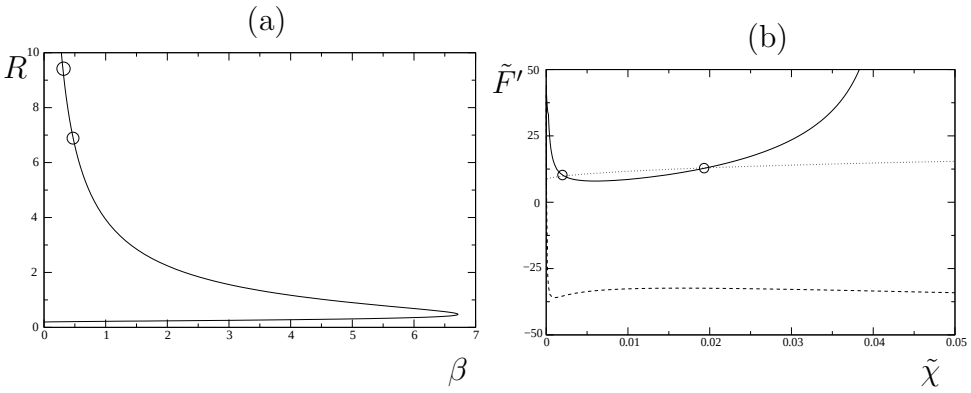

Figure 5.4: Relation between the stability on the bifurcation diagram (a) and the stable area (b) for Le = 0.7, $A = 1.47.10^7$, $\varepsilon = 2.839.10^{-2}$ and $k = 4$

corresponds to the part of the dotted line in 5.3b located after the crossings with the turning point line. We see that we enter and leave the stable area. These points are emphasized by the circles and correspond to the values of β in Figure 5.3a. Therefore, the part between the two circles, corresponds the stable branch of solutions. To conclude these observations, the dotted line and the dashed line in Picture 5.3b will intersect again for large values of $\tilde{\chi}$ meaning that we reach the second vertical turning point, not depicted in Figure 5.3a but visible in Figure 5.2a.

As mentioned earlier, the Lewis number plays an important role in the stability analysis. Indeed, we will see that the stable area exists only for Le < 1, and the stable area becomes larger as Le $\to 0$.

Finally, Section 5.5 deals with the black-body model ($k = 4$). As in the linear case, we are interested in defining the Evans function. Unfortunately, it is harder to define the eigenfunctions on each side of the point $z = R(t)$. To overcome this difficulty, we will consider planes spanned by solutions instead of lines, this analysis being based on [**3**]. Planes on each side are defined by wedging the two solutions on both sides. Because of symmetry arguments, these planes are defined to be with zero derivative in 0, and bounded at infinity. Then one may try to find solutions in these planes which match at $z = R$ through the linearised jump conditions. This matching induces, as in the linear case, the definition of the Evans function.

The analysis of the Evans function can only be done numerically; the main result is shown in Figure 5.4. The interpretation is similar to the linear case. Two main differences occur. The stable area in the nonlinear case diminishes compared to the linear case. Nevertheless, the property concerning the Lewis number still holds, namely the stable area vanish for Le ≥ 1, and becomes bigger as Le $\to 0$. The other difference concerns the vertical turning point line (dashed line). This

curve becomes negative for some parameter value $\tilde{\chi}$, meaning that, for these particular values, there can be no turning points in the bifurcation diagram 5.4a. Note that for large values of $\tilde{\chi}$, the turning point curve becomes positive again and tends to infinity.

5.2. Linearisation of the free boundary problem

In this section we apply the linearisation technique for free boundary problems with jump conditions, see [**8**]. One of the main advantages of this technique is that, under the change of variables needed, it does not denature the problem. In other words, the linear part defined in the original formulation will be the same for the new linearised variables. Before going into the details of linearisation, we first need to fix the free boundary. Strictly speaking, this step is not needed for the linearisation itself, but in order to prove rigorously existence and/or stability properties, it is essential. A standard way to fix the free boundary is to introduce a new variable $z = r - R(t)$. In a traveling wave context (cf [**8**]) this works well, but such a change of variable does not fit in a radially symmetric problem. Indeed, our working interval reads $[0, +\infty)$ and the variable z would lie in $[-R(t), +\infty)$, i.e. shifting time dependence to the domain rather than the variable. One thus needs to incorporate another way of dealing with such problems, as was described in [**11**]. Instead of a translation argument, consider the following change of variables, suitable for radial problems,

$$z = \frac{Rr}{R(t)}. \tag{5.6}$$

Here R is the radius of the *stationary* flame ball, while $R(t)$ is the radius of the perturbed, evolving flame ball. The free boundary is now fixed at $z = R$, and it is convenient to introduce the new variable

$$s(t) = \frac{R(t) - R}{R},$$

hence we may write $r = z(1 + s(t))$. Our goal is, first to linearise Problem (5.2) and its associated jump conditions (5.2d) around a fixed stationary solution. Let us then fix a solution quadruplet

$$(Y(r), \Theta(r), U(r), R)$$

of Problem (5.3). Next we set

$$y(r,t) = Y(z) + s(\tau) z Y'(z) + m(\tau, z), \tag{5.7a}$$

$$\theta(r,t) = \Theta(z) + s(\tau) z \Theta'(z) + n(\tau, z), \tag{5.7b}$$

$$u(r,t) = U(z) + s(\tau) z U'(z) + p(\tau, z). \tag{5.7c}$$

This splitting is adapted from a similar trick in [**13**] for travelling waves. Linearising around the stationary solution and in view of $f(r) =$

$f(z(1+s)) = f(z) + szf'(z) + O(s^2)$, this splitting is naturally induced by the change of coordinates. In the following, we denote by

$$\Delta_z w = w_{zz} + \frac{2}{z} w_z$$

the radial Laplacian in $\mathbb{R}^3$ in the z variable. In the next subsections we introduce an Evans function $D(\lambda)$ to characterize the spectrum in the case $k = 1$. Indeed in this case, computations are explicit while they are of course not in the case $k = 4$. The Evans function for the latter case will be discussed in Section 5.5.

Linearisation of the parabolic equations

Substituting (5.7) in (5.2), we obtain

$$m_\tau = \frac{1}{\mathrm{Le}} \Delta_z m + \mathcal{F}_1(\Delta_z m, s) + \dot{s}\mathcal{F}_2(z, z m_z, s), \tag{5.8a}$$

$$n_\tau = \Delta_z n + p + \mathcal{F}_3(z, \Delta_z n, s) + \dot{s}\mathcal{F}_4(z, z n_z, s), \tag{5.8b}$$

$$3\alpha^2 p = \Delta_z p + k\chi \Delta_z(\Theta^{k-1} n) + \mathcal{F}_5(\Delta_z p, s) + \dot{s}\mathcal{F}_6(z, z p_z, s), \tag{5.8c}$$

where all $\mathcal{F}_i$ for $i = 1, ..., 6$ are nonlinear terms in the (m, n, p) variables. These terms can be written explicitly, see [**27**], where they were used to rigorously prove instability results using semi-group techniques. In our present work their exact form is irrelevant. Clearly these expressions depend on the perturbation $s(\tau)$ and its time derivative $\dot{s}(\tau)$. The linearisation of the the jump conditions $[y] = [\theta] = 0$, (see Section 5.2) allows us to express s and its time derivative in terms of m or n, so that s and $\dot{s}$ can be eliminated from System (5.8). Note that the triplet (m, n, p) are supposed to be small variables. Hence, the linear part of System (5.8) for $z \neq R$ reads, as expected

$$m_\tau = \frac{1}{\mathrm{Le}} \Delta_z m, \tag{5.9a}$$

$$n_\tau = \Delta_z n + p, \tag{5.9b}$$

$$0 = \Delta_z p - 3\alpha^2 p + k\chi \Delta_z(\Theta^{k-1} n). \tag{5.9c}$$

Linearisation of the jump conditions

We consider in the following each jump condition separately. Moreover, if not mentioned otherwise, as we are linearising, we omit all terms that involve a product of two small quantities. By the square brackets we mean the jump in $z = R$, e.g. $[w] = w(R^+) - w(R^-)$.

The jump condition $[y] = [\theta] = 0$. This jump condition gives an expression for the perturbation $s(\tau)$ and its derivative $\dot{s}(\tau)$ in terms of m or n. First it is good to remark that $\Theta + Y/\mathrm{Le}$ is C^2 since U is continuous. Therefore $[\theta + \frac{y}{\mathrm{Le}}] = 0$ implies the first linearised condition

$$[n] = -\frac{1}{\mathrm{Le}} [m] \cdot \tag{5.10}$$

Moreover, since Y is explicitly given by (5.4) and $\frac{y_f}{R\mathrm{Le}} = F(\theta(R))$, $[y] = 0$ implies that, using (5.10),

$$s = -\frac{[m]}{y_f} = \frac{\mathrm{Le}}{y_f}[n] = \frac{1}{RF(\theta(R)}[u]. \tag{5.11}$$

This leads to an expression for s and $\dot{s}$, namely $s = \frac{m(\tau,R^+)}{y_f}$ and $\dot{s} = \frac{m_\tau(\tau,R^+)}{y_f}$.

The jump condition $\frac{1}{\mathrm{Le}}[y_r] = -[\theta_r]$. Again from the fact that $\theta + y/\mathrm{Le}$ is C^2, we can conclude that the second linearised jump condition reads

$$[n_z] = -\frac{1}{\mathrm{Le}}[m_z]. \tag{5.12}$$

The jump condition $[\theta_r] = -F(\theta(R))$. Let us start by computing $[\theta_r]$. Since $[\Theta'] = -F(\Theta(R))$ and $[\Theta''] + \frac{2}{R}[\Theta'] = 0$, we obtain using (5.11)

$$\begin{aligned}[\theta_r] &= \frac{1}{1+s}\left([\Theta'] + s[\Theta'] + sR[\Theta''] + [n_z]\right)\\ &= (1-2s)[\Theta'] + [n_z] = -F(\Theta(R)) + \frac{2}{R}[n] + [n_z],\end{aligned}$$

up to higher other terms. On the other hand

$$\begin{aligned}F(\theta(R)) &= F\left(\Theta(R) + sR\Theta'(R) + n(R)\right)\\ &= F(\Theta(R)) + F'(\Theta(R))\left(sR\Theta'(R^\pm) + n(R^\pm)\right).\end{aligned}$$

Without loss of generality, we may choose a sign, say $+$, and using (5.11) and $[\Theta'] = -F(\Theta(R))$, we see that $[\theta_r] = -F(\theta(r))$reduces to

$$[n_z] = -\frac{2}{R}[n] - \frac{F'(\Theta(R))}{F(\Theta(R))}\left(\Theta'(R^-)n(R^+) - \Theta'(R^+)n(R^-)\right)\cdot \tag{5.14}$$

The jump conditions $[u + \chi\theta^k] = 0$ *and* $[u_r + \chi(\theta^k)_r] = 0$. Let us start with the condition $[u + \chi\theta^k] = 0$. Since $U + \chi\Theta^k$ is C^2 and $\theta^k = \Theta^k + k\Theta^{k-1}(sz\Theta' + n)$, it easily follows that

$$[p + k\chi\Theta^{k-1}n] = 0. \tag{5.15}$$

Next, let us concentrate on the condition $[u_r + \chi(\theta^k)_r] = 0$, which is equivalent to $[u_r] + k\chi\theta^{k-1}[\theta_r] = 0$. Using again that $U + \chi\Theta^k$ is C^2, a straightforward computation leads to

$$[p_z] = -k\chi\Theta^{k-1}[n_z] - \chi k(k-1)\Theta^{k-2}[\Theta' n].$$

It will be convenient to rewrite the term $[\Theta' n]$ as follows. From Equations (5.12) and (5.14), we can deduce

$$[\Theta' n] = (\Theta'(R^-) + \Theta'(R^+))[n] + \frac{F(\Theta(R))}{F'(\Theta(R))}([n_z] + \frac{2}{R}[n]),$$

which leads to the linearised jump condition

$$[p_z] = -k\chi\Theta^{k-1}[n_z] \tag{5.16}$$

$$-\chi k(k-1)\Theta^{k-2}\left\{(\Theta'(R^-)+\Theta'(R^+))[n] + \frac{F(\Theta(R)}{F'(\Theta(R))}([n_z]+\frac{2}{R}[n])\right\}.$$

Summary. The linear problem thus becomes

$$m_\tau = \frac{1}{\mathrm{Le}}\Delta_z m \qquad \text{for } z \neq R, \tag{5.17a}$$
$$n_\tau = \Delta_z n + p \qquad \text{for } z \neq R, \tag{5.17b}$$
$$0 = \Delta_z p - 3\alpha^2 p + k\chi\Delta_z(\Theta^{k-1}n), \tag{5.17c}$$

with the jump conditions at $z = R$

$$[n] = -\frac{1}{\mathrm{Le}}[m] \tag{5.18a}$$
$$[n_z] = -\frac{1}{\mathrm{Le}}[m_z] \tag{5.18b}$$
$$[n_z] = -\frac{2}{R}[n] - \frac{F'(\Theta(R))}{F(\Theta(R))}\left(\Theta'(R^-)n(R^+) - \Theta'(R^+)n(R^-)\right) \tag{5.18c}$$
$$[p] = -k\chi\Theta^{k-1}[n] \tag{5.18d}$$
$$[p_z] = -k\chi\Theta^{k-1}[n_z] \tag{5.18e}$$
$$-\chi k(k-1)\Theta^{2}\left\{(\Theta'(R^-)+\Theta'(R^+))[n] + \frac{F(\Theta(R)}{F'(\Theta(R))}([n_z]+\frac{2}{R}[n])\right\}.$$

The Evans function for $k = 1$

The Evans function is an efficient tool for understanding the spectral properties of a problem. Having linearised Problem (5.2), we consider the associated eigenvalue problem, the eigenvalue denoted by λ. The first task consists of computing, in terms of λ, well-behaved solutions near 0 and $+\infty$. By symmetry considerations we are looking for solutions with vanishing derivative in 0, whereas at infinity the solutions should be bounded. Those solutions should then match in $z = R$ through the linear jump conditions. As we will see below, we end up with a 5×5 matrix depending on λ. We compute its determinant (which is by definition the Evans function) and study its zeros. The zeros of this function are the eigenvalues of the problem. In this section, we derive an explicit formulation for this function when $k = 1$.

Let us then consider the eigenvalue problem associated to System (5.17)-(5.18)

$$\lambda m = \frac{1}{\mathrm{Le}}\Delta m \qquad \text{for } z \neq R, \tag{5.19a}$$
$$\lambda n = \Delta n + p \qquad \text{for } z \neq R, \tag{5.19b}$$
$$0 = \Delta p - 3\alpha^2 p + \chi \Delta n. \tag{5.19c}$$

with the jump conditions at $z = R$

$$[n] = -\frac{1}{\mathrm{Le}}[m] \tag{5.20a}$$
$$[n_z] = -\frac{1}{\mathrm{Le}}[m_z] \tag{5.20b}$$
$$[n_z] = -\frac{2}{R}[n] - \frac{F'(\Theta(R))}{F(\Theta(R))}\left(\Theta'(R^-)n(R^+) - \Theta'(R^+)n(R^-)\right) \tag{5.20c}$$
$$[p] = -\chi[n] \tag{5.20d}$$
$$[p_z] = -\chi[n_z]. \tag{5.20e}$$

The radial Laplacian contains a singular $1/z$ term which can be removed via the change of variables $m = \frac{\tilde{m}}{z}$, $n = \frac{\tilde{n}}{z}$ and $p = \frac{\tilde{p}}{z}$. Indeed, this leads to a system of second order ODEs with constant coefficients, namely

$$\lambda \tilde{m} = \frac{1}{\mathrm{Le}}\tilde{m}'' \qquad \text{for } z \neq R, \tag{5.21a}$$
$$\lambda \tilde{n} = \tilde{n}'' + \tilde{p} \qquad \text{for } z \neq R, \tag{5.21b}$$
$$0 = \tilde{p}'' - 3\alpha^2 \tilde{p} + \chi \tilde{n}''. \tag{5.21c}$$

As mentioned above we are interested in well-behaved solutions, e.g. bounded at $z \to \infty$ and $\tilde{m}'(0) = 0$, $\tilde{n}'(0) = 0$ and $\tilde{p}'(0) = 0$. In order to determine the exponential decay rate of the solutions $(\tilde{m}, \tilde{n}, \tilde{p})$, we need to set

$$\begin{pmatrix} \tilde{m} \\ \tilde{n} \\ \tilde{p} \end{pmatrix} = \begin{pmatrix} \Omega_1 e^{Az} \\ \Omega_2 e^{Bz} \\ \Omega_3 e^{Bz} \end{pmatrix}.$$

From (5.21a) one finds $A = \sqrt{\mathrm{Le}\lambda}$, whereas (5.21b) and (5.21c) together lead to a fourth order polynomial for B:

$$-B^4 + (\lambda + 3\alpha^2 + \chi)B^2 - 3\alpha^2\lambda = 0.$$

This polynomial can be solved explicitly, the roots being $B_{1,2} = \pm\sqrt{w_1}$ and $B_{3,4} = \pm\sqrt{w_2}$, where

$$w_1 = \frac{\lambda + 3\alpha^2 + \chi - \sqrt{\Delta}}{2}, \quad w_2 = \frac{\lambda + 3\alpha^2 + \chi + \sqrt{\Delta}}{2}$$

and $\Delta = (\lambda + 3\alpha^2 + \chi)^2 - 12\alpha^2\lambda$. It is important to remark that A, B_i for $i = 1, \ldots, 4$ are analytic functions in λ for λ not belonging to the

half-line $(-\infty, 0]$. This allows us to determine the eigenfunctions on each side of $z = R$. For the eigenfunctions near $+\infty$ we find, for $z \geq R$,

$$\begin{aligned} m_+ &= C_1 \frac{\exp(-\sqrt{\lambda \mathrm{Le}}\, z)}{z}, \\ n_+ &= C_2 \frac{\exp(-\sqrt{w_1}\, z)}{z} + C_3 \frac{\exp(-\sqrt{w_2}\, z)}{z}, \\ p_+ &= C_2(\lambda - w_1) \frac{\exp(-\sqrt{w_1}\, z)}{z} + C_3(\lambda - w_2) \frac{\exp(-\sqrt{w_2}\, z)}{z}, \end{aligned}$$

and near 0, for $z \leq R$,

$$\begin{aligned} m_- &= 0, \\ n_- &= C_4 \frac{\sinh(\sqrt{w_1}\, z)}{z} + C_5 \frac{\sinh(\sqrt{w_2}\, z)}{z}, \\ p_- &= C_4(\lambda - w_1) \frac{\sinh(\sqrt{w_1}\, z)}{z} + C_5(\lambda - w_2) \frac{\sinh(\sqrt{w_2}\, z)}{z}, \end{aligned}$$

where C_i, $i = 1, \ldots, 5$ are constants.

Plugging these expressions in the jump conditions (5.20) we get, after some simplifications, the following linear system

$$\begin{pmatrix} 1 & 1 & 1 & f_1 & f_2 \\ a_1 + \frac{1}{R} & a_2 + \frac{1}{R} & a_3 + \frac{1}{R} & f_3 & f_4 \\ a_1 - \frac{1}{R} & \frac{F'}{F}\theta'(R^-) & \frac{F'}{F}\theta'(R^-) & f_5 & f_6 \\ 0 & \lambda - a_2 + \chi & \lambda - a_3 + \chi & f_7 & f_8 \\ 0 & f_9 & f_{10} & f_{11} & f_{12} \end{pmatrix} \begin{pmatrix} C_1 \\ C_2 \\ C_3 \\ C_4 \\ C_5 \end{pmatrix} = 0,$$

where

$$\begin{aligned} &f_1 = -\sinh(a_2 R), \quad f_2 = -\sinh(a_3 R), \\ &f_3 = a_2 \cosh(a_2 R) - \frac{\sinh(a_2 R)}{R}, \quad f_4 = a_3 \cosh(a_3 R) - \frac{\sinh(a_3 R)}{R}, \\ &f_5 = -\frac{F'(\theta^*)}{F(\theta^*)} \theta'(R^+) \sinh(a_2 R), \quad f_6 = -\frac{F'(\theta^*)}{F(\theta^*)} \theta'(R^+) \sinh(a_3 R), \\ &f_7 = -\sinh(a_2 R)(\lambda - a_2 + \chi), \quad f_8 = -\sinh(a_3 R)(\lambda - a_3 + \chi), \\ &f_9 = (a_2 + \frac{1}{R})(\lambda - a_2 + \chi), \quad f_{10} = (a_3 + \frac{1}{R})(\lambda - a_3 + \chi), \\ &f_{11} = \left\{ a_2 \cosh(a_2 R) - \frac{\sinh(a_2 R)}{R} \right\} (\lambda - a_2 + \chi), \\ &f_{12} = \left\{ a_3 \cosh(a_3 R) - \frac{\sinh(a_3 R)}{R} \right\} (\lambda - a_3 + \chi), \end{aligned}$$

where $F = F(\theta^*) = F(\theta(R))$, and $F' = F'(\theta^*) = F'(\theta(R))$. By definition, the Evans function $D(\lambda)$ is the determinant of this 5×5 matrix. The remaining step is then to compute this determinant which reads, after simplifications,

$$D(\lambda) = D_0(\lambda) + F'(\Theta^*) D_1(\lambda), \tag{5.25}$$

where

$$D_0(\lambda) = \frac{1}{R} - a_1 = \frac{1}{R} - \sqrt{\lambda \mathrm{Le}},$$

$$D_1(\lambda) = \frac{h}{2(a_2^2 - a_3^2)} + \frac{\Theta'(R^-)}{F(\Theta^*)},$$

$$h = e^{-2Ra_2}\left(1 - \frac{a_1}{a_2}\right)(a_2^2 - 3\alpha^2) + e^{-2Ra_3}\left(1 - \frac{a_1}{a_3}\right)(3\alpha^2 - a_3^2)$$

$$+\frac{a_1}{a_2}(a_2^2 - 3\alpha^2) - a_2^2 + \frac{a_1}{a_3}(3\alpha^2 - a_3^2) + a_3^2$$

and $a_1 = \sqrt{\lambda \mathrm{Le}}$, $a_2 = \sqrt{w_1}$, $a_3 = \sqrt{w_2}$, roots taken with positive real part.

Again, we may scale the analysis to the case $R = 1$ by, in addition to (5.5),

$$\tilde{D}(\lambda) = RD(\lambda), \quad D_0(\lambda) = RD_0(\lambda), \quad D_1(\lambda) = D_1(\lambda),$$

$$\tilde{w} = R^2 w, \quad \tilde{\lambda} = R^2\lambda, \quad \tilde{h} = R^2 h, \quad \tilde{a}_i = Ra_i,$$

for $i = 1, \ldots, 3$, to get

$$\tilde{D}(\lambda) = \tilde{D}_0(\lambda) + \tilde{F}'(\Theta^*)\tilde{D}_1(\lambda), \tag{5.26}$$

where

$$\tilde{D}_0(\tilde{\lambda}) = 1 - \tilde{a}_1 = 1 - \sqrt{\tilde{\lambda}\mathrm{Le}},$$

$$\tilde{D}_1(\tilde{\lambda}) = \frac{\tilde{h}}{2(\tilde{a}_2^2 - \tilde{a}_3^2)} + \frac{\Theta'(1^-)}{\tilde{F}(\Theta^*)},$$

$$\tilde{h} = e^{-2\tilde{a}_2}\left(1 - \frac{\tilde{a}_1}{\tilde{a}_2}\right)(\tilde{a}_2^2 - 3\tilde{\alpha}^2) + e^{-2\tilde{a}_3}\left(1 - \frac{\tilde{a}_1}{\tilde{a}_3}\right)(3\tilde{\alpha}^2 - \tilde{a}_3^2)$$

$$+\frac{\tilde{a}_1}{\tilde{a}_2}(\tilde{a}_2^2 - 3\tilde{\alpha}^2) - \tilde{a}_2^2 + \frac{\tilde{a}_1}{\tilde{a}_3}(3\tilde{\alpha}^2 - \tilde{a}_3^2) + \tilde{a}_3^2$$

and $\tilde{a}_1 = \sqrt{\tilde{\lambda}\mathrm{Le}}$, $\tilde{a}_2 = \sqrt{\tilde{w}_1}$, $\tilde{a}_3 = \sqrt{\tilde{w}_2}$, roots taken with positive real part.

5.3. Bifurcation diagram analysis

Before going to the study of the Evans function and stability properties, we recall an analysis on the bifurcation diagrams from [**53**] and we derive some additional properties. These bifurcation diagrams exhibit the multiplicity of solutions one can get for different control parameters, as shown for example in Figure 5.2. Our purpose is to relate the stability analysis to the bifurcation diagrams in order to determine which branches are stable or unstable.

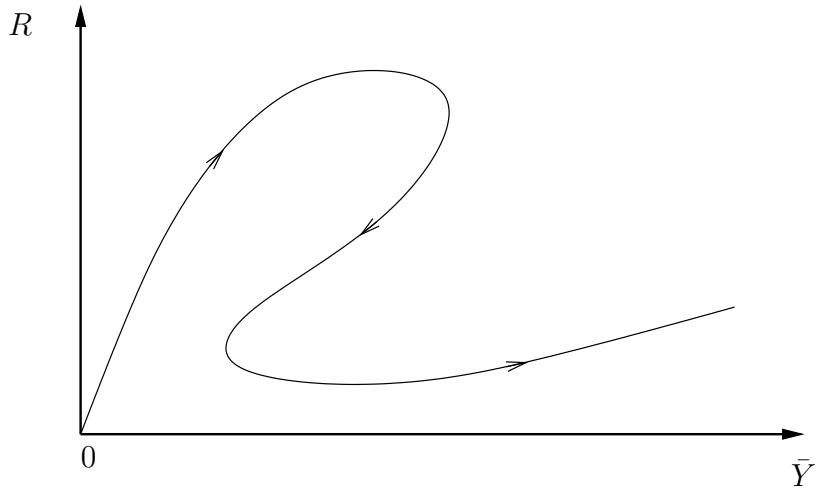

Figure 5.5: Full bifurcation diagram with $\bar{Y}$ as a control parameter. The arrows are indicating increasing flame temperature θ^*.

The bifurcation diagram with y_f as the control parameter

In this section, and if not mentioned otherwise, by $\bar{Y}$, we consider the ratio $\frac{y_f}{\mathrm{Le}}$. Since y_f or Le never appear by themselves in the bifurcation diagram, this simplifies the notation.

Figure 5.5 represents a sketch of a bifurcation diagram for the control parameter $\bar{Y}$. The scales are not preserved, the top part of the curve concerns very large radii while the lower branch on the right of the picture concerns very small ones. The important characteristic here is the shape of the curve. Note that, for some specific values of the parameters, it is possible to obtain a curve without turning points. Moreover, there are no restrictions on the numbers of vertical turning points, and thus, there might be more wiggles. Nevertheless, such a situation did not happen in the numerics we performed.

Let us recall from [**53**] that the bifurcation diagram curve is given by the equation

$$F(\Theta(R;R)) = \frac{\bar{Y}}{R}, \tag{5.27}$$

where $\Theta(R;r)$ is the flame temperature parametrised by the prescribed flame ball radius R. For the linear Eddington equation, one can derive an explicit formula for $\Theta(R;R)$ (see [**53**]). To simplify the notation we introduce

$$\mu = \mu_{\alpha\beta} = \sqrt{3\alpha^2 + \chi}.$$

Then

$$\Theta(R;r) = \begin{cases} \dfrac{B_1}{r}\sinh(\mu r) + B_3 + \theta_f & \text{for } r \le R, \\ \dfrac{B_2}{r}\exp(-\mu r) + \dfrac{B_3 R}{r} + \theta_f & \text{for } r > R, \end{cases}$$

where the constants are given by

$$B_1 = \frac{\chi\bar{Y}}{\mu^3}\exp(-\mu R), \qquad B_2 = \frac{\chi\bar{Y}}{\mu^3}\sinh(\mu R), \qquad B_3 = \frac{3\alpha^2\bar{Y}}{\mu^2}.$$

Therefore the problem reduces to the following system, where $\Theta^* = \Theta(R;R)$,

$$F(\Theta^*) - \frac{\bar{Y}}{R} = 0, \tag{5.28a}$$

$$\Theta^* - \frac{\chi\bar{Y}}{2\mu^3 R}[1 - 2\mu R - \exp(-2\mu R)] - \bar{Y} - \theta_f = 0. \tag{5.28b}$$

We denote by $\bar{\Theta}$ the expression

$$\bar{\Theta} = \frac{\chi\bar{Y}}{2\mu^3 R}[1 - 2\mu R - \exp(-2\mu R)] + \bar{Y} + \theta_f, \tag{5.29}$$

in order to distinguish between this expression and Θ^*, which is also used as a parameter for the bifurcation diagram curve. The implicit function theorem gives a condition for the solutions of (5.28) to be a curve in the $(\bar{Y}, R)$-plane, if we think of $\bar{Y}$ as bifurcation parameter. For control parameter $\bar{Y}$ it reads

$$R\bar{\Theta}_R + \bar{Y}\bar{\Theta}_{\bar{Y}} \neq 0, \tag{5.30}$$

where the subscript R (resp. $\bar{Y}$) denotes the derivative of $\bar{\Theta}$ with respect to R (resp. $\bar{Y}$). If this condition is satisfied the solution set defines a smooth curve parametrised by Θ^*. Due to the fact we have an explicit formula for $\bar{\Theta}$, we can derive an expression for $R\bar{\Theta}_R + \bar{Y}\bar{\Theta}_{\bar{Y}}$ given by Equation (5.30), namely

$$R\bar{\Theta}_R + \bar{Y}\bar{\Theta}_{\bar{Y}} = \bar{Y}\left\{\frac{\chi}{\mu^2}\left(\exp(-2R\mu) - 1\right) + 1\right\},$$

which defines a strictly positive function and therefore does not vanish. Thus Figure 5.5 defines a single curve, as we shall see.

The next step consists of finding the horizontal and vertical turning points. By means of the implicit function theorem, one derives

$$\frac{dR}{d\Theta^*} = \frac{R - R^2\bar{\Theta}_{\bar{Y}}F'(\Theta^*)}{R\bar{\Theta}_R + \bar{Y}\bar{\Theta}_{\bar{Y}}}, \tag{5.31}$$

$$\frac{d\bar{Y}}{d\Theta^*} = \frac{R^2\bar{\Theta}_R F'(\Theta^*) + \bar{Y}}{R\bar{\Theta}_R + \bar{Y}\bar{\Theta}_{\bar{Y}}}. \tag{5.32}$$

From Equations (5.31) and (5.32), we conclude

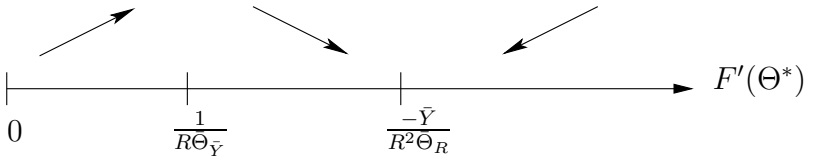

Figure 5.6: Varying Θ^*, the direction in which the bifurcation curve moves in the $(\bar{Y}, R)$-plane depends on $F'(\Theta^*)$.

Lemma 5.2. *We have*

(1) *The condition to have vertical turning points reads*

$$F'(\Theta^*) = -\frac{\bar{Y}}{R^2\bar{\Theta}_R}, \tag{5.33}$$

where $\bar{\Theta}_R$ defines the (negative) derivative w.r.t. R.

(2) *The condition to have horizontal turning points reads*

$$F'(\Theta^*) = \frac{1}{R\bar{\Theta}_{\bar{Y}}}, \tag{5.34}$$

where $\bar{\Theta}_{\bar{Y}}$ defines the (positive) derivative w.r.t. $\bar{Y}$.

Equations (5.31) and (5.32) also lead to Diagram 5.6, via a simple sign inspection. This diagram has to be related to Figure 5.5 and gives the direction along the curve as Θ^* increases. We can prove using (5.28) but also using the fact that $F(\Theta^*)$ is a bounded positive increasing function, the following

Lemma 5.3. *We have*

(1) *If $\Theta^* > \theta_f$ then $\bar{Y}$ and R are positive,*
(2) *If Θ^* is bounded then $\bar{Y}$ and R are bounded,*
(3) *If $\Theta^* \to \infty$ then $\bar{Y} \to \infty$ and $R \to \infty$,*
(4) *If $\Theta^* \to \theta_f$ then $\bar{Y} \to 0$ and $R \to 0$.*

Proof. The conclusions are derived from System (5.28).

(1) Let us suppose $\Theta^* > \theta_f$. Then from Equation (5.28b), as $\frac{\chi\bar{Y}}{2\mu^3 R}[1 - 2\mu R - \exp(-2\mu R)]$ is bounded, it implies $\bar{Y} > 0$. Finally, from Equation (5.28a), we conclude $R = \frac{\bar{Y}}{F(\Theta^*)} > 0$.

Considering similar arguments, one can easily prove (2), (3) and (4).

□

Lemma 5.3 insures that, assuming Θ^* is greater than θ_f and is bounded, $\bar{Y}$ and R are positive and bounded, which means that the bifurcation diagram curve cannot go to infinity for finite R or $\bar{Y}$. Conditions (3) and (4) give the behavior of the curve in R and $\bar{Y}$ in 0 and at infinity. Therefore, bifurcation curves have to link these two points, but at this point we do not have uniqueness of the bifurcation diagram curve yet. In order to get this conclusion, it is enough to prove

that the implicit function theorem is valid at least for one of the extrema. We choose to show that the implicit function theorem is valid for $R = \bar{Y} = 0$ or equivalently for $\Theta^* = \theta_f$.

After multiplying Equation (5.28a) by R to avoid the singularity in $R = 0$, we apply the implicit function theorem to System (5.28), and we see that Condition (5.30) is satisfied. Starting at $\bar{Y} = R = 0$ in $\Theta^* = \theta_f$, System (5.28) defines a unique bifurcation curve. We note that the number of vertical turning points is not restricted to the number shown in Figure 5.5. Summarising:

Proposition 5.4. *The $(\bar{Y}, R)$ bifurcation diagram defined by System (5.28) defines a unique curve parametrised by Θ^* for every given set of parameters.*

Bifurcation diagram with χ as the control parameter

Let us consider the bifurcation diagram 5.2a. We proceed as in the previous section and therefore we omit details and state only results. The implicit function theorem gives a condition for the solutions of (5.28) to be a curve. For control parameter χ it reads

$$\bar{\Theta}_\chi \neq 0. \tag{5.35}$$

If this condition is satisfied the solution set defines a smooth curve parametrised by Θ^*. Because $\bar{\Theta}_\chi$ is a negative strictly decreasing function, this condition is always satisfied. By means of the implicit function theorem, one derives the following

$$\frac{dR}{d\Theta^*} = -\frac{R^2 F'(\Theta^*)}{\bar{Y}}, \tag{5.36}$$

$$\frac{d\chi}{d\Theta^*} = \frac{R^2 \bar{\Theta}_R F'(\Theta^*) + \bar{Y}}{\bar{Y}\bar{\Theta}_\chi}. \tag{5.37}$$

From Equations (5.36) and (5.37), we conclude the

Lemma 5.5. *We have*

(1) *The condition to have vertical turning points reads*

$$F'(\Theta^*) = -\frac{\bar{Y}}{R^2 \bar{\Theta}_R}, \tag{5.38}$$

where $\bar{\Theta}_R$ defines the (negative) derivative w.r.t. R.

(2) *The condition to have horizontal turning points reads*

$$\frac{dR}{d\Theta^*} = -\frac{R^2 F'(\Theta^*)}{\bar{Y}}. \tag{5.39}$$

Note that the condition to have horizontal turning points is never satisfied, thus, in the bifurcation diagram picture, only vertical turning points can be observed. After studying the sign of Equations (5.36)

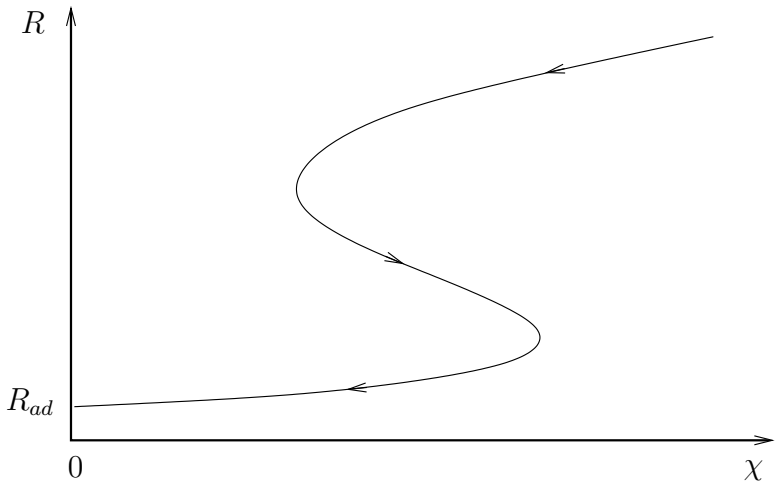

Figure 5.7: Full bifurcation diagram with respect to χ as a control parameter.

and (5.37), it leads to Diagram 5.8. The picture should be related to Figure 5.7, in which the arrows indicate the direction of increasing Θ^*.

As in the previous subsection, we would like to understand the behavior of the bifurcation diagram for $\chi = R = 0$ and χ, $R \to \infty$, corresponding respectively to $\bar{\Theta} = \theta_f$ and $\bar{\Theta} = \theta_f + \bar{Y}$. Note that these two number are natural bounds for Θ^*, which is indeed bounded, whereas when considering $\bar{Y}$ as control parameter, Θ^* was only bounded below. We denote by R_{ad} the adiabatic radius defined by Equation (5.27), when $\Theta^* = \theta_f + \bar{Y}$. This radius is also known as the Zeldovich radius and correspond to the combustion model without radiation (i.e. $\chi = 0$). We derive the following

Lemma 5.6. *We have*

(1) *If Θ^* is bounded then χ and R are bounded,*
(2) *If $\Theta^* \to \theta_f + \bar{Y}$ then $\chi \to 0$ and $R \to R_{ad}$,*
(3) *If $\Theta^* \to \theta_f$ then $\chi \to 0$ and $R > R_{ad}$ is bounded.*

As before, Lemma 5.6 ensures that for finite Θ^* between θ_f and $\theta_f + \bar{Y}$, the bifurcation curve cannot blow up. Moreover, as we know the behavior of the bifurcation curve for $\Theta^* = \theta_f$ and $\Theta^* = \theta_f + \bar{Y}$, one has to apply the implicit function theorem to one chosen extrema in order to get the conclusion that the bifurcation diagram defines a unique curve. It can be easily done, as in the previous subsection. Note that once again, there are no restrictions on the number of vertical turning points. Summarizing

Proposition 5.7. *The (χ, R) bifurcation diagram defined by System (5.28) defines a unique curve parametrised by $\Theta^* \in (\theta_f, \theta_f + \bar{Y})$ for every given set of parameters.*

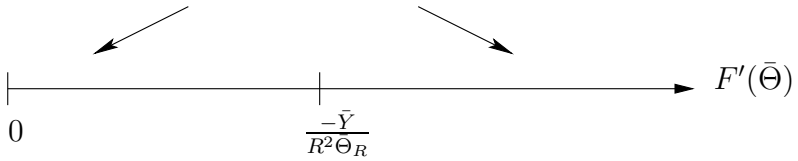

Figure 5.8: Varying Θ^*, the direction in which the bifurcation curve moves in the (χ, R)-plane depends on $F'(\Theta^*)$.

Relation between the Evans function and the bifurcation diagrams

In this subsection, we determine the connection between the Evans function $D(\lambda)$ and the turning points. We expect that in order to have vertical turning points in Figure 5.2, the condition $D(0) = 0$ needs to be satisfied.

Let us recall that the bifurcation diagram equation is given by Equation (5.27). As we are considering in this paragraph a linear Eddington equation, Θ^* can be explicitly computed, so that this equation can be rewritten as

$$f := F\left(\frac{\chi\bar{Y}}{2\mu^3 R}[1 - 2\mu R - \exp(-2\mu R) + \bar{Y} + \theta_f]\right) - \frac{\bar{Y}}{R} = 0, \quad (5.40)$$

where $\mu = \sqrt{3\alpha^2 + \chi}$. Irrespective of considering $\bar{Y}$ or χ as a control parameter, the implicit function theorem leads to (choosing χ),

$$f_\chi + f_R R' = 0.$$

Hence, it suffices to show that $D(0) = f_R$. We recall that the expression of the Evans function in the linear case is given by Equation (5.25), and replacing $\lambda = 0$ in this expression, the roots simplify to $a_1 = 0$, $a_2 = 0$ and $a_3 = \sqrt{3\alpha^2 + \chi}$. This expression can be easily compared to the computation of f_R, and one sees that the two expression are identical. Therefore, the vertical turning points, in the bifurcation diagram curves, are indeed given by the condition $D(0) = 0$.

5.4. Stability analysis for the linear Eddington equation

In this section, we are interested in studying the Evans function $D(\lambda)$ for $k = 1$. We recall that the zeros of the Evans function are the eigenvalues for the linearised problem. Thereby, if we can understand the zeros of $D(\lambda)$, then we can deduce stability properties. Unfortunately, an analytic analysis is extremely hard, hence the analysis will mainly be numerical. Nevertheless, considering $k = 1$, we can put $\alpha = 0$ in the Evans function (5.25) and in the bifurcation diagram equation (5.27), and keeping $\chi > 0$, we obtain a simplified expression

of the Evans function from which one explains analytically the main properties. This limit case was studied in Chapter 2, referred to as the heat loss case. One notes that the heat losses in the temperature equation enters in the form $-(\theta^4 - \theta_f^4)$. We therefore start by describing the main stability properties in the linear heat loss case.

A general overview

Starting from the simpler heat loss case $\alpha = 0$, we take the remaining radiation parameter χ as our main "variable". As explained in the introduction, see also (5.26), we examine stability in the $(\tilde{\chi}, \tilde{F}'(\Theta^*))$-plane, having rescaled to $R = 1$.

The case $\tilde{\alpha} = 0$. This case is interesting to study because the expression of the Evans function is simpler and we can conclude properties of the eigenvalues via an analytical analysis. The Evans function reads

$$\tilde{D}(\tilde{\lambda}) = \tilde{D}_0(\tilde{\lambda}) + \tilde{F}'(\Theta(R))\tilde{D}_1(\tilde{\lambda}), \tag{5.41}$$

where

$$\tilde{D}_0(\tilde{\lambda}) = 1 - \sqrt{\tilde{\lambda}\mathrm{Le}},$$

$$\tilde{D}_1(\tilde{\lambda}) = \frac{1}{2}\left(\sqrt{\frac{\tilde{\lambda}\mathrm{Le}}{\tilde{\lambda}+\tilde{\chi}}} - 1\right)\left(1 - \exp(-2\sqrt{\tilde{\lambda}+\tilde{\chi}})\right) + a(\tilde{\chi})$$

and

$$a(\tilde{\chi}) = \frac{1}{2}\left(1 + \exp(-2\sqrt{\tilde{\chi}}) + \frac{\exp(-2\sqrt{\tilde{\chi}}) - 1}{\sqrt{\tilde{\chi}}}\right).$$

In order to study the "dynamics" of the eigenvalues, we are interested in two particular values of $\tilde{\lambda}$. Namely we consider, first, $\tilde{\lambda}$ to be purely imaginary, i.e. we are looking for Hopf bifurcations. Secondly, as we will relate the stability pictures to the bifurcation diagrams, we are interested in the special value $\tilde{\lambda} = 0$, i.e. $\lambda = 0$, corresponding to vertical turning points in the bifurcation diagrams (see Section 5.3). For a fixed Lewis number, provided $\mathrm{Le} < 1$, a sketch of the curves obtained is shown in Figure 5.9. The solid line corresponds to the Hopf bifurcations while the dashed line corresponds to $\tilde{D}(0) = 0$.

We start by explaining the "dynamics" of the eigenvalues when one follows the parameter values given by the lines L_1 and L_2. A sketch of the situation is represented in Figure 5.10. Beginning from $\tilde{F}'(\Theta^*) = 0$, the analysis of the Evans function implies the existence of one positive real eigenvalue. As we cross the dashed curve, another positive eigenvalue emerges from $\lambda = 0$. These two real eigenvalues meet and continue in the complex plane. Their real part is then decreasing until they cross the imaginary axis, and a Hopf bifurcation occurs. The difference between the parameter lines L_1 and L_2 is simply that following L_1, the eigenvalues will keep negative real part, while following L_2 eigenvalues turn back and become positive again.

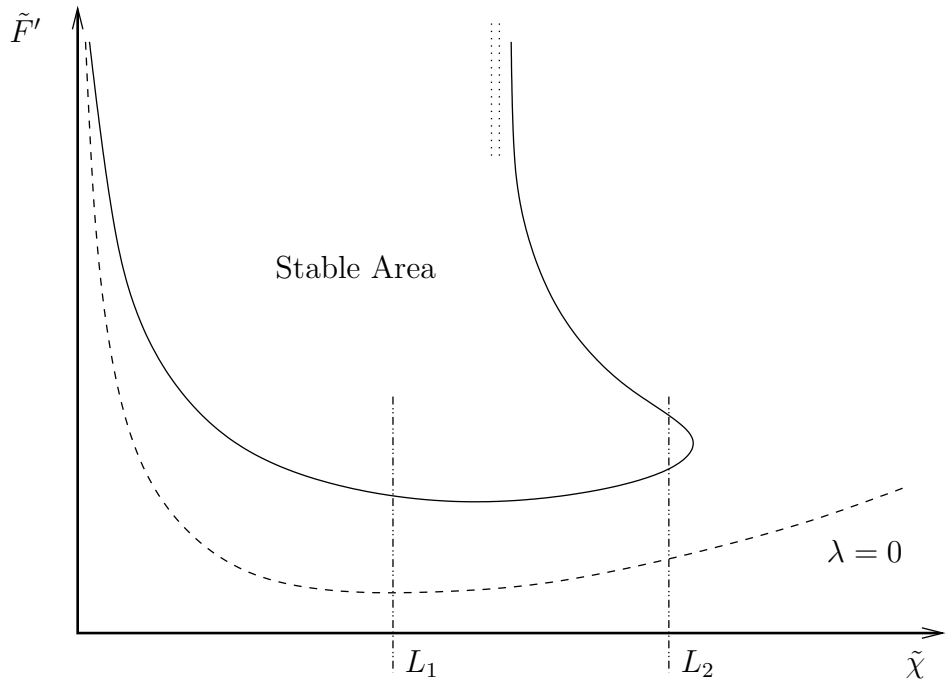

Figure 5.9: General picture of stability in the plane $(\tilde{\chi}, \tilde{F}')$

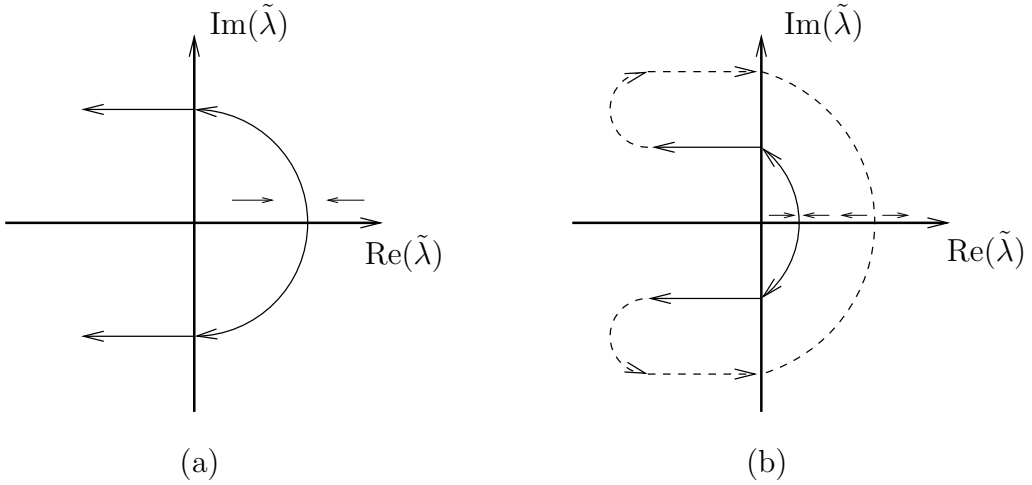

Figure 5.10: Sketch of the dynamic of the eigenvalues along the line (a) L_1 and (b) L_2

Another interesting question is to know how the stable area behaves when varying the Lewis number. The answer to this question is plotted in Figure 5.12. In order to explain this picture, we go back to Figure 5.9 and explain the dynamics of the double-dot asymptote. This asymptote depends on the value of $\tilde{D}_1(+\infty)$. In Figure 5.11 we sketch both $\tilde{D}_0$ and $\tilde{D}_1$. Note that $\tilde{D}_0(0) > 0$, $\tilde{D}_1(0) < 0$, $\tilde{D}_0(\tilde{\lambda}) \sim -\sqrt{\tilde{\lambda}}$ for

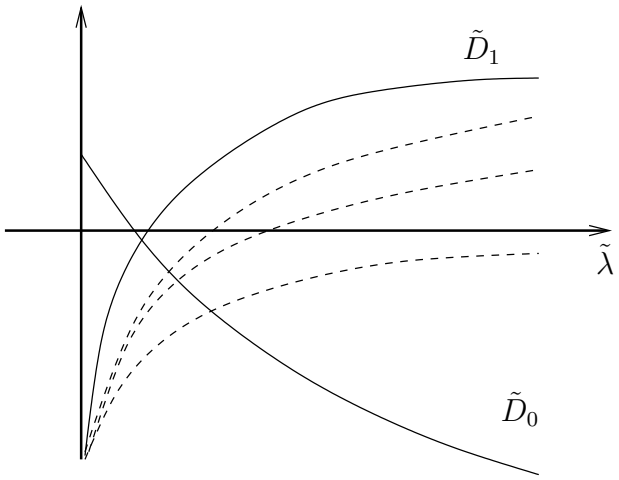

Figure 5.11: Behavior of the components $\tilde{D}_0$ and $\tilde{D}_1$

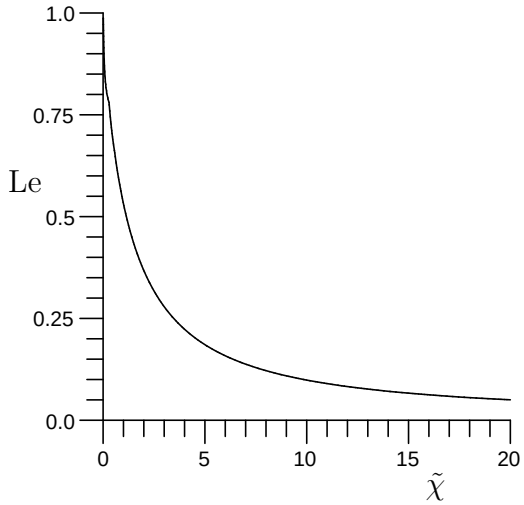

Figure 5.12: Asymptote dynamics in the heat loss case, stability vanish when $\mathrm{Le} = 1$

large $\tilde{\lambda}$, and

$$\tilde{D}_1(+\infty) = \lim_{\tilde{\lambda}\to+\infty} \tilde{D}_1(\tilde{\lambda}) = \frac{\sqrt{\mathrm{Le}}}{2} + \frac{e^{-2\sqrt{\chi}}}{2} + \frac{e^{-2\sqrt{\chi}} - 1}{2\sqrt{\chi}}.$$

The numerics suggest that, for large $\tilde{F}'(\Theta^*)$, the roots of the Evans function are real. Assuming this is valid in general, we can argue as follows. For large $\tilde{F}'(\Theta^*)$, there are two positive roots of $\tilde{D}(\lambda)$ if $\tilde{D}_1(+\infty) > 0$, and no positive roots if $\tilde{D}_1(+\infty) < 0$. Thus the asymptote in Figure 5.9 corresponds to $\tilde{D}_1(+\infty) = 0$. In Figure 5.12 we plot this curve. Recalling that $\tilde{\chi} = R^2\chi$, this picture suggests

that the stable area vanish when $\mathrm{Le} \geq 1$ and become more and more important as $\mathrm{Le} \to 0$.

The case $\tilde{\alpha} \neq 0$. Studying the heat loss case $\tilde{\alpha} = 0$ was a motivation for the study of the general case $\tilde{\alpha} \neq 0$. In the case $k = 1$, the sketch of the situation shown in Figure 5.9 is still valid for $\tilde{\alpha} > 0$. The eigenvalues behave similarly, and the stable area shrinks for Lewis numbers greater or equal to 1, and grows as the Lewis number tends to 0.

Before moving to the numerics, we discuss the choice of the parameter $\tilde{\chi} = R^2\alpha\beta$. In the following, we are interested in plotting the bifurcation diagram 5.2a, for which β is the control parameter, in the parameter plane $(\tilde{\chi}, \tilde{F}'(\Theta^*))$. The parameter $\tilde{\chi}$ is a consistent parameter if we can prove that $\tilde{\chi} = R^2\chi$ is a decreasing function of Θ^*, since Θ^* parametrises the bifurcation curve.

To prove this monotonicity statement, we apply the implicit function theorem, and derive the formulas

$$\frac{dR}{d\Theta^*} = -\frac{R^2}{\bar{Y}}F'(\Theta^*),$$

and

$$\frac{d\chi}{d\Theta^*} = \frac{R^2\bar{\Theta}_R F'(\Theta^*) + \bar{Y}}{\bar{Y}\bar{\Theta}_\chi},$$

where the subscripts R and χ denotes the derivative of $\bar{\Theta}$ with respect to R and χ, and $\bar{Y} = \frac{y_f}{\mathrm{Le}}$. Thus, we have

$$\frac{dR^2\chi}{d\Theta^*} = -\frac{2R^3\chi}{\bar{Y}}F'(\Theta^*) + R^2\frac{R^2\bar{\Theta}_R F'(\Theta^*) + \bar{Y}}{\bar{Y}\bar{\Theta}_\chi}.$$

As Equation (5.29) gives the expression of $\bar{\Theta}$, we can easily compute the expressions of $\bar{\Theta}_R$ and $\bar{\Theta}_\chi$, and prove that right hand side is negative.

The numerical analysis

Let us turn to the numerical investigation of the problem. The following computations are performed using the continuation software AUTO97, see [**21**].

We need an explicit expression for the reaction rate. Following the literature, e.g. [**55, 18**], we choose a simple Arrhenius law

$$F(\theta(R)) = A\exp\left(-\frac{1}{\varepsilon\theta(R)}\right), \tag{5.42}$$

where ε is a normalized inverse activation energy and $A > 0$ is the pre-exponential factor. Next we must choose values for the parameters. Unless mentioned otherwise, in all computations we take

$$\theta_f = 1, \quad y_f = 1, \quad \varepsilon = 0.1, \quad A = 40, \quad \alpha = 10^{-3}.$$

Figure 5.13 depicts the difference of the bifurcation diagrams we consider for $\mathrm{Le} = 0.5$ (solid line) and $\mathrm{Le} = 0.7$ (dashed line). One

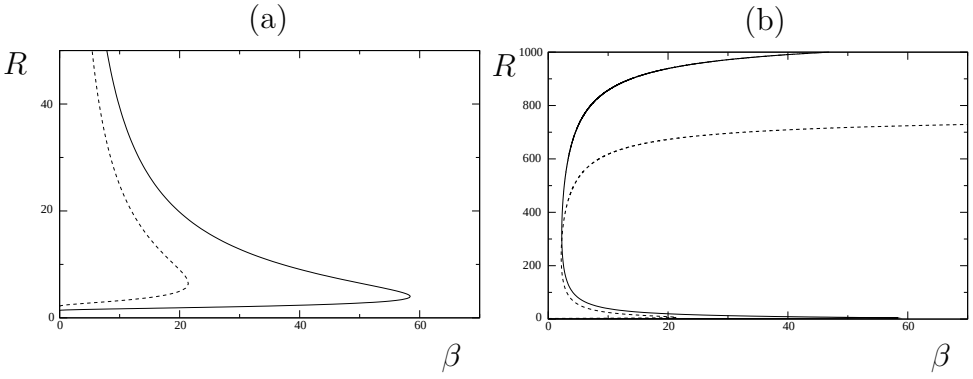

Figure 5.13: Bifurcation diagrams for $k = 1$, Le $= 0.5$ (solid line) and Le $= 0.7$ (dashed line) (a) around the first vertical turning point and (b) a more global picture

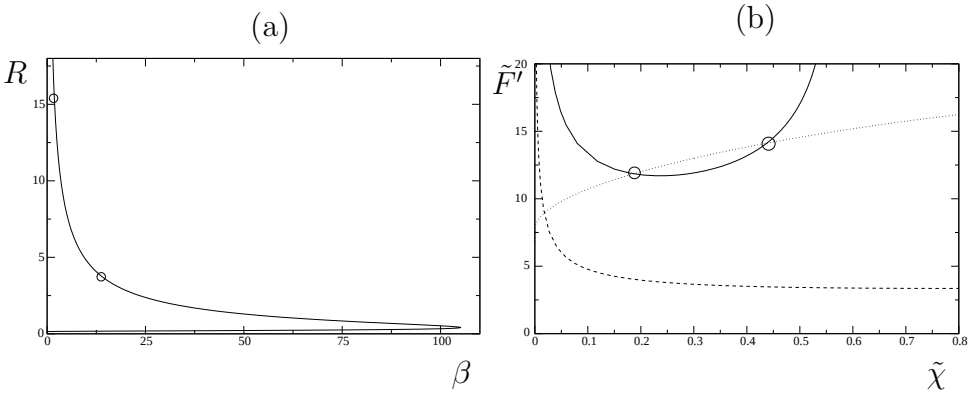

Figure 5.14: Relation between the stability on the bifurcation diagram (a) and the stable area (b) for Le $= 0.7$, $A = 2.29.10^6$, $\varepsilon = 3.35.10^{-2}$ and $k = 1$

notices that the first vertical turning point occurs for bigger values of β when Le $= 0.5$. As suggested by Equation (5.27), Figure 5.13 shows that the bifurcation curve is strongly influenced by the Lewis number

The goal of this section is to relate the bifurcation diagram curves and the stability pictures, as shown in Figure 5.14. We choose to give an example of stability for Le $= 0.7$. We start by plotting the bifurcation diagram 5.14a in the $(\tilde{\chi}, \tilde{F}'(\theta^*))$-plane, corresponding to the dotted line in Figure 5.14b. Note that in order to hit the stable area, we needed to consider a larger value of the pre-exponential term A and a smaller value for the inverse of the activation energy ε.

The interpretation is similar to the description given in the introduction of this chapter. We recall that, in Figure 5.14b, the solid curve corresponds to Hopf bifurcations, the dashed curve to the vertical turning points and the dotted curve is the plot of Figure 5.14a in the $(\tilde{\chi}, \tilde{F}'(\theta^*))$-plane. The circles in the two pictures are related and stability occurs only in between these two points.

Similar qualitative curves can be obtained following similar computations for $0 < \mathrm{Le} < 1$. As soon as the Lewis number reach the value 1, the Hopf bifurcation curve does not exist anymore and thus, no points in the bifurcation diagram curve corresponds to stable solutions, i.e. no stable flame balls.

5.5. The Evans function for the nonlinear Eddington equation

In this section, we are interested in considering the nonlinear Eddington equation, namely, we consider the linearised System (5.17) with the linearised jump conditions (5.18) for $k = 4$. In this case, it is not possible anymore to derive explicit formulas for the Evans function, and the analysis can only be numerical. Let us explain where the difficulties are and how one can overcome them. We consider the eigenvalue problem associated to System (5.17), namely

$$\lambda m(z) = \frac{1}{\mathrm{Le}}\Delta_z m(z) \qquad \text{for } z \neq R, \quad (5.43a)$$

$$\lambda n(z) = \Delta_z n(z) + p(z) \qquad \text{for } z \neq R, \quad (5.43b)$$

$$0 = \Delta_z p(z) - 3\alpha^2 p(z) + k\chi\Delta_z(\Theta^{k-1}n(z)). \quad (5.43c)$$

As in Section 5.2, one can easily compute an expression for $m_\pm$. The problem lies in computing the eigenfunctions for Equations (5.43b) and (5.43c). Indeed, it is no longer possible to easily identify two well-defined solutions which decay at infinity. To overcome this problem, our analysis will be based on the paper by Allen and Bridges [**3**]. The idea is as follows. As one cannot work with individual solutions, it is easier to consider the wedge of the two solutions on both sides of $z = R$. This leads to the definition of a plane of solutions on each side i.e., with zero derivative in 0 and decaying at infinity. Once we have defined these two planes, one may try to find solutions in these planes which match at $z = R$ via the jump conditions (5.18). After matching, this gives us solutions in each plane, satisfying the jump conditions and these are the eigenfunctions we are looking for. In this framework, we extend the work by Allen and Bridges [**3**] in which they consider smooth solutions (i.e. no jump conditions). After this sketch of the general ideas, let us go into more detail.

Wedge formulation

Our first concern is to give a formulation in terms of wedges. For this purpose, we first reduce Equations (5.43b) and (5.43c) into a system of first order ODE's, namely

$$u_x = A(x, \lambda)u, \quad u \in \mathbb{C}^n, \quad \lambda \in \Lambda \subset \mathbb{C}, \quad (5.44)$$

where $u = (\tilde{n}, \tilde{n}', \tilde{p}, \tilde{p}')$ and

$$A(x,\lambda) = \begin{pmatrix} 0 & 1 & 0 & 0 \\ \lambda & 0 & -1 & 0 \\ 0 & 0 & 0 & 1 \\ -B'' - \lambda B & -2B' & 3\alpha^2 + B & 0 \end{pmatrix},$$

where $B = k\chi\Theta^{k-1}$. This system is obtained after a change of variables to "remove" the singularity $\frac{1}{z}$ induced by the radial Laplacian, as in Section 5.2. Let us consider $e_1, \ldots, e_4$ to be the standard basis for $\mathbb{C}^4$ and let $\omega_1, \ldots, \omega_6$ be a basis for the wedge formulation in the lexicographical ordering, namely

$$\omega_1 = e_1 \wedge e_2, \quad \omega_2 = e_1 \wedge e_3, \quad \omega_3 = e_1 \wedge e_4,$$

$$\omega_4 = e_2 \wedge e_3, \quad \omega_5 = e_2 \wedge e_4, \quad \omega_6 = e_3 \wedge e_4.$$

Then following [**3**] in which the authors derive a generic way to obtain the induced 6×6 problem, we define

$$A^{(2)} = \begin{pmatrix} 0 & -1 & 0 & 0 & 0 & 0 \\ 0 & 0 & 1 & 1 & 0 & 0 \\ -2B' & 3\alpha^2 + B & 0 & 0 & 1 & 0 \\ 0 & \lambda & 0 & 0 & 1 & 0 \\ B'' + \lambda B & 0 & \lambda & 3\alpha^2 + B & 0 & -1 \\ 0 & B'' + \lambda B & 0 & 2B' & 0 & 0 \end{pmatrix}.$$

We briefly explain the role of this matrix. Let us take two solutions of System (5.44)

$$u_1 = \sum_{i=1}^{4} u_1^i e_i, \quad u_2 = \sum_{j=1}^{4} u_2^j e_j.$$

The wedge product of u_1 and u_2 defines a 2-form w given by

$$w = u_1 \wedge u_2 = \sum_{1 \le i < j \le 4} (u_1^i u_2^j - u_1^j u_2^i) e_i \wedge e_j.$$

The product derivative of u_1 and u_2 satisfies

$$\frac{d}{dx}(u_1 \wedge u_2) = \sum_{i,j=1}^{4} \left(\frac{du_1^i}{dx} u_2^j + u_1^i \frac{du_2^j}{dx} \right) e_i \wedge e_j,$$

or equivalently using (5.44)

$$\frac{d}{dx}(u_1 \wedge u_2) = \sum_{i,j,k=1}^{4} \left(a_k^i u_1^k u_2^j + u_1^i a_k^j u_2^k \right) e_i \wedge e_j,$$

where a_k^i are the components of the matrix $A(x,\lambda)$. This leads to the formulation

$$\frac{d}{dx}(u_1 \wedge u_2) = Au_1 \wedge u_2 + u_1 \wedge Au_2 \stackrel{def}{=} A^{(2)}(u_1 \wedge u_2), \qquad (5.45)$$

where $A^{(2)}(x,\lambda) \in \mathbb{C}^{6\times 6}$. By linearity, the coefficients of $A^{(2)}(x,\lambda)$ are computed using

$$A^{(2)}(e_i \wedge e_j) = Ae_i \wedge e_j + e_i \wedge Ae_j = \sum_{k=1}^{4} a_i^k e_k \wedge e_j + a_j^k e_i \wedge e_k,$$

for $1 \leq i < j \leq 4$. We define w^- as the plane spanned by two independent solutions for $z < R$ with $\tilde{n}(0) = \tilde{p}(0) = 0$, and w^+ as the plane spanned by two independent solutions for $z > R$ that decay as $z \to \infty$.

Then from (5.45) it follows that the 2-forms $w^\pm \in \mathbb{C}^6$ satisfy

$$(w^\pm)' = A^{(2)}(x,\lambda)w^\pm, \quad x \neq R, \quad w^\pm \in \mathbb{C}^6. \tag{5.46}$$

The boundary conditions

Having defined the differential equations to be solved for the wedge formulation, one needs to derive the boundary conditions which must be satisfied. Once again, our derivation is widely inspired by [**3**].

The boundary condition in 0. We defined the vector $X = (x_i)_{i=1,\dots,4}$, which corresponds to the vector (n, n', p, p'). In order to get two independent solutions, one can consider $e_2 = (0,1,0,0)$ and $e_4 = (0,0,0,1)$, where the constant 1 can be taken as any other constant. Then the boundary condition in 0 is simply given by wedging e_2 and e_4 and so we get $a = (0,0,0,0,1,0)$. Therefore in 0, we should solve Equation (5.46) with the initial condition

$$w_-(0,\lambda) = a. \tag{5.47}$$

The boundary condition at infinity. As one can notice, the matrix $A^{(2)}$ is not a constant matrix, so that it is not straightforward to solve such a problem. The technique proposed by [**3**] is as follows. When $x = +\infty$, the matrix $A(x,\lambda)$ is asymptotically constant (independent of x):

$$\lim_{x\to+\infty} A(x,\lambda) = A_\infty(\lambda), \quad \forall \lambda \in \Lambda. \tag{5.48}$$

We start with $\lambda > 0$, then A_∞ has two positive eigenvalues and more importantly, two negative ones, σ_1 and σ_2. The most negative eigenvalue of $A_\infty^{(2)} = \lim_{x\to\infty} A^{(2)}(x,\lambda)$ is $\sigma^+(\lambda) = \sigma_1 + \sigma_2$. Let $\xi^+(\lambda)$ be an eigenvector of $A_\infty^{(2)}(\lambda)$ associated to the eigenvalue $\sigma^+(\lambda)$,

$$A_\infty^{(2)}(\lambda)\xi^+(\lambda) = \sigma^+(\lambda)\xi^+(\lambda).$$

Since $\sigma^+(\lambda)$ is simple, the eigenvector $\xi^+(\lambda)$ can also be chosen to be an analytic function.

By standard arguments from the theory of differential equations (see for example [**19**]), there exists a unique solution of the differential equation (5.46) which satisfies

$$\lim_{x\to+\infty} e^{-\sigma^+(\lambda)x} U^+(x,\lambda) = \xi^+(\lambda).$$

Again, $U^+(x,\lambda)$ depends analytically on λ, and is the plane spanned by solutions decaying to zero.

The Evans function

Having defined the solutions $w^\pm$, we now need to express the Evans function in terms of the variables $w^\pm$ instead of individual solutions of Equation (5.44). As Equation (5.4) provides an explicit solution for the mass fraction, we can compute explicitly the jump conditions (5.18). They read, after simplifications,

$$\begin{aligned}
[n] &= -1 \\
[n_z] &= \sqrt{\lambda \mathrm{Le}} \\
\frac{1}{R} - \sqrt{\lambda \mathrm{Le}} &= \frac{F'(\Theta(R))}{F(\Theta(R))}\left(\Theta'(R^-)n(R^+) - \Theta'(R^+)n(R^-)\right) \\
[p] &= k\chi\Theta^{k-1} \\
[p_z] &= -k\chi\Theta^{k-1}\sqrt{\lambda \mathrm{Le}} - \chi k(k-1)\Theta^2\sqrt{\lambda \mathrm{Le}}[\Theta'(R^-) + \Theta'(R^+)] \\
&\quad - \frac{F(\Theta(R))}{F'(\Theta(R))}k(k-1)\chi\Theta^2\sqrt{\lambda \mathrm{Le}}
\end{aligned}$$

We define the vector $q = (q^i)$, $i = 1, \ldots, 6$, to be

$$\begin{pmatrix} q^1 \\ q^2 \\ q^3 \\ q^4 \\ q^5 \\ q^6 \end{pmatrix} = \begin{pmatrix} -1 \\ \sqrt{\lambda \mathrm{Le}} \\ k\chi\Theta^{k-1} \\ -k\chi\Theta^{k-1}\sqrt{\lambda \mathrm{Le}} - \chi k(k-1)\Theta^2\sqrt{\lambda \mathrm{Le}}[\Theta'_- + \Theta'_+] \\ \frac{1}{R} - \sqrt{\lambda \mathrm{Le}} \\ k(k-1)\chi\Theta^2\sqrt{\lambda \mathrm{Le}} \end{pmatrix}.$$

As $w^- = u_1 \wedge u_2$ and $w^+ = u_3 \wedge u_4$, for $u_j \in \mathbb{C}^4$, $j = 1, \cdot\cdot, 4$, we can rewrite the jump conditions (5.18) as the following linear system

$$MC = \begin{pmatrix} -u_1^1 & -u_2^1 & u_3^1 & u_4^1 & -q^1 \\ -u_1^2 & -u_2^2 & u_3^2 & u_4^2 & -q^2 \\ -u_1^3 & -u_2^3 & u_3^3 & u_4^3 & -q^3 \\ -u_1^4 & -u_2^4 & u_3^4 & u_4^4 & -q^4 \\ -a^-F'u_1^1 & -a^-F'u_2^1 & a^+F'u_3^1 & a^+F'u_4^1 & -q^5 \end{pmatrix} \begin{pmatrix} C_1 \\ C_2 \\ C_3 \\ C_4 \\ C_5 \end{pmatrix}$$

$$-\frac{F}{F'}\begin{pmatrix} -u_1^1 & -u_2^1 & u_3^1 & u_4^1 & 0 \\ -u_1^2 & -u_2^2 & u_3^2 & u_4^2 & 0 \\ -u_1^3 & -u_2^3 & u_3^3 & u_4^3 & 0 \\ -u_1^4 & -u_2^4 & u_3^4 & u_4^4 & -q^6 \\ -a^-F'u_1^1 & -a^-F'u_2^1 & a^+F'u_3^1 & a^+F'u_4^1 & 0 \end{pmatrix} \begin{pmatrix} C_1 \\ C_2 \\ C_3 \\ C_4 \\ C_5 \end{pmatrix} = 0,$$

where $C = (C_1, C_2, C_3, C_4, C_5)^T$ is a constant vector, $a^- = \frac{\Theta'(R^-)}{F(\theta^*)}$, $a^+ = \frac{\Theta'(R^+)}{F(\theta^*)}$ and F' denotes $F'(\theta^*)$. In order to have a nontrivial solution of this system, the matrix M should have a non zero determinant.

This determinant is called the Evans function, and its zeros correspond to the eigenvalues. Computing this determinant leads, after simplifications to the following expression of the Evans function

$$D(\lambda) = q^5 s + \Theta'_- s_1^- + \Theta'_+ s_1^+ - \frac{\mathrm{Le}\, R}{Y_f} F'(\theta^*)[\Theta'_- s^- + \Theta'_+ s^+], \quad (5.49)$$

where $\Theta'_\pm = \Theta'(R^\pm)$. We denote by $\bar{q} = (q^1, q^2, q^3, q^4)$ and $\bar{p} = (0, 0, 0, q^6)$. The quantities s, s^-, s^+, s_1^- and s_1^+ are then defined by

$$\begin{aligned}
s &= \det(u_1, u_2, u_3, u_4),\\
s^- &= u_1^1 \det(\bar{q}, u_2, u_3, u_4) + u_2^1 \det(u_1, \bar{q}, u_3, u_4),\\
s^+ &= u_3^1 \det(u_1, u_2, \bar{q}, u_4) + u_4^1 \det(u_1, u_2, u_3, \bar{q}).\\
s_1^- &= u_1^1 \det(\bar{p}, u_2, u_3, u_4) + u_2^1 \det(u_1, \bar{p}, u_3, u_4),\\
s_1^+ &= u_3^1 \det(u_1, u_2, \bar{p}, u_4) + u_4^1 \det(u_1, u_2, u_3, \bar{p}).
\end{aligned}$$

There is an easy way to compute these determinants in terms of $w^\pm$ as explained below. Let us denote by $\delta(i)$ the permutation symbol for $i = (i_1, i_2, i_3, i_4)$. In the following we denote by i_l, $l = 1, \dots, 4$ the different indexes for i. We recall that $w^- = u_1 \wedge u_2$ and $w^+ = u_3 \wedge u_4$, so that we can write

$$\begin{aligned}
s &= \det(u_1, u_2, u_3, u_4),\\
&= \sum_{i_l=1}^{4} \delta(i) u_1^{i_1} u_2^{i_2} u_3^{i_3} u_4^{i_4},\\
&= \sum_{i_1<i_2, i_3<i_4} \delta(i)(u_1^{i_1} u_2^{i_2} - u_1^{i_2} u_2^{i_1})(u_3^{i_3} u_4^{i_4} - u_3^{i_4} u_4^{i_3}),\\
&= \sum_{i_1<i_2, i_3<i_4} \delta(i) w^-_{i_1 i_2} w^+_{i_3 i_4},\\
&= w^-_{12} w^+_{34} - w^-_{13} w^+_{24} + w^-_{14} w^+_{23} + w^-_{23} w^+_{14} - w^-_{24} w^+_{13} + w^-_{34} w^+_{12},
\end{aligned}$$

where w^-_{ij} denotes the component of w^- associated to the vector basis $e_i \wedge e_j$.

In the same way we compute the expression for s^-:

$$\begin{aligned}
s^- &= \sum_{i_l=1}^{4} \delta(i) q^{i_1} u_2^{i_2} u_3^{i_3} u_4^{i_4} u_1^1 + \delta(i) u_1^{i_1} q^{i_2} u_3^{i_3} u_4^{i_4} u_2^1,\\
&= \sum_{i_l=1}^{4} \delta(i) q^{i_1} u_3^{i_3} u_4^{i_4} (u_1^1 u_2^{i_2} - u_2^1 u_1^{i_2}),\\
&= \sum_{i_3<i_4} \delta(i) q^{i_1} (u_3^{i_3} u_4^{i_4} - u_3^{i_4} u_4^{i_3})(u_1^1 u_2^{i_2} - u_2^1 u_1^{i_2}),\\
&= \sum_{i_3<i_4} \delta(i) q^{i_1} w^+_{i_3 i_4} w^-_{1 i_2}.
\end{aligned}$$

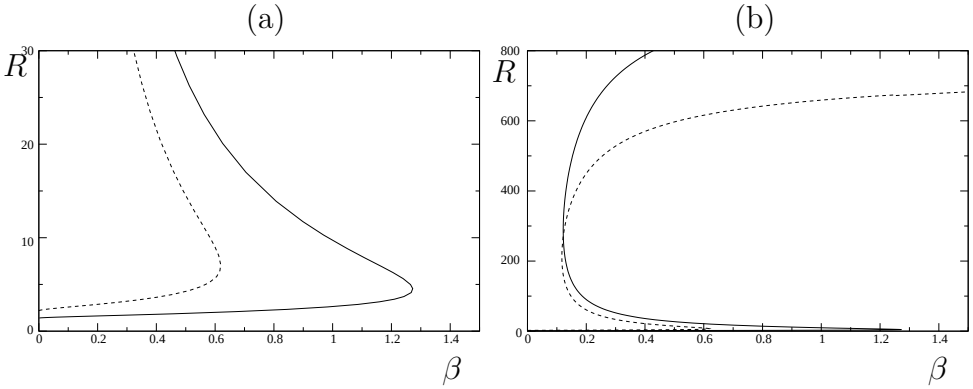

Figure 5.15: Bifurcation diagrams for $k = 4$, Le $= 0.5$ (solid line) and Le $= 0.7$ (dashed line) (a) around the first vertical turning point and (b) a more general picture

Similarly we find

$$\begin{aligned} s^+ &= \sum_{i_1<i_2} \delta(i) q^{i_3} (u_1^{i_1} u_2^{i_2} - u_1^{i_2} u_2^{i_1})(u_3^1 u_4^{i_4} - u_4^1 u_3^{i_4}), \\ &= \sum_{i_1<i_2} \delta(i) q^{i_3} w^+_{i_1 i_2} w^-_{1 i_4}. \end{aligned}$$

Expanding the terms for s^- and s^+, we find

$$\begin{aligned} s^- = {} & q^1(w^-_{34}w^+_{12} - w^-_{24}w^+_{13} + w^-_{23}w^+_{14}) + q^2(w^-_{14}w^+_{13} - w^-_{13}w^+_{14}) \\ & + q^3(w^-_{12}w^+_{14} - w^-_{14}w^+_{12}) + q^4(w^-_{13}w^+_{12} - w^-_{12}w^+_{13}), \end{aligned}$$

and

$$\begin{aligned} s^+ = {} & q^1(w^-_{12}w^+_{34} - w^-_{13}w^+_{24} + w^-_{14}w^+_{23}) + q^2(w^-_{13}w^+_{14} - w^-_{14}w^+_{13}) \\ & + q^3(w^-_{14}w^+_{12} - w^-_{12}w^+_{14}) + q^4(w^-_{12}w^+_{13} - w^-_{13}w^+_{12}). \end{aligned}$$

The expression for s_1^- and s_1^+ are

$$\begin{aligned} s_1^- &= q^6(w^-_{13}w^+_{12} - w^-_{12}w^+_{13}), \\ s_1^+ &= q^6(w^-_{12}w^+_{13} - w^-_{13}w^+_{12}). \end{aligned}$$

The numerical analysis

Since we have defined the Evans function, we are able to perform a similar analysis as in Section 5.4. The reaction rate and the parameter values we consider are, unless mentioned otherwise the same as the ones defined in Section 5.4. We exhibit similar curves and comment only on differences.

Let us define a large interval length L_∞ in order to reduce our problem to a bounded domain and to allow us to perform numerics.

The numerical strategy to compute the solution is to integrate the differential equation (5.46) from $x = L_\infty$ to $x = R$ with $\xi^+(\lambda)$ as the starting vector. Unfortunately, one can see that for large value of L_∞

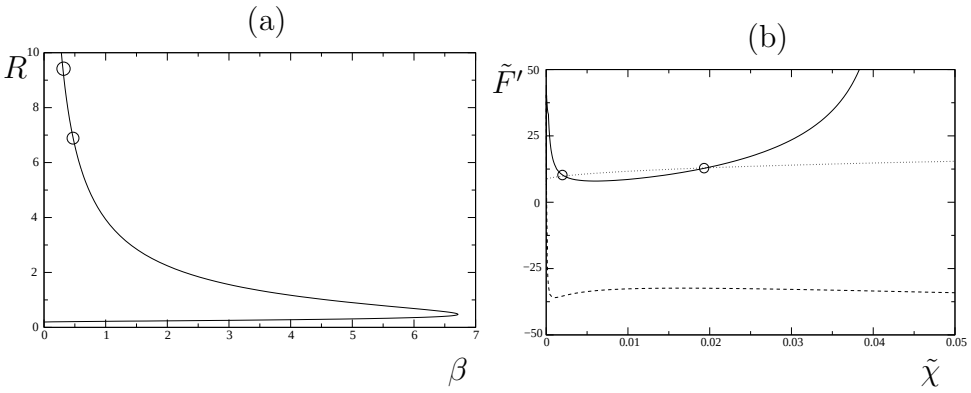

Figure 5.16: Relation between the stability on the bifurcation diagram (a) and the stable area (b) for Le = 0.7, $A = 1.47.10^7$, $\varepsilon = 2.839.10^{-2}$ and $k = 4$

the solution $w^+ = \xi^+ e^{\sigma^+ L_\infty}$ becomes almost zero. Therefore, we rescale w^+ by $e^{\sigma^+ x}$. Thus the problem to solve at infinity reads

$$(\tilde{w}^+)' = (A^{(2)}(x,\lambda) - \sigma^+(\lambda) I_6)\tilde{w}^+, \quad x \neq R, \tag{5.50}$$

where I_6 denotes the identity 6×6-matrix. We can explicitly compute $\xi^+(\lambda)$:

$$\xi^+(\lambda) = \begin{pmatrix} a_2 - a_3 \\ a_2^2 - a_3^2 \\ -(a_2 - a_3)(a_3^2 + a_2 a_3 + a_2^2 - \lambda) \\ (a_3 - a_2)(a_2 a_3 + \lambda) \\ a_2 a_3 (a_2^2 - a_3^2) \\ (a_2 - a_3)(\lambda - a_3^2)(\lambda - a_2^2) \end{pmatrix},$$

where a_2 and a_3 are defined in Section 5.2 and the associated eigenvalue reads

$$\sigma^+(\lambda) = \sqrt{\lambda + 3\alpha^2 + \chi B_\infty + 2\sqrt{\lambda(3\alpha^2 + \chi B_\infty)}},$$

where $B_\infty = k\chi\theta_f^{k-1}$.

As in the linear stability analysis, Figure 5.15 shows that the bifurcation diagram curve is Lewis dependent. Moreover, we can, for a fixed value of the Lewis number relate the bifurcation diagram and the stability curves as shown in Figure 5.16. The major difference occurring between the linear and nonlinear case concerns the vertical turning point line (dashed curve). Indeed, in the nonlinear case, it becomes negative for some parameter value (and tends to $+\infty$ as $\tilde{\chi} \to \infty$), whereas in the linear case, this curve was always positive.

Bibliography

[1] http://exploration.grc.nasa.gov/combustion/sofball/sofball_index.htm.

[2] P. Acquistapace and B. Terreni. Hölder classes with boundary conditions as interpolation spaces. *Math. Z.*, 195:451–471, 1987.

[3] L. Allen and T.J. Bridges. Numerical exterior algebra and the compound matrix method. *Numer. Math.*, 92:197–232, 2002.

[4] J. Audounet, V. Giovangigli, and J.-M. Roquejoffre. A threshold phenomenon in the propagation of a point source initiated flame. *Physica D*, 121:295–316, 1998.

[5] J. Audounet, J.-M. Roquejoffre, and H. Rouzaud. Numerical simulation of point-source initiated flame ball with heat losses. *Mathematical Modelling and Numerical Analysis*, 36:2:273–291, 2002.

[6] O. Baconneau, J.B. van den Berg, C.M. Brauner, and J. Hulshof. Multiplicity and stability of travelling wave solutions in a free boundary combustion-radiation problem. *European J. Appl. Math.*, 15:79–102, 2004.

[7] H. Berestycki and B. Larrouturou. Quelques aspects mathématiques de la propagation de flammes prémélangées. *Collège de France Seminar, Pitmar*, 10:65–129, 1987-1988.

[8] C.M. Brauner, J. Hulshof, and A. Lunardi. A general approach to stability in free boundary problems. *J. Differential Equations*, 164:1:16–48, 2000.

[9] C.M. Brauner, J. Hulshof, A. Lunardi, and C. Schmidt-Lainé. Instabilities, bifurcations and saddle-points in some free boundary problems in combustion. *FBP: theory and applications, Crete*, pages 105–114, 1997.

[10] C.M. Brauner, J. Hulshof, and J.-F. Ripoll. Existence of travelling wave solutions in a combustion-radiation model. *Discrete and Contin. Dyn. Syst. Ser. B*, 1:193–208, 2001.

[11] C.M. Brauner, J. Hulshof, and C. Schmidt-Lainé. The saddle point property for focussing selfsimilar solutions in a free boundary problem. *Proc. Amer. Math. Soc.*, 127:473–479, 1999.

[12] C.M. Brauner and A. Lunardi. Instabilities in a two-dimensional combustion model with free boundary. *Arch. Ration. Mech. Anal.*, 154:157–182, 2000.

[13] C.M. Brauner, A. Lunardi, and C. Schmidt-Lainé. Stability of travelling waves with interface conditions. *Nonl. Anal.*, 19:455–474, 1992.

[14] J.D. Buckmaster and T.L Jackson. The effects of radiation on the thermal-diffusive stability boundaries of premixed flames. *Comb. Sci. and Tech.*, 103:299–313, 1994.

[15] J.D. Buckmaster and G. Joulin. The structure and stability of nonadiabatic flame balls. *Combustion and Flame*, 79:381–392, 1990.

[16] J.D. Buckmaster, G. Joulin, and P.D. Ronney. The structure and stability of non adiabatic flame balls. *Combust. Flame*, 79:381–392, 1990.

[17] J.D. Buckmaster, G. Joulin, and P.D. Ronney. The structure and stability of non adiabatic flame balls: 2. effects of far field losses. *Combust. Flame*, 84:411–422, 1991.

[18] J.D Buckmaster and G.S.S. Ludford. *Theory of laminar flames*. Cambridge University Press, 1982.

[19] E. A. Coddington and N. Levinson. *Theory of Ordinary Differential Equations*. McGraw–Hill Book Co., 1955.

[20] H.B. Dixon. On the movements of the flame in the explosion of gases. *Proceedings of the Royal Society of London*, 70:471–483, 1902.

[21] E.J. Doedel, A.R. Champneys, T.F. Fairgrieve, Y.A. Kuznetsov, B. Sandstede, and X. Wang. Auto97, continuation and bifurcation software for ordinary differential equations (with homcont). 1997. Available by anonymous ftp from ftp.cs.concordia.ca, directory pub/doedel/auto.

[22] J.W. Dold, A.A. Shah, and R.W. Thachter. Stability of a spherical flame ball in a porous medium. *Combust. Theory Modelling*, 4:511–534, 2000.

[23] J.W. Dold, R.W. Thatcher, and Shah A.A. High order effects in one step reaction sheet jump conditions for premixed flames. *Combust. Theory Model., no.1*, 7:109–127, 2003.

[24] B. Dubroca and J.L. Feugeas. Etude théorique et numérique d'une hiérarchie de modèles aux moments pour le transfert radiatif. *C. R. Acad. Sci. Paris I*, 329:915–920, 1999.

[25] L.C. Evans. *Partial Differential Equations*, volume 19 of *Graduate Studies in Mathematics*. American Mathematical Society, 1998.

[26] V.A. Galaktianov, J. Hulshof, and J.L. Vazquez. Extinction and focusing of spherical and annular flames described by a free boundary problem. *J. Math. Pure Appl.*, 9:76:563–608, 1997.

[27] V. Guyonne and L. Lorenzi. Instability in a flame ball problem. *Discrete Contin. Dyn. Syst Ser. B*, 7:315–350, no.2, 2007.

[28] V. Guyonne and P. Noble. On a model of flame ball with radiative transfer. *SIAM Journal of Applied Mathematics*, 67(3):854–869, 2007.

[29] J. Hulshof and L. Lorenzi. Stability in a two-dimensional combustion model. *Interfaces Free Bound.*, 6:1–29, 2004.

[30] G. Joulin. Point source initiation of lean spherical flames of light reactants: an asymptotic theory. *Comb. Sci. Tech.*, 43:99–113, 1985.

[31] G. Joulin and B. Deshaies. On radiation-affected flame propagation in gaseous mixtures seeded with inert particules. *Combust. Sci. and Tech.*, 47:299–315, 1986.

[32] G. Joulin and M. Eudier. Radiation-dominated propagation and extinction of slow, particle-laden gaseous flames. *22nd Int. Symp. on combustion*, 1:1579–1585, 1988.

[33] C. Lederman, J.-M. Roquejoffre, and N. Wolansky. Mathematical justification of a nonlinear integrodifferential equation for the propagation of spherical flames. *Ann. Mat. Pura Appl.*, 183:2:173–239, 2004.

[34] C. Lee and J.D. Buckmaster. The structure and stability of flame balls: a near-equidiffusional flame analysis. *SIAM Journal on Applied Mathematics*, 51:1315–1326, 1991.

[35] D. Levermore. Moment closure hierarchies for kinetic theories. *J. Stat. Phys.*, 83:1021–1065, 1996.

[36] L. Lorenzi. A free boundary problem stemmed from combustion theory, part i: existence, uniqueness and regularity results. *J. Math. Anal. Appl.*, 274:505–535, 2002.

[37] L. Lorenzi. Regularity and analyticity in a two-dimensional combustion model. *Adv. Differential Equations*, 7:11:1343–1376, 2002.

[38] L. Lorenzi and A. Lunardi. Stability in a two-dimensional free boundary combustion model. *Nonlinear Anal. T.M.A.*, 53:227–276, 2003.

[39] A. Lunardi. *Analytic semigroups and optimal regularity in parabolic problems*. Birkhäuser, 1995.

[40] D. Mihalas and B. Mihalas. *Foundation of radiation hydrodynamics*. Oxford University Press, 1984.

[41] M.-F. Modest. *Radiative heat transfer*. Series in Mechanical Engineering. McGraw-Hill, Inc, 1993.

[42] M.-N. Ozisik. *Radiative transfer*. Wiley, 1973.

[43] G.-C. Pomraning. *The equation of radiation hydrodynamics*. Pergamon Press, 1973.

[44] P.D. Ronney. On the mechanisms of flame propagation limits and extinction processes at microgravity. *Twenty Second Symposium (International) on Combustion, Combustion Institute*, pages 1615–1623, 1988.

[45] P.D. Ronney. Near-limit flame structures at low lewis number. *Combust. Flame*, 82:1–14, 1990.

[46] P.D. Ronney, M.S. Wu, H.G. Pearlman, and K.J. Weiland. Experimental study of flame balls in space: Preliminary results from sts-83. *AIAA Journal*, 36:1361–1368, 1998.

[47] H. Rouzaud. Long-time dynamics of an integro-differential equation describing the evolution of a spherical flame. *Rev. Mat. Complut.*, 16:207–232, 2003.

[48] D. Sattinger. Monotone methods in nonlinear elliptic and parabolic boundary value problems. *Indiana. Univ. Math. J.*, 21:979–1000, 1972.

[49] R. Siegel and J.R. Howell. *Thermal radiation heat transfer*. McGraw-Hill, Inc, 1972.

[50] G.I. Sivashinsky. On flame propagation under condition of stoichiometry. *Siam J. Appl. Math.*, 39:67–82, 1980.

[51] H. Triebel. *Interpolation theory, Function Spaces, Differential Operators*. North-Holland, Amsterdam, 1978.

[52] C.A. Truesdell. On the foundations of mechanics and energetics. *Continuum Mechanics II: The Rational Mechanics of Materials*, pages 292–305, 1965.

[53] J.B. van den Berg, V. Guyonne, and J. Hulshof. Flame balls for a free boundary combustion model with radiative transfer. *SIAM J. Appl. Math.*, 67:116–137, no.1, 2006.

[54] J.B. van den Berg, V. Guyonne, and J. Hulshof. Stability properties for a flame balls problem with radiative transfer. *In preparation*, 2007.

[55] F.A. Williams. *Combustion theory*. Addison Wesley, 1994.

[56] Y.B. Zeldovich, G.I. Barenblatt, V.B. Librovich, and G.M. Makhviladze. The mathematical theory of combustion and explosions. 1985.

Samenvatting

Wiskundige Modellen voor Bolvlammen

Dit proefschrift gaat over de analyse van wiskundige modellen voor bolvormige vlammetjes. Deze bolvlammetjes, met een grootte van enkele millimeters, worden waargenomen in gasmengels van bijvoorbeeld aardgas en lucht, bij afwezigheid van zwaartekracht. De verhouding tussen de diffusie coefficient van het brandbare gas en de warmte diffusie coefficient speelt hierbij een belangrijke rol en wordt in de literatuur het Lewis getal genoemd. In de wiskundige modelvorming vinden we dit getal terug in de beschrijving van de balans tussen de massa flux die de vlam voedt en de warmte flux die door de vlam verspreid wordt.

De variabelen waarmee we de vlam beschrijven zijn de temperatuur, de fractie brandbaar gas en de straal van de bolvlam. In Hoofdstuk 1 bespreken we de wiskundige modelvorming aan de hand van een reactie-diffusie systeem. Omdat de vlam ruimtelijk beperkt is tot een kleine bolschil, is het gebruikelijk dit model te vervangen door een zogenaamd vrije rand probleem, waarbij de vrije rand het vlamfront is, dat met de tijd varieert. De precieze correspondentie tussen beide modellen is nog steeds onderwerp van studie. In dit proefschift werken we met de vrije rand formulering.

Dat deed ook Zeldovich, die in 1944, lang voor het ruimtevaart-tijdperk en experimenten onder gewichtsloosheid, een eenvoudig model opstelde dat weliswaar liet zien dat bolvlammen theoretisch kunnen bestaan, maar dat ze altijd onstabiel zijn en dus niet waarneembaar. Veertig jaar later werden ze echter toch waargenomen door Ronney. De vraag was en is hoe dat kan. Een zeer heuristische verklaring is dat via straling weglekkende warmte uit de vlambol en de op het bol-oppervlak gegenereerde warmte met elkaar in evenwicht kunnen zijn, waaruit een vaste verhouding tussen inhoud en oppervlakte van de bol volgt, een vaste diameter dus. Is de diameter groter, dan doet de weglekkende energie de vlambol slinken, en bij kleine diameter is het juist omgekeerd.

Het model van Zeldovich werd daarom aangepast met een term in de warmte vergelijking van het model die de door straling weglekkende energie modelleert, via de Stefan-Boltzmann wet met daarin de vierde macht van de temperatuur. Diverse varianten van dit gemodificeerde

model laten wel stabiele bolvlammen toe, maar zijn fysisch gezien toch minder correct, omdat bij straling niet alleen de emissie maar ook de absorptie van fotonen een belangrijke rol speelt.

In dit proefschrift gebruiken we een beter fysisch model voor stralingseffecten, waarbij straling zorgt voor een herverdeling van warmte energie. We koppelen daartoe de Eddington vergelijking voor de stralingsflux aan het verbrandingsmodel. Daarbij verschijnen twee parameters, een parameter in de Eddington vergelijking die de donkerheid, veroorzaakt bijvoorbeeld door stofdeeltjes in het medium, karakteriseert, en het Boltzmann getal dat aangeeft hoe sterk de stralingseffecten zijn in verhouding tot de gewone warmteflux ten gevolge van diffusie. Ook dit model wordt behandeld in Hoofdstuk 1.

Het aldus verkregen vlammodel met stralingeffecten is het onderwerp van dit proefschrift. We zoeken naar stationaire oplossingen en bestuderen hoe eigenschappen, met name stabiliteit, van de diverse parameters afhangen, waarbij we vooral naar het Lewis getal en het Boltzmann getal kijken. In het proefschrift beschouwen we alleen nog radieel symmetrische verstoringen.

In Hoofdstuk 2 bewijzen we eerst het bestaan van stationaire oplossingen, hetgeen nu niet meer vanzelfsprekend is. Als de reactiesnelheid niet is vastgelegd en dus vrij te kiezen, dan bestaat voor elke waarde van de parameters en voor elke voorgeschreven diameter precies één bolvlam met die diameter. De vergelijking voor het profiel van de fractie brandbaar gas ontkoppelt daarbij en is expliciet oplosbaar, net als bij Zeldovich. De diameter van de vlam volgt daarna door te eisen dat de voor het bestaan van de vlam benodigde reactiesnelheid consistent is met de vlamtemperatuur. Dat laatste leidt tot bifurcatie diagrammen waarbij generiek voor gegeven waarden van de parameters het aantal stationaire oplossingen oneven is.

Daarna beschrijven we verstoringen van stationaire oplossingen met een gelineairiseerde vergelijking die op een vernuftige manier wordt afgeleid uit het vrije rand probleem. Dit stelt ons in staat de zogenaamde spectrale stabiliteit van de oplossingen te bestuderen. Dit doen we met een Evans functie, een analytische functie gedefinieerd op een deelverzameling van het complexe vlak. De nulpunten van deze functie zijn bepalend voor de stabiliteit van de vlam. Ruwweg gezegd: nulpunten met positief reëel deel maken de vlam onstabiel. Vandaar dat we uitgebreid onderzoeken hoe nulpunten van de Evans functie weg te drijven zijn uit het complexe rechter halfvlak door aan de (controle) parameters/knoppen van ons model te draaien.

De Eddington vergelijking zelf bevat de vierde macht van de temperatuur. In een eerste analyse wordt ook deze term gelineariseerd, waarmee de Evans functie een semi-expliciete vorm krijgt die beter aan te pakken is met exacte methoden. De zo verkregen resultaten worden daarna numeriek gecontinueerd naar het model met de echte Eddington

vergelijking. We zien daarbij dat de tak van stabiele bolvlammen wat kleiner wordt. De rol van het Lewis getal is steeds hetzelfde. Dit getal moet klein genoeg zijn voor stabiliteit. Hoe dichter het bij de waarde 1 komt, hoe minder waarschijnlijk het wordt dat bolvlammen stabiel zijn, en voorbij 1 zijn er helemaal geen stabiele bolvlammen mogelijk. Dit alles komt aan de orde in Hoofdtuk 5.

Hoofdstuk 3 is het meeste theoretische hoofdstuk, waarin we proberen de stap van spectrale stabiliteit via gelineariseerde stabiliteit naar niet-lineaire stabiliteit te maken. Dit lukt alleen voor instabiliteit. Voor een gedeelte van het bifurcatiediagram bewijzen we met halfgroep technieken dat de bolvlammen ook werkelijk onstabiel zijn. Dit gebeurt in de context van zogenaamde volledig niet-lineaire problemen. Het grote open probleem hier blijft om hetzelfde te doen voor stabiele oplossingen. De wezenlijke moeilijkheid hier is gerelateerd aan het feit dat de Evans functie in nul een vertakkingspunt heeft.

In Hoofdstuk 4 tenslotte bekijken we het model met de gelineariseerde Eddington vergelijking en doen extra aannamen waarmee een integraal-differentiaalvergelijking voor de diameter van een veranderende bolvlam is af te leiden. Stabiliteit van bolvlammen is dan meer globaal te beschrijven. We laten numeriek zien dat als er twee stationaire oplossingen zijn, de grotere stabiel en de kleinere onstabiel is.

Summary

This thesis is devoted to the analysis of mathematical models for flame balls. Flame balls are tiny (4mm), stable, stationary, spherically symmetric flames that occur in combustible gas mixtures (such as lean hydrogen-air mixtures), having low Lewis numbers. They are visible only in a microgravity environment. The Lewis number is a measure of the rate of diffusion of fuel into the flame ball relative to the rate of diffusion of heat away from the flame ball, and is an important parameter throughout this thesis. The reaction zone, where the fuel is burning, occurs at the boundary of the ball and is assumed to be thin. Through this flame sheet, fuel and oxygen diffuse inward while heat and products diffuse outward.

The main variables we are interested in to describe the behavior, are the temperature, the fuel mass fraction and the flame ball radius. The classical governing equations for combustion are rederived in Chapter 1 as a reaction-diffusion system (RDS). Since we assume the flame to occur in a narrow region, it is possible to reduce this RDS to a free boundary problem (FBP), the free boundary being the a priori unknown radius, which may vary in time. Going from one formulation to the other is a hard issue and requires involved asymptotic analysis. In this thesis, we will consider the FBP formulation.

A first mathematical model to describe flame balls was derived in 1944 by Zeldovich, and he showed that such flames were unstable, and hence certainly not observable. Nevertheless, forty years later, flame balls were experimentaly found by Ronney. Therefore, a physical mechanism for stabilising the flame balls had to be sought. It has been argued that radiative effects could strongly influence the stability properties of flame balls. One can give an heuristic argument explaining why radiation can stabilise flame balls. We remark first that the total heat release is proportional to the flame ball surface area and that the total radiative heat loss is proportional to the flame ball volume. Hence, if the flame radius is large, the surface area to volume ratio is small, thus the ratio of total heat release to total radiative heat loss is large, and the flame ball becomes weaker and shrinks. Conversely, if the radius is small, the flame ball grows stronger and expands. Hence, flame balls with volumetric heat losses could be stable to radial disturbances.

New models were then derived introducing heat loss terms in the temperature equation, where the power radiated by a body is proportional to the fourth power of the temperature (Stefan-Boltzmann law). The analysis of such models leads to stability results.

In this thesis, we go one step further in describing the radiation effects. Indeed, radiation does not involve only emission of photons but also absorption. A more physical model of this phenomenon is described by the Eddington equation (radiative transfer equation) which we couple to the equations for the temperature and the fuel mass fraction. Radiation is even more important when the medium is filled with dust. The opacity of the medium is then another natural parameter to consider. The model and more physical explanations are discussed in Chapter 1.

Thus we are interested in studying the FBP involving the radiative transfer equation and, more specifically, we would like to prove stability results. Throughout this thesis, we suppose that flame balls are radially symmetric.

We start by proving the existence of stationary solutions. This is the objective of Chapter 2, in which we first prove that for each fixed radius, there exist a unique associated temperature profile if the reaction rate is not specified. The fuel mass fraction equation is decoupled from the system, and therefore we can compute explicitly its solution. The final step is to determine the radius of the flame given a specific temperature dependent reaction rate. In this way we can prove that there exist stationary solutions, and moreover, for a generic choice of the parameters, the number of solutions is odd. The existence of multiple solution is shown in various bifurcation diagrams.

In order to study stability properties, we are interested in perturbing slightly a fixed stationary solution. The perturbations that we consider in this thesis are radial (nonradial perturbations are part of work still in progress). For this purpose, we consider the FBP and linearise around a fixed stationary solution. It leads to a linear problem for which spectral properties have to be derived. To understand the "dynamics" of the eigenvalues considering different parameter values, we construct a special function known as the Evans function. It is an analytical function and its zeros are the eigenvalues. The analysis consists of two steps. We first consider the linearised Eddington equation and show that, for some specific range of the parameters, a branch of solutions of the bifurcation diagram is stable. This case is more accessible because we can derive explicit formulas. We then extend these results to the nonlinear Eddington equation (black body radiation model). In this case there are no explicit formulas and the computations are more involved but lead to similar stability results. Compared to the linear case, a smaller branch of the bifurcation diagram is stable under radial perturbations. We moreover show that stability depends strongly on

the Lewis number. More precisely, if the ratio of radiative and thermal fluxes is greater or equal to 1, then stability cannot occur. This analysis is performed in Chapter 5.

Chapter 3 is the most theoretical chapter of this thesis. We prove rigorously instability results, using semi-group techniques. Part of a branch of the bifurcation diagrams obtained in Chapter 2 corresponds to unstable solutions. The analysis performed in this chapter relates first the spectral stability to linear stability. Then, deriving proper estimates, we can deduce instability results from the previous linear analysis. Because the linearisation of the FBP leads to a fully nonlinear problem, it introduces theoretical difficulties. Indeed, instability results can still be proved in this setting, but stability issues are, on the theoretical level, an open problem.

Finally, Chapter 4 takes another approach. Considering the linearised Eddington law, under suitable assumptions, it is possible, from the initial FBP to derive an integro-differential equation describing the growth of the radius of the flame ball. The analysis of this model equation allows us to understand the behavior of flame balls for long times. After a mathematical analysis of this equation, we perform numerics and show that, when two steady flame balls exist, the smaller one is unstable while the larger one is stable.

Résumé

Modèles Mathématiques pour Flammes Sphériques

Cette thèse de cotutelle entre Amsterdam et Bordeaux, est consacrée à l'étude de modèles mathématiques décrivant des flammes sphériques. Ces flammes sont petites, de l'ordre de quelques millimètres, stables, stationnaires, à symétrie sphérique, brûlant des mélanges gazeux (comme, par exemple, des mélanges air-hydrogène appauvris), possédant un nombre de Lewis petit. Enfin, il est uniquement possible de les observer en microgravité. La zone de réaction, dans laquelle le carburant est brûlé, se trouve à la surface de la flamme et est supposée être fine.

Les inconnues de ce modèle sont la température, la fraction massique du carburant et le rayon de la flamme sphérique. Les équations générales décrivant l'écoulement d'un mélange gazeux réactif sont écrites dans le chapitre 1 sous la forme d'un système de réaction-diffusion (RDS). La zone de réaction étant mince, il est possible de réduire ce RDS en un problème à frontière libre (FBP), la frontière libre étant ici le rayon qui peut évoluer au cours du temps. Le passage d'une formulation à l'autre est le résultat d'une analyse asymptotique. Dans le cadre de cette thèse, nous considérons le FBP.

Le premier modèle décrivant des flammes sphériques est dû à Zeldovich en 1944. L'analyse qui en suivit révéla que ces flammes étaient instables et donc qu'il ne serait a priori pas possible de les observer. Cependant, quarante ans plus tard, des flammes sphériques ont été observées expérimentalement par Ronney. De ce fait, un mécanisme physique stabilisant ces flammes devait être trouvé. Des études ont montré que les effets radiatifs pouvaient influencer de manière importante leur stabilité.

D'une manière heuristique, il est possible de comprendre pourquoi les effets radiatifs peuvent rendre une flamme sphérique stable. Le dégagement total de chaleur de la flamme est proportionnelle à sa surface et les pertes de chaleur totales sont, elles, proportionnelles au volume de la flamme sphérique. Ainsi, si la flamme possède un grand rayon, le rapport entre surface et volume est petit, et donc le rapport entre dégagement de chaleur et perte de chaleur est grand, avec pour conséquence d'aller jusqu'à son extinction. Au contraire, si le rayon est

petit, la flamme croît et s'étend. Ainsi, une flamme ayant des pertes de chaleur volumétriques peut être stabilisée par des perturbations radiales.

En conséquence de nouveaux modèles ont été dérivés, incorporant un terme de pertes de chaleur dans l'équation de température, tout en considérant que la puissance radiative d'un corps est proportionnelle à T^4 (loi de Stefan- Boltzmann). Les analyses découlant de ces modèles ont amené à l'existence de solutions stables.

Au cours de cette thèse, nous allons plus loin dans la description des effets radiatifs. En effet, ces phénomènes ne prennent pas en compte seulement l'émission des photons mais aussi leur absorption. L'équation d'Eddington est plus proche d'une description physique, et nous la couplerons donc aux équations de température et de fraction massique. La radiation est d'autant plus importante que le milieu est opaque. Ainsi, il est naturel de considérer l'opacité du milieu comme un paramètre du modèle. La présentation de ce dernier mais aussi une description physique plus détaillée est le sujet du chapitre 1.

Ainsi, nous voulons étudier le FBP tout en y incorporant une équation de transfert radiatif et plus précisément, nous voudrions prouver des résultats de stabilité. Nous supposerons, tout au long de cette thèse que les flammes sphériques sont à symétrie radiale.

Le point de départ est de prouver l'existence de solutions stationnaires et est l'objet du chapitre 2. Nous montrons tout d'abord, que, pour tout rayon fixé, il existe un profil de température unique si le taux de réaction n'est pas spécifié. L'équation sur la fraction massique est découplée du système et donc il est possible de calculer de manière explicite son expression. Le dernier point consiste à déterminer le rayon de la flamme après avoir fixé un taux de réaction qui est une fonction de la température. Ainsi, nous prouvons qu'il existe des solutions stationnaires et de plus, pour un choix générique des paramètres, le nombre de solutions est impair. Afin d'illustrer la non-unicité des solutions, nous présentons différents diagrammes de bifurcation.

En vue d'étudier la stabilité, nous perturbons faiblement une solution stationnaire fixée. Les perturbations considérées sont radiales (les perturbations non radiales font l'objet d'un travail en cours). Nous linéarisons le FBP autour d'une solution stationnaire obtenant ainsi un problème linéaire dont nous devons étudier les propriétés spectrales. Afin de mettre en évidence la "dynamique" des valeurs propres vis à vis des différents paramètres, nous construisons une fonction d'Evans. Cette dernière est analytique et ses racines sont les valeurs propres. L'analyse se fait en deux étapes. Dans un premier temps, nous considérons l'équation d'Eddington linéaire et montrons, que pour certaines valeurs des paramètres, une partie du diagramme de bifurcation correspond à des solutions stables. Ce cas simplifié est plus accessible

car il est possible d'écrire des formules explicites. Nous étendons ensuite, ces résultats à l'analyse de l'équation d'Eddington non linéaire. Dans ce cas précis, les formules ne sont pas explicites et, de ce fait, l'étude numérique est plus poussée mais débouche sur des résultats similaires. De plus, nous montrons que les résultats de stabilité dépendent fortement du nombre de Lewis. En effet, si celui-ci est supérieur ou égal à 1, il n'est pas possible de trouver de solutions stables. Cette analyse est présenté dans le chapitre 5.

Le chapitre 3 présente des développements plus abstraits. Nous prouvons rigoureusement des résultats d'instabilité, grâce à la théorie des semi-groupes analytiques. Une partie du diagramme de bifurcation obtenu au chapitre 2 correspond à des solutions instables. L'analyse produite au cours de ce chapitre relie tout d'abord l'analyse spectrale à une analyse de stabilité linéaire. Par la suite, obtenant des estimations adéquates, il est possible de déduire des résultats d'instabilité non linéaire à partir de l'analyse linéaire. Comme la linéarisation du FBP aboutit à un problème totalement non linéaire, certaines difficultés théoriques apparaissent cependant.

Enfin, le chapitre 4 est consacré à une approche différente. Prenant en compte une version linéaire de l'équation d'Eddington, il est possible, à partir du FBP, de dériver une équation intégro-différentielle décrivant l'évolution du rayon de la flamme sphérique. L'analyse de ce modèle nous permet de mieux comprendre l'évolution du rayon pour les temps long. Après une analyse mathématique de cette équation, une étude numérique confirme que lorsque deux rayons stationnaires existent, le plus petit est instable alors que le plus grand est stable.

Au cours de cette thèse, nous avons étudié un modèle de combustion avec transfert radiatif. Des méthodes d'analyse différentes (que ce soit d'un point de vue dynamique ou abstrait) nous ont amenés à des résultats globaux concernant la stabilité du FBP. Une extension naturelle de ces travaux est l'étude des perturbations non-radiales ainsi que le couplage à d'autres moèles décrivant les effets radiatifs, comme le modèle M_1.